# miRNA biogenesis and developmental phase transition in the liverwort *M. polymorpha*


Susanna Streubel

Magdalen College

Department of Plant Sciences

University of Oxford

A thesis submitted in partial fulfilment of the requirement for the degree of

Doctor of Philosophy (D. Phil.)

Michaelmas 2019

# miRNA biogenesis and developmental phase transition in the liverwort *M. polymorpha*

Susanna Streubel
Magdalen College
Department of Plant Sciences
University of Oxford

A thesis submitted in partial fulfilment of the requirement for the degree of Doctor of Philosophy (D. Phil.)
Michaelmas 2019

## Abstract

microRNAs (miRNAs) are important regulators of gene expression and plant development. Some miRNAs, together with their target genes, have conserved functions among the major land plant lineages. An important miRNA-regulated developmental pathway is the ageing pathway that controls the juvenile to adult transition and the vegetative to reproductive transition in flowering plants. This thesis presents evidence that the function of *HASTY* (*HST*), a regulator of the ageing pathway through miRNA processing in the flowering plant *Arabidopsis thaliana*, is conserved in the bryophyte *Marchantia polymorpha*. Mp*HST* negatively regulates the timing of the reproductive transition in male *M. polymorpha*, which is consistent with At*HST* inhibiting phase transitions in *A. thaliana*. In contrary, Mp*HST* positively regulates the reproductive transition in female *M. polymorpha* plants. This suggests a sex-specific function of Mp*HST* in the dioecious liverwort and presents a new aspect of phase change regulation. This thesis also reports that another core regulator of miRNA biogenesis, *DICER-LIKE 1* (*DCL1*), controls growth, morphogenesis and organ differentiation through miRNA processing in *M. polymorpha*, as it does in angiosperms. Moreover, a novel role was discovered for Mp*DCL1* – Mp*DCL1* represses the reproductive phase transition in the absence of the normally required far-red light inductive signal. This occurs in a sex-dependent manner – similar to the requirement of Mp*HST* to delay phase transition in male plants, Mp*DCL1* represses phase change under non-inductive conditions in male plants. I propose that miRNAs, including sex-specific miRNAs, are involved in controlling phase change in the early divergent embryophyte *M. polymorpha*. This suggests that *HST*-regulated phase change operated in the common ancestor of liverworts and angiosperms, one of the first land plants.

# Acknowledgments

First and foremost, I would like to thank Liam Dolan, my supervisor and the reason why I returned to Oxford to do a DPhil. Thank you for sharing your endless passion for science with me, and some valuable life lessons. Thanks for continuously reminding me that it was going to be great when I didn't want to believe it, yet. I would also like to thank Lee Sweetlove for volunteering to be my second supervisor and for his support and valuable advice during my PhD. Thank you also to Nicholas Harberd and Justin Goodrich for examining this thesis. I want to express my gratitude to the DTP and the BBSRC for not only providing funding for my DPhil project and a fantastic internship, but also for a lot of very friendly support. That also came from my colleagues in the Dolan lab – thanks to everybody who sat through long lab and DPhil meetings and test presentations with me and still managed to provide priceless input and feedback on my research. Special thanks go to Anna and Suvi for sharing their wisdom on everything around FRH1; to Sandy for lots of useful and encouraging feedback on presentations and help with phylogenetic trees; to Reka for sharp feedback on many presentations and written pieces and to Chloe for support on the mutagenesis screen. Thanks also to George Ryan and Zoe Nahas for their help in generating and phenotyping the Mp*hst* mutant. I would also like to thank a few other members of the department for their support: Marta Mendez for her help and wise advice on qPCR; John baker for not getting tired of photographing my mutants; Gem Toes and Nicholas Kruger for taking such good care of us helpless DPhil students in the Plant Sciences department; Helen Prescott for tireless efforts to keep the lab running. Thank you also to Magdalen college, which provided a beautiful home, especially in my first years at Oxford.

Finally, I cannot express enough gratitude to all my friends, who massively improved my past four years in Oxford. Most of all to my best friend, Elli, who stood by my side from the beginning 'til the end, with never-ending moral support and care packages that kept me going. Nobody believed in me as much as you did, thank you so much! To Giulio – thanks for making my life in Oxford so much better and for accompanying me through bright and bleak times! To my house mates, who truly made me feel at home in Oxford and who shared much laughter. To my awesome Volleyball team and our special coaches, who sometimes made me forget that I was supposed to be doing a DPhil – special memories remain of the 2017/2018 team with some incredible action on and off court; they will never be forgotten. Finally, I want to thank my family, who, even though stumped with things happening in Oxford, are always there for me unconditionally.

# Table of content

# List of abbreviations

| | |
|---|---|
| **5'RLM-RACE PCR** | RNA-ligase mediated rapid amplification of complementary DNA ends PCR |
| **aa** | amino acid(s) |
| **AGO** | ARGONAUTE |
| **AP1** | APETALA 1 |
| **AP2** | APETALA 2 |
| **ARF** | AUXIN RESPONSE FACTOR |
| **bHLH** | basic helix-loop-helix |
| **bp** | base pairs |
| **CaMV** | Cauliflower Mosaic Virus |
| **CDF1** | CYCLING DOF FACTOR 1 |
| **CDS** | coding sequence |
| **CO** | CONSTANS |
| **CRISPR/Cas9** | clustered regulatory interspaced palindromic repeats/ CRISPR associated protein 9 |
| **dd$H_2O$** | double-distilled water |
| **DCL** | DICER-LIKE |
| **dsRNA** | double stranded RNA |
| **EF1α** | ELONGATION FACTOR 1α |
| **Exp5** | Exportin 5 |
| **FKF1** | FLAVIN-BINDING, KELCH-REPEAT, F-BOX 1 |
| **FRH1** | FEW RHIZOIDS 1 |
| **GI** | GIGANTEA |
| **GL2** | GLABRA 2 |
| **gRNA** | guide RNA |
| **HD-ZIP** | HOMEODOMAIN LEUCINE ZIPPER |
| **HD-ZIP III** | class III HOMEODOMAIN LEUCIN ZIPPER |
| **HEN1** | HUA ENHANCER 1 |
| **HST** | HASTY |
| **HYL1** | HYPONASTIC LEAVES 1 |
| **kb** | kilo base pairs |

| | |
|---|---|
| **LCA** | last common ancestor |
| **miRNA** | microRNA |
| **mRNA** | messenger RNA |
| **nt** | nucleotide |
| **PCR** | polymerase chain reaction |
| **PHA** | PHABULOSA |
| **PHV** | PHAVOLUTA |
| **PIF** | PHYTOCHROME-INTERACTING FACTOR |
| **pri-miRNA** | primary miRNA |
| **qRT-PCR** | quantitative real-time PCR |
| **RdDm** | RNA-directed DNA methylation |
| **RISC** | RNA-Induced Silencing Complex |
| **RITS** | RNA-Induced Transcript Silencing |
| **RNase III** | ribonuclease III |
| **rpm** | revolutions per minute |
| **RSL1** | ROOT HAIR DEFECTIVE 6-LIKE 1 |
| **RT-PCR** | reverse transcription PCR |
| **SBP** | SQUAMOSA BINDING PROTEIN |
| **SE** | SERRATE |
| **siRNA** | short interfering RNA |
| **SNP** | single nucleotide polymorphism |
| **snRNA** | small non-coding RNA |
| **SPL** | SQUAMOSA PROMOTER BINDING PROTEIN-LIKE |
| **sRNA** | small RNA |
| **T-DNA** | transfer DNA |
| **Tak-1/2** | Tagaragaike-1/2 |
| **ta-siRNA** | transacting short interfering RNA |
| **UTR** | untranslated region |

# Chapter 1 – Introduction

At all stages of a plant's life cycle, developmental processes must be tightly controlled to ensure developmental progression. This relies on complex genetic networks that are in place to integrate endogenous cues and external environmental information. These networks consist of different layers of regulation that interact with each other, for example through feedback loops, to create stable molecular responses.

## 1.1. miRNAs are highly conserved post-transcriptional regulators of plant development

The expression of genes in specific timely and spatial patterns during plant development is controlled by different mechanisms. Transcription factors are activators or inhibitors of gene expression and are themselves being regulated transcriptionally, post-transcriptionally or post-translationally (Liu, White and Macrae, 1999; Gill, 2003). A post-transcriptional mechanism by which some transcription factors and a variety of other genes are regulated, is through the activity of small non-coding RNAs (snRNAs) (Samad *et al.*, 2017). snRNAs function based on sequence specificity and complementarity to their target genes, whose activity they control post-transcriptionally through initiation of mRNA cleavage or translational inhibition (Axtell, 2013). Besides short interfering RNAs (siRNAs), microRNAs (miRNAs) represent the most important class of snRNAs in the regulation of plant developmental processes (Bonnet, Van De Peer and Rouzé, 2006; Chen, 2012). miRNAs are conserved post-transcriptional regulators of gene expression not only in plants but also in metazoans (He and Hannon, 2004; Tétreault and De Guire, 2013). In fact, miRNAs were first discovered in *Caenorhabditis elegans*, where the *lin-4* miRNA was identified to control larval developmental transitions in the nematode (Feinbaum, Ambros and Lee, 2004). Plant and animal miRNAs share similarities, but there are substantial differences in their processing pathways and modes of action (Axtell, Westholm and Lai, 2011). For example, while animal miRNAs mainly regulate their target genes by

translational repression, plant miRNAs predominantly initiate mRNA cleavage to inhibit the expression of their target genes (Iwakawa and Tomari, 2015). The processing of both animal and plant miRNAs requires the activity of endoribonucleases; while animal miRNA precursors are cleaved by Dicer and Drosha proteins, plant miRNAs are processed by DICER-LIKE 1 (DCL1) proteins (Millar and Waterhouse, 2005). Whether plant and animal miRNAs have evolved from a common ancestor or are the result of convergent evolution remains unclear (Moran *et al.*, 2017). Either possibility highlights the crucial existence of miRNAs in controlling eukaryotic gene regulation.

Seven plant miRNAs, together with their target genes, are highly conserved among different land plant lineages, including the late divergent angiosperms (flowering plants) and the early divergent bryophytes: miR160, miR166, miR171, miR319, miR390, miR156/529 and miR408 (Axtell and Bowman, 2008; Lin and Bowman, 2018). Conserved miRNAs tend to be more highly expressed in plant tissues than non-conserved miRNAs, which are usually low-abundant (Willmann and Poethig, 2007). Furthermore, they tend to control central developmental processes of ancestral origin, for example dorsoventral patterning, phase change control, secondary metabolism and cell cycle progression, and ubiquitous processes of growth and cell differentiation through the activity of *HOMEODOMAIN-LEUCIN ZIPPER CLASS III* (*HD-ZIP III*), *SQUAMOSA PROMOTER BINDING PROTEIN-LIKE* (*SPL*), *MYB* and *AUXIN RESPONSE FACTOR* (*ARF*) transcription factors, respectively (Jin and Martin, 1999; Chandler, 2016; Tsuzuki *et al.*, 2016). This suggests that certain miRNA functions might have been crucial for the colonialization of the terrestrial environment (Floyd and Bowman, 2007).

### 1.1.1. miRNAs control the formation of rooting structures

The evolution of rooting structures in plants was crucial for the colonialization of the terrestrial environment (Kenrick and Crane, 1997). Rooting structures provide anchorage in the ground and regulate water and nutrient uptake. Different rooting structures develop different architectures, ranging from single-celled filamentous rhizoids in bryophytes (Bowman *et al.*, 2017) to complex roots consisting of various specialised cell types in vascular plants (Dolan *et al.*, 1993). Through interaction with the soil environment, roots perceive and integrate abiotic information, which dictates their spatial organisation for ideal resource acquisition. The differentiation and morphogenesis of cells and tissues with rooting function is thereby carefully coordinated. It involves the activity of miRNAs and their target genes, many of which are transcription factors (Khan and Hartmann, 2011). These regulatory units are often self-controlled and self-reinforcing through negative feedback loops to create precise and stable patterns of gene expression.

#### 1.1.1.1. Different miRNAs control the development of complex roots in vascular plants

Dicotyledonous vascular plants like *A. thaliana* form primary roots that emerge from the seedling and produce lateral roots to increase the surface area for water and nutrient uptake. The primary root consists of specialised tissues, which are generated from the root apical meristem. They form the epidermis, cortex, endodermis and pericycle, which surround the central vascular cylinder in a radial pattern (Ueda, Koshino-Kimura and Okada, 2005). The embryonic root is derived from the uppermost suspensor cell of the embryo. MiRNA activity is pivotal for this developmental step, as evident by the fact that mutants of *SERRATE* (*SE*), a core promoter of miRNA biogenesis, are embryonic lethal (Prigge and Ry Wagner, 2001). Insufficient accumulation of miR165/166 in *se* mutants fails to restrict the expression of HD-Zip III transcription factors *PHABULOSA* (*PHB*) and *PHAVOLUTA* (*PHV*) to specific

domains, compromising embryo viability and correct embryonic root development (Grigg *et al.*, 2005). During post-embryonic root development, the conserved miR160 miRNA inhibits auxin response factors *ARF10*, *ARF16* and *ARF17* to regulate root growth and gravitropism by restricting cell divisions and promoting cell elongation and differentiation (Wang *et al.*, 2005). The differentiation of the functional cell layers of the root is controlled through a complex signalling cascade involving the *SHORTROOT* (*SHR*) and *SCARECROW* (*SCR*) transcription factors and miR165/166 members. Cell-to-cell movement and communication of the components in a regulatory loop ensure correct radial patterning of the root layers (Carlsbecker *et al.*, 2010). The pericycle layer of the root can develop founder cells, from which lateral roots are initiated. This process is positively regulated by auxin, which promotes cell divisions in the pericycle (Fukaki, Okushima and Tasaka, 2007). In response to auxin, miR164 negatively regulates lateral root initiation by repressing the *NAC1* transcription factor. On the other hand, miR160 has a positive influence on lateral root development by controlling lateral root density through repression of *ARF16* (Wang *et al.*, 2005). Proper growth of lateral roots is controlled through miR390, which produces ta-siRNAs to restrict *ARF2*, *ARF3* and *ARF4* levels in the newly initiated lateral root primordium. In addition to lateral roots, several monocot species like *Oryza sativa* produce adventitious roots, which emerge from the stem. This process involves the partly conserved activity of auxin-sensitive miRNAs (Meng *et al.*, 2009). Ultimately, miRNAs are also involved in the integration of environmental stresses to adapt root growth (Couzigou and Combier, 2016), and in the formation of nitrogen-fixing nodules when establishing symbioses with *Rhizobium* bacteria (Simon, Meyers and Sherrier, 2009).

#### 1.1.1.2. The FEW RHIZOIDS 1 (FRH1) miRNA controls rhizoid differentiation in liverworts

To maximise the surface area for water and nutrient uptake, specialised epidermal cells in the roots of vascular plants bulge out and elongate into root hairs (Datta *et al.*, 2011). In *A. thaliana*, *Oryza sativa* and *Brachypodium distachyon*, this process was shown to be dependent on the activity of *ROOT HAIR DEFECTIVE6-LIKE* (*RSL*) bHLH transcription factors (Menand *et al.*, 2007; Zalewski *et al.*, 2013; Kim and Dolan, 2016). *RSL1* genes are ancestral regulators in the networks controlling the development of filamentous rooting structures (Pires *et al.*, 2013). While promoting root hair differentiation in vascular plants, *RSL1* genes promote the differentiation of single-celled rhizoids, which are rooting structures in bryophytes, in *P. patens* and *M. polymorpha* (Menand *et al.*, 2007; Proust *et al.*, 2016). Root hairs and rhizoids are analogous structures with rooting function and are both initiated from single epidermal precursor cells, in which *RSL1* is expressed. While the *GLABRA 2* (*GL2*) transcription factor suppresses At*RSL1* expression in non-root hair cells in the angiosperm *A. thaliana* (Lin *et al.*, 2015), Mp*RSL1* expression is restricted to rhizoid precursor cells by the Mp*FRH1* miRNA in the liverwort *M. polymorpha* (Honkanen *et al.*, 2018, internal communications). Throughout the liverworts, *FRH1* target sites are conserved in *RSL1* genes, whereas they are absent in other land plants. This indicates the evolution of independent regulatory pathways upstream of *RSL1*, a conserved master regulator, to control rooting function in land plants. Mp*rsl1* loss of function and Mp$FRH1^{GOF}$ gain of function mutants both form fewer rhizoids compared to wild type, suggesting opposite functions (Proust *et al.*, 2016; Honkanen, Thamm, Arteaga-Vazquez, *et al.*, 2018). Also, fewer gemmae (asexual propagules of *M. polymorpha*) and no mucilage papillae develop upon loss of Mp*RSL1* or gain of Mp*FRH1* function. On the contrary, when over-expressed, Mp*RSL1* causes the formation of supernumerary rhizoids but not gemmae or mucilage papillae in the Mp$RSL1^{GOF}$ mutant. These phenotypes indicate firstly that Mp*RSL1*

positively controls the outgrowth of specialised structures from epidermal cells, and secondly that Mp*RSL1* is required and sufficient for the initiation of rhizoids, but likely not sufficient for mucilage papillae and gemma formation. Consistent with this, Mp*RSL1* is expressed in epidermal cells that give rise to specialised epidermal structures. Likewise, Mp*FRH1* is expressed in these cells, where it regulates Mp*RSL1* activity under a negative feedback loop – although Mp*RSL1* mRNA levels were lower in Mp$FRH1^{GOF}$ mutants compared to wild type, Mp*FRH1* levels were also lower in Mp*rsl1* mutants than wild type and higher in Mp$RSL1^{GOF}$ mutants (Honkanen *et al.*, 2018). Finally, the post-transcriptional regulatory mechanism by which Mp*FRH1* represses Mp*RSL1* activity, is cleavage of the Mp*RSL1* mRNA, as confirmed by 5'RLM-RACE PCR. *FRH1* target sites are only conserved in liverwort *RSL1* genes, but not in other land plants. This demonstrates that an independent miRNA-mediated mechanism of *RSL1* regulation has evolved to control rooting function in liverworts. Furthermore, it provides an example of a non-conserved miRNA that has evolved to fulfil a crucial function in a specific land plant lineage, which is a common evolutionary trend in land plants (Axtell and Bowman, 2008).

### 1.1.2. miRNAs control developmental phase changes in flowering plants

miRNAs were first discovered in the process of phase change in the nematode *C. elegans*, where the *lin-4* and *let-7* miRNAs control the developmental timing of larval transitions (Reinhart *et al.*, 2000; Feinbaum, Ambros and Lee, 2004). Plants equally undergo developmental transitions as they mature (Poethig, 2003). As the seedling passes through juvenile vegetative growth, it is not competent to reproduce. Upon entering the adult vegetative phase, the plant becomes responsive to floral inductive signals. Flowering marks the transition to reproductive growth, which is triggered by photoperiod and different light qualities. Only adult, not juvenile plants, are capable of initiating flowering when exposed to these triggers (Bäurle and Dean, 2006). The juvenile and adult phases are morphologically

distinguishable – while juvenile leaves have trichomes only on the adaxial surface, adult leaves become competent to also form abaxial trichomes (Telfer and Poethig, 1998). The juvenile developmental phase is promoted by members of the miRNA156 family, which are highly conserved among angiosperms (Morea *et al.*, 2016). miR156 is highly expressed in juvenile leaves, where it represses members of the *SPL* family of transcription factors. Over-expression of miR156 prolongs the juvenile phase and delays the vegetative transition in *A. thaliana* and maize (G. Wu and Poethig, 2006; Chuck, Meeley, *et al.*, 2007). In successive leaf primordia, miR156 levels decrease to allow accumulation of SPL protein (He *et al.*, 2018). This gradually enables the expression of adult traits in later rosette leaves and provides competence to the shoot apical meristem to respond to floral inducers. Like the vegetative transition, the reproductive transition is under control of miR156/SPL modules. Induction of flowering depends on the activation of miR172 by *SPL* transcription factors, mainly *SPL9* and *SPL15*, as miR156 levels decrease. Gain of function mutations in *SPL9* and *SPL15*, like over-expression of miR172, shorten the vegetative phase and accelerate flowering. Both transcription factors directly bind to the promoter of *MIR172*. miR172 miRNAs activate flowering by targeting *APETALA 2*-like (*AP2*-like) transcription factors, which are repressors of the floral transition (Aukerman and Sakai, 2003). Additionally, *SPL* and *AP2*-like genes promote expression of their repressors miR156 and miR172. Taken together, opposite expression patterns of miR156 and miR172 are central to the ageing pathway that negatively influences the reproductive transition in flowering plants (Figure 1.1). Negative feedback regulations with their respective target genes contribute to the stability of the floral transition.


**Figure 1.1: The ageing pathway regulates flowering through miR156 and miR172 in *A. thaliana***. from (Wang and Wang, 2015) – miR156 expression is high in the seedling and declines as the plant ages. Because miR156 functions in repressing *SPL* target genes, SPL protein accumulates until a certain threshold is reached that triggers flowering. *SPL* transcription factors directly promote the expression of floral inducers and miR172. Levels of miR172 therefore increase as the plant ages, in an opposite manner to miR156. miR172 targets and represses AP2-like genes, which are inhibitors of floral integrators that activate flowering.

#### 1.1.2.1. The miR156/SPL module is a core regulator of vegetative and reproductive phase changes in flowering plants

The *SPL* family of transcription factors takes up fundamental roles in controlling plant growth and development, including vegetative and reproductive phase transitions (Xu *et al.*, 2016). SPL proteins contain a highly conserved SBP domain of 76 amino acids, which is involved in nuclear import and sequence-specific DNA binding (Cardon *et al.*, 1999; Preston and Hileman, 2013). Many *SPL* genes are under negative regulation of members of the miR156 family. Together, they control developmental phase changes and the expression of the reproductive phase (Fornara and Coupland, 2009). In order to activate phase changes, the expression of partly redundant *SPL* genes must exceed a certain threshold, which is set by the activity of miR156 (Xu *et al.*, 2016; He *et al.*, 2018). Thereby, miR156-mediated translational inhibition and transcript cleavage confer different miR156-sensitivity to different *SPL* members. In *A. thaliana*, the transition from juvenile to adult vegetative development is primarily controlled by At*SPL9*, At*SPL13* and At*SPL15*, which also control the transition to flowering together with At*SPL2/10/11* and At*SPL3/4/5*, some of which

interact directly with floral integrators (Xu *et al.*, 2016). Unlike its paralog At*SPL9*, At*SPL15* has a stronger effect on flowering in short days than in long days (Hyun *et al.*, 2016). It is active in the SAM earlier before the floral transition than At*SPL9* in conferring floral primordium identity. Under non-inductive conditions, gibberellic acid activates At*SPL15* to initiate flowering, similar to activation of At*SPL3*/*4*/*5* (Jung *et al.*, 2012). This demonstrates that although many members of the At*SPL* gene family function redundantly, there has been functional diversification to control the floral transition in both short day and long day. miR156/SPL modules are universal in developmental regulation among land plants and some representative regulators have been described in different angiosperms as summarised in the following.

The *Corngrass1* (*Cg1*) mutant in maize ectopically overexpresses *zma-miR156*, which results in the production of more leaves with juvenile identity, late flowering and abnormal florescence architecture. Like miR156 in *A. thaliana*, the expression of *zma-miR156* is highest during the juvenile vegetative phase and decreases with age. Among at least 13 target genes of *zma-miR156* is *teosinte glume architecture1* (*tga1*), which is target gene of *Cg1* and has highest similarity to At*SPL13* (Chuck, Cigan, *et al.*, 2007). Another SBP-box gene and target of *zma-miR156* in maize is *tasselheath4* (*tsh4*), which is required for the initiation and maintenance of branch meristems (Chuck *et al.*, 2010).

The flowering plant *Antirrhinum majus* encodes two genes that are similar to At*SPL3/4/5*, namely Am*SBP1* and Am*SBP2*. Their expressions increase with inflorescence development, during which they positively regulate floral promoter genes (Preston and Hileman, 2010).

In rice, 11 putative Os*miR156*-targeted Os*SPL* genes were identified. Among other phenotypes, overexpression of Os*MIR156* genes resulted in delayed flowering (Xie, Wu and

Xiong, 2006). Overexpression of Os*SPL14* on the other hand increased panicle branching and grain yield (Miura *et al.*, 2010). Both observations indicate that the function of Os*SPL14* in flower development and timing of the reproductive transition is conserved with the function of At*SPL* genes.

In barley, seven miR156-targeted *SPL* genes were identified, which have higher transcript levels in the reproductive than in the vegetative phase. Together with an antagonistic expression pattern of miR156 and miR172 during vegetative and reproductive development, this argues for conservation of the ageing pathway to control the reproductive phase transition in barley (Tripathi, Bregitzer and Singh, 2018).

SBP-box genes and their miR156 regulators were also identified in tomato. Sly*SBP* gene expression was detected in young inflorescences and during fruit development, which suggests that they control reproductive growth (Salinas *et al.*, 2011).

These examples demonstrate that miR156/SPL modules are well-conserved among different angiosperm species, where they control phase transitions and diverse aspects of reproductive development.

#### 1.1.2.2. The miR56/SPL module in the moss *P. patens* plays the opposite role of the angiosperm miR156/SPL module

The regulatory interactions between miR156 and *SPL* genes not only control phase changes in vascular plants but also in the moss *P. patens*. There, the miR156/SPL module regulates the transition from filamentous protonemal growth to the production of leafy gametophores (Cho, Coruh and Axtell, 2012a). Contrary to the inhibitory role of miR156 in flowering plant phase transitions, miR156 promotes the reproductive transition in moss – miR156 levels reach their maximum in the intermediate bud stage between protonema and gametophore. When a *MIM156* target mimic transgene was used to reduce miR156 function, bud initiation was delayed. Furthermore, fewer leafy buds and subsequent gametophores were formed.

miR156 targets three SBP-domain proteins in *P. patens* – SBP3, SBP6 and SBP13. A null mutant of *sbp3* showed the opposite phenotype of the *MIM156* transgenic line: more leafy buds were initiated than in wild type upon loss of *sbp3* function. While controlling the same process of reproductive phase transition, miR156 and SPL genes have opposite expression patterns in moss and in angiosperms. Taken together, these observations show that although the regulatory interaction between miR156 and *SPL* genes is ubiquitous in land plants, it has been modified to function differently in different species. It remains to be determined whether the miR156/SPL expression pattern from *P. patens* is the same among other bryophytes or whether it is specific for moss.

## 1.2. Mature miRNAs are generated in a complex biogenesis pathway in *A. thaliana*

miRNAs are encoded by MIR genes, which, in plants, are mainly independent transcriptional units (Rogers and Chen, 2013). The approx. 70-190 bp-long primary miRNA (pri-miRNA) transcript folds and forms a stem-loop, which contains the 21 nt-long miRNA sequence. This sequence is complementary to part of the mRNA sequence of a target gene. After excision from the stem-loop, the mature miRNA will post-transcriptionally regulate the expression of that target gene. The stepwise processing of pri-miRNAs into precursor miRNAs (pre-miRNAs) and eventually into mature miRNAs is realised by an extensive machinery of enzymes and RNA-binding proteins (Figure 1.2) (Wang, Mei and Ren, 2019). It takes place primarily in the nucleus, whereby the assembled multi-protein complexes can be visually identified as so-called Dicing bodies (Fang and Spector, 2007). After excision from its double-stranded precursor, the short miRNA duplex, consisting of the guide (miRNA) and the passenger (miRNA*) strands, is vulnerable to degradation. 3'-end-methylation provides protection until incorporation of the miRNA guide strand into the RNA-INDUCED SILENCING COMPLEX (RISC), while the miRNA* strand is degraded

(Yu *et al.*, 2005). Core components of the RISC are AGO proteins, which function as RNA slicers (Baumberger and Baulcombe, 2005). According to recent findings, RISC assembly takes place in both the nucleus and the cytoplasm – there is evidence for nucleo-cytosolic shutting of an AGO1:miRNA complex (Figure 1.2B) (Bologna *et al.*, 2018), as well as evidence showing higher accumulation of mature miRNAs in the cytoplasm than in the nucleus (Park *et al.*, 2005). Both scenarios involve the nuclear export of protein complexes or miRNAs to the cytoplasm, where miRNAs exert their functions. Through (nearly) complete base pair complementarity, they identify their target mRNAs and trigger either mRNA cleavage through AGO activity or translational inhibition through the RISC (Axtell, Westholm and Lai, 2011; Iwakawa and Tomari, 2015). While translational inhibition is the main target gene silencing mechanism in animals, transcript cleavage is in plants (Axtell, Westholm and Lai, 2011). Despite the discovery and characterisation of numerous regulators of the plant miRNA processing pathway (see Thesis Chapter 2.3.1 for a more detailed description), certain aspects of miRNA biogenesis have not been fully elucidated and require further investigation. Included in this are the precise mechanisms of nucleo-cytosolic transport of miRNAs, and regulators that determine the occurrence of transcript cleavage versus translational inhibition.

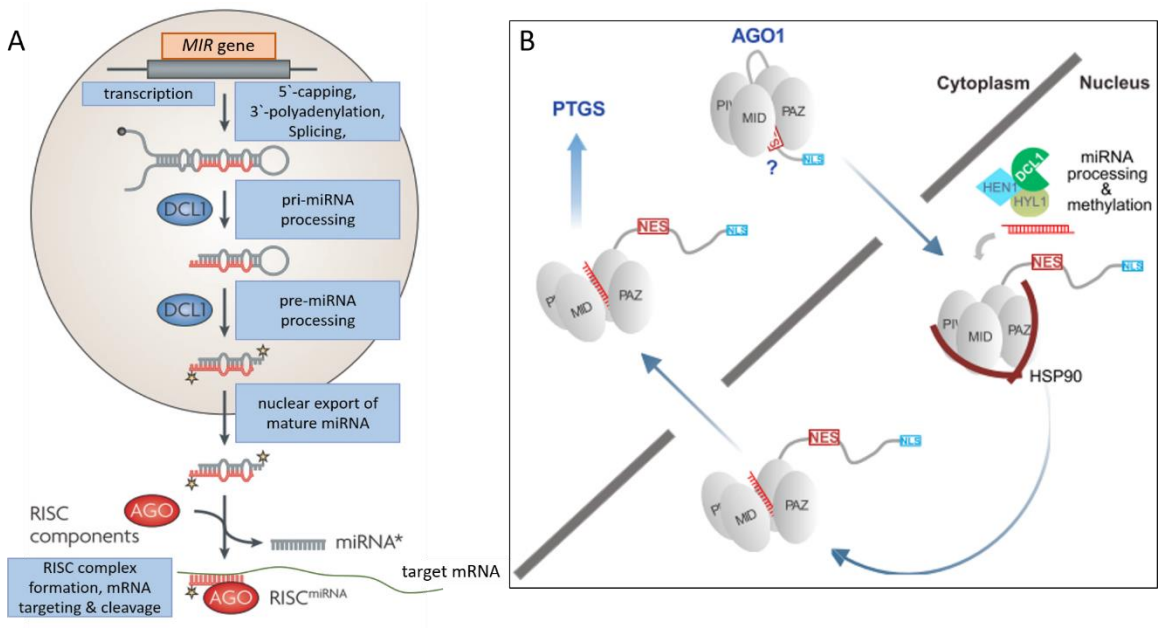


**Figure 1.2: miRNA biogenesis and action in plants.** (A) schematic of the canonical plant miRNA biogenesis pathway from Chapman and Carrington, 2007. (B) modified schematic model of nucleo-cytoplasmic AGO1:miRNA shuttling from Bologna *et al.*, 2018. HEN1 = HUA-ENHANCER 1, HYL1 = HYPONASTIC LEAVES 1, HSP90 = HEAT SHOCK PROTEIN 90, a more detailed description of miRNA biogenesis regulators is presented in Thesis Chapter 2.3.1.

### 1.2.1. DCL1 occupies a central position in plant miRNA biogenesis pathways

The processing of 70-190 nt-long pri-miRNAs into 21 nt-short mature miRNAs takes place in the Dicing complex (Reinhart *et al.*, 2002; Achkar, Cambiagno and Manavella, 2016). Core of this complex forms the endoribonuclease DCL1. Already during transcription, the processing complex assembles while the Elongator complex bridges the association of RNA polymerase II with DCL1 and other dsRNA-binding proteins like SERRATE (SE) (Fang, Cui, *et al.*, 2015). Co-transcriptional occurrence of miRNA processing is supported by the observation that DCL1 and pri-miRNAs associate with the chromatin of *MIR* genes. While assisted by numerous proteins, most importantly SE and HYL1, DCL1 cleaves the double-stranded pri-miRNA in two steps (Iwata *et al.*, 2013). This generates a precursor miRNA

(pre-miRNA) and eventually a short miRNA duplex. This duplex contains the guide miRNA strand that is complementary to the miRNA target gene, and the passenger miRNA* strand. The significant reduction of miRNA abundance in At*dcl1* mutants compared to wild type demonstrates that *DCL1* is essential for the biogenesis of mature miRNAs (Reinhart *et al.*, 2002). Consequently, severe developmental defects in *dcl1* mutants stem from over-expression of genes that are normally under miRNA control (Schauer *et al.*, 2002). The function of *DCL1* in miRNA processing is conserved in many land plants (Margis *et al.*, 2006). miRNA reduction and the resulting increase in target gene mRNA abundance, which are hallmarks *dcl1* mutants, have been demonstrated in rice, soybean, common bean, maize and moss, as summarised in the following paragraphs.

*Oryza sativa* encodes four *DCL* orthologs. According to (Liu *et al.*, 2005), Os*DCL2* and Os*DCL3* are orthologs of At*DCL3*, while Os*DCL1* is most similar to At*DCL1* and At*DCL2*. Os*DCL4* is orthologous to At*DCL4* and processes siRNAs. Through RNA interference (RNAi), the expression of Os*DCL1* was silenced to study the function of the Os*DCL1* gene. RNAi silencing of Os*DCL1* led to reduced accumulation of numerous miRNAs in leaf tissue, as detected by northern blot. Os*dcl1* mutants developed overall shoot and root abnormalities like a dark green colour and dwarfism (Liu et al. 2005). Narrow rolled leaves and reduced root elongation were characteristic, as well as fewer adventitious roots. Adaxial/abaxial leaf polarity defects were speculated to have arisen due to reduced levels of miR165/miR166, because similar phenotypes were observed in transgenic plants with reduced HD-Zip III target gene accumulation in maize and *Arabidopsis* (Schauer *et al.*, 2002; Thompson *et al.*, 2014).

RNAi silencing was also applied to investigate the role of Pv*DCL1*, At*DCL1* ortholog of the common bean *Phaseolus vulgaris* (Valdés-López *et al.*, 2008), in phosphate

starvation. As a consequence of reduced Pv*DCL1* mRNA abundance, different miRNAs accumulated at higher levels in partial Pv*dcl1* loss of function mutants than in wild type. Silencing of Pv*DCL1* had a negative effect on miR399 accumulation, but a positive effect on mRNA abundance of the Pv*PHT1* target gene.

*Glycine max* (soybean) encodes two functional Gm*DCL1* paralogs, Gm*DCL1a* and Gm*DCL1b* (Curtin *et al.*, 2016). To study their roles in miRNA processing, loss of function Gm*dcl1a* and Gm*dcl1b* alleles were generated by a zinc finger nuclease. The observations that Gm*DCL1a* and Gm*DCL1b* mRNA localisation patterns overlapped widely, and that neither the Gm*dcl1a* nor the Gm*dcl1b* single mutant expressed any defective phenotypes, indicates functional redundancy of the paralogs. However, Gm*dcl1a dcl1b* double mutants were embryonic lethal, only few seeds germinated. Consistently, while miRNA accumulation was only minorly reduced in the single mutants, a global reduction in mature miRNA levels was detected in Gm*dcl1a dcl1b* double mutants. This resulted primarily in the inability of the shoot apical meristem to differentiate. The small Gm*dcl1a dcl1b* seedling did therefore neither initiate radial root growth, nor leaves. Furthermore, the short stem of the seedling grew wavy because of lopsided differentiation of the vascular tissue.

Like soybean, the moss *Physcomitrella patens* encodes two *DCL1* genes, Pp*DCL1a* and Pp*DCL1b*. However, these two paralogs take up very distinct functional roles in the miRNA pathway – while Pp*DCL1a* functions in miRNA processing like At*DCL1*, Pp*DCL1b* is only involved in the miRNA-directed target mRNA cleavage step (Khraiwesh, M. Asif Arif, *et al.*, 2010). Loss of Pp*DCL1a* function reduced the accumulation of miRNAs drastically. At the same time, target gene mRNA levels were increased in Pp*dcl1a* mutants compared to wild type. While Pp*dcl1b* mutants developed strong developmental defects like Pp*dcl1a*, this was not explained by a decrease in miRNA abundance. Furthermore, mRNAs of miRNA target genes were not cleaved in Pp*dcl1b*, but instead these genes were hyper-

methylated and lowly expressed. Therefore, it was hypothesised that Pp*DCL1b* might be required for loading of miRNAs into the RNA-Induced Silencing Complex (RISC). If not associated with the RISC, miRNAs would be loaded into an RNA-Induced Transcript Silencing (RITS) complex that induces methylation. Both Pp*dcl1a* and Pp*dcl1b* mutants suffered defects in cell differentiation, size and shape, as well as growth polarity during vegetative protonemal development. In addition, Pp*dcl1a* mutants were more strongly retarded in growth than Pp*dcl1b*, and unable to form leafy stems. This developmental arrest could sometimes be overcome in Pp*dcl1b*, which developed malformed leafy stems, but were sterile (Khraiwesh *et al.*, 2010). Pp*DCL1* is therefore required for the reproductive phase transition in moss.

Among the five *DCL* genes identified in *Zea mays*, there is one ortholog of Zm*DCL1*, Zm*DCL2* and Zm*DCL4* each, while there are two copies of Zm*DCL3* – Zm*DCL3a* and Zm*DCL3b* (Qian and Cheng, 2011). In the Zm*dcl1* mutant *fuzzy tassel* (*fzt*), approximately 50 % of all miRNAs were differentially expressed compared to wild type (Thompson *et al.*, 2014). In about half of these cases, a decrease in mature miRNAs coincided with an increase in miRNA precursor expression. Transcriptome sequencing and qRT-PCR analyses independently confirmed that most predicted and conserved miRNA target genes like *ARF*, MYB-domain and AP2-domain transcription factors, as well as F-box genes were increased in *fzt* mutants. The causative SNP in exon 17 of the RNase III domain produced pleiotropic defective phenotypes in the *fzt* mutant – mutant plants had a short habitus and fewer leaves with mild polarity defects, which were also smaller due to fewer but bigger cells. *fzt* mutants were also severely affected in the development of floral organs, which resulted in complete sterility. Fewer inflorescence branches were formed and sex determination was defective, two phenotypes that likely underly misexpression of miR172 (Chuck, Meeley, *et al.*, 2007). As in At*DCL1* (Schauer *et al.*, 2002), the dsRNA-binding domain of Zm*DCL1* seems to be

crucial for protein function, because another *fzt* mutant, which lacks the last 39 aa due to a premature STOP codon in exon 19, was sterile as well. In other alleles, mutations in exon 1 caused embryo lethality.

Overall, the loss of *DCL1* functions caused pleiotropic developmental defects in angiosperms as well as bryophytes, ranging from growth retardation to organ polarity defects and compromised phase transition, to sterility and embryo lethality. Through miRNA processing, *DCL1* is therefore a conserved regulator of plant growth and development in the vascular and the non-vascular land plants.

#### 1.2.1.1. Mutations in functional domains of At*DCL1* cause pleiotropic developmental defects

DCL proteins are complex enzymes that catalyse the processing of different types of small non-coding RNAs through endonucleolytic cleavage of RNA precursor transcripts (Liu, Feng and Zhu, 2009). Members of the DCL protein family generally contain the following functional domains: a N-terminal RNA helicase domain, a domain of unknown function, a PAZ (Piwi/Argonaute/Zwille) domain, two ribonuclease III (RNase III) domains, and at least one double-stranded RNA-binding (dsRNA-binding) domain at the C-terminus. DCL1 cleaves pri-miRNAs to generate mature miRNAs, which are essential developmental regulators in plants. T-DNA insertions and other mutations in the functional *DCL1* domains have produced different At*dcl1* alleles with various developmental defects in *A. thaliana* (Schauer et al. 2002, Figure 1.3):

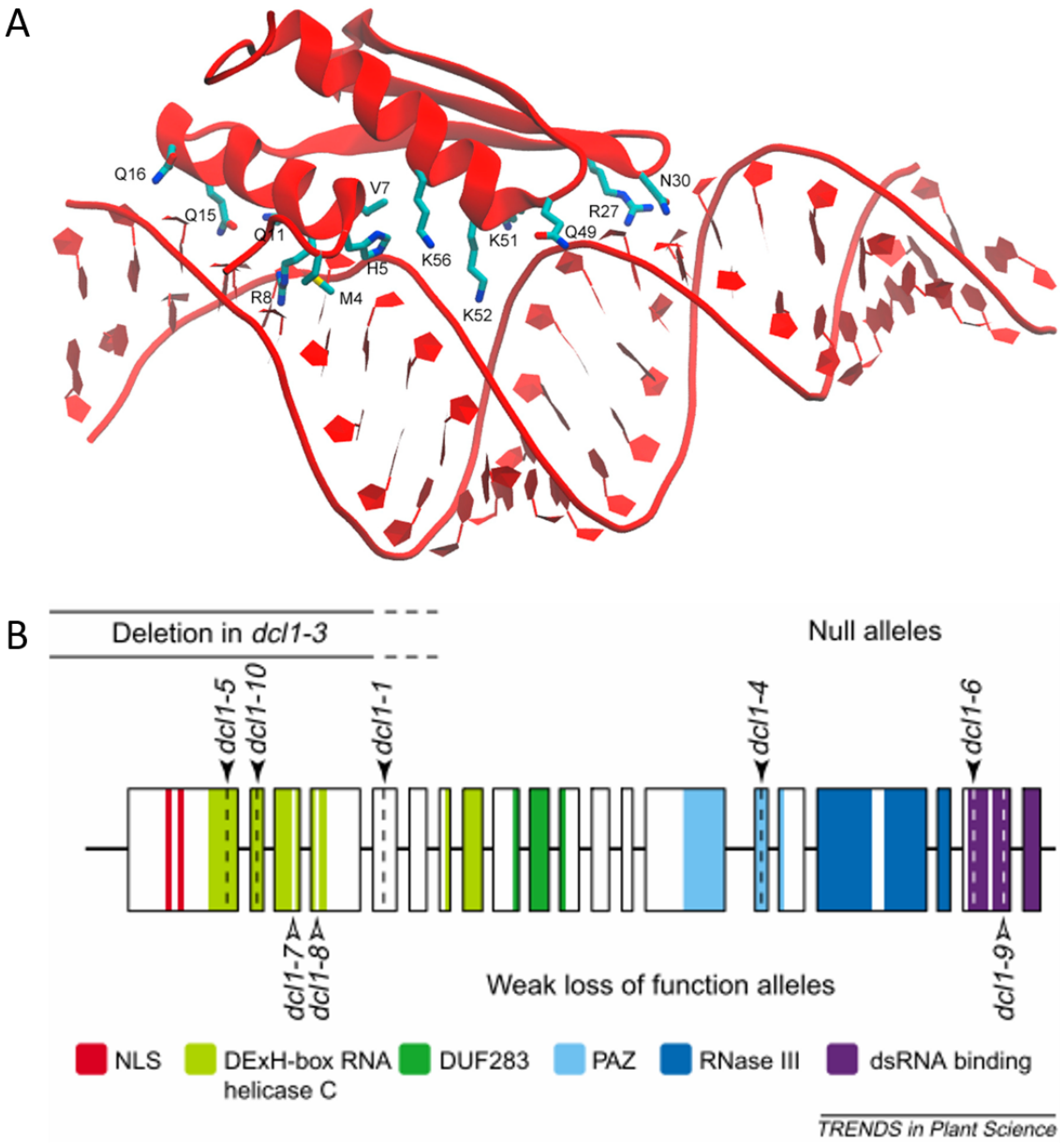


C

| Mutant allele | | Lesion | Position |
|---|---|---|---|
| New name | Old names | | |
| *dcl1-1* | *emb76-1, sus1-1* | T-DNA insert | RNA helicase domain (exon 5) |
| *dcl1-2* | *emb76-2, sus1-2* | Unknown | Unlinked T-DNA insert |
| *dcl1-3* | *emb60, sus1-3* | >20 kb deletion | Removes 5′ end of the ORF |
| *dcl1-4* | *sus1-4* | T-DNA insert | PAZ domain (exon 15) |
| *dcl1-5* | *sus1-5* | T-DNA insert | RNA-helicase domain (exon 1) |
| *dcl1-6* | *sus1-6* | T-DNA insert | First dsRNA-binding domain (exon 19) |
| *dcl1-7* | *sin1-1* | P415S | RNA-helicase domain (exon 3) |
| *dcl1-8* | *sin1-2* | I431K | RNA-helicase domain (exon 4) |
| *dcl1-9* | *caf-1* | T-DNA insert | Second dsRNA-binding domain (exon 19) |
| dcl1-10 | sus1-7 | T-DNA insert | RNA-helicase domain (exon 2) |

**Figure 1.3: Various At*dcl1* mutant alleles were generated and described to elucidate the pleiotropic functions of the complex At*DCL1* enzyme.** From Drusin *et al.*, 2016 – (A) Structure of the AtDCL1 dsRNA-binding domain in complex with dsRNA, main

residues interacting with dsRNA are shown. From Schauer *et al.*, 2002 – (B) Organisation of functional domains and exon-intron structure of the genomic locus encoding At*DCL1*, positions of mutations in different weak At*dcl1* mutants are indicated. (C) Summary of At*dcl1* mutant alleles.

Point mutations in the RNA helicase domain of *DCL1*, which likely inhibit RNA substrate binding, cause defects in female reproductive organ development in the *short integument-1* (*sin-1* or *dcl1-7*) mutant (Robinson-Beers, Pruitt and Gasser, 1992; Schauer *et al.*, 2002, Figure 1.3). Because of defective ovules, *sin-1* mutants are sterile. Furthermore, they flower late and produce many more rosette leaves than wild type (Ray *et al.*, 1996). Since *sin-1* mutants respond to exogenous application of gibberellic acid and to different day lengths, their delayed flowering cannot be explained by defects in the integration of these two flowering determinants. Instead, it was suggested that a defect in the expression of meristem identity genes underlies the late flowering phenotype of *sin-1* (Schauer *et al.*, 2013).

Disruption of the RNA helicase domain by a T-DNA insertion causes even more severe defects in the *suspensor-1* (*sus-1* or *dcl1-5*) mutant of At*DCL1* (Figure 1.3). This mutant, like other *sus-1* null alleles with T-DNA insertions in the PAZ and dsRNA-binding domains, is developmentally arrested at the embryo stage (Schauer et al. 2002). Abnormal cell divisions from the embryonic heart stage on result in an abnormally large suspensor, which is developmentally arrested (Schwartz, Yeung and Meinke, 1994).

Another T-DNA mutant allele affected in the dsRNA-binding domain, is *carpel factory-1* (*caf-1* or *dcl1-9*). A premature STOP codon generated close to the C-terminus of the protein sequence, deleted the last 73 amino acids and therefore presumably the second dsRNA-binding domain (Steven E. Jacobsen, Running and Meyerowitz, 1999, Figure 1.3). While

the likely loss of both dsRNA-binding domains in *sus-1* causes embryo lethality, presence of at least the first dsRNA-binding domain in *caf-1* allows proper embryogenesis (Schauer et al. 2002). Nevertheless, *caf-1* plants express severe pleiotropic developmental defects, which was explained by dsRNA-binding domains being responsible for the recognition of diverse pri-miRNA substrates as well as the positioning of the cleavage sites (Kurihara and Watanabe, 2004; Suarez *et al.*, 2015; Drusin *et al.*, 2016, Figure 1.3A). The *caf-1* mutant has derived its name from the production of supernumerary carpels and stamens. Those multiple carpels are sterile and do not fuse, while a wild type flower consists of two fused carpels. Also leaf morphology is altered in *caf-1* – in the young seedling, which is overall smaller, cotyledons and rosette leaves are thinner. In older leaves, filamentous structures sometimes replace part of the leaf blade. Finally, *caf-1* mutants almost never produce secondary meristems. Altogether, inferred from phenotypic analysis of the *caf-1* mutant allele, it has been proposed that At*DCL1* controls cell divisions and floral meristem proliferation.

Taken together, these mutant alleles outline the multitude of morphological and developmental processes that are regulated by At*DCL1*, including embryogenesis, ovule development, meristem determinacy and leaf morphology. Furthermore, it was found that in embryo-defective At*dcl1* individuals, the underlying At*dcl1* mutation that causes lethality was transmitted maternally (Golden *et al.*, 2002). It was highlighted that the helicase domain (supported by biochemical models) and dsRNA-binding domains are particularly important for AtDCL1 function (Golden et al. 2002). Targeted mutagenesis of other At*DCL1* domains will reveal their precise functions. It is likely that simultaneous disruption of multiple AtDCL1 domains would inhibit the enzymatic function of AtDCL1 even more severely by globally preventing the processing of miRNAs.

### 1.2.2. HASTY, a nucleocytoplasmic transport protein, controls the processing of miRNAs

Plant miRNAs are processed in the nucleus and exert their functions as mediators of target mRNA cleavage or translational inhibition in the cytoplasm (Park *et al.*, 2005; Bologna *et al.*, 2018b; Wang, Mei and Ren, 2019). Accordingly, mature miRNAs were found to accumulate more highly in the cytoplasm than in the nucleus, primarily as single stranded molecules and presumably protected against degradation through 3'-end methylation and through association with proteins (Park *et al.*, 2005; Ji and Chen, 2012). The mechanisms by which miRNAs leave the nucleus have not fully been elucidated to date. A strong candidate for this role is AtHST. Based on size and amino acid sequence, AtHST is the Arabidopsis importin β-like protein most similar to the mammalian karyopherin Exportin 5 (Exp5) and the yeast ortholog Msn5p, which regulate nucleocytoplasmic transport of proteins and small RNAs, respectively (Bollman *et al.*, 2003; Park *et al.*, 2005). Characteristic for a nucleocytoplasmic transport protein, AtHST was shown to interact with the small GTPase Ran, which drives nuclear transport through nuclear pores. More supporting evidence for the function of the AtHST protein as a nucleocytoplasmic transport receptor was its localisation in close vicinity to the nuclear membrane. At*hst-1* mutants are defective in global organ growth, causing pleiotropic morphological defects. Since this coincides with a reduction in the levels of some miRNAs in At*hst-1*, it suggested that HST might also be involved in the transport of small regulatory RNAs. At*hst-1*, At*hst-6* and At*hst-3* are putative null alleles. While At*hst-3* is affected by a 3 bp deletion in exon 1, defects in At*hst-1* and At*hst-6* are caused by premature stop codons – in At*hst-1*, a premature stop codon resulted from mutation of the conserved GT splice donor site at intron 12, which abolished splicing, while in At*hst-6*, a G to A transition caused a premature stop codon that eliminates 91 % of the full-length protein sequence. Blotting of various mature miRNAs in

the At*hst-1* mutant revealed an overall reduction of miRNA abundance compared to wild type, but only for certain miRNAs and to different extents. For example, At*hst-1* had strongly reduced levels of miR156 in immature rosette leaves but accumulation of miR172 was not affected (Park *et al.*, 2005). Despite an overall reduction of miRNAs in At*hst* mutants, there is no evidence for over-accumulation of miRNAs in the nucleus and miRNA deprivation in the cytoplasm. In the At*hst-3* allele, the mutation in exon 1 blocks the interaction with RAN1, which is crucial for nucleocytoplasmic transport function. It suggests that reduced miRNA levels in At*hst-3* are caused by a transport-related defect, which is consistent with a function of At*HST* in nuclear export. Furthermore, there is the possibility that At*HST* interacts with pre-miRNAs, as does Exp5 (Yi *et al.*, 2003), or mature miRNAs to provide stability. Nevertheless, its exact mechanism remains elusive, since At*HST* is not absolutely required for nuclear miRNA export and there is no evidence for its involvement in siRNA or t-RNA export (Hunter, 2003; Park *et al.*, 2005). In conclusion, At*HST* is important for the processing of certain miRNAs that control plant development. The described data from At*hst* mutant analyses suggest that At*HST* might share miRNA export function with other nucleocytoplasmic transporters and possibly takes up another role in stabilising miRNA intermediates in the nucleus.

#### 1.2.2.1. At*HST* regulates cell growth, specification of organ polarity and developmental phase transitions

At*HST* was discovered in an *A. thaliana* mutagenesis screen for genes that affect the juvenile-to-adult transition during vegetative growth (Telfer and Poethig, 1998). Mutations in *Athst* reduce the duration of the juvenile phase of rosette leaf development, so that adult leaves with trichomes on both the adaxial and the abaxial surfaces (juvenile leaves only develop adaxial trichomes) are produced earlier in At*hst-1* than in wild type. Wild type inflorescence leaves characteristically lose trichomes on their adaxial surface. In At*hst-1*,

conditions that promote flowering cause a more rapid loss of adaxial trichomes on inflorescence leaves than in wild type. At*HST* is therefore required for the expression of juvenile vegetative traits. Another characteristic defect is the upwards-curling and narrow shape of At*hst-1* mutant leaves. This is a phenotype that is also expressed in other core miRNA biogenesis mutants like At*hua enhancer 1* (At*hen1*) and At*hyponastic leaves 1* (At*hyl1)* (Vazquez, Gasciolli and Cre, 2004) and is attributable to misexpression of miR166, miR390 and miR139a (Liu *et al.*, 2011). At*hst-1* mutants not only undergo accelerated vegetative phase change, but also early flowering, the opposite of the delayed flowering phenotype in At*dcl1-7*, At*hen-1* and At*hyl-1* mutants (Ray *et al.*, 1996; Park *et al.*, 2002; Vazquez, Gasciolli and Cre, 2004). To explain this phenotype, Telfer and Poethig, 1998 concluded that At*HST* specifically controls the competence of the shoot to respond to floral meristem identity genes like *LEAFY* (*LF*) and *APETALA-1* (*AP1*). They excluded the possibility that At*HST* influences flowering through the gibberellic acid pathway, which is also involved in the control of flowering. Floral organs in At*hst-1* were smaller but more abundant than wild type, possibly a compensatory effect for the reduced seed set resulting from male and female sterility defects. Other phenotypes of the mutant are a disrupted inflorescence phyllotaxis and an abnormally short hypocotyl and primary root due to reduced root elongation rate and premature cessation of root growth (Bollman *et al.*, 2003). All these phenotypic defects in the likely null mutant At*hst-1* can be attributed to defects in cell growth, specification of organ polarity, and phase change (Bollman *et al.*, 2003). They demonstrate that although the precise function of At*HST* remains to be elucidated, At*HST* is important for plant developmental processes through miRNA processing.

### 1.3 Conserved and non-conserved miRNAs and their target genes were identified in *M. polymorpha*

The functions of miRNAs have been characterised in angiosperms, but few miRNAs have been studied in the early divergent lineages of land plants (Axtell, Snyder and Bartel, 2007; Arazi, 2012; Honkanen, Thamm, Arteaga-vazquez, *et al.*, 2018). While some miRNAs are highly conserved in land plants, the majority have evolved species-specifically (Axtell and Bowman, 2008). Recently, small RNA sequencing and degradome analysis have provided insight into the miRNA repertoire of the liverwort *M. polymorpha* (Lin *et al.*, 2016). 129 identified miRNA species including pri-miRNAs and pre-miRNAs, were classified into 23 miRNA families. These miRNAs were predicted to target a total of 171 mRNAs. Of 91 annotated genes giving rise to these mRNAs, 26 % were transcription factors, which present the largest group of miRNA target genes in *M. polymorpha*. Some of them are targets of seven highly conserved land plant miRNA families, which are miR166a, miR390, miR529c/miR156, miR171-3p, miR408a, miR160 and miR319a (Lin and Bowman, 2018). For example, miR166a cleaves the Mp*C3HDZ1* mRNA, ortholog of a highly conserved class III HD-ZIP transcription factor from *A. thaliana* (Tsuzuki *et al.*, 2016). Overexpression of miR166a caused a reduction in Mp*C3HDZ1* mRNA abundance, which resulted in epinastic curling of the thallus in transgenic plants. Another highly conserved miRNA, miR160, cleaves Mp*ARF3*, an ortholog of At*ARF* genes, which are conserved transcription factors of the auxin response gene family. Other *M. polymorpha* genes, which have *A. thaliana* homologs that exert crucial developmental functions, are targeted by 15 novel miRNAs. For example, instead of miR168 regulating At*AGO1* in *A. thaliana*, the liverwort-specific miRNA Mpo-miR11707 regulates Mp*AGO1* (Gazzani *et al.*, 2009). Another example of a novel but important miRNAs is miR529c, which is a close relative of miR156, a conserved phase change regulator outside the liverwort family (Cho, Coruh and Axtell, 2012a; Zhang *et al.*, 2015; Morea *et al.*, 2016). According to small RNA sequencing

analysis, miR156 is encoded but not or very lowly expressed in *M. polymorpha*, likely due to it forming a clumsy hairpin structure that cannot be recognised by DCL proteins. Instead, it was shown that in the liverwort, miR529c cleaves the transcript of Mp*SPL2*, member of the conserved *SPL* family of transcription factors (Tsuzuki *et al.*, 2016). The mRNA of another Mp*SPL* gene, Mp*SPL1*, is cleaved by the liverwort-specific miRNA Mpo-MR-13. At*SPL8*, homolog of Mp*SPL1*, is not a target of any miRNA, but the discovery of Mpo-MR-13 suggests that *M. polymorpha* has likely evolved multiple miRNAs to control the expression of Mp*SPL* genes. Despite its very low abundance, the liverwort-specific miRNA Mp*FRH1* was discovered through a mutagenesis screen for genes involved in rhizoid development. Together with its target gene Mp*RSL1*, Mp*FRH1* controls the differentiation of rhizoids from the ventral epidermis of the liverwort thallus (Proust *et al.*, 2016; Honkanen, Thamm, Arteaga-vazquez, *et al.*, 2018). Mp*FRH1* provides an example for a non-conserved miRNA that has specifically evolved in the liverworts and which controls a conserved transcription factor, in this case *RSL1*, master regulator of filamentous rooting function. Taken together, it was demonstrated that conserved as well as non-conserved miRNA/target gene modules control core developmental processes in *M. polymorpha*.

### 1.4 *M. polymorpha* is a suitable model for forward and reverse genetics studies to investigate miRNA biogenesis

Land plants evolved about 450 Mya from an ancestral charophyte green alga (Kenrick and Crane, 1997). Liverworts, hornworts and mosses, three early diverging extant land plant lineages, form the bryophyte clade (Puttick *et al.*, 2018). Bryophytes lack vascular tissues and complex roots, but form filamentous rooting structures called rhizoids. Rhizoids were one of the morphological adaptations that enabled land plants to colonialize the terrestrial environment. Besides single-celled rhizoids, it was proposed that the extant liverworts possess other characteristics similar to the ancestor of all land plants (Bowman *et al.*, 2017).

To study the mechanisms and evolution of gene regulation in the early diverging land plants, *Marchantia polymorpha* has been stablished as a bryophyte model system. Although the fundamentally different morphologies reflect the level of evolutionary divergence, core genetic regulators including major transcription factor families, are conserved between bryophytes and seed plants (Floyd and Bowman, 2007; Catarino *et al.*, 2016). *M. polymorpha* possesses features that simplify genetic studies: Its simple genome mostly consists of singlecopy genes. Together with the fact that the haploid gametophyte generation is dominant in the bryophyte life cycle, this simplifies the analysis of gene function, with the advantage of little genetic redundancy. *M. polymorpha* can be propagated clonally and sexually in large scales, can be transformed using *Agrobacterium tumefaciens*, and genetically manipulated by techniques like CRISPR/Cas9, RNA silencing and homologous recombination (Ishizaki *et al.*, 2016).

*M. polymorpha* is a dioecious plant, where gender identity is determined by the presence of a female (X) or male (Y) sex chromosome. Female differentiation in the haploid growth phase is controlled by the expression of an autosome-encoded MYB-type transcription factor, Mp*FGMYB*. Male identity is established through the repression of Mp*FGMYB* by *SUF*, a cis-acting antisense gene that produces a long non-coding RNA from the same locus. While loss of Mp*FGMYB* function caused the expression of male morphology in genetically female plants, the opposite male-to-female sex conversion occurred in *suf* loss of function mutants. These sex conversions are reflected in the production of male instead of female gametangiophores, and vice versa (Hisanaga *et al.*, 2019). The data from this study show that the Mp*FGMYB* transcription factor controls the sexual dimorphism in *M. polymorpha*, but upstream and downstream regulators of Mp*FGMYB* are unknown.

In the dominant gametophyte phase of its life cycle, *M. polymorpha* forms a flat, thalloid plant body, from which specialised structures develop (Pandey and Alam, 2016). Gemma cups form on the dorsal thallus surface and produce small, flat gemmae, which are vegetative propagules. Gemmae are unpolarised and only a few cell layers thick. When removed from the cups and placed on growth medium, they grow out into three-dimensional thalloid gemmalings and finally into mature plants. Rhizoids differentiate from single epidermal cells of the ventral thallus surface. They are tip-growing unicellular filaments with rooting function and in control of water and nutrient uptake. When exposed to long days and far-red light, *M. polymorpha* plants transition from the vegetative to the reproductive developmental phase. This photoperiodic growth phase transition requires the activity of the GIGANTEA (GI) and FLAVIN-BINDING KELCH REPEAT F-BOX1 (FKF1) protein complex, a conserved mechanism operating in flowering plants, too (Kubota, Kita, Ishizaki, Nishihama, Katsuyuki T. Yamato, *et al.*, 2014). The finding that far-red light is required for the reproductive transition suggests that the one phytochrome encoded in the *M. polymorpha* genome is involved in this process (Chiyoda *et al.*, 2008). The reproductive developmental phase starts with the outgrowth of gametangiophores from initial cells in the apical meristematic notches. This process requires the activity of the VIIIa bHlH transcription factor Mp*BONOBO* (Mp*BNB*), which is expressed in the initial cells of the gametophyte in far-red light (Yamaoka *et al.*, 2018). Mp*bnb*$^{ko}$ knock-out mutants never produce gametangiophores, while over-expression of Mp*BNB* causes continuous formation of gametangiophores in the absence of far-red light. This suggests that Mp*BNB* is required and sufficient for gametangiophore development. It remains unknown how Mp*BNB* might interact with the far-red light pathway to control the initiation of reproductive development. The sexual reproductive structures are archegoniophores on the female and antheridiophores on the male plants of the dioecious liverwort. Both structures are composed of a stalk which

elevates a receptacle several centimetres off the ground. In the receptacles of archegoniphores, archegonia are produced with a single egg each, which is fertilised by sperm produced in antheridial receptacles (Shimamura, 2016). After fertilisation, the zygote develops into a multicellular sporophyte. The short diploid sporophyte generation of the life cycle ends with the production of hundreds of thousands of spores through meiotic divisions. These remain encapsulated by the sporangium, which hangs upside down beneath the archegoniophore receptacle. They can be harvested for transformation.

miRNAs and their biogenesis regulators fulfil pleiotropic functions in various processes of angiosperm development. Building on the discovery of homologous miRNAs and regulatory genes in the small RNA transcriptome and the genome of *M. polymorpha*, I set out to study the roles of two conserved miRNA processing components, Mp*DCL1* and Mp*HST*, in the liverwort. I will present the use of CRISPR/Cas9 gene editing for the generation of Mp*dcl1* and Mp*hst* mutants, followed by phenotypic characterisation and gene expression analysis in these mutants. Aiming to gain insight into the barely known miRNA biogenesis pathway of liverworts, I analysed conserved and non-conserved roles of *DCL1* and *HST* in the dioecious *M. polymorpha*. Their roles in rhizoid and thallus development and in controlling the reproductive phase transition in the liverwort will be investigated in the following chapters.

# Chapter 2 – *DICER-LIKE 1* and *HASTY* are conserved regulators of miRNA processing in the liverwort *M. polymorpha*

## 2.1. Abstract

miRNAs are regulators of plant development; they act by targeting mRNAs for cleavage and thereby inhibit the translation of target proteins. miRNA biogenesis requires the activity of the endoribonuclease *DICER-LIKE 1* (*DCL1*) and the nuclear export receptor *HASTY* (*HST*). In *A. thaliana*, strong At*dcl1* loss of function mutations reduce endogenous levels of miRNAs and can cause embryo lethality, suggesting that At*DCL1* is essential for plant development. At*hst* mutants also express pleiotropic defects, demonstrating that At*HST* is involved in diverse developmental processes in flowering plants. Together with most known regulators of the canonical plant miRNA biogenesis pathway, Mp*DCL1* and Mp*HST* orthologs were identified in the genome of the liverwort *M. polymorpha*. This suggests that the miRNA processing pathway exists in the non-vascular land plants. Using the Mp*FRH1*$^{GOF}$ mutant, a mutant that ectopically overexpresses the *Marchantia*-specific miRNA Mp*FRH1*, I tested if Mp*DCL1* and Mp*HST* functioned in miRNA biogenesis in the liverwort. The Mp*FRH1*$^{GOF}$ mutant develops fewer rhizoids than wild type, indicating that Mp*FRH1* is a negative regulator of rhizoid differentiation. The few rhizoids that develop are also shorter than wild type rhizoids. I tested if this phenotype was suppressed by loss of function mutations in Mp*HST* or Mp*DCL1* in the *FRH1*$^{GOF}$ background. I hypothesised that if Mp*DCL1* and Mp*HST* are involved in the processing of miRNAs, mature MpFRH1 miRNA levels would be reduced in Mp*FRH1*$^{GOF}$*;dcl1* and Mp*FRH1*$^{GOF}$*;hst* double mutants because of defective miRNA biogenesis. Indeed, these double mutants developed abundant, long rhizoids. I hypothesised that suppression of the Mp*FRH1*$^{GOF}$ few/short-rhizoids phenotype was caused by reduced levels of Mp*FRH1* because of disruption of the miRNA biogenesis pathway in Mp*FRH1*$^{GOF}$*;dcl1* and Mp*FRH1*$^{GOF}$*;hst* double mutants. Using quantitative real-time PCR, I demonstrated that the steady state levels of mature MpFRH1 miRNA were the same as wild type in the double mutants compared to the high levels of

MpFRH1 in the *FRH1*$^{GOF}$ single mutant. Steady state mRNA levels of the Mp*FRH1* miRNA target gene Mp*RSL1* were higher in the double mutants than in the Mp*FRH1*$^{GOF}$ single mutant. Taken together, mutation of Mp*DCL1* and Mp*HST* reduced steady state abundance of MpFRH1 miRNA compared to wild type, and at the same time promoted accumulation of its target gene Mp*RSL1*, restoring rhizoid development. This confirms the hypothesis that Mp*DCL1* and Mp*HST* are active components in the miRNA biogenesis pathway of *M. polymorpha*. Consequently, since Mp*DCL1* and Mp*HST* function in miRNA biogenesis as their homologs do in flowering plants, this suggests that the two genes evolved to regulate miRNAs before flowering plants and liverworts diverged from each other.

## 2.2. Introduction

Many developmental processes in plants involve the functions of miRNAs as post-transcriptional regulators of gene expression (Jones-Rhoades, Bartel and Bartel, 2006). miRNAs are 21 nt-short non-coding RNAs that originate from *MIR* genes and are produced in a complex biogenesis pathway.

*DCL1 occupies a central position in plant miRNA biogenesis pathways*

miRNA processing involves a large number of proteins, which are required for pri- and pre-miRNA cleavage through the Dicing complex (Wang, Mei and Ren, 2019). Evidence suggests that this multiprotein complex assembles co-transcriptionally, whereby the Elongator complex bridges the interaction of the Dicing complex with the transcriptional machinery (Fang, Cui, *et al.*, 2015). Therefore, processing of pri-miRNAs supposedly starts while *MIR* gene transcription is still taking place. Core enzyme of the Dicing complex is the endoribonuclease DICER-LIKE 1 (DCL1), which is essential for plant development (Kurihara and Watanabe, 2004). This is evident by severe pleiotropic defects and lethality in *dcl1* mutants in the flowering plants *A. thaliana* (Reinhart *et al.*, 2002), *Oryza sativa* (Liu *et al.*, 2005), *Glycine max* (Curtin *et al.*, 2016), *Phaseolus vulgaris* (Valdés-López *et al.*, 2008), and *Zea mays* (Qian and Cheng, 2011), and the moss *Physcomitrella patens* (Khraiwesh, M. Asif Arif, *et al.*, 2010). *DCL1* function is therefore highly conserved in land plants. Developmental defects in *dcl1* mutants commonly result from the over-expression of miRNA target genes because of significantly reduced miRNA levels. Only Pp*DCL1b*, paralog of Pp*DCL1a*, is not involved in the processing of miRNAs, but in miRNA-directed target mRNA cleavage in moss. Therefore, miRNAs are abundant in Pp*dcl1b* mutants, but directed to the RNA-induced transcript silencing (RITS) pathway instead of the RNA-INDUCED SILENCING COMLEX (RISC). Consequently, target gene loci are hyper-

methylated in *Ppdcl1b*, resulting in reduced target gene expression. Phylogenetic analysis in the liverwort *M. polymorpha*, another bryophyte, has revealed Mp*DCL1*, another *DCL1* ortholog in bryophytes (Tsuzuki *et al.*, 2016).

*HST, a putative nucleocytosolic miRNA transporter, controls accumulation of miRNAs in A. thaliana*

After processing in the nucleus, mature miRNAs are translocated to the cytoplasm and associate with the RISC to target mRNAs for cleavage or translational inhibition (Achkar, Cambiagno and Manavella, 2016). To date, knowledge about nuclear miRNA export in plants is limited. Based on homology to the Exp5 and Msn5p karyopherins from mammals and yeast, the nucleocytoplasmic transporter At*HST* was proposed as a miRNA exporter (Bollman, 2003; Park *et al.*, 2005). This proposition was supported by the observation that AtHST protein localises to the nuclear membrane, where it interacts with the Ran GTPase, which drives the export of cargo through nuclear pores (Park *et al.*, 2005). However, since miRNA accumulation in the nucleus is not abolished in At*hst* mutants, additional nuclear export mechanisms are likely in place. It remains to be determined if and how miRNAs are exported in association with ARGONAUTE (AGO) and other RISC components (Chen, 2005). Nevertheless, the levels of certain miRNAs like miR156 in immature rosette leaves, are reduced in At*hst* mutants. This may suggest an additional role for At*HST* in miRNA stabilisation, since part of the Exp5 function is to stabilise mammalian pre-miRNAs (Yi *et al.*, 2003; Park *et al.*, 2005). Since At*hst* mutants express pleiotropic developmental defects including reduced fertility, this suggests that At*HST* has an important function in the miRNA biogenesis pathway, although its precise mode of action remains elusive.

*The FEW RHIZOIDS 1 – RHIZOID-DEFECTIVE6-LIKE 1 (FRH1-RSL1) module controls rhizoid differentiation in M. polymorpha*

Vascular plants develop complex roots with specialised cell layers to ensure efficient uptake and transport of water and nutrients. To maximise resource acquisition over a large surface, lateral roots and root hairs are formed. In *A. thaliana*, the differentiation of filamentous root hairs from specialised cells in the epidermal cell layer requires the activity of the bHLH transcription factor *RSL1* (Kim and Dolan, 2016). In the non-vascular plant *M. polymorpha*, the differentiation of rhizoids, which are functional equivalents to root hairs, also requires *RSL1*. *RSL1* is therefore a conserved master regulator of filamentous rooting structures. In *A. thaliana*, At*RSL1* expression is controlled by the *GLABRA 2* (*GL2*) transcription factor, whereas Mp*RSL1* is negatively regulated by the liverwort-specific miRNA Mp*FRH1* (Lin *et al.*, 2015; Honkanen, Thamm, Arteaga-Vazquez, *et al.*, 2018). The Mp*FRH1*-Mp*RSL1* module controls the differentiation of rhizoids from specialised epidermal cells of the ventral thallus (Proust *et al.*, 2016; Honkanen, Thamm, Arteaga-vazquez, *et al.*, 2018). Therefore, liverworts have evolved an independent miRNA-based mechanism to restrict the expression of Mp*RSL1* to rhizoid precursor cells. Mp*FRH1* and Mp*RSL1* control each other in a negative feedback loop, and Mp*rsl1* loss of function as well as Mp$FRH1^{GOF}$ gain of function mutants form no or few short rhizoids (Honkanen, Thamm, Arteaga-Vazquez, *et al.*, 2018, Figure 2.1). These mutants also produce fewer gemmae and no mucilage papillae, suggesting a more general function of the Mp*FRH1*-Mp*RSL1* module in the differentiation of structures derived from single epidermal cells. In the Mp$FRH1^{GOF}$ mutant, a T-DNA in the Mp*FRH1* promoter increases transcription of Mp*FRH1* up to 10-fold relative to wild type Mp*FRH1* mRNA levels (Figure 2.1). This T-DNA insertion does not affect the transcript sequence of Mp*FRH1* but presumably promotes Mp*FRH1* expression through activity of the contained CamV 35S promoter. The Mp$FRH1^{GOF}$ over-expressor is therefore a suitable

model to study miRNA pathways in *M. polymorpha*, while in wild type backgrounds this is hampered by barely quantifiable amounts of miRNA intermediates. The distinguishing feature of Mp*FRH1*$^{GOF}$ mutants are few short rhizoids, and varying levels of mature MpFRH1 miRNA are reflected in the number of rhizoids produce by the plant, since Mp*RSL1* is sufficient for rhizoid development (Proust *et al.*, 2016).

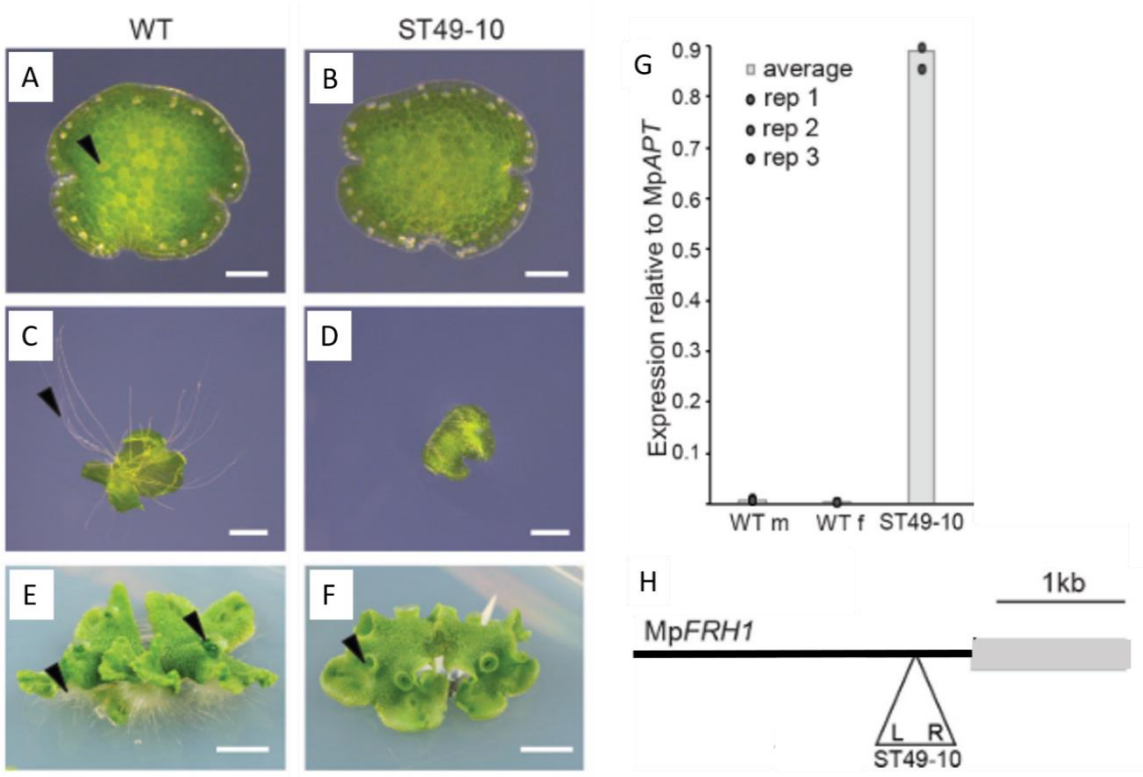


**Figure 2.1: T-DNA insertion in the promoter of Mp*FRH1* causes increased expression of MpFRH1 pri-miRNA, which results in defective rhizoid development.** From Honkanen, Thamm, Arteaga-Vazquez, *et al.*, 2018 – (A-F) Phenotype of wild type and the female Mp*FRH1*$^{GOF}$ mutant ST49-10. (A-B) One-day-old gemma (scale bar 1µm), (C-D) four-day-old gemma (scale bar 1mm) and 28-day-old gemma (scale bar 5mm) of wild type (A, C, E) and the Mp*FRH1*$^{GOF}$ mutant (B, D, F). (G) Localisation and orientation of the T-DNA insertion in the Mp*FRH1*$^{GOF}$ mutant; L and R stand for left and right border of the T-DNA, respectively. (H) qRT-PCR analysis of steady state expression of Mp*FRH1* pri-miRNA in male and female wild type and the female Mp*FRH1*$^{GOF}$ mutant ST49-10 relative to expression of Mp*APT*.

In this chapter, I make use of the Mp*FRH1*$^{GOF}$ mutant to test whether known miRNA biogenesis regulators are functional in miRNA biogenesis in *M. polymorpha*. After performing a protein homology search for conserved components of the pathway in the liverwort, I specifically investigate the roles of Mp*DCL1* and Mp*HST* in miRNA processing. This is because At*DCL1* and At*HST* are central regulators at different steps of the pathway. Moreover, studying *HST* in a distantly related species relative to *A. thaliana* might allow elucidation of the yet the unresolved function of *HST*. I hypothesise that if Mp*DCL1* and Mp*HST* are functional in the miRNA biogenesis pathway in *M. polymorpha*, defective Mp*DCL1* and defective Mp*HST* will produce less mature MpFRH1 miRNA. In the Mp*FRH1*$^{GOF}$ background with few and short rhizoids, this would mean reduced repression of Mp*RSL1* expression, and would cause the development of abundant rhizoids. To test this hypothesis, I use CRISPR/Cas9 to generate Mp*FRH1*$^{GOF}$;*dcl1* and Mp*FRH1*$^{GOF}$;*hst* double mutants. I characterise the rhizoid phenotypes of these double mutants and quantify pri- and mature MpFRH1 miRNA as well as Mp*RSL1* mRNA levels in comparison with the Mp*FRH1*$^{GOF}$ single mutant.

## 2.3. Results

### 2.3.1. Core regulators of the canonical land plant miRNA biogenesis pathway are conserved between *A. thaliana* and *M. polymorpha*

The canonical land plant miRNA biogenesis pathway has been studied thoroughly in *A. thaliana*. To investigate this pathway in liverworts, I searched for *M. polymorpha* orthologs of proteins regulating miRNA processing. *A. thaliana* protein sequences of these regulators were obtained from the TAIR (The Arabidopsis Information Resource) website and protein BLAST was used to identify orthologs in the compiled *M. polymorpha* proteome on the phytozome V12 online database. The found sequence hits with highest identity were subjected to reciprocal protein BLAST search on the NCBI (National Centre for Biotechnology Information) homepage. *A. thaliana* and *M. polymorpha* homologs were then analysed with OrthoFinder, a program that identifies orthologous protein sequence families (Emms and Kelly, 2015). The constructed orthogroups also contained sequences from *P. patens* to provide information on conservation of miRNA processing regulators in another bryophyte.

**Table 2.1: *M. polymorpha* orthologs of *A. thaliana* miRNA biogenesis components as determined by protein BLAST search.** Amino acid sequences from *A. thaliana* proteins were retrieved from the TAIR database, sequence similarity search by BLAST was conducted against the *M. polymorpha* proteome established by the Bowman lab (phytozome V12). Orthogroups were determined by OrthoFinder. Those groups contain all genes descended from a single gene in the last common ancestor of the flowering plant *A. thaliana* (At), the liverwort *M. polymorpha* (Mp) and the moss *P. patens* (Pp). The DCL orthogroup contains two additional RTL-like genes in *A. thaliana* and *M. polymorpha* each, which have similarity to DCL proteins.

| | | | | number of orthogroup members acc. to OrthoFinder | | |
|---|---|---|---|---|---|---|
| **At gene** | **At gene number** | **function** | **Mp ortholog** | **At** | **Mp** | **Pp** |
| **pri-miRNA transcription** | | | | | | |
| ARP6 | AT3G33520.1 | SWR1 chromatin remodelling complex | Mapoly0069s0083 | 1 | 1 | 1 |
| PIE1 | AT3G12810.1 | | Mapoly0111s0052 | 2 | 2 | 5 |
| SEF | AT5G37055.1 | | Mapoly0066s0110 | 1 | 1 | 1 |
| GCN5 | AT3G54610.1 | major histone acetyl transferase | Mapoly0187s0003 | 1 | 1 | 1 |
| NRPB1 | AT4G35800.1 | RNA polymerase II large subunit | Mapoly0070s0048 | 3 | 4 | 5 |
| MED17 | AT5G20170.1 | sub-units of the Mediator complex, general transcriptional activator | Mapoly0010s0026 | 1 | 1 | 2 |
| MED18 | AT2G22370.1 | | Mapoly0023s0045 | 1 | 1 | 1 |
| MED20 | AT4G09070.1, AT2G28230.1 | | Mapoly0097s0017 | 3 | 1 | 1 |
| CDC5 | AT1G09770.1 | positive TF | Mapoly0014s0195 | 1 | 1 | 1 |
| PRL1 | AT4G15900.1 | pri-miRNA processing, co-factor for DCL1 | Mapoly0016s0006 | 2 | 1 | 2 |
| NOT2a | AT1G07705.2 | transcriptional regulator, coordinates recruitment of DCL1 | Mapoly0001s0449 | 2 | 1 | 3 |
| NOT2b/ VIP2 | AT5G59710.1 | | | | | |
| HOS1 | AT2G39810.1 | transcriptional control of miR168 - indirect regulator of AGO1 levels | Mapoly0088s0017 | 1 | 1 | 2 |
| XCT | AT2G21150.1 | positive regulator of DCL expression | Mapoly0015s0022 | 1 | 1 | 2 |
| ELP1 | AT5G13680 | Elongator complex | Mapoly0015s0194 | 1 | 1 | 1 |
| ELP2 | At1G49540 | | Mapoly0064s0032 | 1 | 1 | 1 |

| | | | | | | |
|---|---|---|---|---|---|---|
| ELP3 | AT5G50320.1 | | Mapoly0095s0008 | 1 | 1 | 1 |
| ELP4 | AT3G11220 | | Mapoly0006s0234 | 1 | 1 | 1 |
| ELP5 | At2G18410 | | Mapoly0156s0014 | 1 | 1 | 1 |
| ELP6 | At4G10090 | | Mapoly0003s0199 | 1 | 1 | 1 |
| **pri-miRNA splicing** | | | | | | |
| STA1 | AT4G03430.1 | pri-miRNA splicing | Mapoly0016s0118 | 1 | 1 | 2 |
| CBP20 | AT5G44200.1 | components of the Cap-binding complex | Mapoly0001s0392 | 1 | 1 | 1 |
| CBP80 | AT2G13540.1 | | Mapoly0005s0051 | 1 | 1 | 2 |
| SE | AT2G27100.1 | pri-miRNA splicing and processing | Mapoly0065s0067 | 1 | 1 | 3 |
| **pri- and pre-miRNA cleavage by the micro-processor/Dicing complex** | | | | | | |
| DCL1 | AT1G01040.2 | pri-miRNA cleavage | Mapoly0003s0222 | 6 | 5 | 6 |
| DCL2 | AT3G03300.1 | siRNA and partly miRNA processing | none | | | |
| DCL3 | AT3G43920.2 | | Mapoly0113s0032 | | | |
| DCL4 | AT5G20320.1 | | Mapoly0003s0184 | | | |
| HYL1/ DRB1 | AT1G09700.1 | pri-miRNA processing | Mapoly0146s0045 | 4 | 2 | 4 |
| DRB2 | AT2G28380.1 | tissue-specific influence on pri-miRNA processing | Mapoly0369s0002 | | | |
| DRB3 | AT3G26932.1 | | | | | |
| DRB5 | AT5G41070.1 | | | | | |
| SE | AT2G27100 | pri-miRNA processing | Mapoly0065s0067 | 1 | 1 | 3 |
| PRL1 | AT4G15900.1 | pri-miRNA processing, co-factor for DCL1 | Mapoly0016s0006 | 2 | 1 | 2 |
| RACK1A | AT1G18080.1 | scaffold protein for protein-protein interactions in pri-miRNA transcription and processing | Mapoly0004s0109 | 3 | 1 | 3 |
| RACK1B | AT1G48630.1 | | | | | |
| RACK1C | AT3G18130.1 | | | | | |
| TGH | AT5G23080.1 | assists DCL1 in pri-miRNA processing | Mapoly0043s0012 | 1 | 1 | 1 |
| DDL | AT3G20550.1 | assists DCL1 in pri-miRNA processing | Mapoly0068s0031 | 2 | 1 | 1 |

| | | | | | | |
|---|---|---|---|---|---|---|
| MOS2 | AT1G33520.1 | pri-miRNA processing, recruitment of pri-miRNAs by HYL1 | Mapoly0027s0115 | 2 | 1 | 1 |
| THO2 | AT1G24706.2 | pri-miRNA splicing and transport | Mapoly0001s0369 | 1 | 1 | 1 |
| CPL1 | AT4G21670.1 | phosphorylation/activation of HYL1 | Mapoly0125s0035 | 2 | 1 | 2 |
| **pre-miRNA modification and export** | | | | | | |
| HST | AT3G05040.1 | nuclear export of miRNAs | Mapoly0015s0189 | 1 | 1 | 2 |
| HEN1 | AT4G20910.1 | small RNA methyltransferase | Mapoly0004s0071 | 2 | 1 | 1 |
| HESO1 | AT2G39740.1 | degradation of unmethylated miRNAs | Mapoly0027s0117 | 3 | 1 | 3 |
| URT1 | AT2G45620 | degradation of unmethylated miRNAs | Mapoly0079s0057.1 | 1 | 1 | 1 |
| **miRNA-mediated mRNA cleavage/translational inhibition by the RISC** | | | | | | |
| AGO1<br>AGO5<br>AGO10 | AT1G48410.2<br>AT2G27880.1<br>AT5G43810.1 | RNA slicer component of the RISC associated with miRNAs | Mapoly0001s0149 | 7 | 4 (2 more AGO family proteins) | 6 |
| AGO4<br>AGO6<br>AGO8<br>AGO9 | AT2G27040.1<br>AT2G32940.1<br>AT5G21030.1<br>AT5G21150.1 | RNA slicer component of the RISC associated with siRNAs | Mapoly0065s0059 | | | |
| CYP40 | AT2G15790 | RISC assembly | none | 1 | 0 | 3 |
| TRN1 | AT2G16950 | miRNA loading into the RISC | Mapoly0057s0097.1 | 1 | 1 | 4 |
| EMA1 | AT2G31660 | | Mapoly0014s0213.1 | 2 | 1 | 2 |
| LAMP1<br>AMP1 | AT5G19740.1<br>AT3G54720 | mediates translational inhibition of target mRNA | Mapoly0059s0084 | 1 | 1 | 4 |

*The expression of MIR genes is controlled by conserved chromatin modifiers and general as well as specific transcriptional regulators*

The expression of *MIR* genes underlies epigenetic regulation, analogous to the transcriptional control of protein-coding genes. It involves the activities of the highly conserved histone acetyltransferase GENERAL CONTROL NON-REPRESSED PROTEIN 5 (GCN5) and the SWR1 chromatin remodelling complex (SWR1-C). Both are general regulators of gene expression in *A. thaliana* and influence the abundance of a subset of miRNAs. GCN5 also indirectly represses expression of miRNA biogenesis components such as *DICER-LIKE 1* (*DCL1*), *ARGONAUTE* ( *AGO1*), *HYPONASTIC LEAVES 1* (*HYL1*) and *SERRATE* (*SE*) (Kim *et al.*, 2009). SWR1-C was suggested to render environmentally responsive *MIR* genes in an inactive transcriptional state until their induction (Choi *et al.*, 2016). *M. polymorpha* encodes one homologous GCN5 protein and three conserved components of the SWR1-C complex – ACTIN-RELATED PROTEIN 6 (ARP6), PHOTOPERIOD-INDEPENDENT EARLY FLOWERING 1 (PIE1) and SERRATED LEAVES AND EARLY FLOWERING (SEF).

Transcription of *MIR* genes just like protein-coding genes is completed by RNA-polymerase II (RNAPII) with involvement of CYCLIN-DEPENDENT KINASE F 1 (CDKF1), which phosphorylates the largest subunit of RNAPII to regulate its activity (Achkar, Cambiagno and Manavella, 2016). Both enzymes are highly conserved in the plant kingdom and present in liverworts. Also, general transcriptional regulators that interact with RNAPII, like the MEDIATOR (MED) complex, NEGATIVE ON TATA LESS 2 (NOT2) and the miRNA-specific transcription factor CELL DIVISION CYCLE 5 (CDC5) are encoded in *M. polymorpha* (Kim *et al.*, 2011; Wang *et al.*, 2013; Zhang *et al.*, 2013). However, compared to NOT2a and NOT2b in the angiosperm, only one NOT2 homolog exists in *M. polymorpha*.

The ELONGATOR multi-protein complex is a general transcriptional and translational regulator and highly conserved among eukaryotes (DeFraia and Mou, 2011). Besides other roles, it promotes occupancy of RNAPII at *MIR* gene loci and thereby primary miRNA (pri-miRNA) transcription. Furthermore, the Elongator complex interacts with DCL1 to initiate miRNA processing co-transcriptionally (Fang, Cui, *et al.*, 2015). All six ELP sub-units of the complex are encoded in *M. polymorpha*, indicating that it might regulate miRNA transcription and processing besides controlling the expression of various unrelated genes. Additional to these main transcriptional regulators, different proteins influence the accumulation of subsets of pri-miRNAs. In synergistic action together with CDC5, the WD-40 protein PROTEIN PLEIOTROPIC REGULATORY LOCUS 1 (PRL1) positively affects the abundance of pri-miRNAs (Zhang, Liu and Yu, 2014). Moreover, this RNA-binding protein was proposed to be a co-factor for DCL1 and other DCLs that associate with double-stranded RNAs. Although PRL1 is conserved in *M. polymorpha*, its involvement in miRNA biogenesis in the bryophytes remains to be investigated. As PRL1 was shown to be required for general pathways of immunity and development (Baruah *et al.*, 2009), it might as well fulfil another specialised task in the liverwort.

*Regulation of core miRNA processors*

In another regulatory layer of the miRNA processing pathway, the expression of core processing components is being controlled. The E3 ubiquitin ligase HIGH EXPRESSION OF OSMOTICALLY RESPONSIVE GENES 1 (HOS1) enhances expression of miRNA168b by promoting occupancy of PNAPII at the MIR168b promoter (Wang *et al.*, 2015). This is crucial to ensure the correct accumulation of the core enzyme AGO1, target of miRNA168b. Another nuclear protein is XAP5 CIRCADIAN TIMEKEEPER (XCT). It promotes PNAPII occupancy at the promoter of *DCL1* and thereby controls *DCL1*

abundance (Fang, Shi, *et al.*, 2015). Both proteins, HOS1 and XCT, also fulfil other essential and pleiotropic functions in plants. *M. polymorpha* has single copy orthologs of HOS1 and XCT. Since AGO1 and DCL1 are highly conserved, essential enzymes in miRNA biogenesis, it is likely that their regulators HOS1 and XCT have co-evolved in *M. polymorpha*. However, *M. polymorpha* lacks miR168 and instead, the liverwort-specific Mpo-miR11707 miRNA regulates MpAGO1 (Lin *et al.*, 2016). It remains to be tested whether the liverwort ortholog of HOS1 enhances Mpo-miR11707 expression.

*Conserved splicing factors are crucial for pri-miRNA transcript processing*

Some pri-miRNAs contain introns and undergo splicing just like protein-coding mRNAs. Accordingly, some pre-mRNA splicing factors take up dual roles in pri-miRNA maturation. The most important examples are the zinc-finger protein SERRATE (SE) and the nuclear CAP-BINDING COMPLEX (CBC) (Szweykowska-kulinska, Jarmolowski and Vazquez, 2016). SE and CBC promote splicing of intron-containing pri-miRNAs; their mutants accumulate un-spliced pri-miRNAs, which are less effectively processed into mature miRNAs (Laubinger *et al.*, 2008). Levels of intron-less pri-miRNAs are also elevated in mutants of the CBC, indicating that the CBC, likely in association with SE, promotes general pri-miRNA maturation. Both components are conserved in liverworts, since *M. polymorpha* encodes orthologs of the CBC subunits CBP20 and CBP80, as well as one protein ortholog of SE.

*M. polymorpha encodes core components of the Dicing complex*

Among the DCL proteins, DCL1 is the predominant RNase III enzyme responsible for cleavage of pri-miRNAs into 21 nt-short miRNAs. Its three homologs DCL2, DCL3 and DCL4 add to DCL1 activity in very specific cases, but mainly process short interfering

RNAs (siRNAs) (Liu, Feng and Zhu, 2009; Nagano *et al.*, 2014). *M. polymorpha* has three DCL proteins – one DCL1 and DCL3 ortholog each, and another protein that most closely resembles AtDCL4. This suggests that MpDCL proteins process miRNAs and short interfering RNAs (si-RNAs) in *M. polymorpha*. For the two-step cleavage of pri- and pre-miRNAs, DCL1 associates with several RNA-binding proteins to form the microprocessor/Dicing complex (Fang and Spector, 2007). Some of these are transcription and splicing factors, indicating crosstalk between regulators of different steps of the pathway (Achkar, Cambiagno and Manavella, 2016). For efficient and accurate miRNA cleavage, DCL1 associates with members of the DOUBLE-STRANDED RNA BINDING PROTEIN (DRB) family and the zinc-finger domain-containing protein SE. As fundamental components of the Dicing complex, these integral proteins are present in *M. polymorpha*, too, although the liverwort only encodes two DRB proteins instead of five encoded in *A. thaliana*. One of these two orthologs corresponds to DRB1/HYPONASTIC LEAVES1 (HYL1), which is globally active and indispensable for miRNA biogenesis (Vazquez, Gasciolli and Cre, 2004). Interestingly, the second MpDRB ortholog shows highest similarity to DRB2, DRB3 and DRB5, three members that are exclusively active in regulating miRNA abundance in the shoot apical meristem in flowering plants (Eamens *et al.*, 2012). On top of that, DRB2 has been suggested to guide translational inhibition in *A. thaliana* (Reis *et al.*, 2015). Components of the Dicing complex interact with each other, and the RECEPTOR OF ACTIVATED C KINASE 1 (RACK1) scaffold proteins bridge such interactions. It was shown that they bind to SE and AGO to influence the accumulation of miRNAs (Speth *et al.*, 2013; Speth and Laubinger, 2014). RACK proteins are highly conserved among eukaryotes and function in various signalling pathways. While three RACK proteins exist in *A. thaliana*, a single ortholog is present in *M. polymorpha*. A number of other proteins ensure efficient and accurate miRNA processing in the Dicing complex by

enhancing DCL1 activity as co-factors: TOUGH (TGH), DAWDLE (DDL) and PLEIOTROPIC REGULATORY LOCUS 1 (PRL1) (Yu *et al.*, 2008; Ren *et al.*, 2012; Zhang, Liu and Yu, 2014). All three have single copy orthologs in *M. polymorpha*. MODIFIER OF SNC1 2 (MOS2) and THO2 were proposed to promote miRNA production by binding to pri-miRNAs and facilitating their recruitment by HYL1 (Wu *et al.*, 2013; Francisco-Mangilet *et al.*, 2015). Instead of interacting with the processing machinery, they control the assembly of the Dicing complex. THO2 is one of the eight subunits of the THO/TREX complex, which is involved in various sRNA-dependent processes, and MOS2 is also essential for innate immunity in *A. thaliana*. *M. polymorpha* has single copy orthologs of both proteins; which might be involved in miRNA processing and/or other potentially conserved processes. Other regulators of HYL1 activity are C-TERMINAL DOMAIN PHOSPHATASE-LIKE 1 (CPL1) and CPL2. Apart from promoting correct strand selection and accurate miRNA processing through dephosphorylating HYL1, CPL1 and CPL2 regulate the activity of RNAPII by dephosphorylating its C-terminal domain (Ott *et al.*, 2012; Achkar, Cambiagno and Manavella, 2016). *M. polymorpha* encodes a single CPL1 ortholog, which might be involved in different steps of the miRNA biogenesis pathway.

*Pre-miRNA methylation and nuclear export*

Once the mature miRNA duplex is produced in the Dicing complex, the 3'-ends of each strand are being methylated, which provides protection against uridylation-triggered degradation. The 2'-O-methyltransferase HUA-ENHANCER 1 (HEN1) was shown to influence the accumulation of small RNAs by executing this function (Ji and Chen, 2012). Direct interaction of HEN1 with HYL1 and DCL1 demonstrated that miRNA biogenesis steps are mechanistically linked (Mickut *et al.*, 2015). HEN1 function is conserved – homologs of HEN1 methylate different sRNAs in animals and flies. *M. polymorpha* encodes

a single copy ortholog of HEN1, consistent with the finding that miRNAs are methylated in *M. polymorpha* (Lin *et al.*, 2016). If unmethylated, miRNAs that are bound to AGO1 are uridylated by HEN1 SUPPRESSOR (HESO1) and URIDYLYLTRANSFERASE 1 (URT1). Cooperatively and sequentially, these two predominant nucleotidyl transferases tail miRNAs to be recognised for degradation (Zhao *et al.*, 2012; Tu *et al.*, 2015). *M. polymorpha* encodes single copy orthologs of HESO1 and URT1, which suggests that non-methylated miRNAs are being uridylated in the liverwort. Two ways were proposed in which mature miRNAs reach the cytoplasm, where they meet their target mRNAs – they are shuttled from nucleus to cytosol in association with AGO1 or exported through nuclear pores as miRNA duplexes (Park *et al.*, 2005; Bologna *et al.*, 2018). HASTY (HST), a karyopherin homolog, has a putative function in nuclear miRNA export. However, since cytosolic miRNA accumulation was not abolished in At*hst* mutants, but global accumulation of nuclear and cytosolic miRNAs was reduced, HST was proposed to fulfil a miRNA-stabilising function (Park *et al.*, 2005). *M. polymorpha* encodes a single copy ortholog, which likely functions in the miRNA pathway, although the exact role of HST in miRNA processing remains elusive.

*miRNA-mediated mRNA cleavage and translational repression in the conserved RNA-INDUCED SILENCING COMPLEX (RISC)*

After incorporation of the mature guide miRNA strand, the RISC identifies the complementary target mRNA to either cleave it or inhibit its translation. Core enzymes of RISCs are AGO proteins, which exert RNA slicer activity in sRNA-mediated post-transcriptional gene regulation pathways – in *A. thaliana*, ten AGO proteins regulate miRNA-mediated mRNA cleavage (group 1 AGOs – predominantly AGO1, AGO5 and AGO10), si-RNA-mediated post-transcriptional gene silencing (group 2 AGOs – mainly

AGO4, AGO6, AGO8 and AGO9) and ta-siRNA generation (group 3 AGOs – AGO2, AGO3 and AGO7) (Vazquez, Cre and Bartel, 2004; Baumberger and Baulcombe, 2005). The AGO protein family in *M. polymorpha* is much smaller. It only contains two AGO orthologs – one similar to group 1 AGOs and one similar to group 2 AGOs, suggesting that they regulate miRNA and siRNA pathways. Since presence of ta-siRNAs in *M. polymorpha* was shown, it is likely that one of these two or both MpAGO orthologs are involved in ta-siRNA generation. The assembly of the RISC, with AGO1 and the miRNA guide strand in its core, relies on the activity of the molecular chaperone HEAT SHOCK PROTEIN 90 (HSP90), which was shown to bind to AGO1 (Iki *et al.*, 2010; Iwasaki *et al.*, 2010). HSP90 homologs play roles in the folding and activation of proteins in various signalling processes and cell cycle regulation and are highly conserved in eukaryotes including *M. polymorpha*. The assembly of the RISC is facilitated by the transient association of CYCLOPHILIN 40 (CYP40) with AGO1 and HSP90 (Iki *et al.*, 2012). Cyclophilins are also ubiquitously required in all living organisms and *M. polymorpha* encodes numerous orthologs, but no CYP40 homolog. It is possible that either one of the other *Marchantia*-encoded peptidyl-prolyl isomerases supports RISC assembly or that cyclophilin-like proteins are not involved in this process in *M. polymorpha*. The selective incorporation of miRNAs into the RISC is positively and negatively regulated by two importin β proteins, TRANSPORTIN 1 (TRN1) and ENHANCED MiRNA ACTIVITY 1 (EMA1) (Wang *et al.*, 2011; Cui, Fang and Qi, 2016). Both have orthologs in *M. polymorpha,* which are most likely not exclusively required for the miRNA biogenesis pathway, like TRN1 and EMA in *A. thaliana*. Besides mRNA slicing, which is executed by AGO proteins, the RISC mediates inhibition of mRNA translation. This takes place through steric hindrance of the recruitment or movement of ribosomes along the mRNA by the AtAGO1-RISC complex (Iwakawa and Tomari, 2013). Translational inhibition also requires ALTERED MERISTEM PROGRAM 1 (AMP1) and

its paralog LIKE AMP 1 (LAMP1), which are integral membrane proteins associated with the endoplasmic reticulum (ER). This suggest that miRNA-mediated translational inhibition takes place at the ER, since in the absence of AMP1, the amount of membrane-bound miRNA-associated polysomes was decreased compared to wild type (Li *et al.*, 2013). However, since *amp1 lamp1* double mutants express pleiotropic developmental defects, they might possess miRNA-independent roles. *M. polymorpha* encodes a single copy AMP1/LAMP1 ortholog, which might support the importance of translational inhibition as a mode of miRNA action in liverworts.

It can be concluded that *M. polymorpha* encodes orthologs of core regulators of miRNA processing known from *A. thaliana*. Additional tissue-specific regulators are less conserved, because no highly similar protein sequences were identified in *M. polymorpha*. It remains to be confirmed experimentally whether the identified liverwort orthologs function in the miRNA biogenesis pathway.

### 2.3.2. *M. polymorpha* encodes one *HASTY* and three *DICER-LIKE* homologs

In *A. thaliana*, the endoribonuclease At*DCL1* and the nuclear export receptor At*HST* occupy central positions in the miRNA biogenesis pathway. At*DCL1* is one of four members of the At*DCL* gene family, while At*HST* is a single copy gene. By protein BLAST search, I identified one Mp*HST* ortholog (Mapoly0015s0189) and three Mp*DCL* orthologs (Mapoly0003s0222, Mapoly0113s0032 and Mapoly0003s0184). This suggests that the single copy *HST* gene and the *DCL* gene family are conserved between liverworts and flowering plants. To analyse the phylogenetic relationships between Mp*DCL*s and Mp*HST* with other plant *DCL* and *HST* genes, I built gene trees. In the *DCL1* gene tree, which was generated from orthologous amino acid sequences, I included sequences from *A. thaliana*

and the moss *Physcomitrella patens*. PpDCL orthologs were obtained by BLAST search of the AtDCL amino acid sequences against the *P. patens* proteome on the phytozome database. The amino acid sequences of the four obtained PpDCL orthologs (Pp3c2_15900V3, Pp3c1_24950V3, Pp3c23_3450V3, Pp3c26_370V3) as well as the four AtDCLs and three MpDCLs were aligned online using the MAFFT software (Katoh, Rozewicki and Yamada, 2017). Based on the trimmed alignment, a phylogenetic tree was constructed in MEGA X (Kumar *et al.*, 2018), using the Maximum Likelihood method with 500 bootstrap resampling steps.

The *DCL* gene tree shown in Figure 2.2 consists of three well-supported clades – *DCL1*, *DCL4* and *DCL3* clades (bootstrap support values of 100, 78 and 99), in which at least one ortholog from each of the three species is represented. Mapoly0003s0222, Mapoly0113s0032 and Mapoly0003s0184 were named Mp*DCL1*, Mp*DCL3* and Mp*DCL4* because they were orthologs of At*DCL1*, At*DCL3* and At*DCL4*. Similarly, Pp3c2_15900V3, Pp3c1_24950V3, Pp3c23_3450V3 and Pp3c26_370V3 were termed Pp*DCL1a*, Pp*DCL1b*, Pp*DCL3* and Pp*DCL4*. *DCL1*, *DCL2/4* and *DCL3* genes carry out distinct functions in the processing of miRNAs, siRNAs involved in post-transcriptional gene silencing (PTGS), and siRNAs involved in RNA-directed DNA methylation (RdDM), respectively (Liu, Feng and Zhu, 2009). Since homologs of these three *DCL* groups are present in *M. polymorpha* and *P. patens*, it suggests that different sRNAs are likely processed by the respective DCL proteins in bryophytes (Khraiwesh *et al.*, 2010). Like *M. polymorpha*, *P. patens* does not encode a *DCL2* ortholog, suggesting that *DCL2* genes evolved after the moss, liverwort and flowering plant lineages diverged. Taken together, these results are consistent with the phylogenetic analysis of the MpDCL proteins in Tsuzuki et al. 2016 and confirm that *DCL* genes are conserved among land plants.

For phylogenetic analysis of *HST* genes, I searched for *HST* orthologs in different plant lineages ranging from the green alga *Chlamydomonas reinhardtii* (Cre) to embryophytes. Within the embryophytes, *HST* genes were determined in the bryophytes *Marchantia polymorpha* (Mp), *Physcomitrella patens* (Pp) and *Selaginella moellendorffii* (Sm), in dicotyledonous flowering plants *Arabidopsis thaliana* (At) and *Populus trichocarpa* (Pt), and in the grasses *Oryza sativa* (Os), *Brachypodium distachyon* (Bd) and *Zea mays* (Zm). Amino acid sequence of HST proteins from these species were obtained by protein BLAST search of the AtHST sequence against respective proteomes on the phytozome website. A multiple sequence alignment of these sequences was generated on the MAFFT online website. Based on this, a gene tree was built in MEGA-X using the maximum likelihood method with 500 bootstrap resampling steps. The bootstrap consensus tree was rooted using transportin protein sequences from *H. sapiens*, *A. thaliana* and *M. polymorpha*, different members of the importin-beta protein family, of which *HST* is a member. Phylogenetic analysis demonstrated high conservation of *HST* genes among plants (Figure 2.3). *HST* is consistently present as a single copy gene in plant species, with exception of two *HST* copies in *P. patens*, which are likely product of a whole genome duplication. This suggests that *HST* might have a strongly conserved role in miRNA processing in plants. Furthermore, given the presence of Mp*DCL1* and Mp*HST*, it is likely that a core part of the known miRNA processing pathway from *A. thaliana* is also present in *M. polymorpha*.

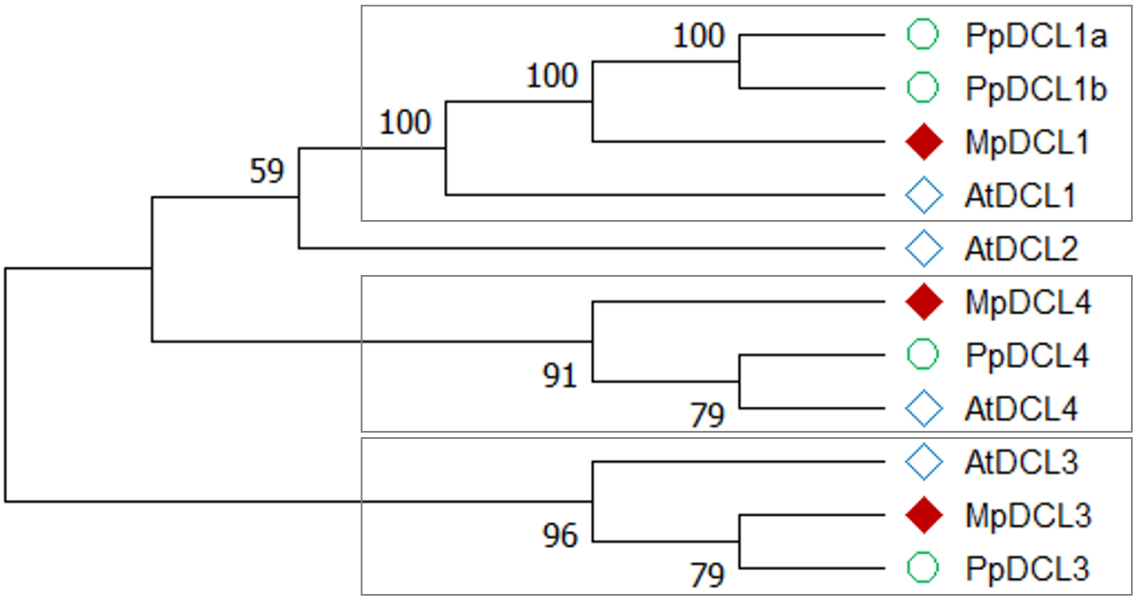


**Figure 2.2**: ***M. polymorpha* encodes three *DCL* orthologs.** Phylogenetic tree of *DCL* genes based on a multiple sequence alignment of amino acid sequences from *A. thaliana*, *P. patens* and *M. polymorpha*. Evolutionary analysis was conducted in MEGA X, where the Maximum Likelihood method based on the Poisson correction model was applied with 500 bootstrap resampling steps. Numbers next to the branches indicate the percentage of trees in which the associated genes cluster together. Branch lengths were measured in the number of substitutions per site, consensus tree is shown. Grey boxes highlight *DCL1*, *DCL3* and *DCL4* gene clades.

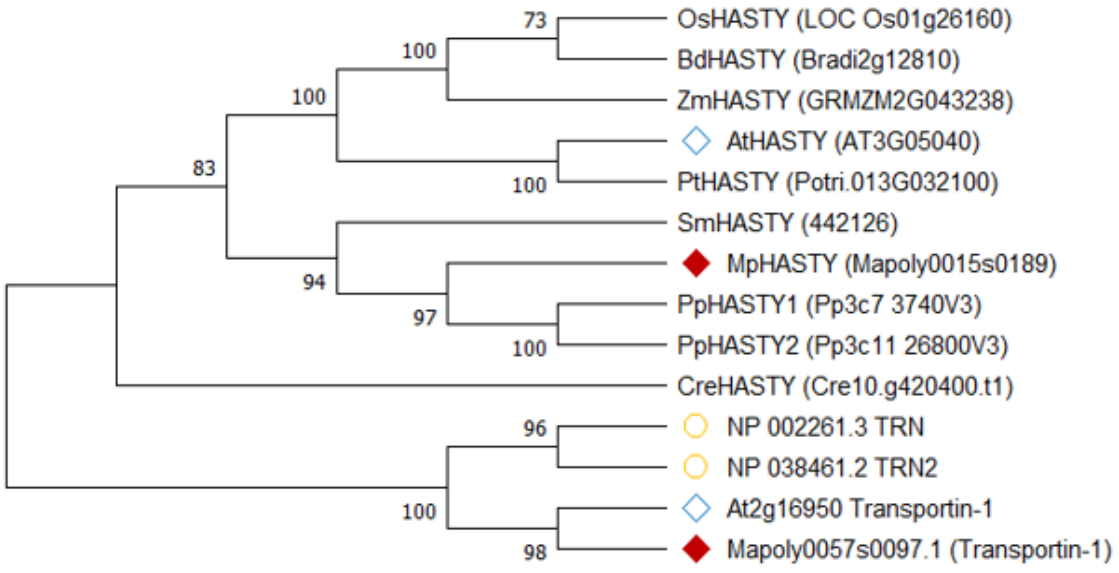

**Figure 2.3**: ***M. polymorpha* encodes a single copy *HASTY* gene.** Phylogenetic analysis of *HST* genes in plants. The tree was constructed using full amino acid sequences from *Chlamydomonas reinhardtii* (Cre), *Arabidopsis thaliana* (At), *Populus trichocarpa* (Pt), *Oryza sativa* (Os), *Brachypodium distachyon* (Bd), *Zea mays* (Zm), *Marchantia polymorpha* (Mp), *Physcomitrella patens* (Pp) and *Selaginella moellendorffii* (Sm). The tree was rooted against transportin genes from the importin-beta family of nuclear transport receptors, of which *HST* is another member. *H. sapiens, A. thaliana* and *M. polymorpha* genes are highlighted by yellow circles, blue rhombuses and red rhombuses, respectively. Branch lengths were measured in the number of substitutions per site.

### 2.3.3. Independent Mp*FRH1*$^{GOF}$*;dcl1* double mutant and Mp*FRH1*$^{GOF}$*;hst* double mutant lines were generated using CRISPR/Cas9 mutagenesis

Mutations in genes encoding proteins that function in miRNA biogenesis lead to reduced accumulation of mature miRNAs, sometimes associated with over-accumulation of pri-miRNAs (Yang *et al.*, 2006). To test if the *M. polymorpha* homologs Mp*DCL1* and Mp*HST* are functional in miRNA biogenesis, I analysed the impacts of Mp*dcl1* and Mp*hst* mutations on the expression of the Mp*FEW RHIZOIDS 1* (*FRH1*) miRNA. As a repressor of rhizoid formation, Mp*FRH1* causes almost complete loss of rhizoids when over-expressed in the Mp*FRH1*$^{GOF}$ mutant. This gain-of-function mutant contains a T-DNA insertion in the promoter of the Mp*FRH1* gene, which increases the steady-state levels of Mp*FRH1* by about 10 compared to wild type (Honkanen, Thamm, Arteaga-Vazquez, *et al.*, 2018). I predicted that if Mp*DCL1* and Mp*HST* promote biogenesis of Mp*FRH1*, loss of function of each gene would disrupt that pathway. Consequently, the amount of mature Mp*FRH1* would decrease to allow rhizoid development in Mp*FRH1*$^{GOF}$;*dcl1* and Mp*FRH1*$^{GOF}$;*hst* double mutants compared to the Mp*FRH1*$^{GOF}$ single mutant. These double mutants would therefore produce abundant rhizoids, as opposed to the few and short rhizoids in Mp*FRH1*$^{GOF}$.

To test this prediction, I generated double mutants using CRISPR/Cas9. For mutagenesis of Mp*DCL1*, I designed two guide RNAs (gRNAs) that bind to the Mp*DCL1* sequence encoding the 1st RNase III domain ca. 380 bp apart from each other (CRISPR 2 gRNAs in Appendix Table A1, Figure 2.4). The 1st RNase III domain is likely necessary for the function of Mp*DCL1* in miRNA cleavage (Schauer *et al.*, 2002). This combination of gRNAs could lead to the deletion of 380 bp if both gRNA target sites were cleaved and the intermediate DNA sequence was released from the chromosome. Alternatively, CRISPR/Cas9 activity could generate smaller mutations in the individual gRNA target sites. To mutagenize the exportin1-like domain of Mp*HST*, two gRNAs were designed to bind 80-90 bp apart from each other to the sequence encoding the functional domain (Figure 2.4). CRISPR activity could therefore delete 80-90 bp of the exportin1-like domain. Using thallus transformation, I independently introduced the CRISPR transgenes containing the respective pairs of gRNAs targeting either Mp*DCL1* or Mp*HST* into the $FRH1^{GOF}$ mutant background. The resulting transformants were screened for abundant rhizoids. Two independent putative Mp$FRH1^{GOF}$;$dcl1^{CRISPR}$ double mutants and one putative Mp$FRH1^{GOF}$;$hst^{CRISPR}$ double mutant that carried CRISPR insertions (indicated by '$^{CRISPR}$'), formed abundant rhizoids compared to the Mp$FRH1^{GOF}$ single mutant. Therefore, I sequenced the genomic regions around the respective gRNA target sites in Mp*DCL1* or Mp*HST* and searched for mutations that might have caused the suppression of the Mp$FRH1^{GOF}$ few-rhizoids phenotype. Using PCR, I amplified 600-1500 bp of DNA sequence encompassing both gRNA target sites in Mp*DCL1* or Mp*HST*. The products were then sequenced; the detected mutations are listed in Table 2.1. Mutations in the two Mp$FRH1^{GOF}$;$dcl1^{CRISPR}$ double mutants are visualised in a gene model in Figure 2.4. CRISPR/Cas9 mutagenesis introduced mutations precisely in the designed gRNA target sites. Of the two Mp$FRH1^{GOF}$;$dcl1^{CRISPR}$ double mutant lines, one

contained an in-frame insertion of 9 bp in exon 17 (position 10628-10636, line Mp*FRH1*$^{GOF}$;*dcl1*$^{CRISPR}$-*1*). This caused the addition of three amino acids – proline, glutamine and isoleucine – which likely affected the conformation and activity of the 1$^{st}$ RNase III domain. The second double mutant line, Mp*FRH1*$^{GOF}$;*dcl1*$^{CRISPR}$-*2*, had a 5 bp deletion in intron 16 (position 10245-10249). The presence of the deletion in an intron suggests that Mp*DCL1* function might be compromised because of defective splicing of the Mp*DCL1* transcript. Similarly, the function of Mp*HST* in the Mp*FRH1*$^{GOF}$;*hst*$^{CRISPR}$ mutant is likely defective due to the deletion of 2 bp in intron 4 (position 2255-2256). Sequencing of the Mp*DCL1* and Mp*HST* transcripts in these two double mutants will clarify whether splicing is affected. The fact that the three identified double mutants formed abundant rhizoids unlike the few rhizoids in Mp*FRH1*$^{GOF}$, suggests that the functionality of Mp*DCL1* and Mp*HST* were altered in the two Mp*FRH1*$^{GOF}$;*dcl1*$^{CRISPR}$ double mutant lines and in the Mp*FRH1*$^{GOF}$;*hst*$^{CRISPR}$ double mutant, respectively.


**Figure 2.4: CRISPR/Cas9 generated mutations in the selected gRNA target sites in Mp*DCL1* and Mp*HST*.** (A) Genomic sequences around gRNA target sites (underlined in

green) in intron 16 (A1) and in exon 17 (A2) as part of the transcript encoding the 1st RNase III domain of Mp*DCL1*. Sequences of wild type and the T1 double mutants Mp*FRH1*$^{GOF}$*;dcl1*$^{CRISPR}$*-2* (A1) and Mp*FRH1*$^{GOF}$*;dcl1*$^{CRISPR}$*-1* (A2) are shown, with mutations highlighted in red. (B) Genomic sequences around gRNA1 and gRNA2 target sites (underlined in green) in the exportin1-like domain in Mp*HST* in wild type and in the double mutant *FRH1*$^{GOF}$*;hst-1*. Open reading frame encoded in exon 5 of Mp*HST* is underlined in blue, mutations highlighted in red. Amino acid sequences corresponding to open reading frames are indicated above the DNA sequences. PAM = protospacer adjacent motif.

To generate stable double mutants by elimination of the CRISPR transgenes by segregation, I crossed T1 double mutants to Tak wild types. This was done to exclude the possibility that the CRISPR transgenes, which had been inserted at random in the genomes of the transformants, would generate new mutations. That could occur either at intact gRNA target sites, or in genomic off-target sites. Both events could happen during growth and development of the two Mp*FRH1*$^{GOF}$*;dcl1*$^{CRISPR}$ double mutant lines and the Mp*FRH1*$^{GOF}$*;hst*$^{CRISPR}$ double mutant and therefore affect rhizoid development. Segregation of the CRISPR transgenes away from the Mp*dcl1* and Mp*hst* mutations by crossing would render these mutant alleles stable, since no novel mutations could be introduced in the absence of the CRISPR transgenes. Co-segregation of the Mp*dcl1* and Mp*hst* mutations with the suppression phenotype, which is abundant rhizoids, would confirm that these mutations were responsible for the observed recovery of rhizoid development.

The male Mp*FRH1*$^{GOF}$*;hst*$^{CRISPR}$ double mutant produced wild type-like antheridiophores, and crossing to the female Tak-2 wild type was successful. However, attempted fertilisation of the two female Mp*FRH1*$^{GOF}$*;dcl1*$^{CRISPR}$ double mutant lines with Tak-1 wild type sperm did not produce spores. Archegoniophores on Mp*FRH1*$^{GOF}$*;dcl1*$^{CRISPR}$*-1* and Mp*FRH1*$^{GOF}$*;dcl1*$^{CRISPR}$*-2* plants were smaller and more fragile and short-living than wild

type archegoniophores (data not shown). Hence, compromised archegoniophore development caused sterility in these double mutants, similar to reduced archegoniophore viability in female Mp*FRH1*$^{GOF}$ single mutants. Although no genetically stable Mp*FRH1*$^{GOF}$*;dcl1* double mutants could be generated, there is evidence from two independent T1 primary transformants, Mp*FRH1*$^{GOF}$*;dcl1*$^{CRISPR}$*-1* and Mp*FRH1*$^{GOF}$*;dcl1*$^{CRISPR}$*-2*, that a defect in Mp*DCL1* restores rhizoid growth in the Mp*FRH1*$^{GOF}$ background.

To select stable Mp*FRH1*$^{GOF}$*;hst* lines, plants grown from the spores produced by the Mp*FRH1*$^{GOF}$*;hst*$^{CRISPR}$ x Tak-2 cross were genotyped by PCR to identify lines that did not contain the CRISPR transgene targeting Mp*HST*. Only plants that lacked the transgene were maintained. To select double mutants, I genotyped these lines for presence of the Mp*FRH1* T-DNA insertion and sequenced the Mp*HST* locus for mutations. One eighth of F2 plants was expected to be stable Mp*FRH1*$^{GOF}$*;hst* double mutants. In 30 genotyped plants, only one stable Mp*FRH1*$^{GOF}$*;hst* line (*FRH1*$^{GOF}$*;hst -1*) was identified as opposed to three to four that were expected. This was the only CRISPR transgene-less plant, which contained the T-DNA in the Mp*FRH1* promoter; no Mp*FRH1*$^{GOF}$ single mutant plant was identified. To obtain Mp*FRH1*$^{GOF}$ mutants and more genetically stable Mp*FRH1*$^{GOF}$*;hst* double mutants, I analysed 40 plants of the F2 progeny of another Mp*FRH1*$^{GOF}$*;hst*$^{CRISPR}$ x Tak-2 cross. This time, there were four stable Mp*FRH1*$^{GOF}$*;hst* double mutants and one Mp*FRH1*$^{GOF}$ single mutant. However, none of the four double mutants showed the expected suppression of the Mp*FRH1*$^{GOF}$ few-rhizoids phenotype. Furthermore, the single Mp*FRH1*$^{GOF}$ F2 mutant grew small and bushy and did not form vegetative propagules. Taken together, among 70 genotyped F2 plants, half of them contained both the Mp*FRH1* T-DNA and the CRISPR transgene targeting Mp*HST*. This suggests genetic linkage between the CRISPR and T-DNA

transgenes. It explains why fewer stable Mp*FRH1*$^{GOF}$*;hst* and Mp*FRH1*$^{GOF}$ plants lacking the CRISPR transgene that targets Mp*HST* were identified than expected from independent segregation. Possibly, the Cas9-gRNA cassette was inserted in close proximity to the endogenous Mp*FRH1* gene including the promoter-located T-DNA. This would have lowered the likelihood of recombination between both loci. Consequently, through crossing, the CRISPR transgene and the Mp*FRH1* T-DNA could only be separated in rare cases, like line Mp*FRH1*$^{GOF}$*;hst -1*. This individual represented a genetically stable double mutant, because the CRISPR transgene targeting Mp*HST* was eliminated from the genetic background, concluded from the lack of an amplification product from PCR genotyping.

Strikingly, in the genetically stable *FRH1*$^{GOF}$*;hst -1* line, the mutation in Mp*HST* had changed after crossing. It suggests that a new mutation was introduced in a formerly wild type Mp*HST* locus through CRISPR/Cas9 activity during the short diploid sporophyte phase. During subsequent meiosis, a rare recombination event might have occurred between the Mp*FRH1* T-DNA and the CRISPR transgene locus. Independent assorting of the chromosomes would then have produced a spore with the Mp*FRH1* T-DNA on one chromosome and the Mp*hst* mutation on another chromosome. This could have happened under the assumption that the Mp*FRH1* and Mp*HST* genes are located on different chromosomes. Eventually, the F2 line Mp*FRH1*$^{GOF}$*;hst -1* carried a 9 bp deletion in intron 4 and an A to T SNP followed by a 6 bp deletion in exon 5 (Figure 2.4 and Figure 2.5).

For precise phenotypic assessment of the rhizoid phenotype of the Mp*FRH1*$^{GOF}$*;hst-1* F2 double mutant compared to Mp*FRH1*$^{GOF}$ and wild type, a segregating population was generated through a Mp*FRH1*$^{GOF}$*;hst-1* x Tak-2 cross. In the resulting population, genetic diversity except for the Mp*hst* mutation and the Mp*FRH1* T-DNA would segregate equally

in all individuals. If all Mp*FRH1*$^{GOF}$*;hst-1* genotypes in this population were linked to the same phenotypic recovery of rhizoid formation, this would confirm that the Mp*hst* mutation alone is causal for it. Therefore, the rhizoid phenotypes of Mp*FRH1*$^{GOF}$*;hst-1*, Mp*FRH1*$^{GOF}$ and wild type from the same segregating genetic backgrounds were compared. Figure 2.5 shows the crossing scheme that describes the steps through which the final comparable lines were generated.

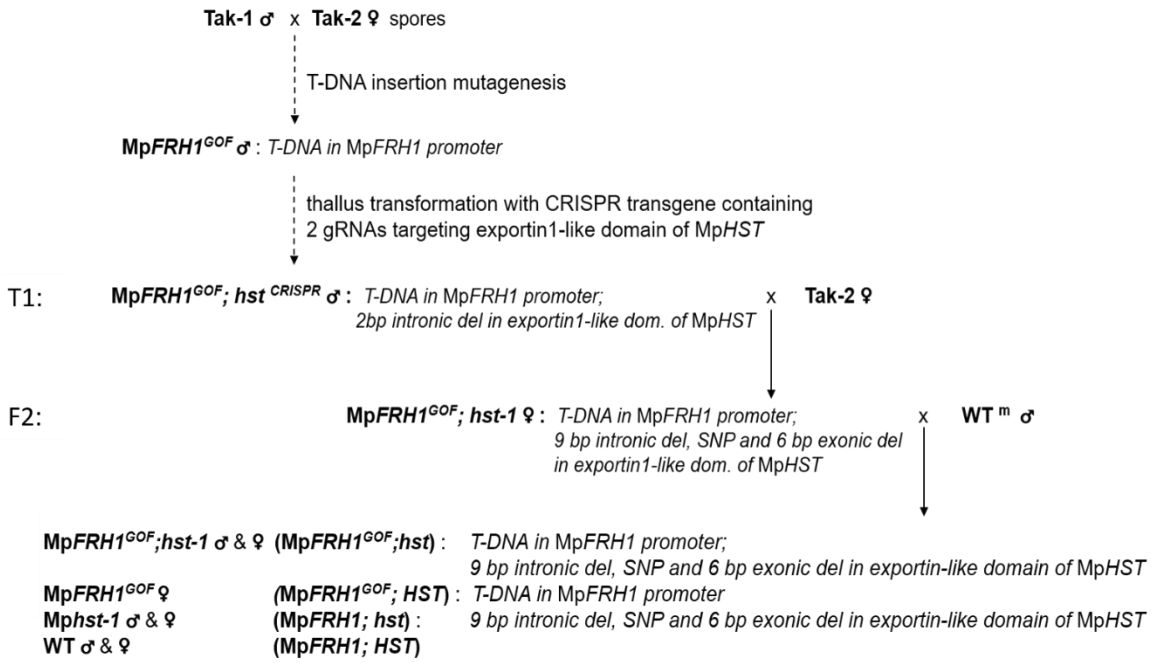


**Figure 2.5: Repeated crossing generated genetically stable and comparable Mp*FRH1*$^{GOF}$*;hst-1* mutants.** Crossing scheme: S. Honkanen identified the Mp*FRH1*$^{GOF}$ mutant in a T-DNA insertion mutagenesis screen (Honkanen et al. 2016). Thallus fragments of Mp*FRH1*$^{GOF}$ plants were transformed with a transgene encoding Cas9 and two gRNAs targeted at the exportin1-like domain of Mp*HST*. The resulting T1 transformant Mp*FRH1*$^{GOF}$*;hst*$^{CRISPR}$, which contained the CRISPR transgene, was crossed to Tak-2. The CRISPR transgene introduced a new mutation, resulting in a novel and stable *FRH1*$^{GOF}$*;hst -1* allele in the F2 progeny of the cross. This CRISPR transgene-less double mutant was crossed to a male wild type F2 line (WT$^{m}$) derived from another *FRH1*$^{GOF}$*;hst*$^{CRISPR}$ x Tak-2 cross. All resulting individuals were genetically stable at the Mp*FRH1* and Mp*HST* loci in a population of equally segregating genetic backgrounds.

Ins = insertion, del = deletion. Only genotype lines of interest for the discussed analyses are shown, they are summarised in Table 2.2. Dashed arrows indicate transformation events, black arrows point at the offspring from crosses.

**Table 2.2: Summary of mutant and wild type lines used to analyse suppression of the Mp*FRH1*$^{GOF}$ few/short-rhizoids phenotype by mutation of Mp*DCL1* and Mp*HST* in the Mp*FRH1*$^{GOF}$ background.** Superscript 'f' or 'm' indicate the female or male sex of the mutant. Superscript 'CRISPR' indicates presence of a CRISPR transgene in the genetic background of the mutant, while mutant lines without that definition are genetically stable.

| | | | mutations | | | |
|---|---|---|---|---|---|---|
| **line** | **♀/♂** | **underlying cross** | **1st RNase III domain** | **exportin1-like domain** | **T-DNA in *FRH1*** | **abundant rhizoids** |
| *FRH1*$^{GOF\,f}$ | ♀ | Tak-1 x Tak-2 | WT | WT | yes | no |
| *FRH1*$^{GOF}$*;dcl1*$^{CRISPR}$ *-1* | ♀ | Tak-1 x Tak-2 | 9 bp ins in exon 17 | WT | yes | yes |
| *FRH1*$^{GOF}$*;dcl1*$^{CRISPR}$ *-2* | ♀ | Tak-1 x Tak-2 | 5 bp del in intron 16 | WT | yes | yes |
| *FRH1*$^{GOF}$*;hst*$^{CRISPR}$ | ♂ | Tak-1 x Tak-2 | WT | 2 bp del in intron 4 | yes | yes |
| *FRH1*$^{GOF}$*;hst-1* | ♀ | *FRH1*$^{GOF}$*;hst*$^{CRISPR}$ x Tak-2 | WT | 9 bp del in intron 4; A→T SNP & 6 bp del in exon 5 | yes | yes |
| *FRH1*$^{GOF}$*;hst-1*$^{f}$ | ♀ | *FRH1*$^{GOF}$*;hst-1* x WT $^{m}$ | WT | 9 bp del in intron 4; A→T SNP & 6 bp del in exon 5 | yes | yes |
| *FRH1*$^{GOF}$*;hst-1*$^{m}$ | ♂ | *FRH1*$^{GOF}$*;hst-1* x WT $^{m}$ | WT | 9 bp del in intron 4; A→T SNP & 6 bp del in exon 5 | yes | yes |
| Wt$^{f}$ | ♀ | *FRH1*$^{GOF}$*;hst-1* x WT $^{m}$ | WT | WT | no | yes |
| Wt$^{m}$ | ♀ | *FRH1*$^{GOF}$*;hst-1* x WT $^{m}$ | WT | WT | no | yes |

### 2.3.4. Loss of Mp*DCL1* or Mp*HST* function in Mp*FRH1$^{GOF}$;dcl1* and Mp*FRH1$^{GOF}$;hst* double mutants suppresses the few/short-rhizoids phenotype of the Mp*FRH1$^{GOF}$* over-expresser mutant

To test if mutation of Mp*DCL1* and Mp*HST* in the Mp*FRH1$^{GOF}$* background could restore wild type-like rhizoid growth, I analysed the phenotypes of Mp*FRH1$^{GOF}$;dcl1$^{CRISPR}$-1*, Mp*FRH1$^{GOF}$;dcl1$^{CRISPR}$-2* and Mp*FRH1$^{GOF}$;hst-1* double mutants. I described rhizoid abundance in the double mutants and compared that to the few rhizoids in the Mp*FRH1$^{GOF}$* single mutant. 3-16-d-old Mp*FRH1$^{GOF}$* gemmae grew fewer rhizoids from their ventral surface than wild types (Figure 2.6A and E, and Figure 2.7A-B, F-G and K-L). However, more abundant rhizoids formed in the two independent Mp*FRH1$^{GOF}$;dcl1$^{CRISPR}$-1* and Mp*FRH1$^{GOF}$;dcl1$^{CRISPR}$-2* double mutants compared to the parental female Mp*FRH1$^{GOF}$* single mutant (Figure 2.6). Also, the stable male and female Mp*FRH1$^{GOF}$;hst-1* double mutants produced more abundant rhizoids than Mp*FRH1$^{GOF}$* from the same segregating population (Figure 2.7). These results indicate that independent mutagenesis of both Mp*DCL1* and Mp*HST* genes suppressed the few-rhizoids phenotype of the Mp*FRH1$^{GOF}$* over-expresser mutant.

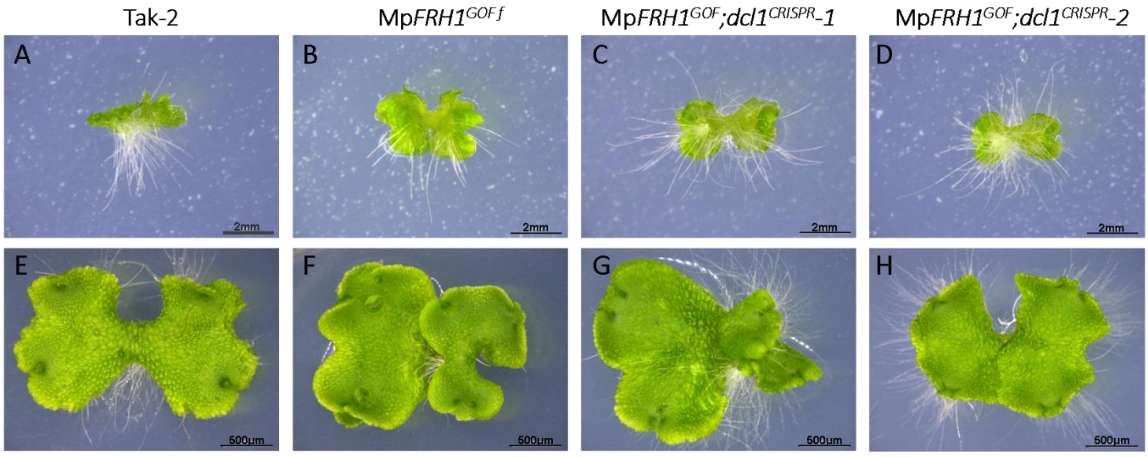


**Figure 2.6: Rhizoid abundance is restored in Mp*FRH1*$^{GOF}$*;dcl1*$^{CRISPR}$ double mutants compared to the few rhizoids in Mp*FRH1*$^{GOF}$.** Two genetically distinct T1 double mutant lines Mp*FRH1*$^{GOF}$*;dcl1*$^{CRISPR}$*-1* and Mp*FRH1*$^{GOF}$*;dcl1*$^{CRISPR}$*-2* are presented compared to their parental Mp*FRH1*$^{GOF}$ single mutant and the Tak-2 wild type, all female plants. Images are of 7-d-old and 16-d-old gemmea grown on 0.8 % Johnson's medium. (A-D) 7-d-old gemmae, (E-H) 16-d-old gemmae.

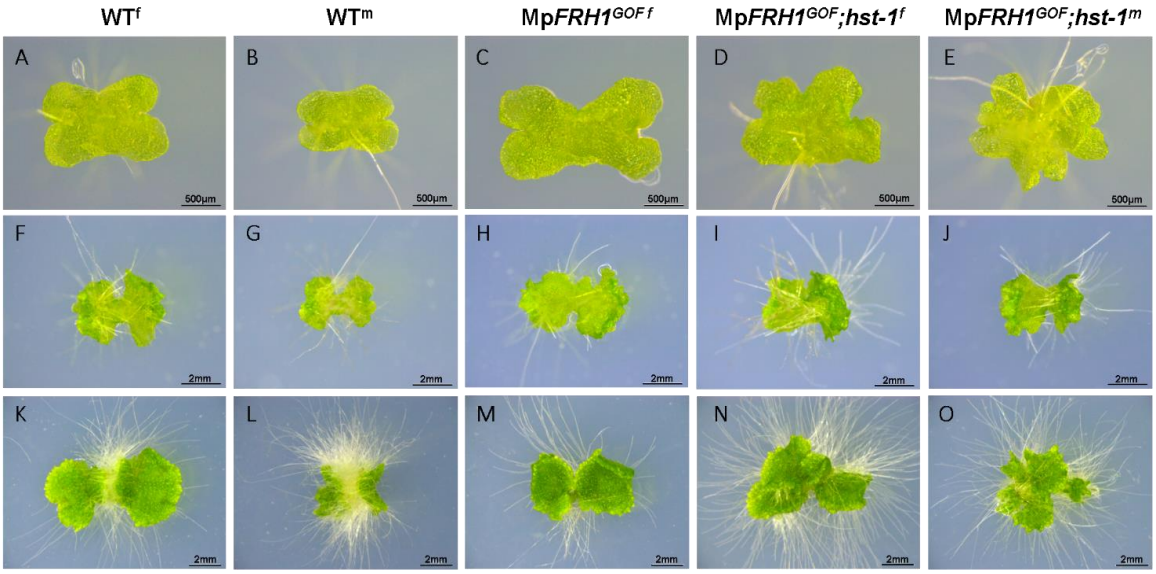


**Figure 2.7**: **Rhizoid abundance is restored in Mp*FRH1*$^{GOF}$*;hst-1* double mutants compared to the few rhizoids in the Mp*FRH1*$^{GOF}$ single mutant.** Male and female Mp*FRH1*$^{GOF}$*;hst-1* double mutant lines (D-E, I-J, N-O) are presented compared to male and female wild type (A-B, F-G, K-L) and female Mp*FRH1*$^{GOF}$ (C, H, M), all lines originated from the same segregating population. Images are of 3-11-d-old gemmae grown on 0.8 % Johnson's medium. (A-E) 3-d-old gemmae, (F-J) 6-d-old gemmae, (K-O) 11-d-old gemmae.

The few rhizoids that form in Mp*FRH1*$^{GOF}$ single mutants are shorter than wild type rhizoids. I predicted a recovery of wild type-like rhizoid length in the double mutants. To test this prediction, I measured rhizoid length in the Mp*FRH1*$^{GOF}$*;dcl1*$^{CRISPR}$*-1*, Mp*FRH1*$^{GOF}$*;dcl1*$^{CRISPR}$*-2* and Mp*FRH1*$^{GOF}$*;hst* double mutants. I grew eight gemmae from each double mutant, Mp*FRH1*$^{GOF}$ and wild type in plastic tubes filled with growth medium. I took weekly measurements of rhizoid length with a ruler and over the course of 28 or 42 days. The primary CRISPR lines Mp*FRH1*$^{GOF}$*;dcl1*$^{CRISPR}$*-1* and Mp*FRH1*$^{GOF}$*;dcl1*$^{CRISPR}$*-2* were compared to their parental female Mp*FRH1*$^{GOF}$ mutant and to Tak-2 wild type. One male and one female Mp*FRH1*$^{GOF}$*;hst-1* double mutant line were analysed in comparison to female Mp*FRH1*$^{GOF}$ (no suitable male Mp*FRH1*$^{GOF}$ line was identified in the sampled population) and male and female wild type; all genotype lines originated from the same segregating population. Rhizoid length in both Tak-2 and the other wild types increased carefully within the first two weeks of gemma growth (Figure 2.8). After two weeks, rhizoid elongation was more rapid, reaching an average length of up to 4.8 cm after four weeks in Tak-2. Rhizoids on the other wild types reached an average length of about 4 cm after six weeks. By contrast, rhizoid growth in Mp*FRH1*$^{GOF}$ single mutants ceased after two weeks, ending in a final rhizoid length of about 1 cm. This observation confirmed the importance of the Mp*FRH1* miRNA as a negative regulator of rhizoid development. Over-expression of Mp*FRH1* drastically reduced rhizoid growth. The Mp*FRH1*$^{GOF}$ short-rhizoids phenotype was suppressed in the Mp*FRH1*$^{GOF}$*;dcl1*$^{CRISPR}$*-1*, Mp*FRH1*$^{GOF}$*;dcl1*$^{CRISPR}$*-2* and Mp*FRH1*$^{GOF}$*;hst-1* double mutants, where rhizoid length resembled wild type as a consequence of restored rhizoid development. This is consistent with the hypothesis that mutating Mp*DCL1* and Mp*HST* would reduce Mp*FRH1* activity. Mp*DCL1* and Mp*HST* therefore exert negative regulatory functions on rhizoid development through positive

regulation of Mp*FRH1*. The observation that Mp*FRH1*$^{GOF}$*;hst-1* double mutant rhizoids grew longer than wild type implies that the underlying Mp*hst* mutation was strong enough to reduce Mp*FRH1* biogenesis below wild type level.

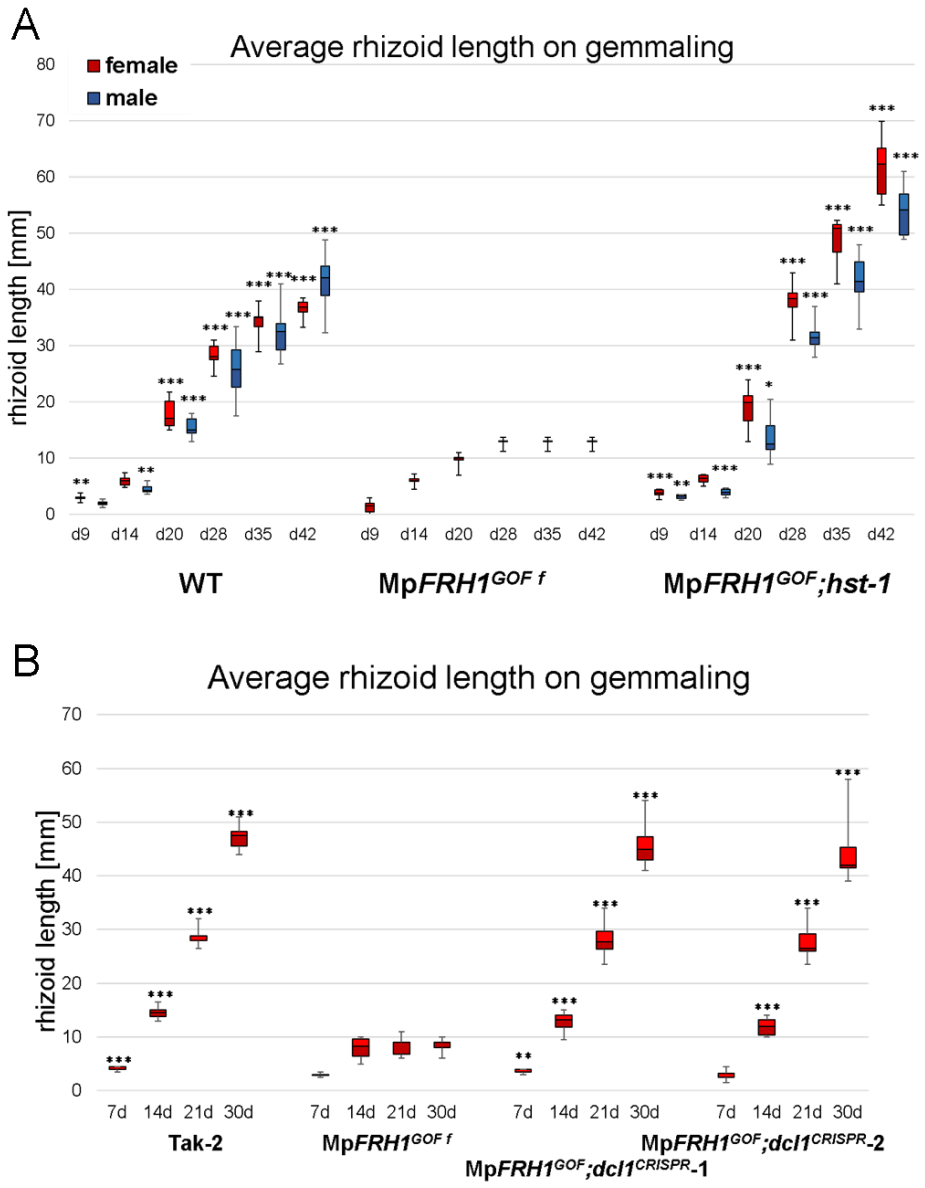


**Figure 2.8: Wild type-like rhizoid length is restored in Mp*FRH1*$^{GOF}$*;dcl1*$^{CRISPR}$ and Mp*FRH1*$^{GOF}$*;hst-1* double mutants compared to the short-rhizoids in the Mp*FRH1*$^{GOF}$ single mutant.** Weekly length measurements of rhizoids of gemmalings grown on 0.8 % Johnson's medium supplemented with phytagel. (A) Mp*FRH1*$^{GOF}$*;hst-1* compared to wild type and female Mp*FRH1*$^{GOF\,f}$ from the same progeny, female lines in

red and male lines in blue, no male Mp*FRH1*$^{GOF}$ line was available (B) female T1 lines Mp*FRH1*$^{GOF}$*;dcl1*$^{CRISPR}$*-1* and *MpFRH1*$^{GOF}$*;dcl1*$^{CRISPR}$*-2* compared to Tak-2 and parental female Mp*FRH1*$^{GOF}$. N = 8, significant differences in rhizoid length relative to female Mp*FRH1*$^{GOF}$ were calculated by two-tailed student's t-test with unequal variances. * $p < 0.05$, ** $p < 0.01$, *** $p < 0.001$.

### 2.3.5. Mp*DCL1* and Mp*HST* control biogenesis of the Mp*FRH1* miRNA

The few/short-rhizoids phenotype of the Mp*FRH1*$^{GOF}$ mutant was suppressed by mutation of Mp*DCL1* or Mp*HST* in Mp*FRH1*$^{GOF}$*;dcl1*$^{CRISPR}$*-1* , Mp*FRH1*$^{GOF}$*;dcl1*$^{CRISPR}$*-2* and Mp*FRH1*$^{GOF}$*;hst-1* double mutants. I hypothesized that a reduction in the steady state level of mature MpFRH1 miRNA was responsible for this phenotype. If Mp*DCL1* and Mp*HST* were promoters of miRNA processing in *M. polymorpha*, a reduction in Mp*FRH1* levels would be expected in Mp*FRH1*$^{GOF}$*;dcl1*$^{CRISPR}$*-1*, Mp*FRH1*$^{GOF}$*;dcl1*$^{CRISPR}$*-2* and Mp*FRH1*$^{GOF}$*;hst-1* double mutants with compromised Mp*DCL1* or Mp*HST* activity. Lower steady state levels of Mp*FRH1* in the double mutants would remove the observed hyper-repression of rhizoid development in the Mp*FRH1*$^{GOF}$ over-expresser mutant. This would explain abundant rhizoid formation in Mp*FRH1*$^{GOF}$*;dcl1*$^{CRISPR}$*-1*, Mp*FRH1*$^{GOF}$*;dcl1*$^{CRISPR}$*-2* and Mp*FRH1*$^{GOF}$*;hst-1* plants. To test this hypothesis, steady state levels of mature MpFRH1 miRNA were quantified in the Mp*FRH1*$^{GOF}$*;dcl1*$^{CRISPR}$ *-1* and Mp*FRH1*$^{GOF}$*;dcl1*$^{CRISPR}$ *-2* double mutant lines and the female *FRH1*$^{GOF}$*;hst-1*$^{f}$ double mutant compared to female Mp*FRH1*$^{GOF}$ and wild type lines. Steady state levels of primary transcript (pri-miRNA) of Mp*FRH1* were measured, because evidence from *A. thaliana* suggest co-transcriptional occurrence of miRNA processing (Fang, Cui, *et al.*, 2015). The pri-miRNA forms a characteristic hairpin-like structure, which is specifically recognised by the Dicing complex. As soon as transcription is completed, processing factors including DCL1 associate with the pri-miRNA to provide stability and to initiate dsRNA cleavage. If Mp*DCL1* and Mp*HST* were required for the early steps in miRNA biogenesis involving the primary Mp*FRH1*

transcript (pri-MpFRH1), a reduction of pri-MpFRH1 would be expected in M*FRH1*$^{GOF}$*;dcl1*$^{CRISPR}$*-1*, Mp*FRH1*$^{GOF}$*;dcl1*$^{CRISPR}$ *-2* and Mp*FRH1*$^{GOF}$*;hst-1* double mutants. Pri-Mp*FRH1* steady state levels were quantified to test whether there was evidence for co-transcriptional processing in *M. polymorpha*.

Mature miRNAs are 21 nt long. For quantification of RNA abundance by PCR, a template long enough to facilitate binding of two specific PCR primers, is required. Therefore, stem-loop PCR is a reverse transcription (RT) method, in which a stem-loop adapter is fused to the mature miRNA molecule. The resulting 60 bp long single stranded RNA can then be used as a template for quantitative PCR. I applied stem-loop RT-PCR followed by quantitative real-time PCR (qRT-PCR) for quantification of mature MpFRH1 levels in the female Mp*FRH1*$^{GOF}$*;dcl1*$^{CRISPR}$*-1*, Mp*FRH1*$^{GOF}$*;dcl1*$^{CRISPR}$ *-2* and Mp*FRH1*$^{GOF}$*;hst-1*$^{f}$ double mutants as well as Mp*FRH1*$^{GOF}$ and wild type lines described in Chapter 2.3.4. Mature MpFRH1 was amplified by stem-loop RT-PCR on total RNA extracted from 12-d-old gemmalings, From the same total RNA, cDNA for quantification of Mp*FRH1* pri-miRNA and the reference gene Mp*ADENINE PHOSPHORIBOSYL TRANSFERASE* (Mp*APT*, Saint-marcoux, Dolan, and Langdale 2015) was prepared by RT-PCR using oligo dT primers.

Steady state expression of pri- and mature MpFRH1 relative to Mp*APT* in the described genotypes is shown in Figure 2.9. Firstly, steady state levels of MpFRH1 are low in wild type plants (Honkanen, Thamm, Arteaga-Vazquez, *et al.*, 2018). Evidently, expression of the MpFRH1 pri-miRNA as well as steady state levels of mature MpFRH1 were close to 0 compared to the Mp*APT* reference gene in wild type. In Mp*FRH1*$^{GOF}$, the amount of mature MpFRH1 miRNA was about 100-times higher in than in wild type, confirming previous

results obtained in the lab (S. Honkanen, doctoral dissertation). By contrast, steady state levels of mature MpFRH1 were almost indistinguishable from wild type in the Mp*FRH1*$^{GOF}$*;dcl1*$^{CRISPR}$*-1*, *MpFRH1*$^{GOF}$*;dcl1*$^{CRISPR}$*-2* and Mp*FRH1*$^{GOF}$*;hst-1*$^{f}$ double mutants Similarly, steady state expression of pri-MpFRH1 in Mp*FRH1*$^{GOF}$ was about 17-times higher than in wild type, but equally low as wild type in the double mutants. These results demonstrate limited accumulation of mature MpFRH1 as a consequence of mutated Mp*DCL1* and Mp*HST* in *FRH1*$^{GOF}$*;dcl1*$^{CRISPR}$*-1*, *MpFRH1*$^{GOF}$*;dcl1*$^{CRISPR}$*-2* and *FRH1*$^{GOF}$*;hst-1* double mutants. They suggest that the activity of Mp*DCL1* and Mp*HST* as miRNA biogenesis regulators in *M. polymorpha* is conserved between liverworts and seed plants. Strikingly, Mp*DCL1* and Mp*HST* also influence the amount of pri-MpFRH1, which is similarly reduced in the Mp*FRH1*$^{GOF}$*;dcl1*$^{CRISPR}$*-1*, *MpFRH1*$^{GOF}$*;dcl1*$^{CRISPR}$*-2* and Mp*FRH1*$^{GOF}$*;hst-1* double mutants compared to Mp*FRH1*$^{GOF}$, as is mature MpFRH1. These data suggest a novel role for Mp*HST* in stabilising miRNA intermediates, and support the hypothesis that in *M. polymorpha*, like in *A. thaliana*, Mp*DCL1* engages with the primary miRNA transcript.

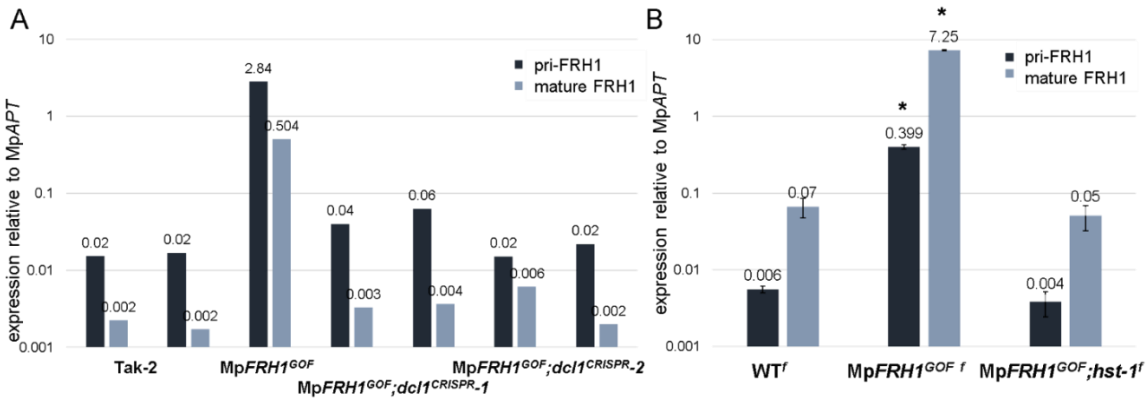


**Figure 2.9: Accumulation of pri- and mature MpFRH1 is reduced to wild type level in Mp*FRH1*$^{GOF}$*;dcl1*$^{CRISPR}$ and Mp*FRH1*$^{GOF}$*;hst-1* double mutants compared to the Mp*FRH1*$^{GOF}$ single mutant.** Average steady state expression of pri- (light blue) and mature (dark blue) MpFRH1 relative to Mp*APT* is shown, measured by qRT-PCR, n=3. Logarithmic y-axes were applied to accommodate the extreme differences in Mp*FRH1* abundance between genotypes. (A) female Mp*FRH1*$^{GOF}$*;dcl1*$^{CRISPR}$ *-1* and Mp*FRH1*$^{GOF}$*;dcl1*$^{CRISPR}$ *-2* lines compared to Tak-2 wild type and the female Mp*FRH1*$^{GOF}$ line from which the double mutants were derived by thallus transformation. Per genotype, two biological replicates were tested, apart from one for Mp*FRH1*$^{GOF}$, (B) female Mp*FRH1*$^{GOF}$*;hst-1* compared to wild type and Mp*FRH1*$^{GOF}$ from the same segregating population. Averages of relative expression were calculated from 3 biological replicates per genotype. Error bars represent standard errors. Significant differences compared to wild type were calculated by two-tailed student's t-test with unequal variances. * $p < 0.05$, ** $p < 0.01$, *** $p < 0.001$.

### 2.3.6. Mp*DCL1* and Mp*HST* negatively regulate accumulation of Mp*RSL1* mRNA, target of Mp*FRH1*

Mp*FRH1* inhibits rhizoid development by directly repressing its target gene Mp*RSL1* (Honkanen, Thamm, Arteaga-Vazquez, *et al.*, 2018). Mp*RSL1* is a conserved regulator of root hair and rhizoid differentiation (Proust et al. 2016). Rhizoids do not develop in Mp*rsl1* loss-of-function mutants, a phenotype that is similar to the Mp*FRH1*$^{GOF}$ mutant. Therefore, I hypothesised that as a consequence of reduced MpFRH1 miRNA, expression of Mp*RSL1* should be increased in Mp*FRH1*$^{GOF}$*;dcl1*$^{CRISPR}$*-1,* *MpFRH1*$^{GOF}$*;dcl1*$^{CRISPR}$*-2* and

Mp*FRH1*$^{GOF}$*;hst-1* double mutants compared to the Mp*FRH1*$^{GOF}$ single mutant. Steady state levels of Mp*RSL1* mRNA were quantified by qRT-PCR. The steady state levels of Mp*RSL1* were reduced by almost half in the Mp*FRH1*$^{GOF}$ mutant compared to wild type, confirming results shown previously in Honkanen et al. 2018. Steady state levels of Mp*RSL1* equalled or exceeded wild type levels in Mp*FRH1*$^{GOF}$*;dcl1*$^{CRISPR}$*-1*, *MpFRH1*$^{GOF}$*;dcl1*$^{CRISPR}$*-2* and Mp*FRH1*$^{GOF}$*;hst-1* double mutants, respectively (Figure 2.10). I conclude that Mp*RSL1* transcript abundance was higher in the double mutants than in the Mp*FRH1*$^{GOF}$ single mutants. In Mp*FRH1*$^{GOF}$*;hst-1*, I observed higher steady state levels of Mp*RSL1* mRNA than in wild type. This is consistent with the increase in rhizoid length beyond wild type rhizoid length in Mp*FRH1*$^{GOF}$*;hst-1* described in Chapter 2.3.4. These results are consistent with the hypothesis that disruption of MpFRH1 miRNA biogenesis by mutation of Mp*DCL1* or Mp*HST* de-represses Mp*RSL1* target gene expression and accounts for rhizoid formation in Mp*FRH1*$^{GOF}$*;dcl1*$^{CRISP}$*-1*, *MpFRH1*$^{GOF}$*;dcl1*$^{CRISPR}$*-2*and Mp*FRH1*$^{GOF}$*;hst-1* double mutants. Therefore, since Mp*DCL1* and Mp*HST* promote Mp*FRH1* miRNA biogenesis, they are negative regulators of the Mp*RSL1* transcription factor in *M. polymorpha*.

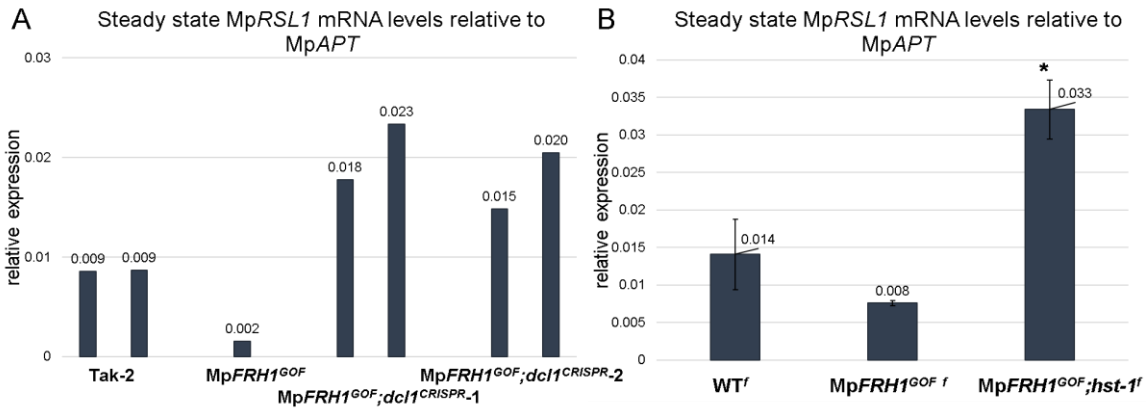


**Figure 2.10: Mp*RSL1* expression is recovered in Mp*FRH1*$^{GOF}$*;dcl1*$^{CRISPR}$ and Mp*FRH1*$^{GOF}$*;hst* double mutants compared to Mp*FRH1*$^{GOF}$.** Average steady state expression of Mp*RSL1* mRNA relative to Mp*APT* is shown, measured by qRT-PCR, n=3. (A) female Mp*FRH1*$^{GOF}$*;dcl1*$^{CRISPR}$ *-1* and Mp*FRH1*$^{GOF}$*;dcl1*$^{CRISPR}$ *-2* lines compared to Tak-2 wild type and the female Mp*FRH1*$^{GOF}$ line from which the double mutants were derived by thallus transformation. Per genotype, 2 biological replicates were tested, apart from one for Mp*FRH1*$^{GOF}$, (B) female Mp*FRH1*$^{GOF}$*;hst-1* compared to wild type and Mp*FRH1*$^{GOF}$ from the same segregating population. Averages of relative expression were calculated from 3 biological replicates per genotype. Error bars represent standard errors. Significant differences compared to wild type were calculated by two-tailed student's t-test with unequal variances. * $p < 0.05$, ** $p < 0.01$, *** $p < 0.001$.

## 2.4. Discussion

In this chapter, I showed that core regulators of the canonical plant miRNA biogenesis pathway, which have been described in *A. thaliana*, are encoded in the genome of *M. polymorpha*. I tested whether At*DCL1* and At*HST*, two important components of the pathway, were functional in miRNA biogenesis, and demonstrated that they control processing of the MpFRH1 miRNA in *M. polymorpha DCL1* and *HST* are therefore conserved regulators of miRNA processing in liverworts and flowering plants. Strikingly, weak Mp*dcl1* and Mp*hst* mutations in Mp*FRH1*$^{GOF}$*;dcl1* and Mp*FRH1*$^{GOF}$*;hst* double mutants caused full recovery of wild type-like rhizoid development in the Mp*FRH1*$^{GOF}$ few/short-rhizoids mutant background. These data are consistent with the hypothesis that Mp*DCL1* and Mp*HST* are involved in miRNA biogenesis in *M. polymorpha*. They also highlight the significance of Mp*FRH1* as a major regulator of rhizoid development in *M. polymorpha*. Mp*FRH1*$^{GOF}$*;dcl1* and Mp*FRH1*$^{GOF}$*;hst* double mutants differed from the Mp*FRH1*$^{GOF}$ single mutant mainly in rhizoid and gemma production; they were otherwise wild type-like apart from impaired reproductive competence in female Mp*FRH1*$^{GOF}$*;dcl1* plants. Strong *dcl1* and *hst* mutations cause pleiotropic developmental defects in flowering plants (Telfer and Poethig, 1998; Schauer *et al.*, 2002) which did not occur in the Mp*FRH1*$^{GOF}$*;dcl1* and Mp*FRH1*$^{GOF}$*;hst* double mutants generated here in *M. polymorpha*. It suggests that the functions of Mp*DCL1* and Mp*HST* were mildly impaired, but enough to reduce mature MpFRH1 levels and therefore allow the accumulation of the Mp*RSL1* target gene to initiate the development of abundant rhizoids. For the first time since discovery of Mp*FRH1* as a miRNA, its functional association with the miRNA biogenesis pathway was proven.

*DCL1* function in bryophyte miRNA processing was previously demonstrated in the moss *P. patens*. There, the Pp*DCL1a* paralog takes up a similar function as At*DCL1*, since the accumulation of various miRNAs is reduced in Pp*dcll1a* mutants, correlating with increased accumulation of miRNA target gene transcripts. This is not the case in Pp*dcl1b*, where miRNA levels are unchanged compared to wild type, but target gene expression is reduced due to hyper-methylation of the encoding genomic loci. My data suggest that Mp*DCL1* is a functional ortholog of At*DCL1* and Pp*DCL1a*, since defective Mp*DCL1* in Mp*FRH1*$^{GOF}$*;dcl1* double mutants reduces processing of mature MpFRH1 and increases accumulation of Mp*RSL1* mRNA. Furthermore, Mp*FRH1*$^{GOF}$*;dcl1* double mutants behave in the same way as Mp*FRH1*$^{GOF}$*;hst* double mutants, which suggests a common function of Mp*DCL1* and Mp*HST* in promoting miRNA biogenesis.

Research in *A. thaliana* has shown that the Dicing complex including AtDCL1 and many other RNA-binding proteins assembles co-transcriptionally, which is largely mediated by the elongator complex (Fang, Cui, *et al.*, 2015). According to these studies, pri-miRNAs, which are highly enriched in the chromatin fraction of the cellular extract, mediate the association of AtDCL1 with chromatin at *MIR* gene loci. It suggests the interaction between pri-miRNAs and AtDCL1 while transcription is taking place and while AtDCL1 is associated with RNA polymerase II through the elongator complex. My results show that not only mature MpFRH1 is reduced in Mp*FRH1*$^{GOF}$*;dcl1* double mutants but also the primary MpFRH1 transcript. This is untypical, since usually the reduction of mature miRNAs coincides with over-accumulation of the respective pri-miRNA due to defective downstream processing (Park *et al.*, 2002; Yang *et al.*, 2006). If Mp*DCL1* was only involved in the processing of the pri-miRNA into mature miRNA, no difference would be expected between pri-MpFRH1 levels in Mp*FRH1*$^{GOF}$*;dcl1* and Mp*FRH1*$^{GOF}$. Since in the absence of

functional Mp*DCL1*, pri-MpFRH1 as well as mature MpFRH1 miRNA accumulate less, my data indicate that Mp*DCL1* promotes accumulation of pri-miRNAs. Whether this regulation takes place through stabilisation of the pri-miRNA transcript, promotion of *MIR* gene transcription or a different mechanism of *MIR* gene expression regulation, remains to be investigated (Zhang, Liu and Yu, 2015). Generally, presence of the elongator complex in *M. polymorpha* (shown in Chapter 2.3.1) suggests occurrence of co-transcriptional miRNA processing.

Mp*HST* also functions in pri-miRNA accumulation, because MpFRH1 pri-miRNA levels were lower in the Mp*FRH1*$^{GOF}$*;hst* double mutant than in the Mp*FRH1*$^{GOF}$single mutant. The *Arabidopsis* homolog At*HST* was shown to control the accumulation of mature miRNAs and pri-miRNAs in nucleus and cytoplasm (Park *et al.*, 2005). Although At*HST* has properties of a nucleocytoplasmic transporter, there is no evidence for abolished cytoplasmic accumulation of miRNAs in At*hst* mutants. Given that At*hst* mutants develop severe pleiotropic defects, an additional function for At*HST* in stabilising pre-miRNAs was proposed. The finding that both mature MpFRH1 and pri-MpFRH1 levels are reduced in Mp*FRH1*$^{GOF}$*;hst* relative to Mp*FRH1*$^{GOF}$ mutants, suggests that Mp*HST* interacts not only with mature miRNAs, but also with pri-miRNAs. This suggests that Mp*HST* has a function in the miRNA biogenesis pathway that has not previously been described. Since Mp*HST* encodes an exportin1-like domain, its function in nucleocytoplasmic transport is likely but remains to be demonstrated. Finally, it cannot be excluded that reduction of pri-FRH1 levels together with mature FRH1 miRNA levels is a general effect of disrupted miRNA biogenesis in the Mp*FRH1*$^{GOF}$ background. Since *DCL1* and *HST* fulfil different functions in the canonical miRNA pathway, it was not expected that both Mp*FRH1*$^{GOF}$*;dcl1* and Mp*FRH1*$^{GOF}$*;hst* double mutants would show extremely similar suppression phenotypes.

There is a possibility that in the double mutants, the CamV 35S promoter as part of the T-DNA in the pMp*FRH1* promoter was silenced through interaction with the CRISPR transgene. Assuming that over-expression of Mp*FRH1* in the Mp*FRH1*$^{GOF}$ mutant results from additional CamV 35S promoter activity, stable silencing of the CamV 35S promoter would lead to the observed down-regulation of pri-MpFRH1 and consequently mature MpFRH1 miRNA levels in the Mp*FRH1*$^{GOF}$*;dcl1* and Mp*FRH1*$^{GOF}$*;hst* double mutants. To test whether increased accumulation of pri-miRNAs in these two double mutants underlies specific functions of Mp*DCL1* and Mp*HST* in miRNA biogenesis including pri-miRNA stabilisation, as opposed to T-DNA transgene silencing, pri-miRNA levels could be measured in a mutant of a miRNA pathway regulator that is unlikely to interact with pri-miRNAs. The methyltransferase HEN1 supposedly only interacts with mature miRNA duplexes that were produced by the Dicing complex (Huang *et al.*, 2009). One Mp*HEN1* ortholog is present in *M. polymorpha* and evidence shows that miRNAs are methylated in the liverwort (Lin *et al.*, 2016). Therefore, reduced Mp*HEN1* function in a Mp*FRH1*$^{GOF}$*;hen1* double mutant would not be expected to influence pri-MpFRH1 abundance. Reduced expression of pri-MpFRH1 similar to Mp*FRH1*$^{GOF}$*;dcl1* and Mp*FRH1*$^{GOF}$*;hst* double mutants however might indicate the possibility of silencing of the CamV 35S promoter insert in the Mp*FRH1* promoter.

Taken together, I have presented evidence that the functions of *DCL1* and *HST* as regulators of miRNA processing are conserved between angiosperms and bryophytes. Furthermore, I have discovered a role for Mp*HST* in regulating the abundance of the MpFRH1 pri-miRNA. This finding might help to elucidate the exact function of *HST* in the miRNA processing pathway in bryophytes and angiosperm. It might hint at a function of *HST* in pri-miRNA stabilisation additional to its proposed role in nuclear miRNA export.

# Chapter 3 – *HASTY* is a conserved regulator of the reproductive phase transition in land plants

## 3.1. Abstract

Plants undergo physiological and morphological changes as they mature. Important phase changes in the dominant diploid stage of the angiosperm life cycle are the transition from juvenile to adult vegetative growth and from vegetative to reproductive development, when the sporophyte initiates flowering. These transitions are negatively controlled by *HASTY* (*HST*), a positive regulator of miRNA processing. *HST* influences the activity of miR156/SQUAMOSA PROMOTER BINDING PROTEIN-LIKE (*SPL*) gene modules in flowering plants like *A. thaliana*, *M. truncatula* and *Hordeum vulgare*. In *A. thaliana*, loss of At*HST* function in At*hst* mutants causes the accelerated transition from juvenile to adult vegetative growth, as well as premature flowering and production of more flowers. In the haploid dominant *M. polymorpha*, reproductive phase transition occurs in the gametophyte. There, the development of antheridiophores and archegoniophores, the reproductive structures that produce sperm and eggs, respectively, is induced by far-red light. In Chapter 1 I showed that Mp*HST* is involved in miRNA biogenesis in *M. polymorpha*. Therefore, I hypothesized that the role of At*HST* as a phase change regulator might be conserved in the liverwort. To test this hypothesis, the timing of the reproductive phase transition was measured in Mp*hst* mutants. Male Mp*hst* plants formed antheridiophores earlier than WT, suggesting that Mp*HST* represses phase change. It indicates that repression of phase change through *HST* is an ancient mechanism and was present in the last common ancestor of *M. polymorpha* and *A. thaliana*. While the reproductive transition was accelerated in male Mp*hst*, it was delayed in female Mp*hst* mutants. This suggests that Mp*HST* has opposite functions in male and female *M. polymorpha* – it represses the reproductive transition in males and promotes phase change in females.

In *A. thaliana*, *HST* functions as a phase change regulator by repressing the expression of *SPL* genes, which promote phase change. *M. polymorpha* encodes 4 *SPL*

genes. 2 of those, namely Mp*SPL1* and Mp*SPL2*, contain predicted target sites for the *M. polymorpha*-specific miRNA Mpo-MIR-13 and miR529c, respectively. miR529c is a close relative to miR156, which targets *SPL* genes in *A. thaliana*. To investigate if Mp*HST* controls *SPL* genes in *M. polymorpha*, I quantified the expression of Mp*SPL1* and Mp*SPL2* in Mp*hst* plants grown in far-red light. Steady state levels of Mp*SPL1* and Mp*SPL2* were higher in male Mp*hst* compared to wild type. This is consistent with the accelerated transition to reproductive growth in male Mp*hst* relative to wild type. It suggests that Mp*SPL1* and Mp*SPL2* genes activate phase change and are negatively regulated by Mp*HST*. The observation that *SPL* genes promote phase transitions in *M. polymorpha* and *A. thaliana* suggests that *SPL* genes promoted phase change in the last common ancestor of liverworts and flowering plants. Furthermore, unaltered expression of Mp*SPL2* in female Mp*hst* mutants suggests an *SPL*-dependent basis for sex-specific reproductive timing in the dioecious liverwort.

## 3.2. Introduction

Plants undergo morphological and physiological phase changes during their life cycle. In the dominant sporophyte generation, flowering plants transition from juvenile to adult vegetative growth, and then from vegetative development to flowering (Bäurle and Dean, 2006; Huijser and Schmid, 2011). The only phase transition so far described in liverworts is the vegetative-to-reproductive phase change during the dominant gametophyte stage of the *M. polymorpha* life cycle. This means the formation of reproductive structures – gametangiophores – on male and female plants (Shimamura, 2016). The development of both, flowers and gametangiophores, is initiated from a reproductively competent meristem and is triggered by a change in day length and light quality – long days in the flowering plant and additionally far-red light supplementation in the liverwort under laboratory conditions, induce the reproductive transition (Chiyoda *et al.*, 2008; Pandey and Alam, 2016).

*HST negatively controls vegetative and reproductive phase changes in A. thaliana*

While much is known about the molecular control of phase changes in *A. thaliana*, the molecular mechanisms regulating phase change in *M. polymorpha* remain largely unknown. At*HST* was discovered as a negative regulator of both the vegetative and reproductive transition (Telfer and Poethig, 1998; Bollman *et al.*, 2003). At*hst* mutants produce fewer juvenile leaves (with adaxial trichomes) before transitioning to the adult vegetative growth phase (leaves develop abaxial trichomes in addition to adaxial trichomes (Telfer, Bollman and Poethig, 1997) and overall fewer leaves before flowering. This is explained by reduced levels of miR156, a miRNA that is important for the expression of the juvenile vegetative phase, in At*hst* mutants (Park *et al.*, 2005). Accelerated flowering in At*hst* contrasts with the delayed flowering phenotype characteristic for other miRNA biogenesis mutants like At*dcl1-7*, At*hen-1* and At*hyl-1* (Ray *et al.*, 1996; Park *et al.*, 2002; Vazquez, Gasciolli and

Cre, 2004). In these mutants, a reduction in the accumulation of the positive flowering regulator miR172 underlies defective floral timing (Park *et al.*, 2002; Tsuzuki, Takeda and Watanabe, 2014). In At*hst* on the other hand, miR172 levels were shown to be unaffected, while accumulation of miR156, an antagonist of miR172, was reduced (Park *et al.*, 2005; Gang Wu and Poethig, 2006). Therefore, At*HST* likely inhibits the floral transition as well as the adult vegetative transition by specifically promoting processing of miR156.

*The timing of vegetative and reproductive phase transitions is regulated by miR156/SPL modules*

Similar signalling pathways are active during the vegetative and the reproductive transition in flowering plants. Flowering is controlled by different pathways that integrate exogenous and endogenous cues. They all converge in regulating the expression of floral integrators like FLOWERING LOCUS T (FT) (Mouradov, Cremer and Coupland, 2002; Amasino and Michaels, 2010). Besides the photoperiod and the light quality pathways, which process blue and red/far-red light signals through light receptors, there is the miRNA-regulated ageing pathway (Wang, Czech and Weigel, 2009). This pathway not only negatively controls flowering, but also the juvenile-to-adult transition of vegetative development. It functions through antagonistic expression of miR156 and miR172 and their respective *SPL* and *APETALA 2*-like (*AP2*-like) target genes (Figure 3.1) (Bäurle and Dean, 2006). miR156 is highly expressed in the seedling, where it represses the expression of *SPL* genes, which are promoters of phase transition. As the plant ages, miR156 expression decreases, which allows the accumulation of SPL proteins (Yang, Conway and Poethig, 2011). When SPL levels exceed a certain threshold, the plant becomes competent to undergo phase transitions (He *et al.*, 2018). Vegetative and reproductive phase changes are promoted by direct activation of miR172 and floral inducers by the SPL transcription factors (Fornara and Coupland, 2009).

The function of miR172 is to repress the activity of its *APETALA 2* (*AP2*) and *AP2*-like target genes, which are phase change inhibitors (Teotia and Tang, 2015). SPL proteins constitute a conserved family of transcription factors with 16 members in *A. thaliana*, of which ten are targets of miR156 miRNA family members (Preston and Hileman, 2013). Of these ten, At*SPL9*, At*SPL13* and At*SPL15* are the main regulators of the vegetative transition. They are also involved in controlling the reproductive transition, together with SPL*2/10/11* and SPL*3/4/5* (Xu *et al.*, 2016). The activities of miR156/SPL modules in regulating the reproductive developmental phase have been demonstrated in the vascular plants *Medicago truncatula* (Wang *et al.*, 2019), *Antirrhinum majus* (Preston and Hileman, 2010), wheat (Bingnan Wang *et al.*, 2015), tomato (Salinas *et al.*, 2011), rice (Xie, Wu and Xiong, 2006) and maize (Chuck *et al.*, 2007, 2010). The miR156/SPL module is also conserved in the non-vascular plant *P. patens*. There, miR156 is not a repressor but a promoter of the reproductive transition, while Pp*SPL* genes have inhibitory roles (Cho, Coruh and Axtell, 2012a). This shows that the miR156/SPL module is conserved in land plants but functions differently in different species.

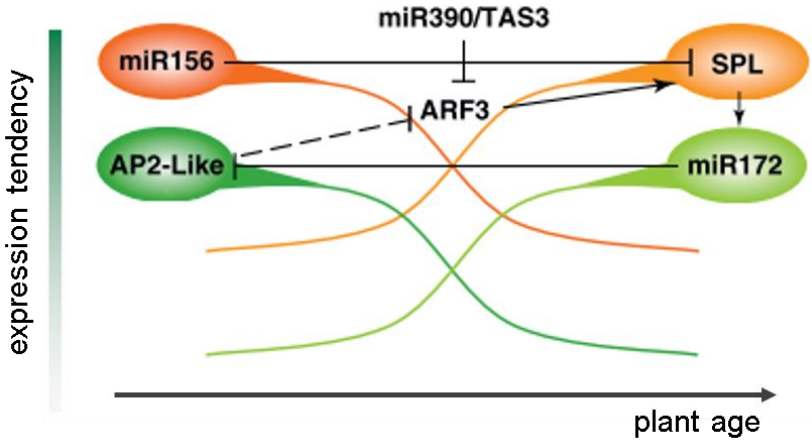


**Figure 3.1: Expression dynamics of phase change regulators during developmental transitions in *A. thaliana*.** From Rubio-somoza and Weigel, 2011. Dashed lines indicate speculative interactions, arrows indicate positive and T-lines indicate negative interactions.

*miRNA-targeted SPL genes were identified in M. polymorpha*

Small RNA sequencing and RACE PCR experiments identified miRNA/SPL gene modules. in *M. polymorpha* (Tsuzuki *et al.,* 2016). Although *MIR156* is present in the liverwort genome, it is not or very lowly expressed, presumably because it forms a bulky hairpin structure that cannot be recognised by DCL proteins. Instead, presence and activity of miR529c was detected, which is a close relative of the miR156 family. *MIR529* was present in the last common ancestor (LCA) of land plants, but was lost in the LCA of eudicots, hence is absent in *A. thaliana* (Cuperus, Fahlgren and Carrington, 2011). miR156 and miR529 share 14-16 bp of sequence homology and have overlapping binding sites in their common targets (Zhang *et al.,* 2015). They cooperatively target SBP-box proteins in maize (Chuck *et al.*, 2010). In *M. polymorpha*, miR529c was shown to cleave the mRNA of Mp*SPL2*, one of four Mp*SPL* genes. Another miRNA, the liverwort-specific Mpo-MR-13, cleaves the Mp*SPL1* transcript. Since the AtSPL8 homolog of MpSPL1 is not a target of miR156 in *A. thaliana* (Unte *et al.,* 2003; Zhang *et al.*, 2007), this suggests an additional miRNA-mediated mechanism of *SPL* gene regulation in *M. polymorpha*. Unlike miR529c as a putative phase change inhibitor, miR172 is not conserved in the liverwort. These findings suggest that although conserved *SPL* genes are present in *M. polymorpha*, they are likely regulated by different miRNAs than the conserved miR156 and miR172 in angiosperms.

In this chapter, I investigate the reproductive phase transition in *M. polymorpha*. I describe the timing of gametangiophore development in wild type and test if mutations in Mp*HST* affect this transition. I analyse the expression of Mp*SPL* genes in Mp*hst* mutants to test if the function of angiosperm *SPL* genes in regulating phase change is conserved in liverworts. Through phenotyping and quantification of Mp*SPL* expression levels in Mp*hst* mutants, I

show that phase change control through *HST* and *SPL* genes is conserved between *A. thaliana* and *M. polymorpha*.

## 3.3. Results

### 3.3.1. *M. polymorpha* undergoes reproductive phase transition upon exposure to far-red light

Far-red light promotes reproductive growth – the development of gametangiophores – in the dominant haploid gametophyte stage of the *M. polymorpha* life cycle (Shimamura, 2016). I first determined the timing of reproductive development in wild type *M. polymorpha*. The described male and female wild types were F2 wild type lines obtained from a crossing between a T1 Mp*hst* CRISPR mutant and a Tak-2 wild type. The Mp*hst* line had been generated by transformation of wild type spores from a Tak-1 x Tak-2 crossing with a CRISPR transgene mutating Mp*HST*. After 19 days of growth in far-red light, male F2 wild type plants produced antheridiophores (Figure 3.2C). Female wild type plants formed archegoniophores after 28 days. Gametangiophore development required far-red light exposure, because no gametangiophores formed in wild type plants grown in cool white light without far-red enrichment for 12 weeks. Therefore, under far-red inductive conditions, female reproductive organs develop on average nine days later than the male ones.

Gametangiophores are initiated in the apical meristems of the thallus (Shimamura, 2016), and male and female gametangiophores are morphologically different in wild type plants (Figure 2.3B). Both form a stalk, which elevates a receptacle above the thallus. The receptacle of the antheridiophore is a flat, round cap (Figure 2.3B), whereas the archegoniophore is an umbrella-like structure with eight to nine pronounced, finger-like lobes (Figure 2.3A). In summary, the reproductive phase transition in the dioecious *M. polymorpha* depends on far-red light and occurs later in female than in male wild type plants.

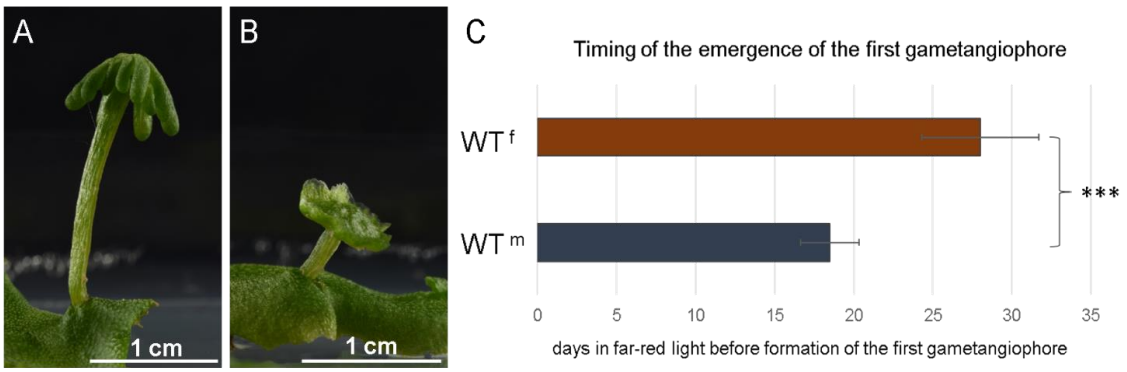


**Figure 3.2: In *M. polymorpha* wild type, male gametangiophores (antheridiophores) are produced earlier than female gametangiophores (archegoniophores).** Images of archegoniophore in Tak-2 (A), and antheridiophore in Tak-1 (B) growing out of thalli after exposure to far-red light, images were taken from 6-weeks-old plants. (C) Timing of the reproductive phase transition is quantified by the number of days in far-red light that passed until the emergence of the first gametangiophore. Male and female wild type are F2 individuals generated by a cross between a T1 Mp*hst* CRISPR mutant and Tak-2. Error bars represent standard deviations. The timely difference in gametangiophore emergence between male and female is highly significant according to a two-tailed student's t-test with unequal variances at *** $p<0.001$, $n = 8$.

### 3.3.2. *HASTY* is a conserved regulator of the timing of the reproductive phase transition in land plants

In flowering plants, developmental phase changes are controlled by *HST*. Since At*hst* loss-of-function mutants flower earlier than wild type, At*HST* is considered as a repressor of the reproductive phase (Telfer and Poethig, 1998). To investigate if this function of *HST* is conserved among land plants, I described the phase change phenotype of Mp*hst-1* mutants in *M. polymorpha*. These Mp*hst-1* mutants were offspring of a cross between the Mp$FRH1^{GOF}$;$hst^{CRISPR}$-*1* double mutant and Tak-2. The Mp$FRH1^{GOF}$;$hst^{CRISPR}$-*1* double mutant had been generated through CRISPR/Cas9 mutagenesis, as described in Chapter 2.3.3, and contained the CRISPR transgene targeting Mp*HST*. Mp*hst-1* plants were identified from the offspring of the Mp$FRH1^{GOF}$;$hst^{CRISPR}$-*1* x Tak-2 cross by genotyping of F2 plants. Absence of the T-DNA from the promoter of Mp*FRH1* confirmed that the

Mp*FRH1* locus was wild type. Absence of the CRISPR transgene targeting Mp*HST* confirmed that Mp*hst-1* mutants were genetically stable because they had lost the CRISPR transgene through independent segregation of the chromosomes. To identify the underlying mutations, the Mp*HST* locus was sequenced around the gRNA target sites. One male and one female Mp*hst-1* line both contained the same 9 bp deletion in intron 4 (position 2253-2261) and an A to T SNP followed by a 6 bp deletion in exon 5 (position 2329-2335), which did not affect steady state expression of Mp*HST* mRNA (Appendix Figure A1). Instead, the mutations in exon 5 caused the exchange of one and the loss of two amino acids. These changes likely influenced the integrity and functionality of the exportin1-like domain. Evidence that this Mp*hst-1* allele caused a loss of function in Mp*HST* came from the observation that the exact same mutation suppressed the few rhizoids phenotype of the Mp$FRH1^{GOF}$ background in Mp$FRH1^{GOF}$;*hst-1* double mutants by inhibiting Mp*FRH1* biogenesis (Chapter2.3.4).

To analyse the timing of the reproductive phase transition, I first grew Mp*hst-1* and wild type of both genders and from the same segregating F2 population in cool white light and on agar medium for 14 days. The mature thalli were then transferred to soil and grown in far-red light conditions to stimulate transition to reproductive development. For each genotype and gender, I analysed 8 plants grown from genetically identical gemmae, the vegetative reproductive clones produced by *M. polymorpha*. For each plant, I quantified the emergence of the first gametangiophore, which marks the transition to reproductive growth. This is visible by the outgrowth of a small bulge from an apical notch of the thallus, from which the full gametangiophore, including a stalk, develops. I counted the number of days of growth in far-red light that passed until the first gametangiophore emerged on a plant (Figure 3.3). While male wild type initiated reproductive growth after 19 days, male Mp*hst-*

*1* formed the first gametangiophore after 12 days. Therefore, the reproductive transition was accelerated by seven days in male Mp*hst-1* relative to wild type. This is consistent with the accelerated flowering transition in At*hst-1* and confirms that *HST* is a conserved negative regulator of phase transition in land plants. When Mp*hst* mutants were grown in continuous white light without far-red light supplementation, they did not form gametangiophores. This resembles the requirement of far-red light and long days for flowering in At*hst-1* mutants. It provides supporting evidence that the specific function of *HST* in controlling the timing of reproductive phase change downstream or independent of far-red light signalling pathways is conserved.

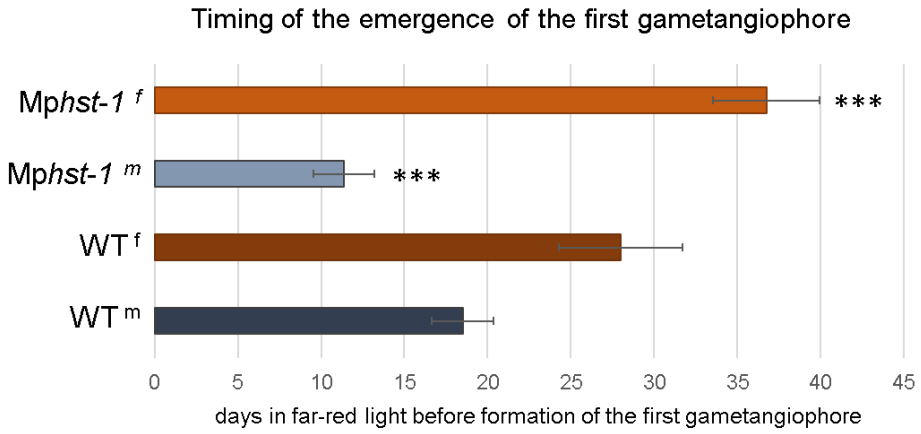


**Figure 3.3: Male and female Mp*hst-1* produce gametangiophores earlier and later than wild type, respectively.** Average number of days of growth in far-red light before emergence of the first gametangiophore, n = 8, error bars represent standard deviations. Significant differences between wild type and mutant of the same sex were calculated by two-tailed student's t-test with unequal variances. * $p < 0.05$, ** $p < 0.01$, *** $p < 0.001$.

### 3.3.3. Mp*HST* negatively regulates the timing of the reproductive phase transition in males and positively regulates the timing of the reproductive phase transition in females

To assess if the Mp*hst-1* mutation also affects female reproductive timing, the timely appearance of the first archegoniophore was compared between Mp*hst-1* and wild type.

While atheridiophores in male Mp*hst-1* appeared before wild type, female archegoniophores developed on average nine days later in Mp*hst-1* than in wild type (Figure 3.3). This suggests that Mp*HST* is a positive regulator of the reproductive transition in female plants. Mp*HST* therefore fulfils opposite functions in the two sexes of the dioecious liverwort *M. polymorpha*. Consequently, the timely delay in reproductive transition between male and female is extended from nine days in wild type to 26 days in Mp*hst-1*.

### 3.3.4. *M. polymorpha* encodes Mp*SPL* genes homologous to miRNA targeted At*SPL* genes from *A. thaliana*

As a promoter of miRNA biogenesis, At*HST* regulates flowering time by modulating the abundance of miR156, which in turn inhibits the expression of *SPL* genes (G. Wu and Poethig, 2006). *SPL* transcription factors are positive regulators of phase transition and conserved throughout the flowering plants; their functions have been demonstrated in *A. thaliana* (Fornara and Coupland, 2009), *Fagopyrum tataricum* (Liu *et al.*, 2019), *Hordeum vulgare* (Tripathi, Bregitzer and Singh, 2018), *Gossypium* (Cai, Guo and Zhang, 2018) *Populus trichocarpa* (Li and Lu, 2014) and *Medicago truncatula* (Wang *et al.*, 2019). There are 16 members in the *A. thaliana SPL* gene family, and Tsuzuki et al. 2016 has reported the presence of two miRNA-targeted *SPL* genes in *M. polymorpha*. To independently confirm Mp*SPL* orthologs and analyse their phylogenetic relationship with the At*SPL* proteins, I undertook BLAST search and built a gene tree. I retrieved amino acid sequences of all 16 At*SPL* members from the TAIR homepage and used the BLAST function to search for Mp*SPL* orthologs in the *M. polymorpha* proteome on the phytozome website. I then confirmed the found hits in OrthoFinder, where orthologous genes are cumulated in orthogroups (Emms and Kelly, 2015). *M. polymorpha* encodes 4 Mp*SPL* genes with highly conserved SBP domains – Mp*SPL1* (Mapoly0014s0224), Mp*SPL2* (Mapoly0014s0223), Mapoly0008s0031 and Mapoly0019s0134. Mp*SPL1* and Mp*SPL2* were predicted to contain

miRNA target sites (Tsuzuki et al. 2016, Figure 3.5). To understand the phylogenetic relatedness of the Mp*SPL*s to the At*SPL*s, I constructed a phylogenetic tree based on amino acid sequences of the highly conserved SBP domains, which confer DNA-binding activity and nuclear localisation (Figure 3.6). I included 7 *SPL* genes from the moss *Physcomitrella patens*, which I identified by BLAST search of At*SPL* protein sequences against the *P. patens* proteome on the phytozome homepage. The amino acid sequences of the SBP domains were retrieved from the TAIR (At*SPL*s) and phytozome (Mp*SPL*s and Pp*SPL*s) websites and aligned online in MAFFT (Katoh, Rozewicki and Yamada, 2017). On the MAFFT website, a phylogenetic tree was built using neighbour joining with 1000 bootstrap resampling steps, and visualisation in phylo.io (Kuraku *et al.*, 2013; Robinson, Dylus and Dessimoz, 2016).

The At*SPL* genes fall into eight separate clades (Preston and Hileman, 2013). Clades IV-VIII comprise At*SPL* genes that are regulated by the miR156/157 family (Figure 3.5 and Figure 3.6), whereas At*SPL* genes in clades I-III do not contain these miRNA target sites. Three Mp*SPL*s are members of clades I, II and III: Mapoly0008s0031 groups in clade I, which indicates that it is most similar to At*SPL7*. Mapoly0019s0134 is in clade II and therefore most similar to At*SPL14*, At*SPL12* and At*SPL1*. Mp*SPL1*, most similar to At*SPL8*, falls into clade III. Mp*SPL2* forms a clade that is sister branch to three Pp*SPL*s, Pp3c16_7490V3, Pp3c25_8630V3 and Pp3c16_7480V3. Therefore, Mp*SPL2* is most closely related to these three moss *SPL*s. Furthermore, it is more closely related to the miRNA-targeted At*SPL* genes in clades IV, V, VII and VIII than to the At*SPL* genes that are not regulated by miRNAs. Since Mp*SPL2* contains a target site for miR529c, a close relative of the miR156 family (Figure 3.5), this supports its phylogenetic position close to the miR156-targeted At*SPL* clades IV, V, VII and VIII. However, with a bootstrap value of 10,

this branch is not well-supported. Hence, only vague assumptions can be made about functional resemblance of Mp*SPL2* to the At*SPL* members of clades IV, V, VII and VIII based on sequence similarity.

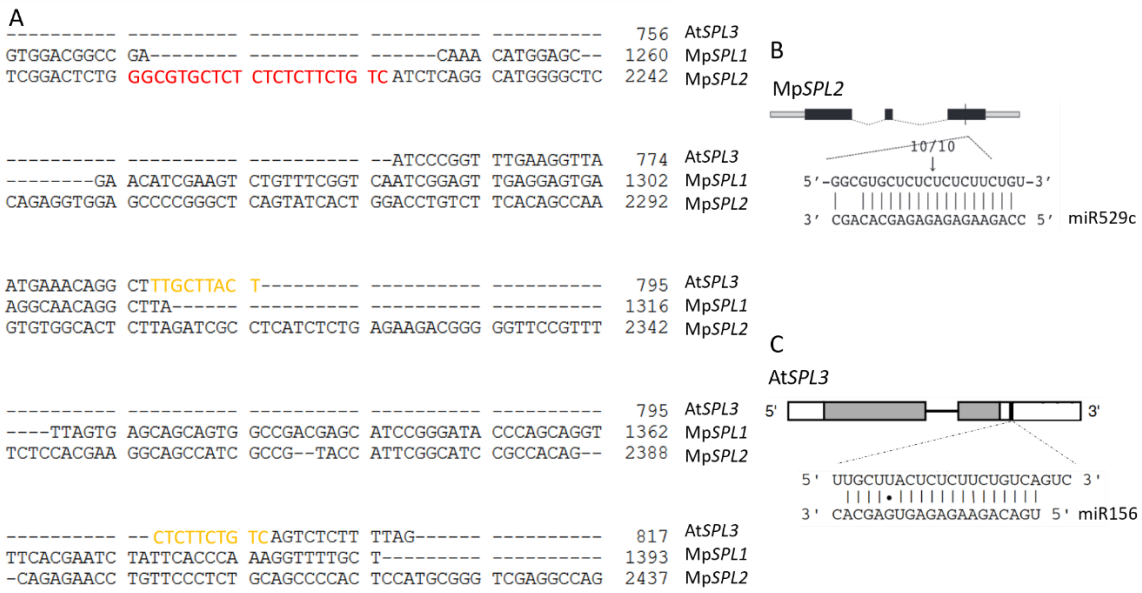


**Figure 3.5: Mp*SPL1* and Mp*SPL2* genes lack the miR156 target site that is conserved in At*SPL* genes.** (A) Multiple sequence alignment of At*SPL3*, Mp*SPL1* and Mp*SPL2* transcript sequences around miR156 (yellow) and miR529c (red) target sites. (B) from Tsuzuki *et al.*, 2016 – miR529c cleavage site in Mp*SPL2* as determined by 5'RACE PCR, miR529c target position is indicated by arrowheads, together with the number of RACE clones. Black bars represent exons and white bars represent untranslated regions in Mp*SPL2*. (C) from Wu and Poethig, 2006 – miR156 cleavage site in At*SPL3* as determined by 5'RACE PCR, its position in At*SPL3* is indicated by a black vertical line. In the genomic structure of At*SPL3*, grey boxes indicate coding sequences and white boxes indicate untranslated regions.

The At*SPL* members of clades IV, V, VII and VIII partly redundantly regulate processes associated with vegetative and reproductive phase change, including flowering. Regulation by miR156/157 contributes to a timely precise At*SPL* gene expression pattern. Since Mp*SPL2*, which has sequence similarity to At*SPL* members of these four clades, is target of

miR529c (Figure 3.5), this module might also regulate phase change in *M. polymorpha*. At*SPL8* regulates the development of anthers, the male reproductive organs in flowering plants, as well as gibberellic acid signalling, both of which are relevant for reproductive development (Unte *et al.*, 2003; Zhang *et al.*, 2007). If the gibberellic acid signalling pathway is somehow conserved in *M. polymorpha*, the Mp*SPL1* ortholog might be a regulator of the development of reproductive structures. This possibility is supported by the finding that Mp*SPL1* mRNA is cleaved by Mpo-MR-13 (Tsuzuki *et al.*, 2016), resembling miR156-mediated regulation of phase change-related At*SPL* genes. Mapoly0019s0134 and its ortholog At*SPL14* are not miRNA targets; however, At*SPL14* was shown to delay the adult reproductive growth phase and therefore flowering (Stone, Nekl and Stiers, 2005). This indicates the possibility that Mapoly0019s0134 might also affects reproductive transition in *M polymorpha*. Taken together, the phylogenetic relationships between Mp*SPL*s and functionally characterised At*SPL*s suggest that Mp*SPL*s likely control different aspects of phase transition or the expression of the reproductive phase. This would indicate that *SPL*-mediated regulation of developmental transitions is an ancestral mechanism that was adapted in plant families with different life cycles and reproductive structures. I began to test this hypothesis in the following paragraphs.

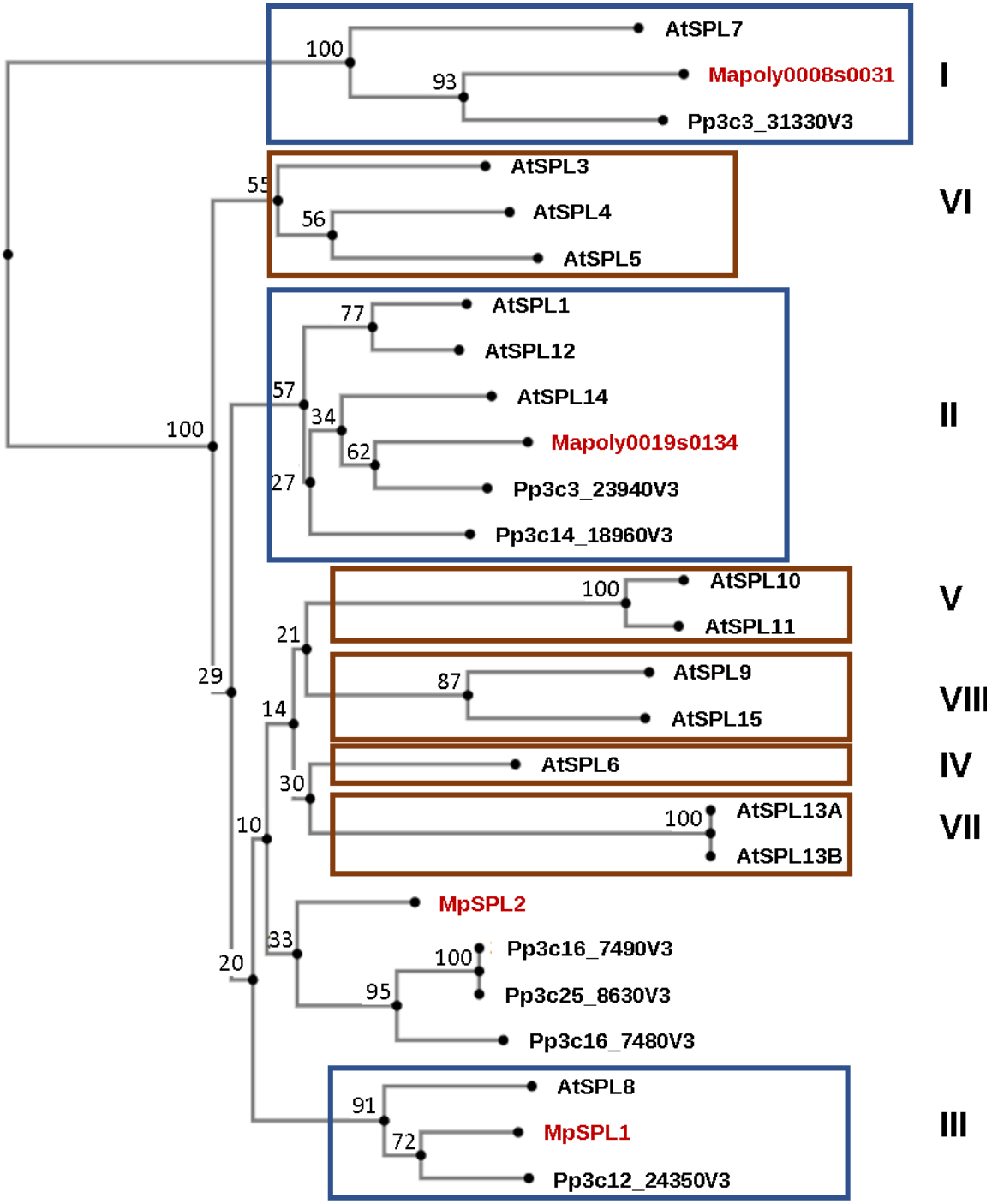


**Figure 3.6: *M. polymorpha* encodes four Mp*SPL* genes that are orthologous to SBP domain containing At*SPL* genes in *A. thaliana*.** The phylogenetic tree was built using the SBP domains from *A. thaliana*, *P. patens* and *M. polymorpha* SPL proteins. Since At*SPL2* and its *M. polymorpha* and *P. patens* orthologs do not contain SBP domains, those were excluded from the phylogenetic analysis. Amino acid sequences were retrieved from the TAIR and phytozome online repositories. They were aligned online in MAFFT, where subsequently a tree was constructed through neighbour joining with 1000 bootstrap

resampling steps. The phylogenetic tree was visualised in phylo.io. *M. polymorpha* orthologs are highlighted in red. Numbers at the nodes indicate support values for the respective clades. *SPL* clades were assigned according to (Preston and Hileman, 2013) – dark blue boxes frame clades whose At*SPL* members are not target genes of miR156/miR157, whereas members of clades in brown boxes are.

### 3.3.5. *SPL* gene-mediated control of phase change is an ancestral mechanism in land plants

Wu and Poethig, 2006 discovered that At*HST* negatively regulates At*SPL3*, since steady state levels of At*SPL3* were higher in the At*hst-6* mutant than in wild type during the juvenile-to-adult transition of vegetative development (Gang Wu and Poethig, 2006). To investigate if *HST*-mediated repression of *SPL* genes during phase transition is conserved in the non-flowering plants, I quantified steady state mRNA levels of Mp*SPL* genes in Mp*hst-1* mutants. Mp*SPL1* and Mp*SPL2* mRNA levels were measured in gemmalings that grew in white light without far-red light enrichment for 12 days. Using qRT-PCR, I measured steady state expression of Mp*SPL1* and Mp*SPL2* mRNAs relative to the Mp*APT* reference gene as described in Chapter 2.3.5-2.3.6. Figure 3.6A shows that Mp*SPL1* and Mp*SPL2* mRNA levels are similar in Mp*hst-1* and wild type. This suggests that Mp*HST* does not regulate Mp*SPL1*and Mp*SPL2* expression during vegetative growth in cool white light. I hypothesised that exposure to far-red light would trigger the molecular response that initiates reproductive transition, including an increase in Mp*SPL* mRNA levels. As the reproductive transition occurs earlier in male Mp*hst-1* mutants than in wild type, I predicted higher steady state levels of Mp*SPL1* and Mp*SPL2* mRNAs in male Mp*hst-1* compared to wild type. To test this prediction, I transferred Mp*hst-1* and wild type gemmalings to far-red light conditions for nine days, after initial growth in cool white light for five days. Before outgrowth of gametangiophores, gemmalings were harvested and frozen. Total RNA was isolated from this plant material and Mp*SPL1* and M*SPL2* mRNA levels were quantified by

qRT-PCR. The abundance of Mp*SPL1* mRNA relative to Mp*APT* was significantly higher in male and female Mp*hst-1* mutants compared to wild type (Figure 3.7B). This suggests that Mp*SPL1* expression is increased in the absence of functional Mp*HST*. Since this reflects the behaviour of At*SPL3* in At*hst-6*, I conclude that *SPL* gene-mediated control of phase change is a conserved mechanism in flowering and non-flowering plants and is repressed by *HST*.

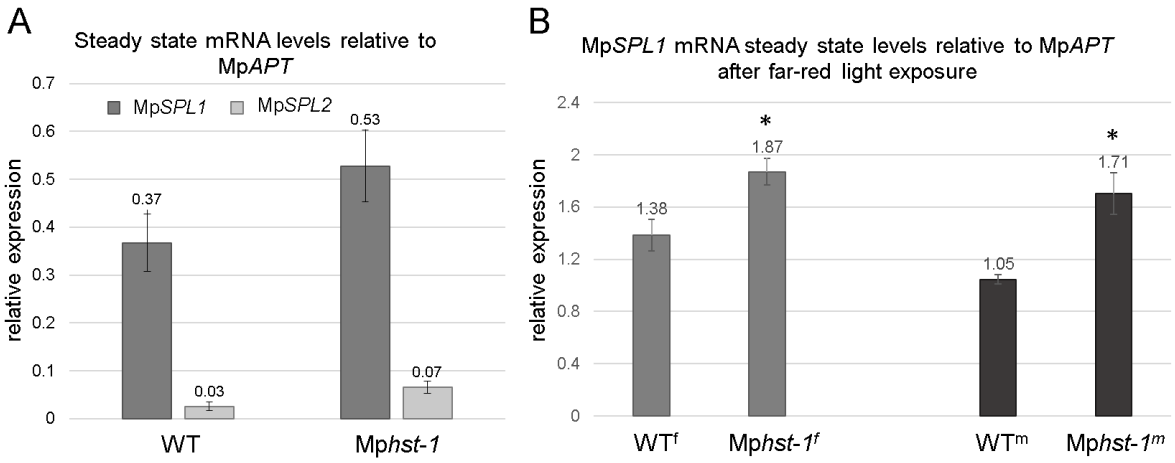


**Figure 3.7: Induction of reproductive phase transition by far-red light causes higher steady state levels of Mp*SPL1* in Mp*hst-1* than in wild type.** (A) steady state levels of Mp*SPL1* and Mp*SPL2* mRNA during vegetative growth in 12-d-old female wild type and Mp*hst-1* gemmalings grown in white light. (B) Steady state levels of Mp*SPL1* mRNA in female (light grey) and male (dark grey) wild type and Mp*hst-1* gemmalings after five days of growth in white light followed by far-red light supplementation for nine days. Mean relative expression from three biological replicates, with standard error. Significant differences between wild type and mutant were calculated by two-tailed student's t-test with unequal variances. * $p < 0.05$, ** $p < 0.01$, *** $p < 0.001$.

#### 3.3.5.1. Mp*SPL2* is expressed differently in the two sexes of the dioecious *M. polymorpha* during reproductive phase transition

Male and female Mp*hst-1* mutants develop opposite defects in reproductive phase transition – while males enter reproductive development about seven days earlier than wild type,

females transition around nine days later than wild type. In Mp*hst-1* mutants of both genders, Mp*SPL1* mRNA levels are higher than in wild type after nine days of growth in far-red light conditions. To investigate if the gender-specific phase change phenotype in Mp*hst-1* can be explained by differential expression of other Mp*SPL* genes, I measured steady state levels of Mp*SPL2* mRNA. I tested the same genotype lines with the same experimental setup as in Chapter 3.3.6. While Mp*SPL2* was expressed similarly in female wild type and female Mp*hst-1* after nine days of far-red light induction, steady state levels of Mp*SPL2* in male Mp*hst-1* were almost three times higher than in male wild type (Figure 3.8). This gender-specific difference in gene expression suggests that higher levels of Mp*SPL2* transcript in male Mp*hst-1* mutants might be responsible for the accelerated timing of the reproductive transition in male relative to female Mp*hst-1* plants. In summary, I demonstrated that Mp*SPL2* levels increase in response to defective Mp*hst* in male *M. polymorpha*. This suggests that Mp*SPL2*, like Mp*SPL1*, is usually repressed by Mp*HST*, but activated during reproductive phase change. Since flowering plant *SPL*s are positive regulators of phase change, this indicates an ancestral function of *SPL* genes to promote the reproductive growth phase. In the dioecious *M. polymorpha*, the enhanced shift in reproductive timing between male and female Mp*hst-1* mutants is reflected in differential Mp*SPL2* expression between the sexes. Therefore, Mp*SPL* genes are likely involved in regulating the sexual dimorphism in male and female *M. polymorpha* plants during the reproductive phase transition.

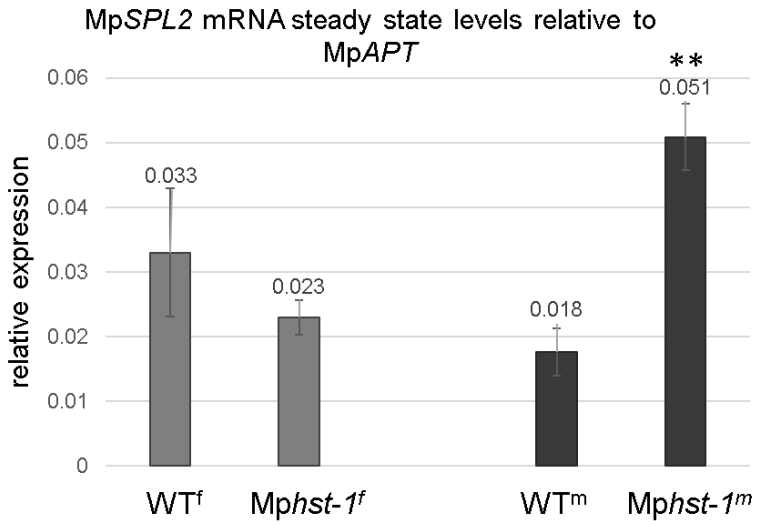


**Figure 3.8: Induction of reproductive phase transition by far-red light causes an increase in Mp*SPL2* mRNA levels in male Mp*hst-1* compared to male wild type, but not in female Mp*hst-1* compared to female wild type.** Steady state levels of Mp*SPL2* mRNA in female (light grey) and male (dark grey) wild type and Mp*hst-1* gemmalings after five days of growth in white light followed by nine days of far-red light supplementation. Mean relative expression from three biological replicates, with standard error. Significant differences between wild type and mutant were calculated by two-tailed student's t-test with unequal variances. * $p < 0.05$, ** $p < 0.01$, *** $p < 0.001$.

## 3.4. Discussion

In this chapter I demonstrated that the function of *HST* as a negative regulator of phase transitions in angiosperms is conserved in the liverwort *M. polymorpha*. Gametangiophores developed precociously in male Mp*hst-1* mutants. Taken together with the accelerated flowering phenotype in At*hst-1* mutants, this suggests that *HST*-mediated control of the timing of the reproductive phase transition is a mechanism that was likely present in the common ancestor of liverworts and flowering plants. However, while this is true in male *M. polymorpha*, gametangiophore development was delayed in female Mp*hst* mutants. Therefore, Mp*HST* inhibits phase change in male plants and promotes phase change in female plants. This suggests that Mp*HST* is involved in controlling the sexual dimorphism during the reproductive phase transition, whereby it might interact with sex-specifically expressed genetic factors. There is no obvious evidence that the development of carpels and stamens, the female and male floral organs, is affected differently in flowers of At*hst* mutants, although At*hst* mutants produce a reduced seed set (Telfer and Poethig, 1998). It would be instructive to study if *HST* has a gender-specific effect on the timing of the reproductive phase transition in other dioecious species.

To investigate if Mp*SPL* genes regulate phase change, I measured Mp*SPL* expression in gemmalings of the Mp*hst-1* mutant after nine days of growth in inductive far-red light conditions. A loss of Mp*hst* function caused higher accumulation of Mp*SPL1* and Mp*SPL2* transcripts in male Mp*hst-1* mutants than in wild type. This suggests that Mp*HST* negatively regulates the expression of Mp*SPL1* and Mp*SL2* in male plants. Since the reproductive transition is accelerated in male Mp*hst-1* mutants, this suggests that Mp*SPL1* and Mp*SPL2* activate this transition. My results are consistent with the observation that steady state levels of At*SPL3* mRNA are higher in At*hst-6* mutants than in wild type in later stages of

development but not until 14 days after germination. Taken together, the mechanism by which accumulation of SPL transcription factors promotes phase change under negative regulation by *HST*, is conserved between *A. thaliana* and *M. polymorpha*. In the moss *P. patens*, the expression pattern of Pp*SPL3* is opposite to that of At*SPL3* – Pp*SPL3* mRNA levels are lowest during the transition from protonemal growth to leafy gametophore (Cho, Coruh and Axtell, 2012). Therefore, the mechanism of phase change regulation is more similar in *M. polymorpha* and *A. thaliana* than it is in *P. patens*. This indicates that *SPL* genes as regulators of phase change are conserved among bryophytes but operate differently in different bryophyte lineages. It would be informative to see whether the negative regulatory function of SPL genes during phase change in *P. patens* is specific to this moss species, or whether it can be found in other bryophytes and even angiosperms.

While Mp*SPL1* mRNA levels were higher than wild type in Mp*hst-1* mutants of both genders of the dioecious liverwort, Mp*SPL2* transcript levels were only higher than wild type in male Mp*hst-1* mutants, but unchanged in female Mp*hst-1*. This suggests that while Mp*SPL1* regulates phase transition in both genders, Mp*SPL2* activity is required differently for antheridiophore development than for archegoniophore development. The observation that Mp*SPL2* transcript levels were not elevated in female Mp*hst-1* mutants, is consistent with the delayed gametangiophore development in these plants. To analyse the distinct requirement of Mp*SPL2* for female and for male reproductive development, steady state expression of Mp*SPL2* must be measured at different time points during growth in far-red light. Here, I have only quantified Mp*SPL2* levels in Mp*hst-1* mutants after nine days of far-red light induction, when gametangiophores had not formed. According to measurements of the timing of gametangiophore formation in Mp*hst-1* mutants, antheridiophores develop approximately 12 days after the start of far-red light supplementation and archegoniophores

develop after approximately 37 days under these growth conditions (Figure 3.3). In *A. thaliana*, *SPL* levels increase gradually until they exceed a threshold, which allows phase transition to occur (Fornara and Coupland, 2009). It is possible that gametangiophore formation also coincides with a certain high level of Mp*SPL2* expression. If this was the case, high Mp*SPL2* levels in female Mp*hst-1* mutants would be predicted to occur later than at the investigated time point of nine days after the onset of far-red light supplementation. It is possible that in female plants, Mp*SPL2* accumulation occurs later than in male plants, possibly prevented by the activity of Mp*HST*. Similarly, I cannot predict how the expression of Mp*SPL1* might change in male and female Mp*hst-1* mutants after longer growth under inductive conditions. In an ideal experimental setup, the timely expression pattern of Mp*SPL1* and Mp*SPL2* must be analysed simultaneously under two growth conditions: under cool white light with far-red light supplementation and in control conditions without far-red light supplementation. This will more clearly demonstrate how Mp*SPL1* and Mp*SPL2* expression behaves over time in response to the far-red light inductive signal. Taken together, my results suggest that Mp*SPL1* and Mp*SPL2* regulate phase change in *M. polymorpha*, and Mp*SPL2* is differently expressed in male than in female plants. It remains to be tested how these two and potentially other Mp*SPL* genes are responsible for the timely delay in archegoniophore formation relative to antheridiophore formation in wild type and even more extremely in Mp*hst-1* mutants. Nevertheless, the presented data indicate that SPL genes are involved in the expression of the sexual dimorphism in *M. polymorpha* during the reproductive phase transition.

In *A. thaliana*, At*HST* influences flowering by specifically regulating miR156 processing (Park *et al.*, 2005). Through post-transcriptional repression of *SPL* genes, miR156 regulates the ageing pathway that negatively controls flowering. In this pathway, miR156 is expressed

in an antagonistic pattern to miR172. Neither miR156 nor miR172 were detected in *M. polymorpha* by small RNA sequencing analysis (Tsuzuki *et al.*, 2016). However, a miRNA very similar to miR156, namely miR529c, is expressed in *M. polymorpha* and was shown to cleave Mp*SPL2* (Figure 3.5). Another liverwort-specific miRNA, Mpo-MR-13, was predicted to cleave Mp*SPL1* (Figure 3.5). Based on the function of the Mp*SPL1* homolog At*SPL8*, which mainly controls male fertility (Unte *et al.*, 2003), I speculated that the Mpo-MR-13/MpSPL1 module might control aspects of gametangiophore production or morphology. Steady state levels of Mp*SPL1* were higher than wild type in both male and female Mp*hst-1* mutants after growth under inductive far-red light conditions. This suggests that Mp*SPL1* is negatively controlled by Mp*HST* and positively regulates gametangiophore development in both sexes. Therefore, the MpSPL1/Mpo-MR-13 interaction might be a novel and liverwort-specific regulatory module in the control of phase change.

To investigate if miR529c and Mpo-MR-13 are processed by Mp*HST* to control the timing of the reproductive transition, their miRNA steady state levels need to be quantified in Mp*hst-1* mutants. If miR529c behaved in a similar manner as miR156 in *A. thaliana*, high miR529c expression would be predicted during vegetative growth in cool white light. After supplementation of far-red light, miR529c levels would decline and reach their minimum during gametangiophore formation. This scenario would argue for a role of miR529c in inhibiting the reproductive transition in *M. polymorpha*, like miR156 inhibits flowering. However, if in Mp*hst-1* mutants, miR529c levels were low during vegetative growth and reached their maximum during gametangiophore formation after far-red light induction, this would suggest similarity to the phase change mechanism in *P. patens*. miR156 promotes phase change in the moss, where its expression is highest during formation of the leafy bud that proceeds the gametophore. Since transcript levels of Mp*SPL1* and Mp*SPL2* were higher

in Mp*hst-1* mutants than in wild type under far-red inductive conditions, it is more likely that this is a consequence of low Mpo-MR-13 and miR529c levels. Therefore, my data indicate that if miR529c and Mpo-MIR-13 controlled the expression of Mp*SPL2* and Mp*SPL1* during phase change, their expression patterns would more likely resemble those of miR156 miRNAs in *A. thaliana* than in *P. patens*.

In wild type, antheridiophores on male plants form approximately nine days later than archegoniophores on female plants. In Mp*hst-1* mutants, this shift is increased to 26 days between male and female plants, which indicates that Mp*HST* inhibits phase change in males and promotes phase change in females. This suggests that Mp*HST* interacts with factors that control the sexual dimorphism. These might be sex-specifically expressed in male or female plants. Gender identity in the dioecious *M. polymorpha* is determined by the presence of a Y chromosome in male plants and an X chromosome in female plants. Very little is known about sex chromosome-encoded genes that control morphological differences between the two genders (Okada *et al.*, 2001). Recently, the autosomal gene FEMALE GAMETOPHYTE MYB (MpFGMYB) was shown to control the sexual dimorphism in *M. polymorpha* gametangiophores (Hisanaga *et al.*, 2019). Mp*FGMYB* is predominantly expressed in archegoniophores, where it is required for female development. Under far-red light conditions, Mp*FGMYB* is expressed in the apical notch where archegoniophores will develop. As a transcription factor, Mp*FGMYB* activates autosomal and X-chromosomal genes that promote female differentiation. In male plants, Mp*FGMYB* is repressed by its antisense transcript *SUF*, a long non-coding RNA. Repression of Mp*FGMYB* allows the expression of autosomal and Y-chromosomal genes that promote male differentiation. The reproductive cues that activate Mp*FGMYB* expression to confer female gametangiophore identity are yet unknown and so are downstream targets of Mp*FGMYB*. It might be that

Mp*SPL2* and other Mp*SPL* genes somehow interact with the Mp*FGMYB* pathway that determines male and female gametangiophore identity. Possibly, Mp*SPL* genes regulate the timely expression of Mp*FGMYB* and *SUF* so that antheridiophores are formed earlier than archegoniophores. To determine a possible link between the ageing pathway and regulators of the sexual dimorphism, it will be worth investigating the regulatory relationship between Mp*HST*, Mp*SPL* genes and sex-specifically expressed factors like MpFGMYB.

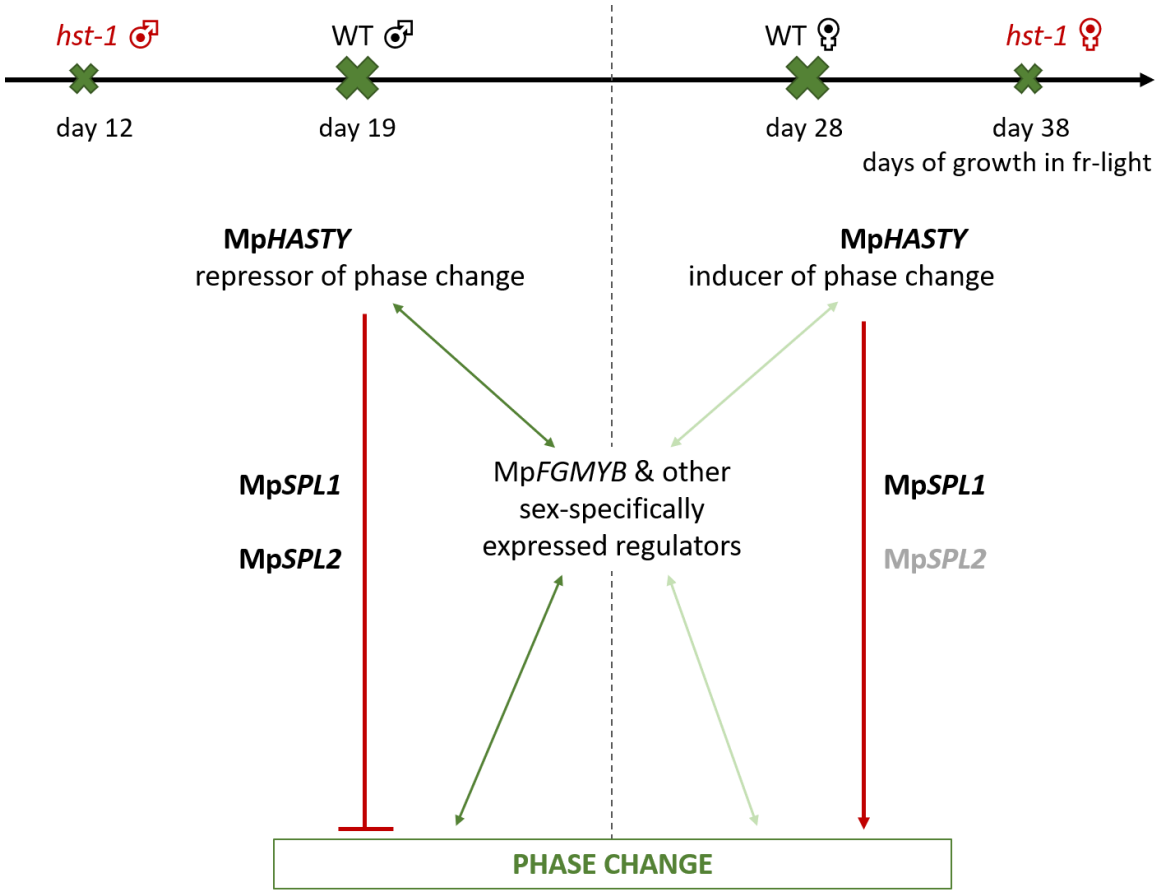


**Figure 5.9: Proposed model of sex-dependent regulation of phase change through MpHST.** The observation that male Mp*hst-1* mutants undergo phase change earlier than male wild type and female Mp*hst-1* mutants undergo phase change later than female wild type, suggests that Mp*HST* is a repressor of phase change in males and a promote rof phase change in females. The expression of MpSPL1 and MpSPL2 is altered in mild Mphst-1 loss of function mutants in far-red light, suggesting interaction between Mp*HST* and Mp*SPL1* and Mp*SPL2*, although partly differently in males and females. More experiments are required to determine the exact effect of Mp*HST* on Mp*SPL* gene

expression in white light and in far-red light. Sex-specifically expressed regulators like Mp*FGMYB* might determine the opposite function of Mp*HST* in males and in females and might generally interact with the phase change regulatory pathway, producing the observed sexual dimorphism in phase change timing. Unidirectional arrow indicates a positive interaction, while bidirectional arrows indicate an unknown mode of interaction. The T-shaped line indicates a negative regulatory interaction.

Taken together, I demonstrated that the function of *HST* and *SPL* genes in controlling developmental phase transitions in a common pathway is conserved between *A. thaliana* and *M. polymorpha*. While At*HST* is a negative regulator of flowering in the monoecious *A. thaliana*, Mp*HST* negatively or positively regulates gametangiophore development in male or female *M. polymorpha* plants, respectively. While Mp*SPL2* expression in male Mp*hst-1* mutants was increased in response to inductive far-red light, Mp*SPL2* expression was unchanged in female Mp*hst-1* mutants relative to wild type. This observation suggests an interaction between specific regulators of the sexual dimorphism and the ageing pathway that controls the reproductive transition in *M. polymorpha*.

# Chapter 4 – Mp*DICER-LIKE 1* controls thallus development and reproductive phase transition in *M. polymorpha*

## 4.1. Abstract

DICER-LIKE (DCL) endoribonucleases constitute the core enzymes in biogenesis pathways of small non-coding RNAs in plants. In the flowering plant *A. thaliana*, the At*DCL* gene family consists of four single copy members. One of these, At*DCL1*, primarily mediates the cleavage of 21 nt-long miRNAs, many of which are important developmental regulators. Therefore, At*DCL1* is essential for plant development; in fact, strong At*dcl1* mutations cause lethality. Other defects resulting from partial loss of At*DCL1* function range from developmental arrest of the embryo to abnormal flower and ovule development connected with delayed flowering and sterility. *DCL1* functions have been investigated thoroughly in the flowering plant *A. thaliana* and in the moss *P. patens*, where Pp*dcl1a* suffers severe growth defects and fails to transition to the reproductive phase. Another bryophyte, the liverwort *M. polymorpha*, also encodes one *DCL1* ortholog, Mp*DCL1*. Previously, I demonstrated that Mp*DCL1* functions in the biogenesis of the *Marchantia*-specific miRNA Mp*FRH1*. To investigate other developmental roles of Mp*DCL1*, I generated Mp*dcl1* mutants with CRISPR/Cas9-induced mutations and characterised their development. These loss-of-function mutants showed strong defects in thallus growth and morphology. In severe cases, mutant thalli barely expanded or branched, but instead curled epinastically and did not form any gemma cups or gemmae. Moreover, strong Mp*dcl1* alleles caused defects in male reproductive phase transition – not only did male Mp*dcl1* plants form gametangiophores earlier than wild type, but this occurred without the exposure to far-red light required by wild type. Female Mp*dcl1* mutants did not show these phase change-related phenotypes. My findings indicate an essential role for Mp*DCL1* in thallus development and differentiation, and in the repression of reproductive growth in the absence of far-red light. Furthermore, they suggest a miRNA-mediated regulatory mechanism of sexual reproductive organ formation in the dioecious *M. polymorpha*.

## 4.2. Introduction

A major morphological and physiological transition in a plant's life cycle is the transition from vegetative to reproductive development. This transition takes place in response to exogenous and endogenous inductive cues that are integrated by different signalling pathways. While in the monoecious *A. thaliana* this leads to flowering, a similar transition occurs with the formation of sexually dimorphic gametangiophores that develop on male and female plants of the dioecious liverwort *M. polymorpha*.

*A similar mechanism controls long-day-dependent reproductive phase transition in A. thaliana and M. polymorpha*

Induction of flowering in *A. thaliana* and the formation of gametangiophores in *M. polymorpha* depend on long days; they are regulated by photoperiod (Mouradov, Cremer and Coupland, 2002; Amasino and Michaels, 2010). The photoperiod signal, coming from growth in long days, is integrated by the interaction of FLAVIN-BINDING KELCH REPEAT F-BOX1 (FKF1) and GIGANTEA (GI) proteins (Sawa *et al.*, 2007). Formation of the FKF1-GI complex upon long-day perception is critical for the reproductive transition in *A. thaliana* and *M. polymorpha* (Sawa *et al.*, 2007; Kubota *et al.*, 2014). While knock-out of Mp*fkf1* and Mp*gi* completely abolished gametangiophore development, overexpression of Mp*FKF1* and Mp*GI* increased the amount of MpFKF1-MpGI complex, which induced gametangiophore formation regardless of photoperiod. This suggests that overproduction of the MpFKF1-MpGI complex can overcome the requirement for the photoperiod signal to transition to reproductive development. In *A. thaliana*, the FKF1-GI complex promotes flowering by degrading CYCLING DOF FACTOR 1 (CDF1), which is a transcriptional repressor of the flowering activator *CONSTANS* (*CO*). *CO* activates expression of *FLOWERING LOCUS T* (*FT*), a mobile signal that is transmitted from leaves, where day

length is perceived, to the shoot apical meristem. In the meristem, it induces the expression of the flower meristem identity gene *APETALA1* (*AP1*), which triggers the conversion of the shoot meristem to a floral meristem with competence to flower (Bäurle and Dean, 2006). Knowledge about the molecular pathway regulating gametangiophore initiation downstream of the MpFKF1-MpGI complex in *M. polymorpha* is very limited, and possible adaptation of any of the described *A. thaliana* components has not been investigated to date.

*dicer-like 1 (dcl1) mutants in flowering plants and the moss P. patens develop pleiotropic developmental defects*

miRNAs play an important role in the control of gene expression (Chen, 2005). Loss of *DCL1* function has detrimental effects on plant development because DCL1 proteins are core enzymes in the biogenesis pathway of plant miRNAs (Reinhart *et al.*, 2002). In *A. thaliana*, rice, maize, bean and the moss *P. patens*, *dcl1* mutants commonly express pleiotropic defects in growth, morphology, cell differentiation, meristem determinacy and developmental phase change (Liu *et al.*, 2005; Khraiwesh *et al.*, 2010; Thompson *et al.*, 2014; Curtin *et al.*, 2016). Complete *dcl1* loss of function alleles are commonly embryonic lethal (Schauer *et al.*, 2002). In partial *dcl1* loss of function mutants of vascular plants, rolled leaves with leaf polarity defects are characteristic, as well as sterility due to defective floral organ development (Aukerman and Sakai, 2003). These defective phenotypes also occur in other mutants of core miRNA biogenesis components in *A. thaliana*, like *argonaute (ago)*, *hyponastic leaves 1* (*hyl1*), *hua enhancer 1* (*hen1*) and *serrate* (*se*) (Park *et al.*, 2002; Kidner and Martienssen, 2004; Vazquez, Gasciolli and Cre, 2004; Grigg *et al.*, 2005). The At*dcl1-7* mutant allele develops a late flowering phenotype, which is likely caused by a reduction in miR172, promoter of the expression of floral integrators in the shoot apical meristem (Ray *et al.*, 1996). In the moss *P. patens*, Pp*dcl1a* mutants fail to transition to the reproductive

phase, but the underlying miRNAs and target genes have not been identified. The pleiotropic defective phenotypes of various *dcl1* mutants demonstrate the conserved requirement of *DCL1* function for plant development through global miRNA processing.

*DCL1 genes encode complex enzymes with several functional domains that are active in miRNA processing*

DCL1 endoribonucleases are complex proteins that contain several functional domains required for miRNA processing (Jacobsen, Running and Meyerowitz, 1999; Kurihara and Watanabe, 2004; Margis *et al.*, 2006). These include an N-terminal RNA helicase domain, a domain of unknown function, a PAZ (Piwi/Argonaute/Zwille) domain, two ribonuclease III (RNase III) domains, and at least one double-stranded RNA-binding (dsRNA-binding) domain at the N-terminus (Schauer *et al.*, 2002). While the RNase III domains execute cleavage of pri- and pre-miRNAs, the dsRNA-binding domains are responsible for selective miRNA binding, the positioning of the miRNA cleavage sites and interaction with other proteins of the Dicing complex (Kurihara and Watanabe, 2004; Margis *et al.*, 2006). The analysis of different mutant alleles of *dcl1* in *A. thaliana* and *Zea mays* have demonstrated the significance of the dsRNA-binding and RNase III domains for correct DCL1 activity and therefore for plant development (Golden *et al.*, 2002; Schauer *et al.*, 2002; Liu, Axtell and Fedoroff, 2012; Thompson *et al.*, 2014). Altogether, while complete loss of DCL1 function causes lethality, the analysis of different weak *dcl1* alleles in numerous plant species has demonstrated the conserved requirement of DCL1 proteins for various developmental processes (Jacobsen, Running and Meyerowitz, 1999; Park *et al.*, 2002; Schauer *et al.*, 2002).

To date, miRNA processing has not been studied extensively in non-flowering plants. In *P. patens*, Pp*dcl1a* and Pp*dcl1b* mutants demonstrated the requirement of Pp*DCL1* for regulating growth and developmental transition in moss (Khraiwesh *et al.*, 2010). This study suggests conservation of plant DCL1 function between angiosperms and bryophytes. The liverwort *M. polymorpha*, another bryophyte, encodes one Mp*DCL1* gene that possesses an N-terminal RNA helicase domain, a designated dimerization domain, a PAZ domain followed by two RNase III domains, and one C-terminal dsRNA-binding domain (see Figure 4.1). In this chapter, I investigated the significance of Mp*DCL1* for the development of the liverwort thallus. The morphology of *M. polymorpha* differs fundamentally from flowering plants, which made it difficult to predict Mp*dcl1* phenotypes. *M. polymorpha* lacks vascular tissue and therefore forms a flat thallus body with dorsal-ventral polarity (Shimamura, 2016; Pandey and Alam, 2016; Bowman *et al.*, 2017). The thallus expands from the apex, where meristematic cells cause radial growth with repeated dichotomous branching. Rhizoids, filamentous rooting structures, develop on the ventral surface of the thallus, while gemma cups differentiate from the dorsal surface. Rather than flowers as in the angiosperms, the reproductive organs of *M. polymorpha* are gametangiophores – umbrella-like structures with a stalk elevating a receptacle several centimetres above the thallus. Antheridiophores (male gametangiophores) and archegoniophores (female gametangiophores) develop from apical meristematic notches (Shimamura, 2016). The dioecious *M. polymorpha* has a fundamentally different morphology compared to angiosperms. Studying the function of Mp*DCL1* in the development of the *M. polymorpha* thallus will reveal conserved and novel roles of *DCL1* and miRNA activity in plant development.

In addition to a large number of non-conserved miRNAs, *M. polymorpha* encodes seven highly conserved miRNAs, of which some regulate important developmental processes

(Tsuzuki *et al.*, 2016; Lin and Bowman, 2018). Therefore, it was likely that severe disruption of the Mp*DCL1* gene sequence could result in sterility or embryo lethality if Mp*DCL1* is essential for miRNA processing. Using CRISPR/Cas9, I generated mutations in exon 1 and in the RNase III and the dsRNA-binding domains of Mp*DCL1* and characterised the phenotypes of different Mp*dcl1* mutant alleles. These revealed a crucial function of Mp*DCL1* for growth and differentiation of the liverwort thallus, including an important role in regulating the reproductive phase transition.

## 4.3. Results

### 4.3.1. CRISPR/Cas9 mutagenesis generated strong Mp*dcl1* mutants defective in the 1st RNase III domain and the dsRNA-binding domain

Loss of *DCL1* function causes severe pleiotropic defects, and in strong mutant backgrounds embryo lethality in the vascular plant *A. thaliana* and the moss *P. patens*. To investigate the developmental role of Mp*DCL1* in the liverwort *M. polymorpha*, I generated Mp*dcl1* single mutants using CRISPR/Cas9 mutagenesis. Three different regions of the Mp*DCL1* gene were independently targeted for mutagenesis (Figure 4.1). Using a combination of two complementary guide RNAs (gRNAs) per genomic target site, I attempted to generate long deletions in Mp*DCL1* to disrupt gene function. With a pair of gRNAs in construct CRISPR 1, I intended to make a strong Mp*dcl1* loss-of-function allele by deleting ~980 bp of exon 1. Besides deleting ~980 bp, this could potentially cause a shift in the open reading frame, or a premature stop codon, which would render most of the protein dysfunctional. gRNAs for construct CRISPR 2 were designed to produce a ~380 bp deletion in the 1st RNase III domain, likely an essential domain for the RNA cleavage activity of MpDCL1. The 3'-end of the Mp*DCL1* coding sequence encodes one dsRNA-binding domain. Two gRNAs designed there could potentially generate a weaker Mp*dcl1* allele with a ~65 bp deletion (construct CRISPR 3). I used the CRISPR-P online tool to design and select gRNAs with the lowest probability for off-target site mutagenesis activity (Appendix Table A1).

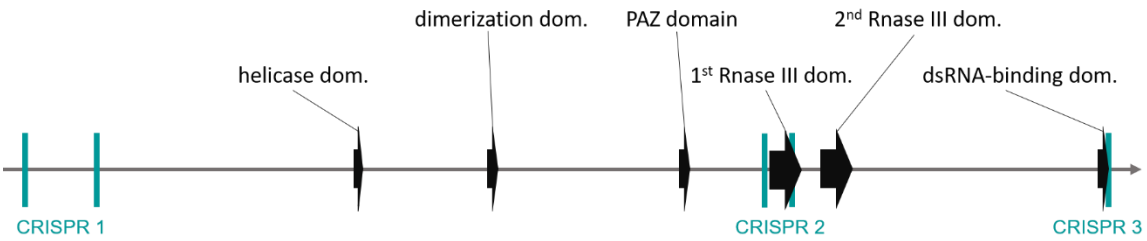


**Figure 4.1: Pairs of gRNAs target three different regions of the Mp*DCL1* gene for CRISPR/Cas9 mutagenesis.** Gene model of the 15.352 kb long Mp*DCL1* gene, showing gRNA target sites as turquoise lines. For CRISPR/Cas9 mutagenesis, one pair of gRNAs each was designed to target either exon 1 (CRISPR 1 transgene), the 1st RNase III domain (CRISPR 2 transgene), or the dsRNA-binding domain (CRISPR 3 transgene). CRISPR gRNA target sites in Mp*DCL1* are indicated by turquoise vertical lines. Functional domains are indicated as black arrows, they were designated after search for conserved domains on the NCBI (National Centre for Biotechnology Information) website.

While transformation of the CRISPR 2 and CRISPR 3 constructs into wild type spores yielded putative mutants, no surviving plants were obtained after transformation and selection of spores with the CRISPR 1 construct. Given that all three transformations were performed at the same time, using spores of the same age and condition, similar transformation efficiencies had been expected. Furthermore, all gRNAs had been designed with the same online tool, CRISPR-P, and selected based on the highest predicted mutagenesis efficiency and lowest likelihood for off-target site binding. Therefore, the CRISPR/Cas9 activity of each pair of gRNAs had been expected to be similar. If transformation of the CRISPR 1 construct into young sporelings was successful, it is likely that disruption of the Mp*DCL1* coding sequence at its 5'-end has resulted in complete loss of gene function. If Mp*DCL1* is essential for plant growth, this could have had a lethal effect, like deletion of > 20 kb of the 5'-end of the open reading frame in the At*dcl1-3* allele (Golden *et al.*, 2002). It would suggest that those transformants died very early and escaped observation.

Two out of 13 genotyped transformants from the CRISPR 2 mutagenesis approach were identified as mutants. Their genotypes were determined by PCR amplification of the region around the gRNA target sites, and subsequent sequencing of the PCR products. The CRISPR 2 transformants did not contain the predicted large deletion in the 1st RNase III domain; instead, short mutations in one of the gRNA target sites were found. Line Mp*dcl1-1* contained a 3 bp deletion in exon 17, and line Mp*dcl1-2* carried a AAA to CCC substitution followed by a 1 bp deletion in intron 16. Absence of any large mutation suggests that integrity of the 1st RNase III domain is essential for the function of Mp*DCL1*. Instead, small mutations allowed the isolation of two weak Mp*dcl1* alleles, Mp*dcl1-1* and Mp*dcl1-2*. They formed irregularly shaped thalli with incisions, but otherwise developed like wild type (Figure 2 A-C).

Two mutants obtained from transformation of the CRISPR 3 construct carried large deletions of 57 bp (line Mp*dcl1-3*) and 59 bp (line Mp*dcl1-4*) between the two gRNAs. These deletions removed 19 aa and therefore the second half of the dsRNA-binding domain. Additionally, the 59 bp out of frame deletion in Mp*dcl1-4* shifted the stop codon towards the 3'-end, adding eleven new aa. The mutant plants developed narrow, elongated thalli and were generally inhibited in growth and thallus expansion (Figure 4.2 D-I). They sometimes failed to produce gemma cups and gemmae (Figure 4.2 H). The phenotypes of these two alleles suggest that the dsRNA-binding domain of Mp*DCL1* is important for growth and thallus development. However, loss of the second half and therefore a substantial part of this domain does not cause severe developmental defects. In contrast, large deletions in the RNase III domain might have caused strong developmental retardation, concluding from the fact that the vital mutants that were identified only carried small DNA sequence alterations.

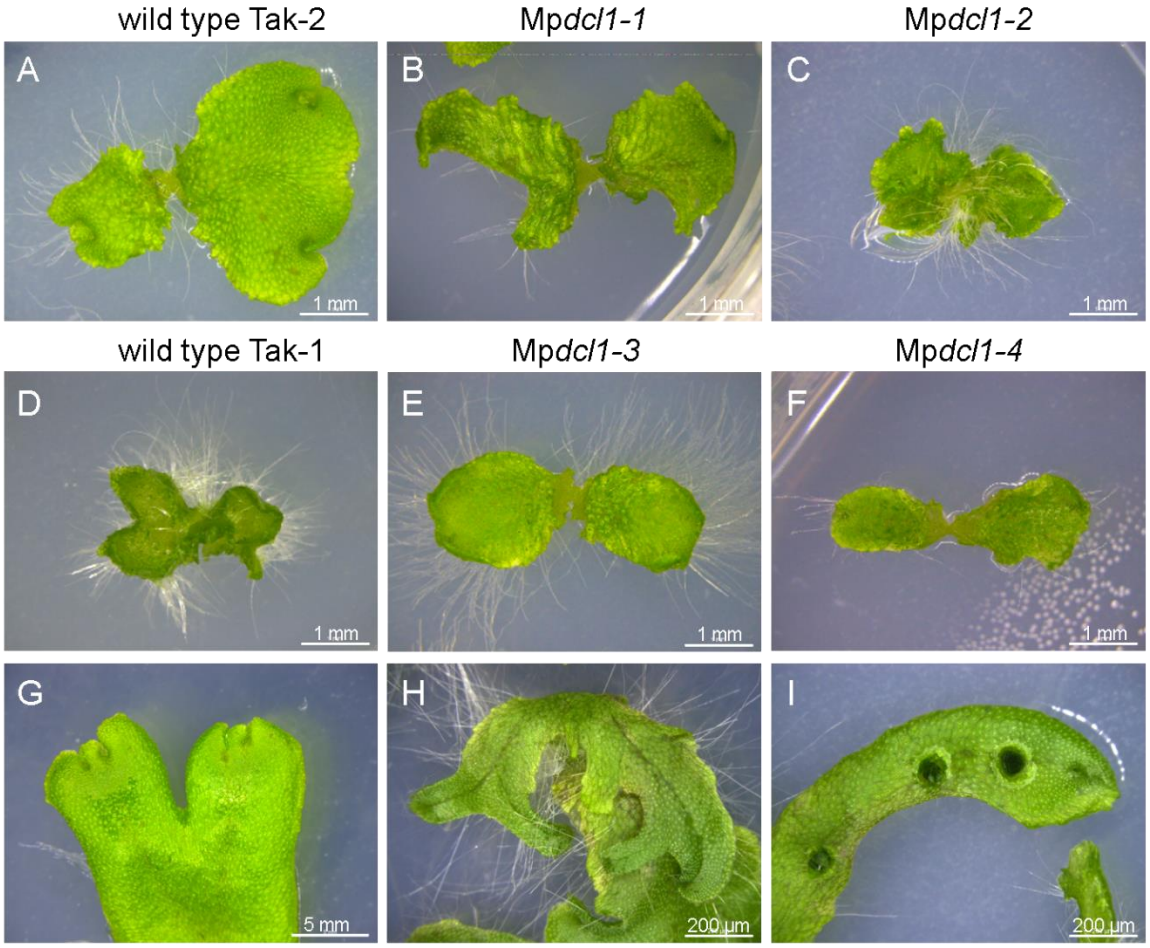


**Figure 4.2: Mp*dcl1* mutants defective in either the 1st *RNase*III domain or the dsRNA-binding domain of Mp*DCL1* are affected in thallus growth and morphology.** 2-weeks-old (A-F) and 6-weeks-old (G-H) gemmalings of Tak wild types (A, D, G) and T1 Mp*dcl1-1/2* (B-C) and Mp*dcl1-3/4* (E-F, H-I) mutants defective in the 1st RNase III domain or the dsRNA-binding domain, respectively. Mutations are listed in Table 1.

Mp*dcl1* mutants obtained from both CRISPR 2 and CRISPR 3 mutagenesis events, produced reproductive structures, the gametangiophores. To further investigate the significance of Mp*DCL1* in *Marchantia* development, I set out to create stronger Mp*dcl1* mutants defective in both the 1st RNase III and the dsRNA-binding domains. For this purpose, I crossed the male Mp*dcl1-3/4* mutants to the female Mp*dcl1-1/2* mutants. If in these parental lines the CRISPR 2 and CRISPR 3 transgenes were inserted on different chromosomes and unlinked

to the mutated Mp*dcl1* loci, they would segregate independently of the Mp*dcl1* mutations. In the offspring, each of the segregating transgenes would then have the potential to induce new mutations in addition to the already existing, inherited Mp*dcl1* mutation. Therefore, Mp*dcl1* mutants defective in both domains could be generated. Following Mendelian inheritance, F2 individuals were expected to carry one of the parental mutations in either the 1st RNase III domain (50 % of offspring) or the dsRNA-binding domain (50 % of offspring). In addition, in 50 % of individuals from both groups, the other non-parental CRISPR transgene would have been assorted into the same gamete, carrying the potential to generate a second Mp*dcl1* mutation.

The following genotyping and phenotyping experiments present a combined analysis of the offspring of the two crosses Mp*dcl1-1* x Mp*dcl1-3* and Mp*dcl1-2* x Mp*dcl1-4*. By sequencing, I identified about 25% of progeny to be single mutants with mutations in either the 1st RNase III domain or the dsRNA binding domain. The other 75 % of individuals carried mutations caused by both the CRISPR 2 and CRISPR 3 transgenes, hence were mutated in both domains. The obtained ratio suggests that the CRISPR 2 and CRISPR 3 transgenes became active during the short diploid sporophyte stage. If the non-parental CRISPR transgenes had only been active in the gametophytes of the F2 plants, only 50 % of progeny with mutations in both Mp*DCL1* domains would have been expected. Instead, CRISPR/Cas9 activity in the sporophyte must have generated mutations in the Mp*DCL1* gRNA target site of the other parent, and after meiosis this has resulted in Mp*dcl1* spores with mutations in both domains. Consequently, 75 % of F2 individuals were mutated in both Mp*DCL1* domains. Figure 4.3 presents a flow chart that describes the generation of Mp*dcl1* mutants defective at both the 1st RNase III and the dsRNA-binding domains, by transformation and crossing.

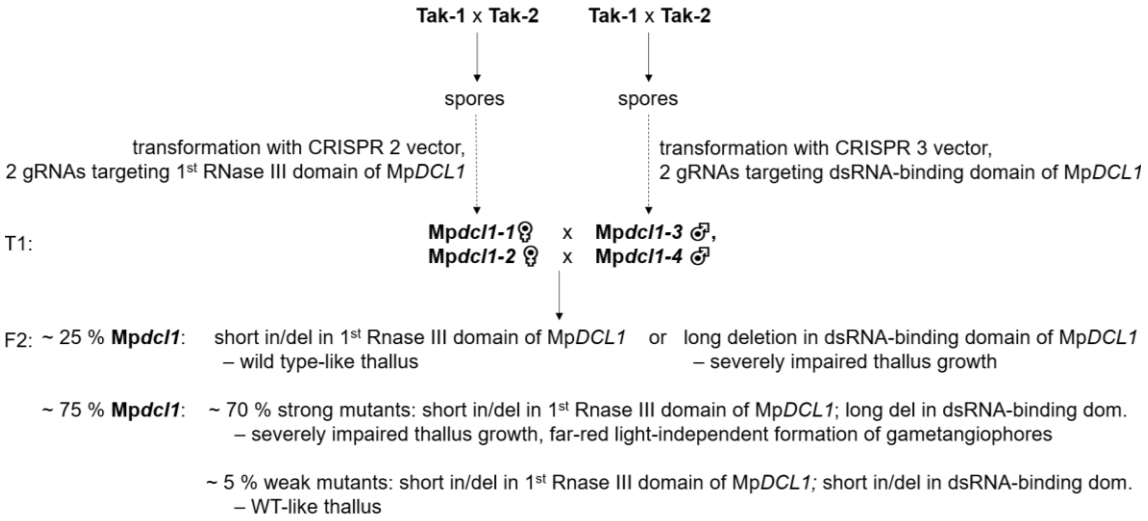


**Figure 4.3: Strong Mp*dcl1* mutants defective in both the 1st RNase III and the dsRNA-binding domains were generated by crossing of two weaker Mp*dcl1* alleles mutated in only one domain each.** Crossing scheme for generation of strong *Mpdcl1* mutant individuals defective in both the 1st RNase III domain and the dsRNA-binding domain. A Tak-1 x Tak-2 cross yielded wild type spores to be transformed for mutagenesis with either the CRISPR 2 or the CRISPR 3 transgene. From each transformation, two individuals were identified with mutations in the 1st RNase III domain (Mp*dcl1-1* and Mp*dcl1-2*, both female) and the dsRNA-binding domain (Mp*dcl1-3* and Mp*dcl1-4*, both male). Mp*dcl1-1* x Mp*dcl1-3* and Mp*dcl1-2* x Mp*dcl1-4* crosses were performed. 75 % of F2 individuals were Mp*dcl1* alleles with mutations in both the 1st RNase III domain and the dsRNA-binding domain introduced both during the diploid sporophyte and the haploid gametophyte stage. in/del = insertion/deletion. Dashed arrows indicate transformation events, black arrows point at the generation succeeding from a cross.

### 4.3.2. Mp*DCL1* is essential for thallus expansion, branching and differentiation

From two Mp*dcl1-1/2* x Mp*dcl1-3/4* crosses, I obtained 75 % Mp*dcl1* mutant alleles with mutations in both the 1st RNase III domain and the dsRNA-binding domain of Mp*DCL1*. To investigate the developmental significance of Mp*DCL1* in *M. polymorpha*, I analysed such mutants from offspring of both Mp*dcl1-1/2* x Mp*dcl1-3/4* crosses. To determine the genetic mutations, I amplified 66-1000 bp around each CRISPR/Cas9 target locus by PCR and

sequenced the products. Sequenced Mp*dcl1* plants contained either the parental mutation from Mp*dcl1-1* in the 1st RNaseIII domain – a 3 bp deletion in exon 17 – or a AAA to CCC substitution followed by a 1 bp deletion in intron 16 and a 12 bp deletion in exon 17. The latter mutation was a combination of the parental mutation from Mp*dcl1-2* and an additional insertion of 12 bp in exon 17. The dsRNA-binding domain was more variable regarding novel mutations. While few of the F2 Mp*dcl1* plants with mutations in both domains inherited the parental 57 bp deletion, the majority had similarly long deletions ranging from 56-62 bp (termed strong Mp*dcl1* mutants, see individual genotypes in Table 4.1). Few individuals contained either SNPs or short deletions in the individual gRNA target sites in the dsRNA-binding domain instead (termed weak Mp*dcl1* mutants, see individual genotypes in Table 4.1). These mutations have likely arisen by CRISPR/Cas9 mutagenesis activity during the diploid sporophytic phase preceding meiosis. Any small mutation in the dsRNA-binding domain was associated with a wild type-like thallus phenotype in F2 Mp*dcl1* plants with both domains mutated. On the other hand, long deletions in the dsRNA-binding domain caused severe growth defects in Mp*dcl1* mutants with additional mutations in the 1st RNase III domain. Images of these two classes of mutants are shown in Figure 4.4, their genotypes are listed in Table 4.1. Weak Mp*dcl1* lines developed flat, widely expanding and frequently branching thalli, which resembled wild type in their morphology and growth (Figure 4.4). On the contrary, strong Mp*dcl1* mutants showed strongly retarded growth. Their thalli barely expanded and were defective in meristem formation and branching, which resulted in a small and narrow morphology. Meristematic notches were under-developed and remained close to each other, possibly as a result of retarded growth and inhibited branching. Moreover, epinastic twisting of the thallus was characteristic, suggesting an imbalance in cell division or expansion between the central cells along the midrib, and cells at the edges of the thallus. Strong Mp*dcl1* mutants lacked dorsal gemma cups and were unable to form gemmae. This

phenotype could be a secondary effect of the described general growth defects. It might also suggest a role for *DCL1* in the control of epidermal cell specification, besides being a general regulator of thallus growth. However, mutants formed air pore complexes and therefore developed some specialised epidermal cell types. Also, ventral epidermal cells specified to form rhizoids, and qualitative phenotypic assessment indicated increased rhizoid length relative to thallus size in strong Mp*dcl1* lines compared to wild type (Figure 4.4). This suggests that upon loss of *DCL1* function, growth is defective, which may result from mis-expression of growth-regulatory genes. It is consistent with the observation that in *P. patens*, protonemal growth is retarded in Pp*dcl1* mutants, and that At*dcl1* mutants develop a small habitus. Taken together, the results suggest a conserved function of the *DCL1* gene in regulating plant growth and morphology in fundamentally distinct lineages of land plants. Furthermore, they indicate a role of Mp*DCL1* in the differentiation of epidermis-derived, specialised thallus structures.

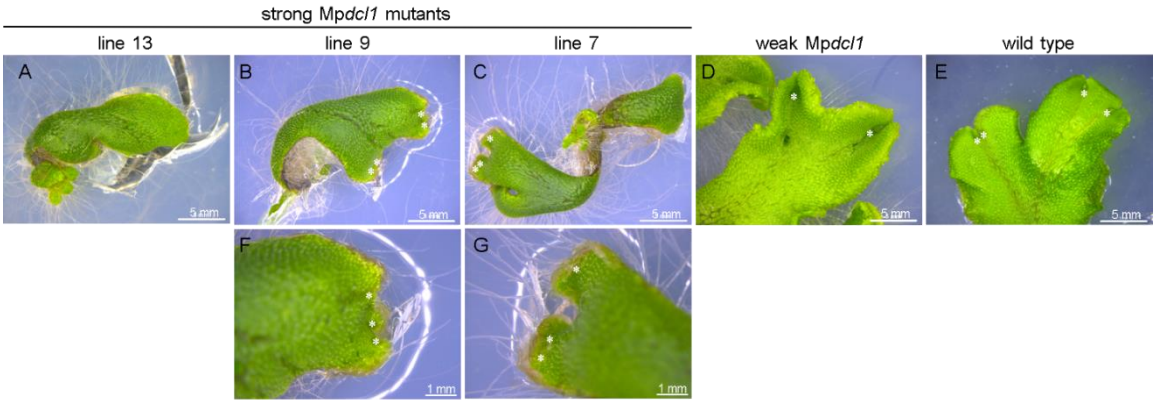


**Figure 4.4: Strong Mp*dcl1* mutants mutated in both the 1st RNase III and the dsRNA-binding domains, are defective in thallus growth and development.** 6.5-weeks-old plants grown from spores (mutants) or gemmae (wild type Tak-2, E). Three strong Mp*dcl1* mutants are shown – line 13 (A), line 9 (B, F) and line 7 (C, G). The weak Mp*dcl1* mutant is line 1 (D). Genotypes with mutations are listed in Table 1. White asterisks indicate the positions of meristematic notches.

**Table 4.1: Summary of the analysed weak and strong Mp*dcl1* mutant lines generated by CRISPR/Cas9 mutagenesis and crossing.** All 'lines' are independent Mp*dcl1* mutants with mutations in both targeted Mp*DCL1* domains. They represent a subset of mutants identified among 30 genotyped and phenotyped offspring plants originated from the two Mp*dcl1-1/2* x Mp*dcl1-3/4* crosses. Any of these mutants that have a deformed and growth-retarded thallus, as well as non-induced gametangiophore outgrowths when male, are termed 'strong Mp*dcl1* mutant' (highlighted in grey). Line 1 and line 2, which do not express these phenotypes, are termed 'weak Mp*dcl1* mutants'.

| line | ♀/♂ | underlying crossing | mutation in 1st RNase III domain | mutation in dsRNA-binding domain | deformed and growth-retarded thallus | gametan-giophores in white light |
|---|---|---|---|---|---|---|
| Mp*dcl1-1* | ♀ | Tak-1 x Tak-2 | 3 bp del in ex17 | WT | no | no |
| Mp*dcl1-2* | ♀ | Tak-1 x Tak-2 | AAA→CCC subst. & 1 bp del in int16 | WT | no | no |
| Mp*dcl1-3* | ♂ | Tak-1 x Tak-2 | WT | 57 bp del in exon 20 | partly | no |
| Mp*dcl1-4* | ♂ | Tak-1 x Tak-2 | WT | 59 bp del in exon 20 | partly | no |
| line 8 | ♀ | Mp*dcl1-1* x Mp*dcl1-3* | 3 bp del in ex17 | 16 bp & 9 bp ins in exon 20 | yes | no |
| line 9 | ♀ | Mp*dcl1-1* x Mp*dcl1-3* | 3 bp del in ex17 | 57 bp del in exon 20 | yes | no |
| line 13 | ♀ | Mp*dcl1-1* x Mp*dcl1-3* | 3 bp del in ex17 | 6 bp del & 15 bp ins in exon 20 | yes | no |
| line 12 | ♂ | Mp*dcl1-1* x Mp*dcl1-3* | 3 bp del in ex17 | 16 bp & 9 bp ins in exon 20 | yes | yes |
| line 7 | ♀ | Mp*dcl1-2* x Mp*dcl1-4* | AAA→CCC subst & 1 bp del in int16, 12 bp del in ex17 | 57 bp del in exon 20 | yes | no |
| line 3 | ♂ | Mp*dcl1-2* x Mp*dcl1-4* | AAA→CCC subst & 1 bp del in int16, 12 bp del in ex17 | 56 bp del in exon 20 | yes | yes |
| line 5 | ♂ | Mp*dcl1-2* x Mp*dcl1-4* | AAA→CCC subst & 1 bp del in int16, 12 bp del in ex17 | 57 bp del in exon 20 | yes | yes |
| line 6 | ♂ | Mp*dcl1-2* x Mp*dcl1-4* | AAA→CCC subst & 1 bp del in int16, 12 bp del in ex17 | 62 bp del in exon 20 | yes | yes |
| line 1 | ♀ | Mp*dcl1-2* x Mp*dcl1-4* | AAA→CCC subst & 1 bp del in int16, 12 bp del in ex17 | 3 bp del in exon 20 | no | no |
| line 2 | ♂ | Mp*dcl1-2* x Mp*dcl1-4* | AAA→CCC subst & 1 bp del in int16, 12 bp del in ex17 | A→C SNP in exon 20 | no | no |

### 4.3.3. Mp*DCL1* represses reproductive growth in the absence of far-red light

Thalli of various strong Mp*dcl1* mutant alleles developed general morphological defects and growth retardation. A more detailed phenotypic analysis of these mutants was undertaken during growth in constant cool white light without supplemented far-red light. It revealed that two different types of outgrowths formed on the main thallus. Firstly, new thallus parts were observed emerging from different regions of the main thallus. These outgrowths formed on both, male and female plants and usually developed dorsal-ventral polarity with rhizoids developing from the ventral epidermis. A second type of tissue outgrowth appeared in a synchronised manner, after 6-7 weeks of growth in cool white light. Bulges emerged from the apical notches of the thallus meristems and differentiated into cap-like structures with more or less pronounced, epinastically bending lobes (examples of different alleles/lines shown in Figure 4.5). These meristem-derived structures did not form rhizoids. In contrast to the previously described non-meristematic thallus outgrowths, they only emerged on strong male Mp*dcl1* mutants. Meristematic outgrowths never appeared on female plants grown in cool white light. This sex-specific difference in the development of a meristem-derived structure is reminiscent of the reproductive phase transition described in Chapter 3.3.1 – in wild type, male antheridiophores develop from meristems about nine days earlier than female archegoniophores. Similarly, in strong Mp*dcl1* mutants, meristem-derived structures grew out precociously on male but not female plants. Therefore, I hypothesised that these structures, unlike the first class of thallus outgrowths, had gametangiophore identity. However, wild type plants require far-red light as a signal to trigger the formation of reproductive organs (Figure 4.5A, F). By contrast, gametangiophores in strong male Mp*dcl1* mutants formed without exposure to far-red light, indicating a role for Mp*DCL1* in repressing male reproductive phase transition under non-inductive conditions.

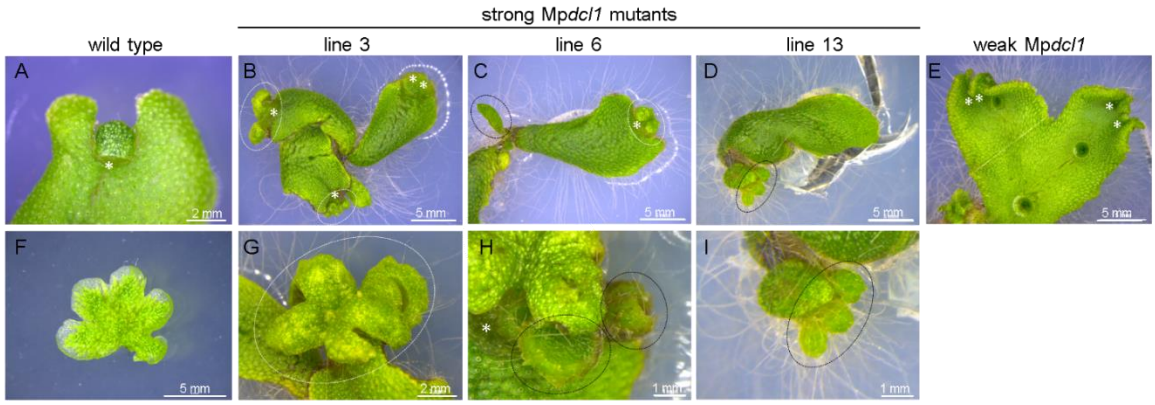


**Figure 4.5: Precocious gametangiophore outgrowths in strong Mp*dcl1* mutants defective in both the 1st RNase III and the dsRNA-binding domains, are distinct from non-meristematic thallus outgrowths.** Thalli of 6.5-weeks-old plants grown from spores in cool white light (mutants, B-E, I), or grown from gemma under far-red light conditions for 4 weeks (wild type Tak-1, A, F). Close-ups of gemetangiophore outgrowths (circled in white) and non-meristematic outgrowths (circled in black) in 9-weeks-old strong Mp*dcl1* mutants after growth under far-red light conditions (G-H). (F) mature, 6.5-weeks old, flat Tak-1 wild type gametangiophore receptacle after 4 weeks of growth under far-red light conditions. Three strong male Mp*dcl1* mutants are shown – line 3 (B, G), line 6 (C, H) and line 13 (D, I). The weak male Mp*dcl1* mutant is line 2 (E). Genotypes with mutations are listed in Table 1. White asterisks indicate positions of meristematic notches.

### 4.3.4. Mp*DCL1* represses the reproductive growth transition in the absence of far-red light in male *M. polymorpha*

In strong male but not female Mp*dcl1* mutants, gametangiophores formed in the absence of far-red light, which is an inducer of reproductive growth. I tested the hypothesis that this male-specific defect was the result of sex-specific development as opposed to genetic differences in Mp*DCL1* between males and females. I compared the phenotypes of independent strong Mp*dcl1* males and females that were genetically identical around the gRNA target sites in Mp*DCL1*. Two independent pairs of one male and one female each were analysed (pair 1: line 12 and 8, pair 2: line 5 and 7, see Table 1 for genotypes). Whereas

male and female of each pair were genetically identical, the two allelic pairs differed from each other in the DNA sequences of the 1st RNase III and the dsRNA-binding domains. This is because they were derived from two different crosses between a CRISPR 2 and a CRISPR 3 Mp*dcl1* mutant (Figure 4.2). Lines 8 and 12 were F2 individuals obtained from the cross Mp*dcl1-1* x Mp*dcl1-3*, whereas lines 5 and 7 were F2 plants produced by the Mp*dcl1-2* x Mp*dcl1-4* cross. Their genotypes at the two Mp*dcl1* loci are listed in Table 4.1. Lines 8 and 12 had 3 bp deleted from exon 17, and 25 bp inserted in exon 20, whereas lines 5 and 7 contained a substitution of AAA to CCC followed by a 1 bp deletion in intron 16 and a 12 bp deletion in exon 17, as well as a 57 bp deletion in exon 20. I compared the phenotypes of the male and the female individual of each pair after six to seven weeks of growth in cool white light without supplementation of far-red light. Their phenotypes confirmed that only the two males produced gametangiophores under these conditions. Until death or growth cessation due to senescence after about 12 weeks, no gametangiophores had formed on female plants. In conclusion, strong Mp*dcl1* mutations do not induce archegoniophore production in non-inductive conditions in female plants. This is consistent with the requirement of far-red light for female reproductive transition in wild type. It suggests that Mp*DCL1* represses reproductive phase transition in male but not in female *M. polymorpha*. More precisely, combined integrity of the 1st RNaseIII domain and the dsRNA-binding domain are necessary to inhibit the male reproductive transition in the absence of far-red light.

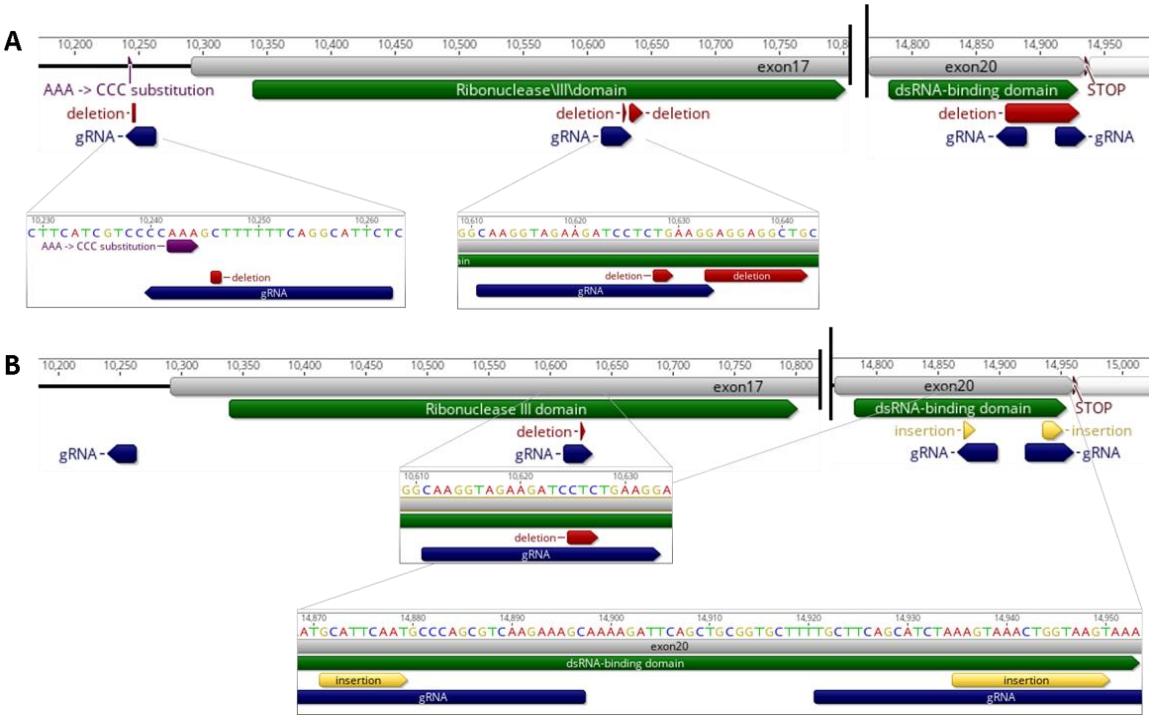


**Figure 4.6: Two distinct pairs of male and female plants contain different CRISPR/Cas9 mutations in both the 1st RNase III domain and the dsRNA-binding domain of Mp*DCL1*.** Gene models of MpDCL1 in strong Mp*dcl1* mutant lines obtained by CRISPR/Cas9 mutagenesis and subsequent crossing of mutants as schematically presented in Figure 4.3. For Mp*dcl1* line 5 and 7 (A), and line 8 and 12 (B), gene models with genomic mutations before and in the 1st RNase III domain (left sequence stretch) and in the dsRNA-binding domain (right sequence stretch) are presented. Boxes show close-ups of the mutated sequences in the gRNA target sites. Blue arrows represent gRNA target sites, grey bars exons, green arrows functional domains, yellow arrows insertions, red arrows deletions and purple arrows substitutions.

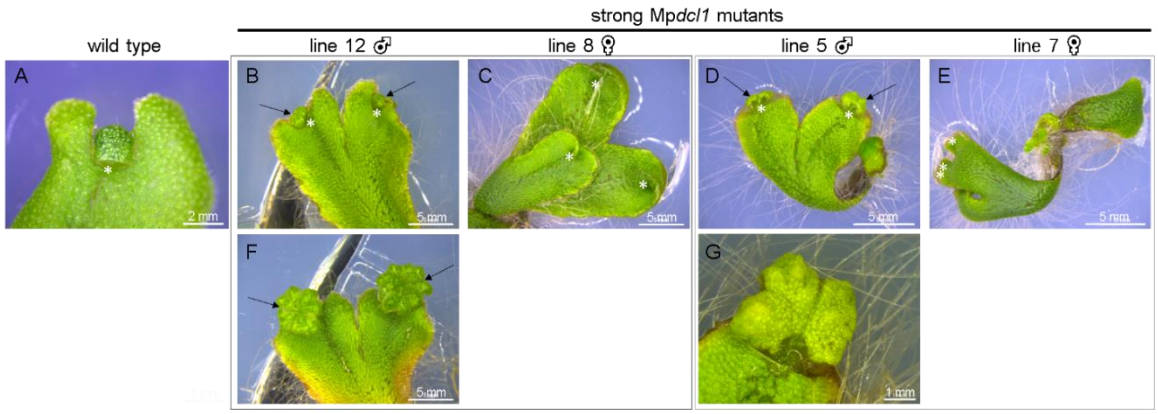


**Figure 4.7: Strong male but not female Mp*dcl1* mutants form gametangiophores without exposure to far-red light.** Phenotypes of individuals from two genetically distinct pairs of one male and one female strong Mp*dcl1* mutant each. (B/F and C) as well as (D/G and E) are two pairs of male (B/F, D/G) and female (C, E) strong Mp*dcl1* mutant lines. The male and female line of each pair are genetically identical at Mp*DCL1*. Genotypes with mutations are listed in Table 1- (B, F) are line 12, (C) is line 8, (D, G) are line 5, and (E) is line 7. White asterisks indicate positions of meristematic notches. Thalli of 6.5-weeks-old plants grown from spores in cool white light without supplemented far-red light (mutants, B-E), or grown from gemma under far-red light conditions for four weeks (wild type Tak-1, A). (F, G) close-ups of gemetangiophore outgrowths in (B, D, pointed out by black arrows) in 9-weeks-old strong Mp*dcl1* plants mutated in both the 1$^{st}$ RNase III and the dsRNA-binding domains.

### 4.3.5. Mp*DCL1* controls antheridiophore morphology

Defects in different aspects of thallus morphology in strong Mp*dcl1* mutants suggest a broad regulatory function of Mp*DCL1* in the morphogenesis of the *M. polymorpha* plant body. To assess the impact of Mp*DCL1* on gametangiophore morphology, I analysed how different Mp*dcl1* mutations affected gametangiophore shape and development. I compared three independent strong male Mp*dcl1* mutants, line 3, 5 and 12. Their genotypes are listed in Table 1: lines 3 and 5 both contained a substitution of AAA to CCC followed by a 1 bp deletion in intron 16 and a 12 bp in-frame deletion in exon 17. However, they differed in the dsRNA-binding domain – while line 5 had a 57 bp in-frame deletion, causing loss of 19 aa,

line 3 contained an out-of-frame deletion of 56 bp, which removed 18 aa and shifted the stop codon by 12 bp into the 3' UTR, thereby adding 12 new amino acids. Line 12 had 3 bp deleted from exon 17, and a total of 25 bp (9 bp in the first gRNA target site and 16 bp in the second gRNA target site) inserted in the dsRNA-binding domain (figure 4.6). These insertions added 3 aa in the first gRNA target site and introduced a premature stop codon in the second gRNA target site in the dsRNA-binding domain, effectively shortening the protein sequence of MpDCL1 by 6 aa.

To analyse the impacts of the three different Mp*dcl1* mutant alleles on antheridiophore development and morphology, I compared their phenotypes. Wild type antheridiophores consist of a receptacle, which is a disc-like cap, attached to an elongated stalk, which connects to the apical notch of the thallus (Figure 4.8D). Unlike wild type, the antheridiophore structures in all strong male Mp*dcl1* mutants stayed closely attached to the meristem, lacking an elongated stalk. As opposed to flat and round, mildly lobed caps in wild type (Figure 4.8H), the mutant receptacles displayed varying degrees of deformation. Antheridiophores in line 12 formed fully round caps, which were attached to the main thallus through a very short stalk. The main difference to wild type was a minorly fragmentation of the round cap into eight to nine finger-like segments, which bent epinastically on the edges (Figure 4.8). This defect was more pronounced in lines 3 and 5, where the receptacle caps were divided into four to five strongly bending, finger-like segments. This kind of deformation is strongest in line 3. The observation that antheridiophores in line 3 and line 5 are more strongly deformed than in line 12, might correlate with the types of underlying Mp*dcl1* mutations. While in all three lines, the second half of the dsRNA-binding domain is significantly interrupted, the RNase III domain contains a deletion of 12 bp in lines 3 and 5 compared to a smaller deletion of 3 bp in line 12. In agreement with the previously raised

hypothesis that functionality of Mp*DCL1* is particularly sensitive to defects in the RNase III domain, the loss of four aa in lines 3 and 5 might likely cause a stronger defective phenotype than the loss of one amino acid in line 12. Overall, the described defects in antheridiophore morphology suggest that Mp*DCL1* regulates antheridiophore development with requirement for integrity of the 1st RNase III and the dsRNA-binding domains. Moreover, the level of Mp*DCL1* activity not only seemed to determine antheridiophore morphology, but also thallus development. Qualitative comparison of thallus size and shape in lines 3, 5 and 12 (Figure 4.8) indicated that thallus expansion and branching in the weaker mutant line 12 was less defective, but more similar to wild type – the thallus of line 12 formed widely expanded, flat lobes with defined apical notches, however, with fewer branches than wild type. On the contrary, lines 3 and 5 formed narrow, bending thallus arms, each terminating in a single, small meristematic region. Taken together, variations of morphological defects in thallus and antheridiophores were correlated with different Mp*dcl1* mutations. This suggests a regulatory activity of Mp*DCL1* in the morphological development of the liverwort thallus and the reproductive structures derived from it. Combined integrity of the 1st RNase III and the dsRNA-binding domains of Mp*DCL1* is required for thallus development and reproductive phase transition.

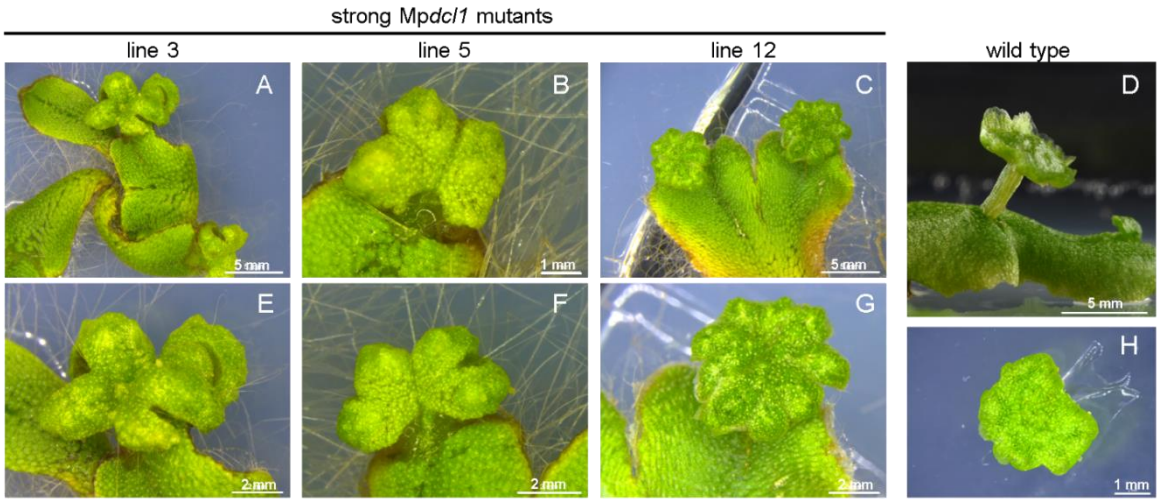


**Figure 4.8: Different mutations in Mp*DCL1* cause different strengths of thallus and antheridiphore morphology defects in strong Mp*dcl1* mutants.** (A-C, E-G) Thalli with antheridiophores of 9-weeks-old plants grown from spores in cool white light without far-red light supplementation (strong male Mp*dcl1* mutants). (D) thallus of a 6.5-weeks-old Tak-1 wild type grown from gemma under far-red light conditions. (H) Close-up from above of the mature receptacle of Tak-1 shown in (D). Mutations in the strong Mp*dcl1* lines are listed in Table 1: (A, E) are line 3, (B, F) is line 5, (C, G) are line 12, all male. White asterisks indicate positions of meristematic notches.

## 4.4. Discussion

Through CRISPR/Cas9-mediated mutagenesis of Mp*DCL1* and phenotyping of different Mp*dcl1* mutant alleles, I have demonstrated that Mp*DCL1* is required for proper development of the *M. polymorpha* thallus. Integrity of the dsRNA-binding domain of Mp*DCL1* is important for thallus growth and expansion, since deletion of the second half of this domain caused slower growth and a narrower thallus relative to wild type. Moreover, fewer gemma cups formed on the mutant than on wild type, suggesting importance of the dsRNA-binding domain for the differentiation of the vegetative reproductive structures. These phenotypic defects were more pronounced in strong Mp*dcl1* mutants with long insertions or deletions in the dsRNA-binding domain and additionally mutations in the 1$^{st}$ RNase III domain. Thalli of Mp*dcl1* plants in which both domains were mutated, were much more defective than Mp*dcl1* mutants in which only the dsRNA-binding domain or the 1$^{st}$ RNase III domain alone was mutated. Instead of a radially expanding flat thallus that bifurcates from the meristematic notches, they developed a narrow and strongly inwards-bending small thallus structure without gemma cups and with few under-developed meristematic notches. During reproductive growth, antheridiophore stalks were strongly stunted and receptacles were irregularly shaped, with epinastically bending lobes instead of a flat, round cap. These phenotypes are consistent with severe growth retardation during the vegetative phase in Pp*dcl1a* mutants, where cell size, shape and differentiation of the protonemal filaments are defective (Khraiwesh *et al.*, 2010). The growth defects of strong Mp*dcl1* mutants are also consistent with general growth retardation and floral organ deformations in At*dcl1* and Zm*dcl1* mutants (Schauer *et al.*, 2002; Thompson *et al.*, 2014). This suggests that the function of *DCL1* genes in regulating plant growth and tissue differentiation is conserved between liverworts, moss and flowering plants. It likely reflects the ancestral nature of *DCL1*, from which *DCL1* paralogs with redundant or specialised

functions evolved after gene duplications, like in *Glycine max* and *P. patens*, respectively (Khraiwesh *et al.*, 2010; Curtin *et al.*, 2016).

The transition from vegetative to reproductive growth in the absence of far-red light is a striking phenotype of strong Mp*dcl1* mutants defective in both the 1st RNase III and the dsRNA-binding domains. Far-red light is an inductive signal required for the development of gametangiophores from meristematic notches of the horizontally expanded thallus in wild type *M. polymorpha*. The small, underdeveloped thallus structures of strong Mp*dcl1* mutants formed gametangiophores when grown in cool white light without supplemented far-red light. It suggests that Mp*DCL1* is important for the inhibition of the reproductive phase in the absence of this inductive light quality. This role of Mp*DCL1* requires the combined integrity of the 1st RNase III domain and the dsRNA-binding domain. In *A. thaliana*, flowering is under control of different pathways that respond to external and internal cues – the photoperiod pathway, the light-quality pathway and the ageing pathway. They all converge in positive or negative regulation of floral integrators like FT (Figure 4.9). The photoperiod pathway mainly responds to blue light, but also to red and far-red light. Far-red light is also processed within the light-quality pathway, which involves phytochrome B (PhyB) receptors. The ageing pathway integrates internal cues and is based on the antagonistic expression and function of the miR156 and miR172 miRNAs. While these three pathways and other regulators of flowering have been studied extensively in *A. thaliana*, very little is known about analogous mechanisms controlling the reproductive phase transition in *M. polymorpha*. Findings from *M. polymorpha* and *A. thaliana* might help to understand the basis of far-red light-independent gametangiophore formation in strong Mp*dcl1* mutants:

Firstly, I have shown in Chapter 3.3.6 that Mp*HST* and downstream of it Mp*SPL1* and Mp*SPL2* are functional components of the ageing pathway that inhibits and promotes gametangiophore development in male and in female *M. polymorpha*, respectively. According to Lin et al. 2016 and Tsuzuki et al. 2016, Mp*SPL1* and Mp*SPL2* are targets of the miRNAs Mpo-MR-13 and miR529c. The observation that Mp*hst-1* mutants require far-red light to produce gametangiophores, suggests that this light quality signal affects the reproductive transition independently of the ageing pathway in *M. polymorpha*.

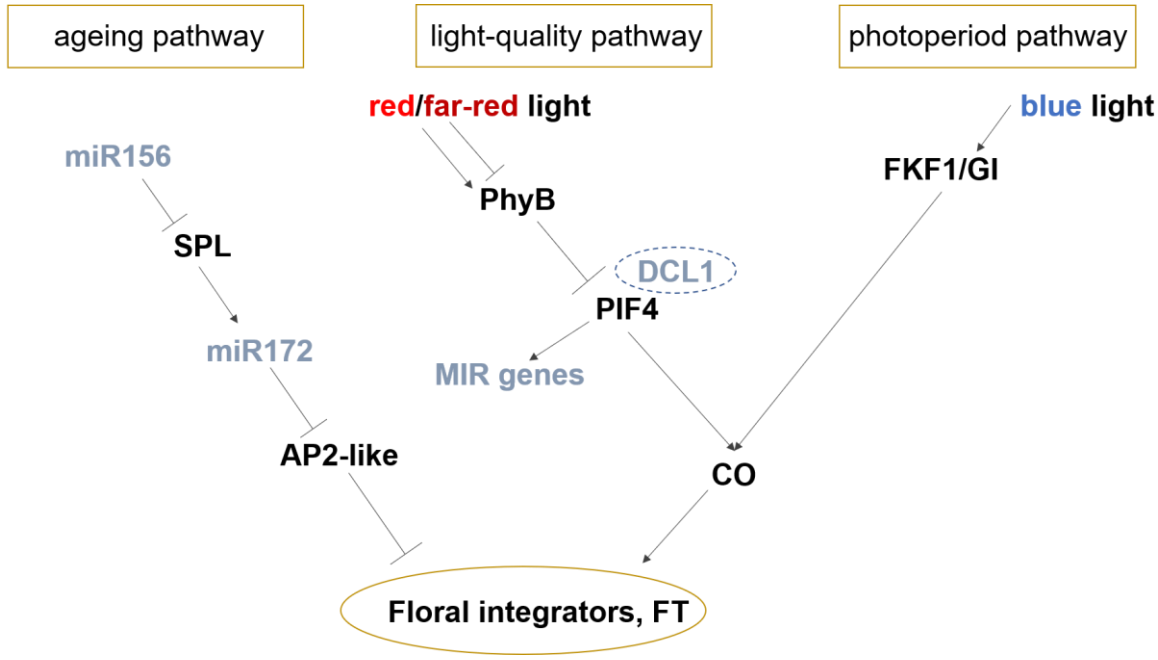


**Figure 4.9: Control of flowering through three main pathways in *A. thaliana*.** While the ageing pathway represses flowering in response to endogenous cues, the light-quality and photoperiodic pathways promote flowering in response to external light cues. Arrows indicate positive interactions, T-lines indicate inhibitory interactions. Pathway components highlighted in grey are associated with miRNA-mediated regulation. Dashed circle around DCL1 indicates a hypothetical interaction with PIF4, which was demonstrated during photomorphogenesis, but was not tested during flowering (Sun *et al.*, 2018).

In *A. thaliana*, red and far-red light activate and inactivate PhyB photoreceptors, respectively. PhyB triggers flowering in response to a low red/far-red ratio, as evident by the late flowering phenotype of At*phyB* mutants (Reed *et al.*, 1993; Costa *et al.*, 2019). PhyB signalling involves PHYTOCHROME INTERACTING FACTOR proteins (PIFs), bHLH transcription factors that are inhibited by activated PhyB (Leivar and Monte, 2014). *M. polymorpha* encodes single copy Mp*PHY* and Mp*PIF* genes, which were shown to regulate gemma germination (Inoue *et al.*, 2016). Moreover, Mp*PHY* is required for the far-red dependent development of gametangiophores, because Mp*phy* loss of function mutants fail to form gametangiophores in far-red light (Inoue *et al.*, 2019). So do Mp*pif* knock-out mutants, suggesting that PIFs are conserved positive regulators of phytochrome signalling in far-red light in angiosperms and liverworts. These findings suggest that a phytochrome signalling pathway integrates the inductive far-red light signal to control the reproductive phase transition in *M. polymorpha*. There is no evidence for the involvement of miRNAs in this process though. However, in *A. thaliana*, an interaction between miRNA processing and red-light signalling in directing plant photomorphogenesis was discovered – At*PIF4* was shown to positively or negatively regulate the transcription of some *MIR* genes (Sun *et al.*, 2018). Furthermore, AtDCL1 and AtHYL1 directly interact with AtPIF4, but the effects of At*dcl1* mutations on far-red dependent flowering have not been elucidated. Since there is an interaction between the miRNA pathway and phytochrome signalling in *A. thaliana*, Mp*DCL1* and certain miRNAs might be required in the far-red light signalling pathway that regulates gametangiophore formation in *M. polymorpa*.

Far-red light also influences the photoperiod pathway, in which it promotes mRNA and protein accumulation of the floral inducer CONSTANS (AtCO) (Sang, Yu and Michaels, 2008). It was speculated that far-red light enrichment stabilises the GIGANTEA (AtGI) protein upstream of AtCO to promote expression of AtCO. This was based on the

observation that in At*gi* mutants, far-red light enrichment does not increase AtCO mRNA levels. The effect of far-red light on AtGI protein accumulation has not been determined, yet. The activity of GI, in complex with FKF1, is required for long-day-dependent reproductive transition in *A. thaliana* as well as in *M. polymorpha* (Sawa *et al.*, 2007; Kubota *et al.*, 2014). It was shown that formation of the MpFKF1-MpGI complex is critical for growth phase transition in the liverwort, because Mp*fkf1* and Mp*gi* knock-out mutants never produced gametangiophores in long days, while wild type produced gametangiopores within 20 days of growth under these conditions. Furthermore, over-expression of Mp*FKF1* or Mp*GI* led to reproductive growth transition regardless of photoperiod (Kubota *et al.*, 2014). In *A. thaliana*, the AtFKF1-AtGI complex degrades CYCLING DOF FACTOR 1 (AtCDF1), a transcriptional inhibitor of the flowering inducer At*CO*. Possible *M. polymorpha* orthologs of these genes have not been characterised, yet, and regulators downstream as well as upstream of the MpFKF1-MpGI complex remain unknown to date. While overexpression of the MpFKF1-MpGI complex enabled gametangiophore formation regardless of day length, it had no effect in the absence of far-red light (Kubota *et al.*, 2014). This could either mean that far-red light influences gametangiophore development independent of the photoperiod pathway, or that far-red light is required for stabilisation of MpGI, as it was proposed for AtGI in *A. thaliana* (Sang, Yu and Michaels, 2008).

The obtained results suggest that Mp*DCL1* is required to repress the reproductive transition in the absence of the inductive far-red light signal. Little is known about the mechanisms that control the reproductive transition, in *M. polymorpha*. There is incomplete evidence that three main pathways that control the reproductive transition in flowering plants, exist in *M. polymorpha* – the ageing pathway, the light-quality pathway and the photoperiod pathway. The latter two promote the reproductive transition, while the ageing pathway inhibits it. The involvement of miRNAs, which are processed by Mp*DCL1*, was

only demonstrated in the ageing pathway (Lin *et al.*, 2016; Tsuzuki *et al.*, 2016). Nevertheless, there is a possibility that liverworts have evolved an independent miRNA-mediated mechanism for far-red light-dependent phase change control, which might be part of the other two or yet another pathway. Generally, the activities of different pathways inhibiting or promoting the reproductive transition must be in balance to ensure correct reproductive timing. Reproductive development might be triggered in response to different disturbances of this balanced network, through changes in the expression of reproductive integrators analogous to floral integrators. The precise regulators that are disturbed in strong Mp*dcl1* mutants because of defective Mp*DCL1* remain to be discovered.

Only male Mp*dcl1* mutants produce antheridiophores without inductive far-red light. Until death through accelerated senescence after three to four months, female plants never transition to the reproductive phase when grown in cool white light without far-red light supplementation. If the signalling pathway that integrates far-red light to control reproductive phase transition was the same in male and female plants, it would be defective in female Mp*dcl1* mutants, too. Therefore, female Mp*dcl1* mutants would form archegoniophores in the absence of far-red light, like male Mp*dcl1* mutants form antheridiophores under these conditions. Since this is not true, this archegoniophore development might be abolished in Mp*dcl1* mutants. To test the hypothesis that Mp*DCL1* is required for female reproductive organ development, archegoniophore formation must be investigated in strong female Mp*dcl1* mutants under inductive conditions. Failure to produce archegoniophores under inductive conditions would confirm this hypothesis, whereas the appearance of archegoniophores would argue against a Mp*dcl1*-induced defect in archegoniophore development. Instead, it would argue for a gender-specific function of Mp*DCL1* in repressing antheridiophore formation under non-inductive conditions. It is

possible that gender-specifically expressed miRNAs that are processed by Mp*DCL1*, are involved in the pathways that control the formation of either antheridiophores or archegoniophores. Taken together, Mp*DCL1* is involved in the sex-specific development of gametangiophores in response to the far-red light signal.

I have shown that the combined activity of the 1st RNase III domain and the dsRNA-binding domain is required for proper growth, differentiation and morphogenesis of the *M. polymorpha* thallus, as well as for the correct timing of the reproductive phase transition. Mp*dcl1* plants mutated in both domains expressed much stronger defects than plants mutated in only one of the two domains. The latter group of mutants showed defects in thallus growth and shape but developed fertile gametangiophores when exposed to far-red light. This suggests that miRNA production is compromised more strongly upon dysfunctionality of multiple Mp*DCL1* domains. Furthermore, if different miRNAs require different activities of the Mp*DCL1* domains for processing, likely a larger set of miRNAs fail to be processed upon dysfunctionality of multiple domains. When considering both domains separately, it becomes apparent that the quality of CRISPR/Cas9-induced mutations differ: Mutagenesis of the dsRNA-binding domain yielded long deletions between both designated gRNA target sites, as well as long insertions. On the contrary, only short deletions and SNPs were identified in individual gRNA target sites in the1st RNase III domain of Mp*dcl1* mutants. Furthermore, after crossing of two Mp*dcl1* CRISPR mutants with mutations in one of the two domains each, several new mutations originated in the dsRNA-binding domain in F2 individuals. By contrast, only parental and no new mutations were identified in the 1st RNase III domain of Mp*dcl1* offspring. This suggests that the inherited CRISPR transgenes generated a wide range of novel mutations in the dsRNA-binding domain, but only a specific type of small mutation in the 1st RNase III domain. Therefore, it is likely that Mp*DCL1* can

tolerate different mutations in the second half of the dsRNA-binding domain, whereas it is more sensitive to mutations in the 1st RNase III domain. The fact that no plants with larger mutations in this domain were observed, might argue for embryo-lethality upon severe disruption of the sequence encoding the 1st RNase III domain. An alternative explanation for the presence of exclusively small mutations in the 1st RNase III domain might be lower efficiency of the two gRNAs designed and used in the CRISPR 2 construct.

The *fuzzy tassle* mutant of Zm*DCL1* develops pleiotropic developmental phenotypes in maize, which underlie a SNP in exon 17 as part of the 1st RNase III domain (Thompson *et al.*, 2014). Similarly, short in-frame deletions in exon 17 in the here investigated Mp*dcl1* mutants contribute to the described developmental defects in *M. polymorpha*. In A. *thaliana*, different At*dcl1* alleles contain mutations in the two encoded dsRNA-binding domains. While deletion of both dsRNA-binding domains causes embryo-lethality in At*dcl1-6*, loss of only the second dsRNA-binding domain through a T-DNA insertion enables proper embryogenesis in At*dcl1-9*, but causes severe pleiotropic developmental defects including sterility (Jacobsen, Running, and Meyerowitz 1999; Schauer et al. 2002). Unlike most land plant DCL1 proteins, MpDCL1 contains only one dsRNA-binding domain. Integrity of the first half of this single dsRNA-binding domain enables partial activity of MpDCL1, including fertility. Whether the abnormal antheridiophores produced by strong Mp*dcl1* mutants produce fertile sperm, remains to be tested. Overall, the defective phenotypes corresponding to various Mp*dcl1* alleles suggest that the 1st RNase III and the dsRNA binding domains are required for proper activity of MpDCL1 to control plant development, as they are for DCL1 proteins in angiosperms.

Taken together, my results demonstrate the pleiotropic requirement of Mp*DCL1* for growth and differentiation of the horizontal thallus. The role of *DCL1* in regulating overall plant

growth and morphology is therefore conserved between angiosperms and bryophytes. So is the importance of the 1st RNase III domain and the dsRNA-binding domain for functionality of *DCL1*. My data suggest that significant disruption of the 1st RNase III domain of Mp*DCL1* could cause embryo lethality. Moreover, it severely affects the expression of the reproductive phase when combined with large mutations in the dsRNA-binding domain. Strong Mp*dcl1* mutants that are defective in both domains develop a phenotype that has not been described in any plant *dcl1* mutant before – the requirement of far-red light as an inducer of reproductive phase transition in wild type is abolished in strong Mpdcl1 mutants. Furthermore, this is only true in male Mp*dcl1* mutants, while female Mp*dcl1* mutants do not form gametangiophores without far-red light supplementation. This observation suggests that there is a role for Mp*DCL1* in repressing reproductive development in the absence of inductive far-red light, which is influenced by sex-specific factors in the two genders of the dioecious liverwort.

# Chapter 5 – Establishment of a suppressor mutant screen to identify novel components of miRNA biogenesis in *M. polymorpha*

## 5.1. Abstract

microRNAs (miRNAs) form a specific class of small non-coding RNAs, which act as post-transcriptional regulators of gene expression. miRNAs are mainly derived from independent *MIR* genes; their primary transcripts (pri-miRNAs) fold into hairpin structures, which contain sequences that are complementary to specific target gene sequences. miRNA processing is initiated co-transcriptionally and in a stepwise manner, pri-miRNAs are cleaved into precursor miRNAs (pre-miRNAs) and eventually into 21-nt-short mature miRNAs. This biogenesis pathway involves numerous RNA-binding proteins interacting with the core endoribonuclease DICER-LIKE1 (DCL1) and the RNA slicer protein ARGONAUTE 1 (AGO1). The canonical plant miRNA biogenesis pathway was mainly discovered in *A. thaliana* and knowledge about it is limited in the bryophytes. I have previously shown that *M. polymorpha* encodes core regulators of the canonical miRNA processing pathway, suggesting that a large part of it is conserved between flowering plants and liverworts. I have demonstrated that Mp*DCL1* and Mp*HASTY* (Mp*HST*), a putative nuclear exporter of miRNAs, regulate the accumulation of miRNAs and their target genes. To verify the functions of other putative miRNA biogenesis regulators and to identify more components of the pathway in *M. polymorpha*, I set up a mutagenesis screen. By screening for suppressors of the few/short-rhizoids phenotype of the Mp*FRH1*$^{GOF}$ mutant, which overexpresses the Mp*FEW RHIZOIDS 1* (Mp*FRH1*) miRNA, I aimed to discover genes that encode proteins involved in miRNA processing. I previously showed that disruption of MpFRH1 biogenesis by reducing Mp*DCL1* or Mp*HST* function restored rhizoid development in Mp*FRH1*$^{GOF}$*;hst* and Mp*FRH1*$^{GOF}$*;dcl1* double mutants. Therefore, I predicted that other genes encoding proteins that regulate miRNA accumulation could be discovered by carrying out a suppressor screen in the Mp*FRH1*$^{GOF}$ background. This would allow the identification of genes in which a mutation would restore the development of

abundant, long rhizoids. I have established UV-B and T-DNA suppressor mutant screens in the Mp*FRH1*$^{GOF}$ background. Among 36,400 plants that survived UV-B treatment, three putative partial suppressor mutants with longer and slightly more abundant rhizoids than Mp*FRH1*$^{GOF}$ were identified. However, they could not be confirmed as suppressor mutants due to sterility. The generation of approximately 400 chlorsulfuron-resistant T-DNA insertion lines validated functionality of a newly cloned T-DNA vector conferring chlorsulfuron resistance. Based on previously observed UV-B and T-DNA mutagenesis efficiencies, screening more than 100,000 mutated lines will more likely enable the discovery of suppressor mutants of Mp*FRH1*$^{GOF}$ in the future.

## 5.2. Introduction

miRNAs are encoded by *MIR* genes. Their primary transcripts (pri-miRNAs) are processed into 21 nt-short mature miRNAs in a complex biogenesis pathway. This involves the activity of numerous RNA-binding proteins, including the central effectors DCL1 and AGO1 (Achkar, Cambiagno and Manavella, 2016). The canonical plant miRNA biogenesis pathway has been described in *A. thaliana*, but barely studied in bryophytes (Wang, Mei and Ren, 2019). Using protein BLAST search, I discovered that most of the known proteins involved in *A. thaliana* miRNA biogenesis are also present in the *M. polymorpha* genome (thesis Chapter 2.1).

*Steps that are unknown in plant miRNA processing*

Although the genes encoding core regulators of miRNA processing are present in *M. polymorpha*, their involvement in miRNA production in liverworts remains to be shown. Studying miRNA biogenesis regulators in *M. polymorpha* will not only elucidate the evolution of the miRNA pathway in the early divergent embryophytes but may also clarify yet unresolved functions in global plant miRNA processing. For example, it was assumed that miRNAs are processed to maturity in the nucleus and subsequently exported to the cytoplasm to inactivate their mRNA targets there. This was supported by the observation that more mature miRNAs accumulated in the cytoplasm than in the nucleus (Park *et al.*, 2005). However, no nuclear exporter could be assigned responsible for nucleo-cytosolic trafficking of miRNAs. The closest candidate to fulfil this function is the nuclear export receptor At*HST*, which contains an exportin1-like domain. Although At*HST* positively regulates overall miRNA levels in the cell, cytoplasmic miRNA accumulation was not abolished in At*hst-1* mutants (Park *et al.*, 2005). At*HST* is therefore likely not the only protein responsible for the nuclear export of miRNAs. Recent findings revealed nucleo-

cytosolic shuttling of AGO1 to be required for the translocation of mature, methylated miRNAs (Bologna *et al.*, 2018b). This depends on EXPORTIN 1 (EXPO1) transporters and suggests that mature miRNAs are loaded into AGO1 to be exported to the cytosol as AGO1:miRNA complexes. It remains unknown how the partitioning of both translocation mechanisms – nuclear export of miRNAs and nucleo-cytosolic shuttling of AGO1 – are regulated. Overall, there is more potential to discover new components and mechanisms involved in the fine-tuning of miRNA processing steps from the stabilisation of miRNA intermediates to the timely and spatial control of the assembly of the Dicing complex and the RNA-INDUCED SILENCING COMPLEX (RISC).

*M. polymorpha is a suitable system in which to carry out a mutagenesis screen for miRNA biogenesis regulators*

*M. polymorpha* is a good system for forward mutagenesis screens. Haploidy of the dominant phase of its life cycle and low genetic redundancy facilitate the functional analysis of mutant genes. The fact that one fertilisation event produces one sporangium containing several hundred thousand small spores approximately 10 µm in diameter, means that large-scale screens can be carried out easily. Few individual miRNAs have been studied in *M. polymorpha*, but Mp*FRH1* has been functionally characterised (Tsuzuki *et al.*, 2016; Honkanen, Thamm, Arteaga-Vazquez, *et al.*, 2018). Mp*FRH1* is a regulator of rhizoid differentiation. By initiating mRNA cleavage, it represses the activity of its target Mp*RHIZOID DEFECTIVE 6-LIKE 1* (Mp*RSL1*), a bHLH transcription factor that promotes rhizoid differentiation from rhizoid precursor cells in the ventral epidermis of the thallus. Overexpression of Mp*FRH1* in the Mp*FRH1*$^{GOF}$ mutant abolishes rhizoid formation, resulting in mutants with fewer and shorter rhizoids than wild type. Additionally, Mp*FRH1*$^{GOF}$ mutants produce fewer gemmae than wild type due to Mp*RSL1* being a general

regulator of specialised epidermal cell differentiation (Proust *et al.*, 2016). In Chapter 2, I demonstrated that the few/short-rhizoids phenotype of the Mp*FRH1*$^{GOF}$ mutant was suppressed by weak mutations in the Mp*DCL1* gene in the Mp*FRH1*$^{GOF}$*;dcl1* double mutant and by weak mutations in Mp*HST* in the Mp*FRH1*$^{GOF}$*;hst* double mutant. These suppressor phenotypes, which were wild type-like rhizoids in the double mutants, were correlated with a reduction in the steady state levels of MpFRH1 and an increase in mRNA levels of Mp*RSL1*. Therefore, the few/short-rhizoids phenotype of the Mp*FRH1*$^{GOF}$ mutant responded to changes in MpFRH1 levels caused by defects in the biogenesis of the MpFRH1 miRNA. This feature makes the Mp*FRH1*$^{GOF}$ mutant a suitable system in which to study miRNA biogenesis, because in a wild type background instead, changes in the abundance of different miRNA intermediates are difficult to detect.

I set out to mutagenize spores with a genetic Mp*FRH1*$^{GOF}$ background in a suppressor screen to identify novel components of miRNA processing. This mutagenesis screen was intended to improve our knowledge about the pre-existing plant miRNA processing pathway and to characterise the miRNA biogenesis pathway in *M. polymorpha*. Besides identifying potentially conserved core regulators of the pathway, I hoped to discover liverwort-specific as well as tissue-specific regulators of miRNA processing. UV-B and T-DNA mutagenesis screens were established to discover suppressor mutants of the Mp*FRH1*$^{GOF}$ few-rhizoids phenotype.

## 5.3. Results

### 5.3.1. Establishment of a UV mutagenesis screen for suppressor mutants of the Mp*FRH1*$^{GOF}$ few-rhizoids phenotype

In Chapter 2, I demonstrated that Mp*DCL1* and Mp*HST*, conserved core regulators of the miRNA biogenesis pathway in land plants, process the liverwort-specific miRNA MpFRH1. The Mp*FRH1*$^{GOF}$ over-expresser mutant thereby served as a genetic tool to test for MpFRH1 miRNA abundance in response to Mp*dcl1* and Mp*hst* mutations. Making use of the Mp*FRH1*$^{GOF}$ mutant again, I set out to establish a UV-B mutagenesis screen to discover novel genes involved in miRNA biogenesis. I hypothesised that mutagenesis of spores of the Mp*FRH1*$^{GOF}$ mutant using UV-B irradiation would cause mutations in genes encoding proteins required for MpFRH1 miRNA biogenesis (Figure 5.1). Mutations that compromise gene function would cause reduced processing of MpFRH1 in the Mp*FRH1*$^{GOF}$ over-expresser background. In suppressor mutants, MpFRH1 levels would be restored to nearer wild type, allowing rhizoid development. Therefore, suppressor mutants could be selected based on restored rhizoid growth ability compared to the Mp*FRH1*$^{GOF}$ short rhizoids. The screening procedure was similar to the experimental setup in Chapter 2, where I assayed the recovery of rhizoid formation in Mp*FRH1*$^{GOF}$*;hst* and Mp*FRH1*$^{GOF}$*;dcl1* double mutants compared to the few rhizoids in the Mp*FRH1*$^{GOF}$ single mutant.

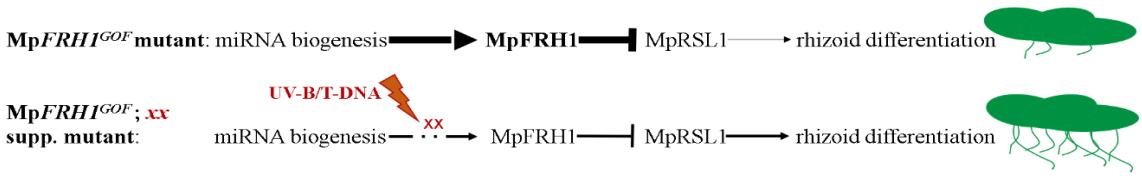


**Figure 5.1: Random mutagenesis of the Mp*FRH1*$^{GOF}$ over-expresser is predicted to reduce MpFRH1 processing and allow rhizoid development**. Simplified model of the genetic interaction between the MpFRH1 miRNA and the Mp*RSL1* transcription factor to control rhizoid development in the Mp*FRH1*$^{GOF}$ single mutant and predicted Mp*FRH1*$^{GOF}$*;x* suppressor mutants . *X* is a mutated gene encoding for a regulator of

miRNA biogenesis. Red arrow indicates mutagenesis by UV-B light or T-DNA insertion. In Mp*FRH1*$^{GOF}$ plants, a T-DNA in the Mp*FRH1* promoter causes up to 100-fold higher expression of MpFRH1 than wild type (Figure 2.7) and therefore post-transcriptional hyper-repression of Mp*RSL1*, master regulator of rhizoid development. Consequently, few rhizoids are formed in the Mp*FRH1*$^{GOF}$ mutant. In suppressor mutants, wild type-like MpFRH1 levels are restored due to compromised miRNA processing. This allows wild type-like expression of Mp*RSL1* to initiate the formation of abundant rhizoids in Mp*FRH1*$^{GOF}$;*x* suppressor mutants.

#### 5.3.1.1. Selection of Mp*FRH1*$^{GOF}$ spores for UV-B mutagenesis

In this suppressor screen, spores of the Mp*FRH1*$^{GOF}$ genotype were mutagenized. To obtain these spores, I crossed male and female T1 Mp*FRH1*$^{GOF}$ mutants to each other. While males produced sperm, female archegoniophores were small and short-lived, and could not be fertilised. As an alternative, I crossed the male Mp*FRH1*$^{GOF}$ mutant, which carried a single T-DNA in the Mp*FRH1* promoter, with Tak-2 wild type. 50 % of the resulting spores carried a wild type Mp*FRH1* allele. Wild type sporelings were phenotypically distinguishable from sporelings with the Mp*FRH1*$^{GOF}$ mutation after germination and formation of the 3D thallus, because they produced abundant rhizoids compared to few rhizoids in Mp*FRH1*$^{GOF}$ spores (Figure 5.2). The suppressor screen relies on mutagenizing a population of spores carrying the Mp*FRH1*$^{GOF}$ mutation, and screening for a suppressor mutation causing reversion of the few-rhizoids phenotype to wild type rhizoid phenotype. Therefore, the F2 progeny of the Mp*FRH1*$^{GOF}$ x Tak-2 cross could not initially be used as the population to be mutagenized and screened, as it contained wild type spores. These form abundant rhizoids, hence are phenotypically indistinguishable from putative suppressor mutants, which were expected to have abundant rhizoids, too. To eliminate wild type spores from the mutagenesis and subsequent screening process, I supplemented the growth medium with hygromycin. Since the T-DNA insertion in the Mp*FRH1*$^{GOF}$ mutant contained a hygromycin resistance gene, Mp*FRH1*$^{GOF}$ spores were able to grow in the presence of the antibiotic, while wild type

spores died. In the lab, a concentration of 10 ng µl$^{-1}$ hygromycin was used to select against non-resistant plants. Since wild type spores are sensitive to hygromycin, I expected approximately 50 % of total spores per plate to die. Additional losses were predicted as a result of spore germination rates below 100% due to long-term storage of sporangia. Indeed, when comparing the number of 2-weeks-old sporelings from a Mp*FRH1*$^{GOF}$ x Tak-2 cross growing on plates with 10 ng µl$^{-1}$ hygromycin to sporelings growing on plates without hygromycin, 56 % of spores were sensitive to the antibiotic. Similarly, 5 ng µl$^{-1}$ hygromycin eliminated about 65 % of spores that would grow without the antibiotic. Sporelings resistant to both concentrations of hygromycin developed fewer or no rhizoids, as illustrated in Figure 5.2.

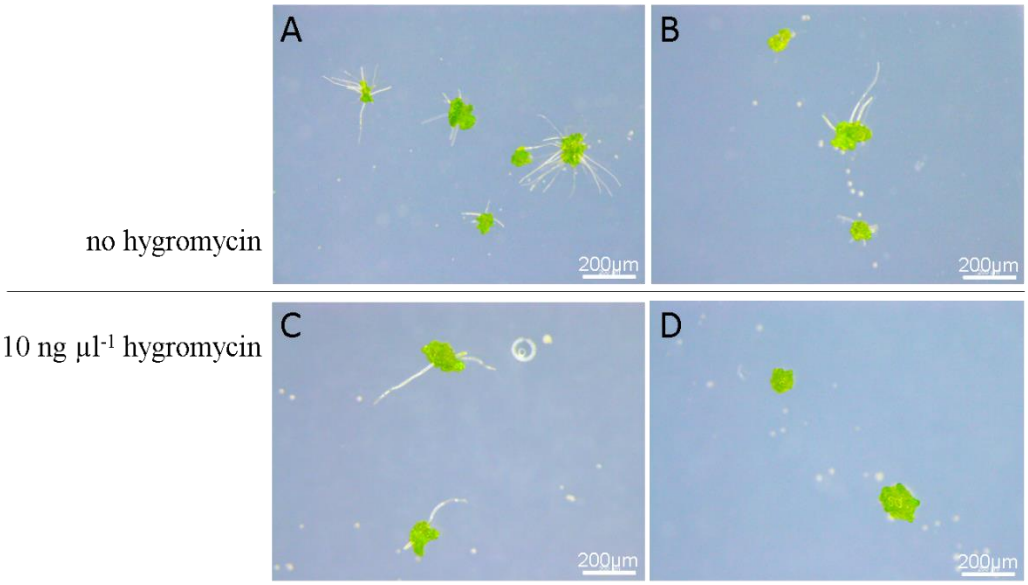


**Figure 5.2: Wild type spores are eliminated from the F2 populations of Mp*FRH1*$^{GOF}$ x Tak-2 crosses by selection on hygromycin.** Images of 9-d-old sporelings, derived from a Mp*FRH1*$^{GOF}$ x Tak-2 cross, grown on solid 1.4 % Johnson's medium with (C-D) or without (A-B) 10 ng µl$^{-1}$ hygromycin. (A-B) show a mix of wild type sporelings with abundant rhizoids and Mp*FRH1*$^{GOF}$ sporelings with few or no rhizoids, while in (C-D) only Mp*FRH1*$^{GOF}$ sporelings grow.

#### 5.3.1.2. UV-B mutagenesis of Mp*FRH1*$^{GOF}$ spores and screening for suppressor mutants

I sterilised F2 spores from Mp*FRH1*$^{GOF}$ x Tak-2 crosses with 1% sodium dichloroisocyanurate. For mutagenesis, I spread sterilised spores on 10 mm x 10 mm square petri dishes (approx. 7,400 spores per plate, counted with a haemocytometer) filled with Johnson's medium supplemented with 5 ng µl$^{-1}$ or 10 ng µl$^{-1}$ hygromycin. I then exposed these plates to UV-B irradiation with a wavelength of 302 nm for 70 sec, the UV-B dose applied in previous mutant screens in the lab (unpublished data). One sporangium's spores were mutagenized per round of mutagenesis (approx. 260,000 spores). For each round, I prepared control plates with or without hygromycin that were not exposed to UV-B light to provide phenotypic references for either non-mutated Mp*FRH1*$^{GOF}$ mutant or wild type, respectively. Immediately after mutagenesis, all plates including the control plates were sealed with micropore tape and wrapped in aluminium foil to be kept in the dark for one day. This prevented the blue light-dependent repair of pyrimidine dimers caused by UV-B irradiation. Such dimers between two subsequent pyrimidine bases form bulky rings, which compromise the precision of the DNA polymerase during DNA replication. If not repaired, mutations are generated, often CC to TT substitutions (Ikehata and Ono, 2011). After a 12-24 h incubation period in the dark, plates were kept in Sanyo cabinets to grow at 23 °C under standard growth conditions. After 14 days and up to 48 days after mutagenesis, I screened the mutated sporelings for formation of abundant rhizoids using the optical light microscope (Leica). Most plants were expected to express the Mp*FRH1*$^{GOF}$ few rhizoids phenotype. I screened for plants that formed abundant rhizoids similar to wild type. To more confidently identify the suppressor phenotype (wild type-like rhizoids), I compared plants on mutagenized plates to plants growing on the control plates that were not mutagenized.

### 5.3.1.3. Characterisation of putative suppressor mutants

After exposure of Mp*FRH1*$^{GOF}$ spores to UV-B irradiation for 70 sec and subsequent growth for at least two weeks, putative suppressor mutants were picked from the mutagenized plates. They were selected by eye based on the formation of more abundant rhizoids. In total, this UV-B mutagenesis screen has involved the mutagenesis of 1,820,000 spores from seven sporangia, of which 36,400 surviving sporelings with a genetic Mp*FRH1*$^{GOF}$ background were screened for abundant rhizoids. Table 1 lists the seven most promising suppressor mutant candidates I have identified in this screen.

**Table 5.1: Summary of putative suppressor mutants after UV-B mutagenesis and screening of approximately 36,400 spores, with analysed traits.** HYG = hygromycin.

| suppressor mutant candidate line | HYG concen-tration | presence of Mp*FRH1* T-DNA | qualitative imaging of gemmae | quantitative rhizoid length measurement | Plant growth on soil |
|---|---|---|---|---|---|
| **R** ♂ | 5 ng µl$^{-1}$ | yes | more abundant rhizoids than Mp*FRH1*$^{GOF}$ | significantly longer rhizoids than in Mp*FRH1*$^{GOF}$ | similar to Mp*FRH1*$^{GOF}$ |
| **P** ♀ | 5 ng µl$^{-1}$ | yes | more abundant rhizoids than Mp*FRH1*$^{GOF}$ | longer rhizoids than in male Mp*FRH1*$^{GOF}$, but lack of female Mp*FRH1*$^{GOF}$ control - inconclusive result | similar to MP*FRH1*$^{GOF}$ |
| **J3** ♂ | 10 ng µl$^{-1}$ | yes | more abundant rhizoids than Mp*FRH1*$^{GOF}$ | rhizoids are not longer than in Mp*FRH1*$^{GOF}$ | similar to Mp*FRH1*$^{GOF}$ |
| **A5 - D5** ♀ | 10 ng µl$^{-1}$ | yes | more abundant rhizoids than Mp*FRH1*$^{GOF}$ | N.A. | grow slightly bigger than Mp*FRH1*$^{GOF}$ |

Firstly, to confirm that the seven plants with abundant rhizoids were putative suppressor mutants as opposed to hygromycin-resistant wild types, I confirmed that their genetic background was Mp*FRH1*$^{GOF}$. This was done by PCR with a forward primer binding to the T-DNA sequence and a reverse primer binding to the promoter of Mp*FRH1* – a PCR product

of 850 bp was amplified in presence of the T-DNA insertion. All seven selected plants had an Mp*FRH1*$^{GOF}$ background and could therefore be suppressor mutants. I performed another genotyping PCR to identify their genders (see Materials and Methods), since from experience, male and female Tak-1 and Tak-2 wild type plants differ in their rhizoid phenotypes with more abundant rhizoids in Tak-1. Therefore, when characterising rhizoid growth in the putative suppressor mutants, I used wild types of the same sex for comparison. The putative suppressor mutants P and R were selected from the same mutagenesis experiment; P was a female plant, while R was a male. Line J3, a male plant, was identified after independent mutagenesis of another sporangium. Lastly, the female lines A5-D5 originated from a third sporangium. In summary, from 36,400 sporelings with a genetic Mp*FRH1*$^{GOF}$ background that were screened for abundant rhizoids, I identified seven putative suppressor mutants. Their phenotypes are described in the following sections.

#### 5.3.1.4. Qualitative imaging of putative suppressor mutants

The putative suppressor mutants produced more abundant rhizoids than the Mp*FRH1*$^{GOF}$ single mutant. However, their suppressor phenotypes were subtle, with rhizoid abundance less than wild type. To test if the appearance of more rhizoids was a stable phenotype, I plated gemmae from the candidate lines on 1.4 % Johnson's medium and compared their rhizoid phenotypes to Mp*FRH1*$^{GOF}$ and Tak wild type rhizoid phenotypes. Figure 5.3 shows microscopic images of 7- and 10-day-old gemmae of P, J3, A5-D5 and the respective controls, with white rhizoids growing out from their ventral sides. The gemmae phenotypes confirmed that slightly more rhizoids were present on the putative suppressor mutants than in the Mp*FRH1*$^{GOF}$ mutant, especially after ten days. This suggests that there was a slight but not full suppression of the Mp*FRH1*$^{GOF}$ few rhizoids phenotype in those lines. The most strikingly different rhizoid phenotype was observed in candidate line R. Although the abundance of rhizoids did not appear significantly higher in R than in Mp*FRH1*$^{GOF}$, rhizoids

were longer in R than in Mp*FRH1*$^{GOF}$ (Figure 5.4). In Mp*FRH1*$^{GOF}$, the few rhizoids that are formed are much shorter than wild type rhizoids (Figure 5.4). When grown on solid agar medium, no significant difference between Mp*FRH1*$^{GOF}$ and the putative suppressor mutants was observed in thallus growth and morphology: Compared to Tak-2, thalli of female Mp*FRH1*$^{GOF}$ mutants as well as the female candidates P and A5-D5 grew smaller and slightly bent upwards on the edges. On the contrary, thalli of male Mp*FRH1*$^{GOF}$ as well as lines R and J3 were flatter and more expanded than Tak-1 thalli. Taken together, the observed rhizoid growth on gemmae confirmed that slightly more rhizoids developed in the putative suppressor mutants than in the Mp*FRH1*$^{GOF}$ mutant, while thallus morphology was similar. This rhizoid phenotype was therefore inherited through vegetative reproduction.

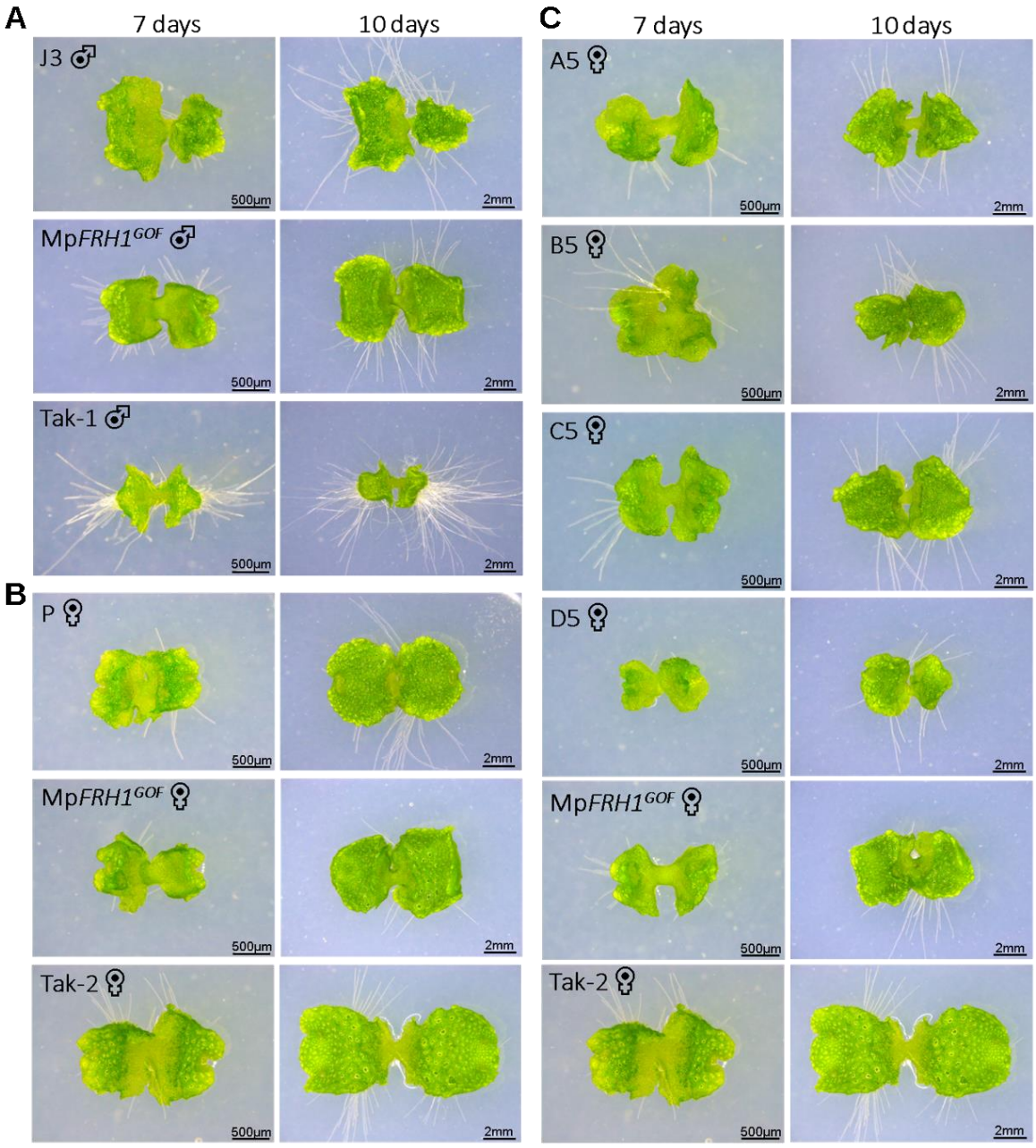


**Figure 5.3: Putative suppressor mutants develop slightly more abundant rhizoids than Mp*FRH1*$^{GOF}$ mutants.** Gemmae from putative suppressor mutants and their parental Mp*FRH1*$^{GOF}$ lines and Tak wild type were grown on solid 1.4 % Johnson's medium and imaged after seven and ten days. Lines J3 (A), P (B) and A5-D5 (C) are shown.

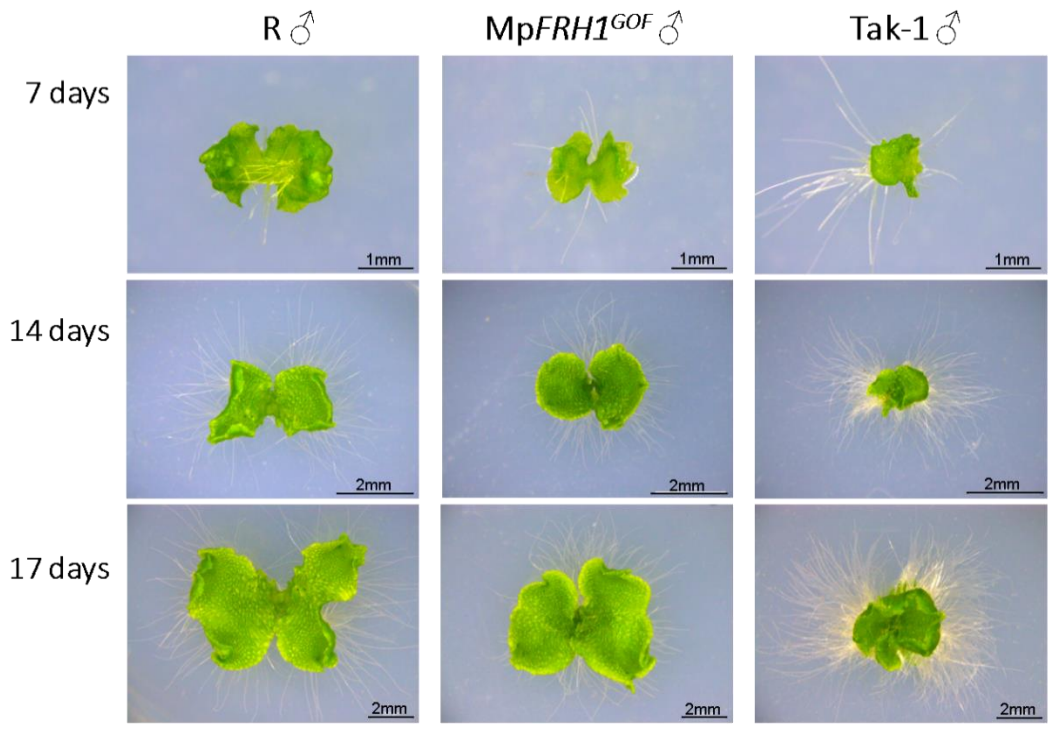


**Figure 5.4: The strongest putative suppressor mutant 'R' develops slightly more abundant and seemingly longer rhizoids than Mp*FRH1*$^{GOF}$.** Gemmae from suppressor mutant candidate R, the parental male Mp*FRH1*$^{GOF}$ line and Tak-1 wild type were grown on solid 1.4 % Johnson's medium and imaged after seven, 14 and 17 days.

#### 5.3.1.5. Quantification of rhizoid length in putative suppressor mutants

To more confidently assess the putative suppressor phenotype in the selected lines, I quantified rhizoid length. Since the few rhizoids in the Mp*FRH1*$^{GOF}$ mutant are shorter than wild type rhizoids, I expected longer rhizoids in suppressor mutants compared to Mp*FRH1*$^{GOF}$. As R, P and J3 showed the strongest potential suppressor phenotypes, I first analysed these lines by growing eight gemmae per line on 0.8 % Johnson's medium in plastic tubes and measuring rhizoid length weekly, up to four weeks for J3 and up to five weeks for P and R. I grew and measured Tak-1 wild type and the male Mp*FRH1*$^{GOF}$ mutant as controls. Candidate lines P and R with controls were analysed in an independent experiment than J3 with the same controls. In both experiments, rhizoid length in Tak-1 reached about 25 mm

after four weeks, with slow growth within the first two weeks (Figure 5.5). On the contrary, Mp*FRH1*$^{GOF}$ rhizoids elongated mainly within the first two weeks, after which rhizoid length stagnated around 7-10 mm. This was not the case in lines P and R, where rhizoid elongation was highest within the first two weeks, but then continued almost linearly. After five weeks, rhizoids from line P had reached around 17 mm in length, and those from line R were around 14 mm long. These rhizoids were therefore significantly longer than Mp*FRH1*$^{GOF}$ rhizoids, although they did not grow to wild type length. This is because rhizoids from lines P and R elongated more slowly than wild type, growing only 1.5-5 mm per week compared to 8-10 mm in wild type. This suggests partial suppression of the short rhizoid phenotype of the Mp*FRH1*$^{GOF}$ mutant in the candidate lines P and R. However, to obtain comprehensive proof that rhizoid development is partly restored in line P, rhizoid length measurement should be repeated including Tak-2 and female Mp*FRH1*$^{GOF}$ controls, since P is a female plant. Rhizoid length in candidate line J3 was almost the same as in Mp*FRH1*$^{GOF}$ over the course of four weeks. The only difference was that J3 rhizoids were as long as wild type rhizoids after one week (4 mm), while Mp*FRH1*$^{GOF}$ rhizoids were only 1 mm long. This observation might suggest that J3 is defective in a process that controls early rhizoid outgrowth or elongation, providing partial suppression of the Mp*FRH1*$^{GOF}$ short-rhizoids phenotype.

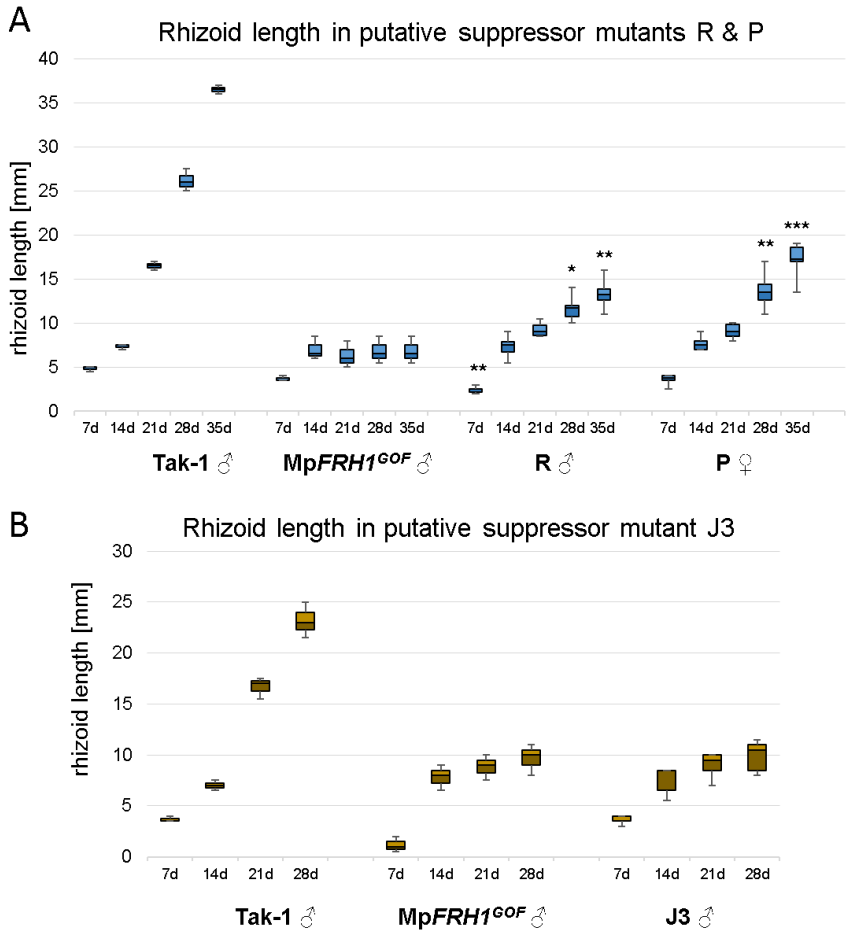


**Figure 5.5: The short rhizoids phenotype of the Mp*FRH1*$^{GOF}$ mutant is partially suppressed in the putative suppressor mutant(s) R (and P).** Boxplots showing rhizoid length on day 7, 14, 21, 28 (and 35 in (B)) after gemmae were brought out to grow on Johnson's medium supplemented with 0.8 % Phytagel in plastic tubes, n = 8. (A) Putative suppressor mutants R (male) and P (female) with male control lines Tak-1 and Mp*FRH1*$^{GOF}$, (B) Male putative suppressor mutant J3 with male control lines Tak-1 and Mp*FRH1*$^{GOF}$. Significant differences in rhizoid length relative to Mp*FRH1*$^{GOF}$ were calculated by two-tailed student's t-test with unequal variances. * $p < 0.05$, ** $p < 0.01$, *** $p < 0.001$.

#### 5.3.1.6. Testing growth and vitality of putative suppressor mutants on soil

Seven candidate mutants identified after UV-B mutagenesis showed partial restoration of rhizoid abundance and length relative to the few and short rhizoids in the Mp*FRH1*$^{GOF}$

mutant. Few and short rhizoids negatively impact overall growth and fitness in Mp*FRH1*$^{GOF}$ mutants, since their limited ability to take up water and nutrients leads to slow growth and desiccation. This phenotype is particularly strong in plants growing on soil, since the short rhizoids of the Mp*FRH1*$^{GOF}$ mutant lack the ability to anchor in the solid ground, where water is available. Mp*FRH1*$^{GOF}$ mutants grow more slowly on soil, where they never reach wild type size and produce gametangiophores late if ever. When Mp*FRH1*$^{GOF}$ plants succeed in entering reproductive growth, then antheridiophores are short-living and archegoniophores are fragile and rarely reach maturity (data not shown). I predicted that if the candidate suppressor mutants had regained the ability to form rhizoids, they would develop a larger, faster-growing thallus than Mp*FRH1*$^{GOF}$ plants. To test this, I first grew the putative suppressor mutant lines, wild type and Mp*FRH1*$^{GOF}$ mutant plants derived from gemmae in plastic pots filled with a layer of soil. I saturated this soil with sterilised water to create as humid an environment as possible, before closing the lids. In the first few weeks, the Mp*FRH1*$^{GOF}$ plants as well as the putative suppressor mutants grew similarly well as wild type. Their thalli were small and flat enough to embed in the watery surface of the soil and take up water sufficiently. Apart from less abundant and shorter rhizoids, the putative suppressor mutants did not develop any obvious thallus growth defects when growing on soil. After about two weeks, once the thalli had grown larger and less flat, Mp*FRH1*$^{GOF}$ mutant plants grew more slowly and smaller compared to wild type. Similarly, the putative suppressor mutants P, R and J3 did not grow notably larger than Mp*FRH1*$^{GOF}$. Also, overall plant growth in lines A5-D5 was very similar to Mp*FRH1*$^{GOF}$, with plants growing slowly and not fully reaching reproductive maturity. This observation suggests that although rhizoid length was partly recovered in P and R compared to Mp*FRH1*$^{GOF}$, overall rhizoid development in any of the putative suppressors was not sufficiently restored to allow wild-type like plant growth. Using plant fitness on soil as an indirect measure of rhizoid

abundance validated that lines P, R and J3 were partial putative suppressor mutants of the Mp*FRH1*$^{GOF}$ short rhizoids phenotype. However, since these lines, as well as the putative suppressor mutants A5-D5 appeared to be sterile, I was not able to test if the suppressor phenotype was inherited. Therefore, further analysis to confirm suppressor mutants was hindered and not pursued because of incompleteness of the suppression phenotypes.

### 5.3.2. Establishment of a T-DNA mutagenesis screen for suppressor mutants of the Mp*FRH1*$^{GOF}$ few-rhizoids phenotype

While I was aiming to discover Mp*FRH1*$^{GOF}$ suppressor mutants with strongly restored rhizoid development similar to the Mp*FRH1*$^{GOF}$*;dcl1* and Mp*FRH1*$^{GOF}$*;hst* double mutants described in Chapter 2, I only identified plants expressing partial suppression. UV-B mutagenesis introduces point mutations, which could cause a range of defects, from minor amino acid changes to the generation of a premature stop codon or the alteration of crucial protein interaction sites. To increase the likelihood of introducing a suppressor mutation strong enough to visibly restore rhizoid development, I also used T-DNA insertion as a mutagen. When T-DNA is inserted into a coding region, this is likely to lead to significant disruption of the affected gene sequence. Moreover, T-DNA insertions are likely to cause gain-of-function mutations when containing enhancers of gene expression. This is the case in the Mp*FRH1*$^{GOF}$ mutant, where a CamV 35S promoter as part of the T-DNA in the Mp*FRH1* promoter presumably increases transcription. T-DNA mutants are selected based on antibiotic resistance, encoded on the T-DNA. I set out to establish a T-DNA mutagenesis screen for suppressors of the Mp*FRH1*$^{GOF}$ few rhizoids phenotype to identify novel components of the miRNA biogenesis pathway in *M. polymorpha*.

#### 5.3.2.1. Cloning and Testing of a chlorsulfuron-resistant T-DNA vector

The Mp*FRH1*$^{GOF}$ mutant itself was produced by T-DNA mutagenesis with the pCAMBIA1300 T-DNA vector and therefore contains a hygromycin resistance gene. To discriminate between hygromycin-resistant Mp*FRH1*$^{GOF}$ single mutants and suppressor mutants, I generated another T-DNA plasmid conferring chlorsulfuron resistance. Selection of transformants on both hygromycin and chlorsulfuron would only allow survival of T-DNA transformants with a Mp*FRH1*$^{GOF}$ background. The chlorsulfuron-resistant T-DNA vector was derived from a modified version of the pCAMBIA1300 vector, pHB444, generated by H. Breuninger (Figure 5.6). Instead of the hygromycin resistance gene, pHB444 encoded the *ALS* chlorsulfuron resistance gene driven by the Cauliflower Mosaic Virus 35S (CaMV 35S) promoter. Additionally, pHB444 contained the *Marchantia*-specific Mp*ELONGATION FACTOR 1α* (Mp*EF1α*) promoter upstream of gateway recombination sites. This gateway cassette and most of the Mp*EF1α* promoter (a total of 2.757 kb), were to be removed to leave behind the two essential components of the T-DNA vector: The *ALS* gene expression cassette flanked by left border (LB) and right border (RB) repeat sequences, and various bacterial genes for expression of the plasmid in *Escherichia coli* and *Agrobacterium tumefaciens*. *SalI* and *XbaI* restriction sites were the best-suited DNA digest sites to cut out the redundant elements of pHB444. Apart from the *ALS* expression unit and the bacterial genes, the final chlorsulfuron-resistant T-DNA vector contained a few additional sequence elements that the digest had not removed by *SalI*/*XbaI* digest: 369 bp of the 3'-end of the MpEF1α promoter, the attR site and a 635 bp long terminator. Hence, a total of 1.004 kb of redundant plasmid sequence was retained (Figure 5.6). This was predicted not to influence the insertion and expression of the T-DNA, since the truncated Mp*EF1α* promoter faces the opposite direction from the 35S promoter and faces the terminator.

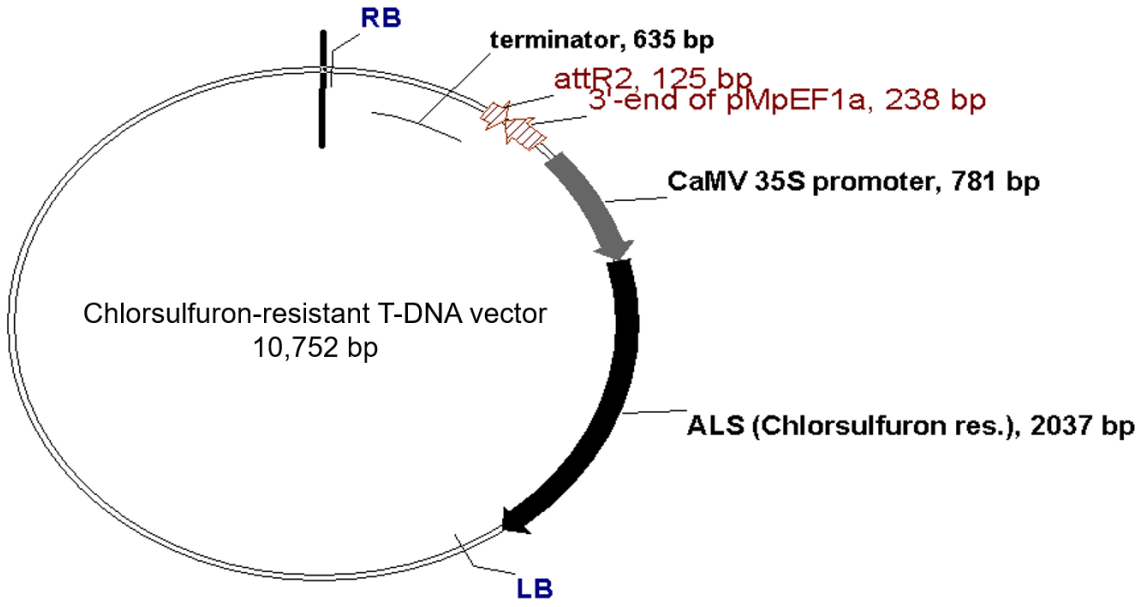


**Figure 5.6: A new pCAMBIA 1300-based T-DNA vector carries a chlorsulfuron resistance gene.** Incomplete plasmid map showing genetic elements encoded on the T-DNA within the left border (LB) and right border (RB) repeat sequences: apart from the 35S promoter driving the *ALS* gene, 1.004 kb of extra sequence remained after digest of the modified plasmid pHB444 (made by H. Breuninger). Not shown are bacterial sequences encoded for expression in *E. coli* and *A. tumefaciens* (https://www.snapgene.com/resources/plasmid-files/?set=plant_vectors&plasmid=pCAMBIA1300).

For T-DNA mutagenesis, spores from a Mp*FRH1*$^{GOF}$ x Tak-2 cross were sterilised and germinated for one week before *Agrobacterium*-mediated transformation of the new T-DNA plasmid. They were then plated for selection on 10 ng µl$^{-1}$ hygromycin and 0.5 µM chlorsulfuron. Only sporelings with the Mp*FRH1*$^{GOF}$ background and those with chlorsulfuron resistance-encoding T-DNA insertions were expected to grow. Control plates did not contain antibiotics. After two weeks of growth on selective medium, fewer sporelings survived on the antibiotic-containing plates relative to the non-antibiotic plates. This confirmed that the new T-DNA vector conferred chlorsulfuron resistance. After plating of approximately 1,040,000 spores from eight sporangia, I screened approximately 400 T-DNA

insertion lines. The screening procedure after antibiotic selection was the same as in the UV-B mutagenesis screen described in Chapter 5.3.1.2. Based on increased rhizoid abundance two weeks after transformation, 27 putative suppressor mutants were selected. However, after another three to four weeks of growth, their rhizoid phenotypes were indistinguishable from Mp*FRH1*$^{GOF}$ plants. Due to time constraints, I was not able to undertake further analyses of these candidates. However, I confirmed that the generated chlorsulfuron-resistant T-DNA vector was functional; since it conferred chlorsulfuron resistance to sporelings, this suggests that the T-DNA sequences were inserted and expressed in the genomes of the transformants.

### 5.3.3. Conclusions

After UV-B mutagenesis, 36,400 sporelings with a genetic Mp*FRH1*$^{GOF}$ background were screened for abundant rhizoids. In a previous screen in the lab, 120,000 UV-B mutagenized plants were screened to discover 97 plants with wavy rhizoids, a rhizoid growth defect (unpublished data). Given that suppression of the few rhizoids phenotype of the Mp*FRH1*$^{GOF}$ mutant is a more specific phenotype, I have likely not screened enough plants to discover a strong suppressor mutant. Equally, while from 150,000 T-DNA insertion lines, 59 tagged rhizoid-defective mutants were discovered in a previous T-DNA mutagenesis screen (Suvi Honkanen, doctoral dissertation 2015), it was very unlikely that I would identify one suppressor mutant in 400 screened T-DNA lines. Time constraints hindered the mutagenesis of more spores. Taken together, I have established UV-B and T-DNA mutagenesis and screening procedures that will enable the identification of suppressor mutants of the Mp*FRH1*$^{GOF}$ few rhizoids phenotype in a larger-scale screen.

To facilitate the identification of true suppressor mutants based on restored rhizoid development, I adjusted the growth and screening conditions for further mutagenesis screens. Growing Mp*FRH1*$^{GOF}$ spores on 1.8 % Johnson's medium and screening for suppressor mutants after more than four weeks, minimizes variability of the Mp*FRH1*$^{GOF}$ rhizoid phenotype. To facilitate the screening procedure, growth plates could be turned upside-down and tapped, which would make Mp*FRH1*$^{GOF}$ plants fall off and only retain putative suppressor mutants.

## 5.4. Discussion

In this chapter, I presented the establishment of UV-B and T-DNA suppressor mutagenesis screens that exploit the *FRH1*$^{GOF}$ over-expresser mutant for the discovery of novel components of miRNA biogenesis in *M. polymorha*. These screens are based on the observation that rhizoid development can be restored in Mp*FRH1*$^{GOF}$*;dcl1* and Mp*FRH1*$^{GOF}$*;hst* double mutants upon inhibition of miRNA biogenesis in the Mp*FRH1*$^{GOF}$ background (presented in Chapter 2). Here, I have shown that partial restoration of rhizoid growth can be achieved through UV-B mutagenesis of Mp*FRH1*$^{GOF}$ spores. I have also cloned and successfully tested the mutagenesis competence of a chlorsulfuron-resistant T-DNA plasmid, which will allow the generation and selection of suppressor mutants in a larger-scale screen.

The putative suppressor mutants I have identified through UV-B mutagenesis, showed partial suppression of the short-rhizoids defect in the Mp*FRH1*$^{GOF}$ mutant. To confirm heritability of this suppression and to identify the underlying mutation(s), these putative candidates had to be crossed, which was impossible due to fragility of the plants. Generally, the likelihood that they carried mutations in genes of the miRNA biogenesis pathway, was

low. Although this screen was developed to identify upstream regulators of the mature MpFRH1 miRNA, a restoration of rhizoid development could just as well result from mutations in different pathways controlling rhizoid growth. Such might be upstream or downstream of MpFRH1, and this can only be determined by testing MpFRH1 abundance using qPCR. Ultimately, I was interested in strong suppressor mutants that show restoration of rhizoid abundance similar to the Mp*FRH1*$^{GOF}$*;dcl1* and Mp*FRH1*$^{GOF}$*;hst* double mutants – full or nearly complete recovery of the wild type plant phenotype would likely be attributable to wild type-like MpFRH1 levels. Partial suppression on the other hand, could as well be caused by impairment of another aspect of rhizoid development than rhizoid differentiation through Mp*FRH1*. Mp*FRH1*, through inhibition of Mp*RSL1*, controls the differentiation of rhizoids from specialised epidermal cells. Rhizoid elongation and polar growth are influenced by other pathways involving auxin-regulated/-regulating genes or protein kinases for example (Ishizaki *et al.*, 2012; Otani *et al.*, 2018). Mutations in such pathways could alter the Mp*FRH1*$^{GOF}$ rhizoid phenotype. They might either occur downstream of the Mp*FRH1*-Mp*RSL1* module, or independent of Mp*FRH1*. Since the identified putative suppressor mutants P, R and J3 developed slightly longer rhizoids, but were not more viable on soil than the Mp*FRH1*$^{GOF}$ mutant, it is likely that they are only defective in rhizoid elongation. Support for this possible conclusion comes from the observation that rhizoid growth rates are altered in P, R and J3. Since the number of outgrowing rhizoids was not quantified on gemmae of these three putative suppressor mutants, it could not be concluded that the primary function of Mp*FRH1*, which is to control rhizoid differentiation from ventral epidermal cells, was restored.

The majority of known plant miRNA biogenesis regulators promote miRNA production. Therefore, a mutation in a core regulator of miRNA biogenesis that leads to reduced

MpFRH1 accumulation would likely either be a knock-out allele or a hypomorphic allele rather than a hypermorphic allele. T-DNA mutagenesis has previously resulted in a number of hypermorphic mutant alleles (Honkanen *et al.*, 2016). Over-expression of the affected genes likely resulted from the promoting effect of the close by inserted CamV 35S promoter on their expression, as assumed in the case of the Mp*FRH1*$^{GOF}$ mutant. Identification of another hypermorphic allele in this Mp*FRH1*$^{GOF}$ background, likely through T-DNA mutagenesis, could be the discovery of an inhibitor of miRNA processing. This could add novel information to our understanding of the miRNA biogenesis pathway, since only few inhibitors of miRNA processing are known to date. However, when using T-DNA mutagenesis to generate suppressor mutations in the Mp*FRH1*$^{GOF}$ background, the phenomenon of transgene silencing must be taken into consideration. Cases have been described in which a transgene became silenced through introduction of a second transgene with homologous CamV 35S promoter sequences (Daxinger *et al.*, 2008). If T-DNA insertion mutagenesis of Mp*FRH1*$^{GOF}$ sporelings resulted in restored rhizoid development, this might be the result of reduced Mp*FRH1* expression through silencing of the inserted CamV 35S promoter in the Mp*FRH1* promoter. Although no cases of T-DNA-induced silencing in the Mp*FRH1*$^{GOF}$ mutant have been reported in our lab to date (internal communications), appropriate tests will have to be performed to exclude this possibility. For example, suppression of the few-rhizoids phenotype of the Mp*FRH1*$^{GOF}$ mutant should be confirmed by multiple suppressor mutant alleles of the same gene, ideally through different mutagenesis approaches. Absence of hypermethylation of the T-DNA in the Mp*FRH1* promoter would support the presence of a true suppression effect as opposed to transgene silencing (Daxinger *et al.*, 2008).

If a core regulator of miRNA processing was mutated, this would likely affect a broad variety of miRNAs, not only Mp*FRH1*, and suppressor mutants might show pleiotropic developmental defects. In severe cases like a null mutation in Mp*DCL1*, this could mean lethality of the sporeling. Ultimately, some UV-B and T-DNA mutations are expected to produce nearly complete suppression and therefore a wild type-like phenotype in the Mp$FRH1^{GOF}$ background. The level of suppression depends on the significance of the affected gene in miRNA biogenesis and on the effect of the introduced mutation. To increase the likelihood of generating and identifying suppressor mutants with a wild type-like rhizoid phenotype, larger-scale screens need to be performed. Screening at least 100,000 T-DNA insertion lines will likely enable the identification of suppressor mutants defective in the miRNA biogenesis pathway. Varying the dose of UV-B irradiation and tripling the number of irradiated spores will increase the chance of identifying Mp$FRH1^{GOF}$ suppressor mutants in another UV-B mutagenesis screen.

# Chapter 6 – Materials and methods

## 6.1. Plant lines and bacterial strains

*M. polymorpha* accessions Tagaragaike-1 and Tagaragaike-2 (Tak-1 and Tak-2) provided by K. Ishizaki (Kobe University, Japan) were used as male and female wild type. Male and female Mp*FRH1*$^{GOF}$ mutants were generated by Suvi Honkanen. All CRISPR lines were generated by transformation of spores derived from a Tak-1 x Tak-2 crossing. Stellar Competent Cells of the *Escherichia coli* HST08 strain were used for molecular cloning (Clontech). For plant transformation, *Agrobacterium tumefactiens* strain GV3101 (Clontech) was used.

## 6.2. Plant growth conditions

*M. polymorpha* was grown on sterile plates containing modified Johnson's medium (Johnson, Stout, Broyer, & Carlton, 1957) supplemented with 1% (w/v) sucrose and 1.4% (w/v) agar (Sigma cat#A9799), pH adjusted to 5.6. To avoid plant desiccation, the amount of agar in the medium was reduced to 0.8% for cultivation of mutant lines with defective rhizoids. For clonal vegetative propagation and phenotypic analyses, gemmae were removed from gemma cups and plated individually on solid medium, using tweezers. Plants were grown at 23 °C in Sanyo growth cabinets providing constant illumination with cool white light. Sexual reproduction was induced by far-red light irradiation as described in Chiyoda *et al.*, 2008. For crossing, plants were grown in pots filled with soil containing a 1:3 mixture of vermiculite:John Innes No 2 soil, at 23 °C under a light:dark period for 16:8 hours.

## 6.3. Phylogenetic analysis

For analysis of the evolutionary relatedness of genes, phylogenetic trees were constructed from multiple sequence alignments of amino acid sequences. These sequences were retrieved from the Tair website for *Arabidopsis* proteins, and from the phytozome website for orthologous protein sequences identified by protein BLAST search. Multiple sequence

alignments of orthologous sequences were generated using the MAFFT online programme (Katoh, Rozewicki and Yamada, 2017). Gene trees were constructed in MEGA-X, using the maximum likelihood method with 500 bootstrap resampling steps.

### 6.4. Statistical analysis

Statistical analysis of data of rhizoid length and phase change timing was undertaken using student's t-test. The difference between two means of n individuals was tested between wild type and a mutant genotype. The student's t-tests used two-tailed distributions and assumed unequal variances of the means and normal distribution of the test statistic. Obtained p-values $< 0.05$ suggested a significant difference between the two means of the tested distributions.

### 6.5. CRISPR/Cas9 mutagenesis

CRISPR/Cas9 mutagenesis vectors were generated by gateway cloning-based recombination of an entry vector containing two guide RNAs (gRNAs) and a destination vector encoding the Cas9 enzyme (vector pMpGEO011), following the protocol provided in Sugano *et al.*, 2014. Guide RNAs were selected using the CRISPR-P online tool. They were ligated into an entry vector containing *BbsI* and *BsmBI* restriction sites, each downstream of a pMpU6 promoter (vector pHB453, a MpEN03 vector modified by Holger Breuninger). The expression plasmids were transformed into competent *A. tumefaciens* cells by heat shock transformation. Mutant plants were then generated by transfection of spores or thallus fragments with transgenic *A. tumefaciens.*

### 6.6. Spore transformation

For transformation of spores, sporangia were harvested in dd$H_2O$, sterilised with 1% sodium dichloroisocyanurate for 3 minutes and rinsed three times with dd$H_2O$. After addition of 600

µl dd$H_2O$, the sporangium was broken to release the spores. This spore suspension was added to 25 ml liquid M51C medium, in which spores were grown for seven days under constant light at 23 ºC (Ishizaki *et al.*, 2008). The germinated spores were then co-incubated with 1 ml of transgenic *A. tumefacies* cells. Those cells carried plasmid vectors with the CRISPR/Cas9 constructs designed for mutagenesis of Mp*DCL1* or Mp*HST*. Before co-cultivation with germinated sporelings, transgenic *A. tumefaciens* cells had grown in liquid LB medium containing selective antibiotics (100 µg/ml rifampicin, 25 µg $ml^{-1}$ gentamycin and 50 µg $ml^{-1}$ spectinomycin) for two days. They had then been harvested and induced with 100 µM acetosyringone in liquid M51C culture, shaking for three to six hours until cells started to clump. 1 µl of these induced *Agrobacteria*, as well as 100 µM acetosyringone were then added to 25 ml of germinated sporelings and co-cultivated on a 120 rpm shaker for two days. After co-cultivation, sporelings were poured through a cell strainer and washed with 150 ml dd$H_2O$. They were then suspended in water and spread on solid Johnson's medium supplemented with 1.4 % Agar and antibiotics in 10 cm x 10 cm square petri dishes. Transformed sporelings were selected on 10 ng $µl^{-1}$ hygromycin or 0.5 µM chlorsulfuron. 100 ng $µl^{-1}$cefotaxime was added to the growth medium to eliminate any remaining *Agrobacteria*.

### 6.7. Thallus transformation

For transformation of CRISPR transgenes into the Mp$FRH1^{GOF}$ mutant, thallus transformation was performed, because these mutants are difficult to cross to produce spores. The used protocol follows thallus transformation described in (Kubota *et al.*, 2013). For thallus transformation, gemmae were grown on solid ½ B5 Gamborg medium supplemented with 0.5 g $l^{-1}$ MES and 0.8% agar in continuous white light for two weeks. Then, the meristems were cut off the thallus using a scalpel, and the remaining thallus was cut in four pieces. These thallus pieces were grown on ½ Gamborg B5 medium

supplemented with 1% sucrose and 1% agar for three days under continuous white light. They were then co-cultivated with induced Agrobacteria exactly as described in Chapter 6.4 on spore transformation. After thorough washing of the plantlets following co-incubation, they were soaked in sterilised water containing 1 g $l^{-1}$ cefotaxime for at least 30 min. Plantlets were then transferred to ½ Gamborg medium with 1.4% agar, 100 ng µ$l^{-1}$cefotaxime and 0.5 µM chlorsulfuron and grown in continuous white light.

## 6.8. Rhizoid length quantification

For quantification of rhizoid length, gemmae were grown in 126 mm x 30 mm plastic tubes (Sarstedt, 60ml, 60.596.001) filled with 45 ml Johnson's medium supplemented with 0.8% phytagel. To guarantee air flow, the lid was perforated and sealed with sun cap closures. Using a ruler, the average length of the majority of a gemmaling's rhizoids was measured.

## 6.9. RNA extraction

For the extraction of total RNA, three to five 10-14-d-old whole gemmalings grown on agar medium were harvested and frozen. The frozen tissue was ground and mixed thoroughly with 700 µl Trizol. After centrifugation at 11,000 rpm for 5 min, the liquid phase was retained in a fresh tube and mixed with an equal amount of 100% ethanol. This mixture was then transferred to a column tube and all further RNA isolation steps were performed using the Direct-zol RNA MiniPrep kit (Zymo Research), including in-column DNase I treatment. The manufacturer's instructions were followed and 30 µl nuclease-free dd$H_2O$ were heated to 65 ºC and incubated on the column for 2 min before final elution by centrifugation. RNA concentration was then measured using a Nanodrop spectrophotometer. To test for DNA contamination, at least 200 ng of RNA were separated on a 1% agarose gel. Presence of only two strong ribosomal RNA bands of 1.2 kb and 1.6 kb without any band or smear at the top of the lane gave an indication of good RNA quality and purity.

## 6.10. cDNA synthesis

Reverse transcription of mRNAs from total RNA was performed using Protoscript II reverse transcriptase. 3 µg of total DNase I-digested RNA together with 1 µl of 10 mM oligo dT primer and 10 mM dNTPs were incubated at 65 ºC for 5 min to dissolve any secondary RNA structures. After addition of 10 X DTT as well as 1 µl murine RNase inhibitor, 1 µl ProtoScript II reverse transcriptase and the corresponding 5 X reverse transcriptase buffer on ice, reverse transcription was performed at 42 ºC for 1 h. Enzyme inactivation was subsequently done by incubation at 80 ºC for 10 min. Finally, cDNA was diluted 1:7 with nuclease-free dd$H_2O$. To test successful synthesis of cDNA, I performed PCR using MANGO Taq DNA polymerase. The manufacturer's protocol was followed, including 1µl of diluted cDNA as well as 10 mM primers amplifying the Mp*ADENINE PHOSPHORIBOSYL TRANSFERASE* (Mp*APT*) housekeeping gene. cDNA quality was assessed as good when clear and uniformly strong bands were visible on a 1% agarose gel after the PCR product was run under addition of 10 X loading dye.

## 6.11. Reverse transcription of miRNAs b stem-loop RT-PCR

Steady state levels of mature miRNAs were measured by quantitative real-time PCR (qRT-PCR) following stem-loop PCR. Stem-loop PCR served to reverse transcribe mature miRNAs after fusion of a 44 bp-long stem-loop adapter to generate a 60 bp-long template for PCR amplification. The adapter sequence was designed according to the protocol published in Chen *et al.*, 2005. 1 µl of 1 mM stem-loop adapter and 0.5 µl of 10 mM dNTPs together with 11.5 µl of nuclease-free dd$H_2O$ were incubated at 65 ºC for 5 min to dissolve any secondary molecular structures. Then, 10 X DTT as well as 0.1 µl murine RNase inhibitor, 0.25 µl Protoscript II RNA polymerase and the corresponding 5 X reverse transcriptase buffer were added on ice. Finally, after addition of 850-1000 ng of DNase-

digested total RNA and adjustment of the total reaction volume to 20 µl with nuclease-free dd$H_2O$, the mix was incubated at 16 ºC for 30 min. Subsequently, pulsed reverse transcription took place in 60 cycles of 30 ºC for 30 sec, 42 ºC for 30 sec and 50 ºC for 1 sec. I tested the success of stem-loop RT PCR by semi-quantitative PCR amplification of the RT product. The PCRBIO Ultra Polymerase kit (PCR Biosystems) served for that purpose, with 2 µl of undiluted stem-loop RT product as template. After initial denaturation at 95 ºC for 2 min, PCR amplification was performed in 33 cycles of 95 ºC for 15 sec, 60 ºC for 15 sec and 72 ºC for 10 sec. The PCR product ran on a 2 % agarose gel to separate bands of 60 bp in size.

### 6.12. Quantification of mRNA expression by qRT-PCR

For measurement of steady-state mRNA and miRNA levels, I used quantitative real-time PCR. Templates were either cDNA, diluted 1:7 with dd$H_2O$, or 60 bp-long stem-loop RT PCR products. The reaction mix contained 2 µl of template together with 2 X SYBR Green master mix, 2 µl of both forward and reverse primer (10 mM) and 4 µl dd$H_2O$. The total sample volume was 20 µl and was kept on ice during preparation. For each biological sample, I used three technical replicates. Mp*APT* served as a housekeeping gene relative to which mRNA and miRNA abundances were measured. After initial denaturation at 95 ºC for 20 sec, qRT-PCR amplification was performed in 40 amplification cycles of 3 sec at 95 ºC and 30 sec at 60 ºC per cycle. For melting curve analysis, samples were denatured at 95 ºC, then cooled to 65 ºC. Fluorescence signals were collected at 530 nm wavelength continuously from 65 ºC to 95 ºC at 0.2 ºC per second. Delta Ct analysis was performed to analyse the obtained data. From three Ct values for each biological replicate, the average was calculated and normalised to that of the housekeeping gene to determine delta Ct values and relative expression levels using the formula $2^{-dCt}$.

## 6.13. Genotyping and Sequencing

For DNA extraction and genotyping, the Phire Plant Direct PCR kit (Thermo Fisher Scientific) was used. A small piece (approximately 1-2 $mm^2$) of thallus tissue, removed from the plant using forceps and a pipette tip, was incubated in 20 µl dilution buffer and incubated at room temperature for at least one hour to facilitate cellular extraction of DNA. After mixing, 1 µl of this solution containing genomic DNA was used per 20 µl PCR reaction. The PCR reaction mix also contained 1 µl of each forward and reverse primer, 10 µl of Phire Tissue Direct PCR master mix (2X) and $ddH_2O$. PCR amplification was performed with the following incubation steps: initial denaturation at 95 ºC for 5 min; 35-40 cycles of denaturation at 95 ºC for 5 sec, annealing at 59 ºC for 5 sec and elongation at 72 ºC for 30 sec; and final elongation of 1 min at 72 ºC. The PCR products were loaded on a 1% agarose gel supplemented with SYBR Safe stain. DNA bands were separated by gel electrophoresis and visualised under UV light. For sequencing of PCR products, the respective bands were excised from the agarose gel and the DNA was purified using the QIAGEN Kit For DNA Extraction From Agarose Gels – after dissolving the agarose gel block at 65 ºC, the DNA was bound to a column membrane, washed and eluted in 20-30 µl elution buffer.

## 6.14. Primers

For sex identification, plants were genotyped using primers that bind to specific markers on the sex chromosomes. For the X chromosome, the rhf73 marker was amplified and for the Y chromosome, the rbm27 marker was amplified.

**Table 6.1: primer sequences and amplicons**

| amplicon | primer name | sequence |
|---|---|---|
| **Mp*DCL1* CRISPR2 target locus** | oS27 | CACAGTGCAGCCAACTCTTGCTTG |
| | oS38 | GTCCCATGGTACATCATTGCGTGA |
| **Mp*DCL1* CRISPR3 target locus** | oS24 | CTCTGCTGCAGGTTAAGGGATGAAG |
| | oS25 | GATACATGTCCATGGCACTCCCAAG |
| **Mp*HST* CRISPR target locus** | oS81 | CAGCAACAAATCATGCATGCTCG |
| | oS86 | CATAGGCTGCATCTTCTTGAGATCG |
| **Mp*DCL1* CRISPR2 transgene** | gRNA_RNAse_2_f | CTCGAGAATGCCTGAAAAAAGCTT |
| | M13R | CAGGAAACAGCTATGAC |
| **Mp*DCL1* CRISPR3 transgene** | gRNA_ex20_2_f | CTCGTGCTTCAGCATCTAAAACGG |
| | M13R | CAGGAAACAGCTATGAC |
| **Mp*HST* transgene** | gRNA4_hst_ex5_f | CTCGAGATGTAACTGTTCATAACG |
| | M13R | CAGGAAACAGCTATGAC |
| **rhf73 marker on X chromosome** | rbf62_F | CAATTGGGAAGATTTGACACTTAGC |
| | rbf62_R | TTCCCAATTGAGTACGAGTAGTCCT |
| **rhm12 marker on Y chromosome** | rhm12_F | GAGAGTATTTGCGATGCGTCAC |
| | rhm12_R | CAAGGGCTCGAATCCATTTCT |
| **Mp*APT1* qPCR** | MpAPT1 F | CGAAAGCCCAAGAAGCTACC |
| | MpAPT1 R | GTACCCCCGGTTGCAATAAG |
| **Mp*FRH1* qPCR** | MpFRH1 F | ACAGCTCGGGGGCTGCAGCACAAAT |
| | MpFRH1 R | TCAGGATGGCCAGGGGACACTGAAG |
| **Mp*RSL1* qPCR** | MpRSL1 F | AGATGAGTCTGGGGCAACC |
| | MpRSL1 R | GGATGAGCGCTTTAGAGTGG |

# Discussion

Since the discovery of the first miRNA, *lin-4*, in the nematode *C. elegans*, a large number of conserved and non-conserved miRNAs have been identified from worm, fly, mammals and plants. After the discovery of the role of *lin-4* in controlling the timing of larval phase transitions, miRNAs were discovered to be regulators of developmental phase transitions in flowering plants, too. This thesis reports on the finding that miRNA-mediated regulation of phase change is an ancestral mechanism in land plants. The presented results demonstrate that two core regulators of miRNA processing, DICER-LIKE 1 (DCL1) and HASTY (HST), respectively regulate the timing and the far-red light dependence of the reproductive phase transition in *M. polymorpha*, a member of one of the first land plant lineages. Since At*HST* controls the timings of the juvenile-to-adult and the vegetative-to-reproductive transitions in the flowering plant *A. thaliana*, a function of *HST* in regulating phase change was likely present in the LCA of all land plants.

The dioecious nature of the liverwort model enabled the discovery that Mp*HST* controls phase change in opposite ways in male and female plants – while inhibiting gametangiophore formation in males, Mp*HST* promotes gametangiophore formation in females. To explain this sex-specific role of Mp*HST*, it would be informative to study how genes underlying the sexual dimorphism in *M. polymorpha* interact with regulators of the reproductive phase transition. Furthermore, it would be interesting to see whether *HST* also exerts a sex-specific regulatory role in dioecious vascular plants.

In wild type *M. polymorpha*, the timing of the reproductive phase transition is different in male and female plants – antheridiophores on male plants develop approximately ten days earlier than the archegoniohores on female plants. The results presented in this thesis suggest

that Mp*HST* is involved in controlling this timely shift in the reproductive transition between males and females. Since Mp*HST* was shown to regulate miRNA processing, this indicates that miRNAs might be involved in this sex-dependent process. Additional evidence for this comes from the observation that Mp*DCL1*, core enzyme of the miRNA processing pathway, affects the reproductive phase transition differently in male and female *M. polymorpha* plants. In male plants, Mp*DCL1* represses the reproductive transition in the absence of far-red light, which is normally required for gametangiophore development. As opposed to strong male Mp*dcl1* mutants, strong female Mp*dcl1* mutants do not undergo reproductive phase transition in the absence of far-red light. This suggests that: (i) Mp*DCL1* does not repress the reproductive transition in female plants or (ii) Mp*DCL1* does repress the reproductive transition in female plants but is essential for archegoniophore development. If the first possibility was true, this would indicate that Mp*DCL1* processes miRNAs that are expressed differently in males and females during phase change. Taken together with the finding that Mp*HST* controls gametangiophore development differently in males and females, it is likely that sex-specifically expressed miRNAs are involved in regulating the reproductive phase transition in the dioecious liverwort. Alternatively, Mp*SPL* genes, which are regulated by Mp*HST*, might have sex-specific functions.

Mp*DCL1* and Mp*HST* both process miRNAs, perhaps including yet unknown miRNAs that regulate the sexual dimorphism in *M. polymorpha*. Nevertheless, they are differently involved in the process of reproductive phase transition. While Mp*HST* regulates reproductive timing under the requirement of inductive far-red light, Mp*DCL1* is likely itself involved in the far-red light signalling pathway that contributes to the correct timing of the reproductive transition. In *A. thaliana,* At*DCL1* is involved in reproductive phase change control by processing of miR172; therefore, it positively regulates the ageing pathway

together with At*HST*. On the other hand, Mp*DCL1* represses the reproductive transition in *M. polymorpha* through integration of the far-red light signal. The role of Mp*DCL1* during far-red light dependent development remains to be tested, as well as the specific involvement of miRNAs in the process of far-red dependent phase change. Nevertheless, the results suggest that Mp*DCL1* regulates a different set of miRNAs than At*DCL1*, perhaps including miRNAs involved in far-red light signalling. Furthermore, the results are consistent with Mp*DCL1* being a global regulator of miRNAs and Mp*HST* likely processing a specific subset of miRNAs, including miRNAs involved in phase change timing.

The presented results suggest that Mp*HST* functions in an ageing pathway in *M. polymorpha*, like At*HST* does in *A. thaliana*. Other components of this pathway are MpSPL1 and MpSPL2, homologs of highly conserved SPL proteins that regulate phase changes in angiosperms. Mp*SPL1* and Mp*SPL2* were shown to be regulated by Mp*HST* in response to inductive far-red light. Mp*SPL1* and Mp*SPL2* are targeted by Mpo-MR-13 and miR529c, respectively. The exact functions of these two miRNAs and their Mp*SPL* target genes during the reproductive phase transition remains to be tested. Since Mpo-MR-13 is a liverwort-specific miRNA and miR529c is a close relative of miR156 but not present in *A. thaliana*, this suggests that the ageing pathway in the liverwort likely comprises different miRNAs than the conserved miR156 and miR172 miRNAs in the ageing pathway of angiosperms.

The dioecious nature of the *M. polymorpha* model has enabled the discovery of new aspects of phase change regulation through *HST* and *DCL1*. The presented results suggest an interaction between regulators of miRNA biogenesis and regulators of the sexual dimorphism during the reproductive phase transition in the liverwort. They will further our

understanding of mechanisms that have evolved to control developmental phase changes not only in bryophytes but in all land plants.

# Appendix

**Table A1: gRNA sequences for CRISPR/Cas9 mutagenesis**

| construct | oligo name | sequence |
|---|---|---|
| Mp*DCL1* CRISPR1 gRNA1 | gRNA_ex1_1_dir_fwd | CTCGACCGCGTTCGCGATGCCTCC |
| Mp*DCL1* CRISPR1 gRNA2 | gRNA_ex1_2_dir_fwd | CTCGCTTGCTCAAGAACTTCCAGC |
| Mp*DCL1* CRISPR2 gRNA1 | gRNA_RNAse_1_dir_fwd | CTCGCAAGGTAGAAGATCCTCTGA |
| Mp*DCL1* CRISPR2 gRNA2 | gRNA_RNAse_2_comp_fwd | CTCGAGAATGCCTGAAAAAAGCTT |
| Mp*DCL1* CRISPR3 gRNA1 | gRNA_ex20_1_comp_fwd | CTCGGCTTTCTTGACGCTGGGCAT |
| Mp*DCL1* CRISPR3 gRNA2 | gRNA_ex20_2_comp_fwd | CTCGTGCTTCAGCATCTAAAACGG |
| Mp*HST* CRISPR gRNA1 | gRNA1_hst_ex3_fwd | CTCGTCGCCAAACCTCATGAGCAA |
| Mp*HST* CRISPR gRNA2 | gRNA3_hst_int4_fwd | CTCGGATCACAAGTAATGACTCTT |

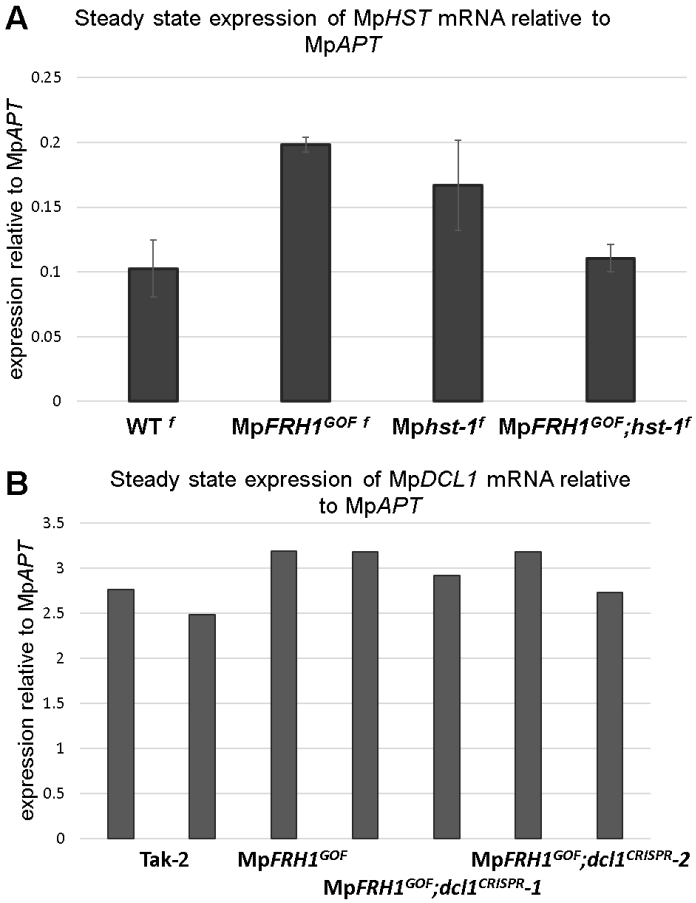


**Figure A1: Steady state expression of Mp*DCL1* and Mp*HST* mRNA is unchanged in mutants of Mp*dcl1* and Mp*hst*.** Average steady state expression of Mp*DCL1* and Mp*HST* mRNA relative to Mp*APT* is shown, measured by qRT-PCR, n=3. (A) female Mp$FRH1^{GOF}$;*hst-1* and Mp*hst-1* compared to wild type and Mp$FRH1^{GOF}$ from the same F2 population. Averages of relative expression were calculated from three biological replicates per genotype. (B) female Mp$FRH1^{GOF}$;$dcl1^{CRISPR}$ *-1* and Mp$FRH1^{GOF}$;$dcl1^{CRISPR}$ *-2* lines compared to Tak-2 wild type and the female Mp$FRH1^{GOF}$ line from which the double mutants were derived by thallus transformation. Per genotype, 2 biological replicates were tested, apart from one for Mp$FRH1^{GOF}$. No significant differences were detected.

# Bibliography


Achkar, N. P., Cambiagno, D. A. and Manavella, P. A. (2016) 'miRNA Biogenesis: A Dynamic Pathway', *Trends in Plant Science*. Elsevier Ltd, xx, pp. 1–11. doi: 10.1016/j.tplants.2016.09.003.

Amasino, R. M. and Michaels, S. D. (2010) 'The Timing of Flowering', *Future Perspectives in Plant Biology*, 154(October), pp. 516–520. doi: 10.1104/pp.110.161653.

Arazi, T. (2012) 'MicroRNAs in the moss Physcomitrella patens', *Plant Molecular Biology*, 80(1), pp. 55–65. doi: 10.1007/s11103-011-9761-5.

Aukerman, M. J. and Sakai, H. (2003) 'Regulation of Flowering Time and Floral Organ Identity by a MicroRNA and Its APETALA2-LIKE Target Genes', *The Plant Cell*, 15(November), pp. 2730–2741. doi: 10.1105/tpc.016238.pression.

Axtell, M. J. (2013) 'Classification and Comparison of Small RNAs from Plants', *Annual Review of Plant Biology*. Annual Reviews, 64(1), pp. 137–159. doi: 10.1146/annurev-arplant-050312-120043.

Axtell, M. J. and Bowman, J. L. (2008) 'Evolution of plant microRNAs and their targets', *Trends in Plant Science*, 13(7), pp. 343–349. doi: 10.1016/j.tplants.2008.03.009.

Axtell, M. J., Snyder, J. A. and Bartel, D. P. (2007) 'Common Functions for Diverse Small RNAs of Land Plants', *The Plant Cell*, 19(June), pp. 1750–1769. doi: 10.1105/tpc.107.051706.

Axtell, M. J., Westholm, J. O. and Lai, E. C. (2011) 'Vive la différence: biogenesis and evolution of microRNAs in plants and animals', *Genome Biology*, 12(4), p. 221. doi: 10.1186/gb-2011-12-4-221.

Baruah, A. *et al.* (2009) 'Modulation of O2-mediated retrograde signaling by the PLEIOTROPIC RESPONSE LOCUS 1 (PRL1) protein, a central integrator of stress and energy signaling', *Plant Journal*, 60(1), pp. 22–32. doi: 10.1111/j.1365-313X.2009.03935.x.

Baumberger, N. and Baulcombe, D. C. (2005) 'Arabidopsis ARGONAUTE1 is an RNA Slicer that selectively recruits microRNAs and short interfering RNAs', *PNAS*, 102, pp. 11928–11933.

Bäurle, I. and Dean, C. (2006) 'The Timing of Developmental Transitions in Plants', *Cell*, 125(May), pp. 655–664. doi: 10.1016/j.cell.2006.05.005.

Bollman, K. M. *et al.* (2003) 'HASTY, the Arabidopsis ortholog of exportin 5/MSN5, regulates phase change and morphogenesis.', *Development*, 130(8), pp. 1493–1504. doi: 10.1242/dev.00362.

Bologna, N. G. *et al.* (2018a) 'Nucleo-cytosolic Shuttling of ARGONAUTE1 Prompts a Revised Model of the Plant MicroRNA Pathway', *Molecular Cell*. Elsevier Inc., 69(4), pp. 709-719.e5. doi: 10.1016/j.molcel.2018.01.007.

Bologna, N. G. *et al.* (2018b) 'Nucleo-cytosolic Shuttling of ARGONAUTE1 Prompts a Revised Model of the Plant MicroRNA Pathway', *Molecular Cell*. Elsevier Inc., 69(4), pp. 709-719.e5. doi: 10.1016/j.molcel.2018.01.007.

Bonnet, E., Van De Peer, Y. and Rouzé, P. (2006) 'The small RNA world of plants', *New Phytologist*, 171(3), pp. 451–468. doi: 10.1111/j.1469-8137.2006.01806.x.

Bowman, J. L. *et al.* (2017) 'Insights into Land Plant Evolution Garnered from the Marchantia polymorpha Genome', *Cell*, 171(2), pp. 287-304.e15. doi: 10.1016/j.cell.2017.09.030.

Cai, C., Guo, W. and Zhang, B. (2018) 'Genome-wide identification and characterization of SPL transcription factor family and their evolution and expression profiling analysis in cotton', *Scientific Reports*, 8(1), p. 762. doi: 10.1038/s41598-017-18673-4.

Cardon, G. *et al.* (1999) 'Molecular characterisation of the Arabidopsis SBP-box genes', *Gene*, 237, pp. 91–104.

Carlsbecker, A. *et al.* (2010) 'Cell signalling by microRNA165/6 directs gene dose-dependent root

cell fate.', *Nature*, 465(May), pp. 316–321. doi: 10.1038/nature08977.

Catarino, B. *et al.* (2016) 'The Stepwise Increase in the Number of Transcription Factor Families in the Precambrian Predated the Diversification of Plants on Land', *Molecular Biology and Evolution*, 33(11), pp. 2815–2819. doi: 10.1093/molbev/msw155.

Chandler, J. W. (2016) 'Auxin response factors', *Plant, Cell & Environment*. John Wiley & Sons, Ltd (10.1111), 39(5), pp. 1014–1028. doi: 10.1111/pce.12662.

Chapman, E. J. and Carrington, J. C. (2007) 'Specialization and evolution of endogenous small RNA pathways.', *Nature reviews. Genetics*, 8(11), pp. 884–896. doi: 10.1038/nrg2179.

Chen, C. *et al.* (2005) 'Real-time quantification of microRNAs by stem-loop RT-PCR', *Nucleic Acids Research*, 33(20), pp. 1–9. doi: 10.1093/nar/gni178.

Chen, X. (2005) 'microRNA biogenesis and function in plants', *FEBS letters*, 579, pp. 5923–5931. doi: 10.1016/j.febslet.2005.07.071.

Chen, X. (2012) 'Small RNAs in development – insights from plants', *Current Opinion in Genetics & Development*, 22(4), pp. 361–367. doi: https://doi.org/10.1016/j.gde.2012.04.004.

Chiyoda, S. *et al.* (2008) 'Direct transformation of the liverwort Marchantia polymorpha L. by particle bombardment using immature thalli developing from spores', *Plant Cell Reports*, 27(9), p. 1467. doi: 10.1007/s00299-008-0570-5.

Cho, S. H., Coruh, C. and Axtell, M. J. (2012a) 'miR156 and miR390 regulate tasiRNA accumulation and developmental timing in Physcomitrella patens.', *The Plant cell*, 24(12), pp. 4837–49. doi: 10.1105/tpc.112.103176.

Cho, S. H., Coruh, C. and Axtell, M. J. (2012b) 'miR156 and miR390 Regulate tasiRNA Accumulation and Developmental Timing in Physcomitrella patens', *The Plant Cell*, 24(December), pp. 4837–4849. doi: 10.1105/tpc.112.103176.

Choi, K. *et al.* (2016) 'Regulation of microRNA-mediated developmental changes by the SWR1 chromatin remodeling complex in Arabidopsis thaliana', *Plant Physiology*, 171(June), p. pp.00332.2016. doi: 10.1104/pp.16.00332.

Chuck, G., Cigan, A. M., *et al.* (2007) 'The heterochronic maize mutant Corngrass1 results from overexpression of a tandem microRNA', *Nature Genetics*. Nature Publishing Group, 39, p. 544. Available at: https://doi.org/10.1038/ng2001.

Chuck, G., Meeley, R., *et al.* (2007) 'The maize tasselseed4 microRNA controls sex determination and meristem cell fate by targeting Tasselseed6/indeterminate spikelet1', *Nature Genetics*, 39(12), pp. 1517–1521. doi: 10.1038/ng.2007.20.

Chuck, G. *et al.* (2010) 'The maize SBP-box transcription factor encoded by *tasselsheath4* regulates bract development and the establishment of meristem boundaries', *Development*, 137(8), pp. 1243 LP – 1250. doi: 10.1242/dev.048348.

Costa, V. *et al.* (2019) 'PIF transcription factors link a neighbor threat cue to accelerated reproduction in Arabidopsis', *Nature Communications*, 10, pp. 1–10. doi: 10.1038/s41467-019-11882-7.

Couzigou, J. M. and Combier, J. P. (2016) 'Plant microRNAs: key regulators of root architecture and biotic interactions', *New Phytologist*, 212(1), pp. 22–35. doi: 10.1111/nph.14058.

Cui, Y., Fang, X. and Qi, Y. (2016) 'TRANSPORTIN1 Promotes the Association of MicroRNA with ARGONAUTE1 in Arabidopsis', *The Plant Cell*, 28(October), p. tpc.00384.2016. doi: 10.1105/tpc.16.00384.

Cuperus, J. T., Fahlgren, N. and Carrington, J. C. (2011) 'Evolution and functional diversification of MIRNA genes', *The Plant cell*. 2011/02/11. American Society of Plant Biologists, 23(2), pp. 431–442. doi: 10.1105/tpc.110.082784.

Curtin, S. J. *et al.* (2016) 'MicroRNA maturation and microRNA target gene expression regulation are severely disrupted in soybean dicer-like1 double mutants', *G3: Genes, Genomes, Genetics*, 6(2), pp. 423–433. doi: 10.1534/g3.115.022137.

Datta, S. *et al.* (2011) 'Root hairs : development , growth and evolution at the plant-soil interface', *Plant Soil*, (346), pp. 1–14. doi: 10.1007/s11104-011-0845-4.

Daxinger, L. *et al.* (2008) 'Unexpected silencing effects from T-DNA tags in Arabidopsis', *Trends in Plant Science*, 13(1), pp. 1–3. doi: 10.1016/j.tplants.2007.11.004.

DeFraia, C. T. and Mou, Z. (2011) 'The role of the Elongator complex in plants', *Plant Signaling and Behavior*, 6(1), pp. 19–22. doi: 10.4161.psb.6.1.14040.

Dolan, L. *et al.* (1993) 'Cellular organisation of the Arabidopsis thaliana root', *Development*, 119(1), pp. 71 LP – 84. Available at: http://dev.biologists.org/content/119/1/71.abstract.

Drusin, S. I. *et al.* (2016) 'dsRNA-protein interactions studied by molecular dynamics techniques. Unravelling dsRNA recognition by DCL1', *Archives of Biochemistry and Biophysics*. Elsevier Inc, 596, pp. 118–125. doi: 10.1016/j.abb.2016.03.013.

Eamens, A. L. *et al.* (2012) 'DRB2 Is Required for MicroRNA Biogenesis in Arabidopsis thaliana', *Plos one*, 7(4). doi: 10.1371/journal.pone.0035933.

Emms, D. M. and Kelly, S. (2015) 'OrthoFinder: solving fundamental biases in whole genome comparisons dramatically improves orthogroup inference accuracy', *Genome Biology*. Genome Biology, 16(1), p. 157. doi: 10.1186/s13059-015-0721-2.

Fang, X., Shi, Y., *et al.* (2015) 'CMA33/XCT Regulates Small RNA Production through Modulating the Transcription of Dicer-Like Genes in Arabidopsis', *Molecular Plant*. Elsevier Ltd, 8(8), pp. 1227–1236. doi: 10.1016/j.molp.2015.03.002.

Fang, X., Cui, Y., *et al.* (2015) 'Transcription and processing of primary microRNAs are coupled by Elongator complex in Arabidopsis', *Nature Plants*, 1(6), pp. 1–9. doi: 10.1038/nplants.2015.75.

Fang, Y. and Spector, D. L. (2007) 'Identification of Nuclear Dicing Bodies Containing Proteins for MicroRNA Biogenesis in Living Arabidopsis Plants', *Current Biology*, 5(17), pp. 818–823. doi: 10.1016/j.cub.2007.04.005.

Feinbaum, R., Ambros, V. and Lee, R. (2004) 'The C. elegans Heterochronic Gene lin-4 Encodes Small RNAs with Antisense Complementarity to lin-14', *Cell*, 116(116), pp. 843–854.

Floyd, S. K. and Bowman, J. L. (2007) 'The ancestral developmental tool kit of land plants', *International Journal of Plant Sciences*, 168(1), pp. 1–35. doi: 10.1086/509079.

Fornara, F. and Coupland, G. (2009) 'Plant Phase Transitions Make a SPLash', *Cell*, 138(4), pp. 625–627. doi: 10.1016/j.cell.2009.08.011.

Francisco-Mangilet, A. G. *et al.* (2015) 'THO2, a core member of the THO/TREX complex, is required for microRNA production in Arabidopsis', *Plant Journal*, 82(6), pp. 1018–1029. doi: 10.1111/tpj.12874.

Fukaki, H., Okushima, Y. and Tasaka, M. (2007) 'Auxin-Mediated Lateral Root Formation in Higher Plants', *International Review of Cytology*. Academic Press, 256, pp. 111–137. doi: 10.1016/S0074-7696(07)56004-3.

Gazzani, S. *et al.* (2009) 'Evolution of MIR168 paralogs in Brassicaceae', *BMC Evolutionary Biology*, 9(1), p. 62. doi: 10.1186/1471-2148-9-62.

Gill, G. (2003) 'Post-translational modification by the small ubiquitin-related modifier SUMO has big effects on transcription factor activity', *Current Opinion in Genetics & Development*. Elsevier Current Trends, 13(2), pp. 108–113. doi: 10.1016/S0959-437X(03)00021-2.

Golden, T. A. *et al.* (2002) 'SHORT INTEGUMENTS1/SUSPENSOR1/CARPEL FACTORY, a Dicer Homolog, Is a Maternal Effect Gene Required for Embryo Development in Arabidopsis',

*Society*, 130(October), pp. 808–822. doi: 10.1104/pp.003491.in.

Grigg, S. P. *et al.* (2005) 'SERRATE coordinates shoot meristem function and leaf axial patterning in Arabidopsis', *Nature*, 437(7061), pp. 1022–1026. doi: 10.1038/nature04052.

He, J. *et al.* (2018) 'Threshold-dependent repression of SPL gene expression by miR156/miR157 controls vegetative phase change in Arabidopsis thaliana', *PLoS Genetics*, 14(4), pp. 1–28. doi: 10.1371/journal.pgen.1007337.

He, L. and Hannon, G. J. (2004) 'MicroRNAs: Small RNAs with a big role in gene regulation', *Nature Reviews Genetics*, 5(7), pp. 522–531. doi: 10.1038/nrg1379.

Hisanaga, T. *et al.* (2019) 'A cis -acting bidirectional transcription switch controls sexual dimorphism in the liverwort', *The EMBO Journal*, (January), pp. 1–12. doi: 10.15252/embj.2018100240.

Honkanen, S. *et al.* (2016) 'The Mechanism Forming the Cell Surface of Tip-Growing Rooting Cells Is Conserved among Land Plants', *Current Biology*, pp. 1–7. doi: 10.1016/j.cub.2016.09.062.

Honkanen, S., Thamm, A., Arteaga-Vazquez, M. A., *et al.* (2018) 'Negative regulation of conserved RSL class I bHLH transcription factors evolved independently among land plants', *eLife*, 7, pp. 1–21. doi: 10.7554/elife.38529.

Honkanen, S., Thamm, A., Arteaga-vazquez, M. A., *et al.* (2018) 'Negative regulation of conserved RSL class I bHLH transcription factors evolved independently among land plants', pp. 1–21.

Huang, Y. *et al.* (2009) 'Structural insights into mechanisms of the small RNA methyltransferase HEN1', *Nature*. Nature Publishing Group, 461(7265), pp. 823–827. doi: 10.1038/nature08433.

Huijser, P. and Schmid, M. (2011) 'The control of developmental phase transitions in plants', *Development*, 4129(138), pp. 4117–4129. doi: 10.1242/dev.063511.

Hunter, C. A. (2003) 'PAUSED Encodes the Arabidopsis Exportin-t Ortholog', *Plant Physiology*, 132(4), pp. 2135–2143. doi: 10.1104/pp.103.023309.

Hyun, Y. *et al.* (2016) 'Multi-layered Regulation of SPL15 and Cooperation with SOC1 Integrate Endogenous Flowering Pathways at the Arabidopsis Shoot Meristem', *Developmental Cell*, 37(3), pp. 254–266. doi: 10.1016/j.devcel.2016.04.001.

Iki, T. *et al.* (2010) 'In vitro assembly of plant RNA-induced silencing complexes facilitated by molecular chaperone HSP90', *Molecular Cell*. Elsevier Ltd, 39(2), pp. 282–291. doi: 10.1016/j.molcel.2010.05.014.

Inoue, K. *et al.* (2016) 'Phytochrome signaling is mediated by PHYTOCHROME INTERACTING FACTOR in the liverwort Marchantia polymorpha', *Plant Cell*, 28(6), pp. 1406–1421. doi: 10.1105/tpc.15.01063.

Inoue, K. *et al.* (2019) 'Reproductive induction is a far-red high irradiance response that is mediated by phytochrome and phytochrome interacting factor in marchantia polymorpha', *Plant and Cell Physiology*, 60(5), pp. 1136–1145. doi: 10.1093/pcp/pcz029.

Ishizaki, K. *et al.* (2008) 'Agrobacterium-mediated transformation of the haploid liverwort Marchantia polymorpha L., an emerging model for plant biology', *Plant and Cell Physiology*, 49(7), pp. 1084–1091. doi: 10.1093/pcp/pcn085.

Ishizaki, K. *et al.* (2012) 'Visualization of auxin-mediated transcriptional activation using a common auxin-responsive reporter system in the liverwort Marchantia polymorpha', *Journal of Plant Research*, 125(5), pp. 643–651. doi: 10.1007/s10265-012-0477-7.

Ishizaki, K. *et al.* (2016) 'Molecular Genetic Tools and Techniques for Marchantia polymorpha Research', *Plant & Cell Physiology*, 2(June 2015), pp. 262–270. doi: 10.1093/pcp/pcv097.

Iwakawa, H. oki and Tomari, Y. (2013) 'Molecular insights into microRNA-mediated translational

repression in plants', *Molecular Cell*. Elsevier Inc., 52(4), pp. 591–601. doi: 10.1016/j.molcel.2013.10.033.

Iwakawa, H. oki and Tomari, Y. (2015) 'The Functions of MicroRNAs: mRNA Decay and Translational Repression', *Trends in Cell Biology*. Elsevier Ltd, 25(11), pp. 651–665. doi: 10.1016/j.tcb.2015.07.011.

Iwasaki, S. *et al.* (2010) 'Hsc70/Hsp90 chaperone machinery mediates ATP-dependent RISC loading of small RNA duplexes', *Molecular Cell*. Elsevier Ltd, 39(2), pp. 292–299. doi: 10.1016/j.molcel.2010.05.015.

Iwata, Y. *et al.* (2013) 'Dissecting the interactions of SERRATE with RNA and DICER-LIKE 1 in Arabidopsis microRNA precursor processing', *Nucleic Acids Research*, 41(19), pp. 9129–9140. doi: 10.1093/nar/gkt667.

Jacobsen, S E, Running, M. P. and Meyerowitz, E. M. (1999) 'Disruption of an RNA helicase/RNAse III gene in Arabidopsis causes unregulated cell division in floral meristems.', *Development (Cambridge, England)*, 126, pp. 5231–5243.

Jacobsen, Steven E., Running, M. P. and Meyerowitz, E. M. (1999) 'Disruption of an RNA helicase/RNAse III gene in Arabidopsis causes unregulated cell division in floral meristems', *Development*, 126(23), pp. 5231–5243.

Ji, L. and Chen, X. (2012) 'Regulation of small RNA stability : methylation and beyond', *Nature Publishing Group*. Nature Publishing Group, 22(4), pp. 624–636. doi: 10.1038/cr.2012.36.

Jin, H. and Martin, C. (1999) 'Multifunctionality and diversity within the plant MYB-gene family', *Plant Molecular Biology*, 41(5), pp. 577–585. doi: 10.1023/A:1006319732410.

Johnson, C. M. *et al.* (1957) 'Comparative chlorine requirements of different plant species', *Plant and Soil*, 8(4), pp. 337–353. doi: 10.1007/BF01666323.

Jones-Rhoades, M. W., Bartel, D. P. and Bartel, B. (2006) 'MicroRNAs and their regulatory roles in plants', *Plant biology*, 57, pp. 19–53. doi: 10.1146/annurev.arplant.57.032905.105218.

Jung, J. H. *et al.* (2012) 'The SOC1-SPL module integrates photoperiod and gibberellic acid signals to control flowering time in Arabidopsis', *Plant Journal*, 69(4), pp. 577–588. doi: 10.1111/j.1365-313X.2011.04813.x.

Katoh, K., Rozewicki, J. and Yamada, K. D. (2017) 'MAFFT online service: multiple sequence alignment, interactive sequence choice and visualization', *Briefings in Bioinformatics*. doi: 10.1093/bib/bbx108.

Kenrick, P. and Crane, P. R. (1997) 'The origin and early evolution of plants on land', *Nature*, 389(4), pp. 33–39. doi: 10.1038/37918.

Khan, G. A. and Hartmann, C. (2011) 'MicroRNAs as regulators of root development and architecture', *Plant Molecular Biology*, (September 2014). doi: 10.1007/s11103-011-9793-x.

Khraiwesh, B., Arif, M. Asif, *et al.* (2010) 'Transcriptional Control of Gene Expression by MicroRNAs', *Cell*. Elsevier Ltd, 140(1), pp. 111–122. doi: 10.1016/j.cell.2009.12.023.

Khraiwesh, B., Arif, M Asif, *et al.* (2010) 'Transcriptional Control of Gene Expression by MicroRNAs', *Cell*. Elsevier Ltd, 140(1), pp. 111–122. doi: 10.1016/j.cell.2009.12.023.

Kidner, C. A. and Martienssen, R. A. (2004) 'Spatially restricted microRNA directs leaf polarity through ARGONAUTE1', *Nature Publishing Group*, 428(March), pp. 81–84. doi: 10.1038/nature02313.1.

Kim, C. M. and Dolan, L. (2016) 'ROOT HAIR DEFECTIVE SIX-LIKE Class I Genes Promote Root Hair Development in the Grass Brachypodium distachyon', *Plos Genetics*, pp. 1–18. doi: 10.1371/journal.pgen.1006211.

Kim, W. *et al.* (2009) 'Histone acetyltransferase GCN5 interferes with the miRNA pathway in

Arabidopsis', *Cell Research*, 19(July), pp. 899–909. doi: 10.1038/cr.2009.59.

Kim, Y. J. *et al.* (2011) 'The role of Mediator in small and long noncoding RNA production in Arabidopsis thaliana', *The EMBO Journal*, 30(5), pp. 814–822. doi: 10.1038/emboj.2011.3.

Kubota, A. *et al.* (2013) 'Efficient Agrobacterium -Mediated Transformation of the Liverwort Marchantia polymorpha Using Regenerating Thalli', *Bioscience, Biotechnology and Biochemistry*, 77(1), pp. 167–172. doi: 10.1271/bbb.120700.

Kubota, A., Kita, S., Ishizaki, K., Nishihama, R., Yamato, Katsuyuki T., *et al.* (2014) 'Co-option of a photoperiodic growth-phase transition system during land plant evolution', *Nature Communications*. Nature Publishing Group, 5, pp. 1–9. doi: 10.1038/ncomms4668.

Kubota, A., Kita, S., Ishizaki, K., Nishihama, R., Yamato, Katsuyuki T, *et al.* (2014) 'Co-option of a photoperiodic growth-phase transition system during land plant evolution', *Nature Communications*. Nature Publishing Group, 5, pp. 1–9. doi: 10.1038/ncomms4668.

Kumar, S. *et al.* (2018) 'MEGA X: Molecular Evolutionary Genetics Analysis across Computing Platforms', *Molecular Biology and Evolution*, 35(6), pp. 1547–1549. doi: 10.1093/molbev/msy096.

Kuraku, S. *et al.* (2013) 'aLeaves facilitates on-demand exploration of metazoan gene family trees on MAFFT sequence alignment server with enhanced interactivity', *Nucleic Acids Research*, 41(W1), pp. W22–W28. doi: 10.1093/nar/gkt389.

Kurihara, Y. and Watanabe, Y. (2004) 'Arabidopsis micro-RNA biogenesis through Dicer-like 1 protein functions', *Proceedings of the National Academy of Sciences*, 101(34), pp. 12753–12758. doi: 10.1073/pnas.0403115101.

Laubinger, S. *et al.* (2008) 'Dual roles of the nuclear cap-binding complex and SERRATE in pre-mRNA splicing and microRNA processing in Arabidopsis thaliana', *PNAS*, 105(25), pp. 8795–8800.

Leivar, P. and Monte, E. (2014) 'PIFs: Systems integrators in plant development', *Plant Cell*, 26(1), pp. 56–78. doi: 10.1105/tpc.113.120857.

Li, C. and Lu, S. (2014) 'Molecular characterization of the SPL gene family in Populus trichocarpa', *BMC Plant Biology*.

Li, S. *et al.* (2013) 'MicroRNAs Inhibit the Translation of Target mRNAs on the Endoplasmic Reticulum in Arabidopsis', *Cell*, 153(3), pp. 562–574. doi: 10.1016/j.cell.2013.04.005.

Lin, P. *et al.* (2016) 'Identification of miRNAs and Their Targets in the Liverwort Marchantia polymorpha by Integrating RNA-Seq and Degradome Analyses', *PCP*, 57(February), pp. 339–358. doi: 10.1093/pcp/pcw020.

Lin, Q. *et al.* (2015) 'GLABRA2 directly suppresses basic helix-loop-helix transcription factor genes with diverse functions in root hair development', *Plant Cell*, 27(10), pp. 2894–2906. doi: 10.1105/tpc.15.00607.

Lin, S.-S. and Bowman, J. L. (2018) 'MicroRNAs in Marchantia polymorpha', *New Phytologist*, 6(May). doi: 10.1111/nph.15294.

Liu, B. *et al.* (2005) 'Loss of function of OsDCL1 affects microRNA accumulation and causes developmental defects in rice', *Plant Physiology*, 139(1), pp. 296–305. doi: 10.1104/pp.105.063420.

Liu, C., Axtell, M. J. and Fedoroff, N. V (2012) 'The helicase and RNaseIIIa domains of Arabidopsis Dicer-Like1 modulate catalytic parameters during microRNA biogenesis.', *Plant physiology*, 159(2), pp. 748–58. doi: 10.1104/pp.112.193508.

Liu, L., White, M. J. and Macrae, T. H. (1999) 'Transcription factors and their genes in higher plants - Functional domains, evolution and regulation', *Eur. j. Biochem*, 257, pp. 247–257.

Liu, M. *et al.* (2019) 'Genome-wide identification of the SPL gene family in Tartary Buckwheat (

Fagopyrum tataricum ) and expression analysis during fruit development stages', pp. 1–14.

Liu, Q., Feng, Y. and Zhu, Z. (2009) 'Dicer-like (DCL) proteins in plants', pp. 277–286. doi: 10.1007/s10142-009-0111-5.

Liu, Z. *et al.* (2011) 'HYL1 regulates the balance between adaxial and abaxial identity for leaf flattening via miRNA-mediated pathways', *Journal of Experimental Botany*, 62(12), pp. 4367–4381. doi: 10.1093/jxb/err167.

Margis, R. *et al.* (2006) 'The evolution and diversification of Dicers in plants', *FEBS letters*, 580, pp. 2442–2450. doi: 10.1016/j.febslet.2006.03.072.

Menand, B. *et al.* (2007) 'An ancient mechanism controls the development of cells with a rooting function in land plants', *Science*, (June), pp. 1477–1481.

Meng, Y. *et al.* (2009) 'Genome-wide survey of rice microRNAs and microRNA-target pairs in the root of a novel auxin-resistant mutant Genome-wide survey of rice microRNAs and microRNA – target pairs in the root of a novel auxin-resistant mutant', *Planta*, (December 2015). doi: 10.1007/s00425-009-0994-3.

Mickut, M. *et al.* (2015) 'Functional mapping of the plant small RNA methyltransferase : HEN1 physically interacts with HYL1 and DICER-LIKE 1 proteins', *Nucleic Acids Research*, 43(5), pp. 2802–2812. doi: 10.1093/nar/gkv102.

Millar, A. A. and Waterhouse, P. M. (2005) 'Plant and animal microRNAs: Similarities and differences', *Functional and Integrative Genomics*, 5(3), pp. 129–135. doi: 10.1007/s10142-005-0145-2.

Miura, K. *et al.* (2010) 'OsSPL14 promotes panicle branching and higher grain productivity in rice', *Nature Genetics*, (May). doi: 10.1038/ng.592.

Moran, Y. *et al.* (2017) 'The evolutionary origin of plant and animal microRNAs', *Nature Ecology and Evolution*. Macmillan Publishers Limited, 1(3), pp. 1–8. doi: 10.1038/s41559-016-0027.

Morea, E. G. O. *et al.* (2016) 'Functional and evolutionary analyses of the miR156 and miR529 families in land plants', *BMC Plant Biology*. BMC Plant Biology, 16(1), p. 40. doi: 10.1186/s12870-016-0716-5.

Mouradov, A., Cremer, F. and Coupland, G. (2002) 'Control of Flowering Time : Interacting Pathways as a Basis for Diversity', *The Plant Cell*, pp. 111–130. doi: 10.1105/tpc.001362.S112.

Nagano, H. *et al.* (2014) 'Distinct substrate specificities of Arabidopsis DCL3 and DCL4', *Nucleic Acids Research*, 42(3), pp. 1845–1856. doi: 10.1093/nar/gkt1077.

Okada, S. *et al.* (2001) 'The Y chromosome in the liverwort <em>Marchantia polymorpha</em> has accumulated unique repeat sequences harboring a male-specific gene', *Proceedings of the National Academy of Sciences*, 98(16), pp. 9454 LP – 9459. doi: 10.1073/pnas.171304798.

Otani, K. *et al.* (2018) 'An evolutionarily conserved NIMA-related kinase directs rhizoid tip growth in the basal land plant Marchantia polymorpha', *Development (Cambridge)*, 145(5). doi: 10.1242/dev.154617.

Ott, F. *et al.* (2012) 'Fast-Forward Genetics Identifies Plant CPL Phosphatases as Regulators of miRNA Processing Factor HYL1', *Cell*, 151(9), pp. 859–870. doi: 10.1016/j.cell.2012.09.039.

Pandey, S. and Alam, A. (2016) 'Marchantia polymorpha L .: An Emerging Model Plant System to Study Contemporary Plant Biology - A Review', *Plant Science Today*, 3(April), pp. 88–99.

Park, M. Y. *et al.* (2005) 'Nuclear processing and export of microRNAs in Arabidopsis', *PNAS*, 102(10), pp. 3691–3696.

Park, W. *et al.* (2002) 'CARPEL FACTORY , a Dicer Homolog , and HEN1 , a Novel Protein , Act in microRNA Metabolism in Arabidopsis thaliana', *Current Biology*, 12(02), pp. 1484–1495.

Pires, N. D. *et al.* (2013) 'Recruitment and remodeling of an ancient gene regulatory network during land plant evolution', *PNAS*, 110(23), pp. 9571–9576. doi: 10.1073/pnas.1305457110.

Poethig, R. S. (2003) 'Phase change and the regulation of developmental timing in plants', *Science*, 301(5631), pp. 334–336. doi: 10.1126/science.1085328.

Preston, J. C. and Hileman, L. C. (2010) 'SQUAMOSA-PROMOTER BINDING PROTEIN 1 initiates flowering in Antirrhinum majus through the activation of meristem identity genes', *Plant Journal*, 62(4), pp. 704–712. doi: 10.1111/j.1365-313X.2010.04184.x.

Preston, J. C. and Hileman, L. C. (2013) 'Functional Evolution in the Plant SQUAMOSA-PROMOTER BINDING PROTEIN-LIKE (SPL) Gene Family', *Frontiers in Plant Science*, 4(April), pp. 1–13. doi: 10.3389/fpls.2013.00080.

Prigge, M. J. and Ry Wagner, D. (2001) 'The Arabidopsis SERRATE gene encodes a zinc-finger protein required for normal shoot development', *Plant Cell*, 13(6), pp. 1263–1279. doi: 10.1105/tpc.13.6.1263.

Proust, H. *et al.* (2016) 'RSL Class I Genes Controlled the Development of Epidermal Structures in the Common Ancestor of Report RSL Class I Genes Controlled the Development of Epidermal Structures in the Common Ancestor of Land Plants', *Current Biology*, pp. 93–99. doi: 10.1016/j.cub.2015.11.042.

Puttick, M. N. *et al.* (2018) 'The Interrelationships of Land Plants and the Nature of the Ancestral Embryophyte', *Current Biology*. Elsevier Ltd., 28(5), pp. 733-745.e2. doi: 10.1016/j.cub.2018.01.063.

Qian, Y. and Cheng, Y. (2011) 'Identification and characterization of Dicer-like , Argonaute and RNA- dependent RNA polymerase gene families in maize Identification and characterization of Dicer-like , Argonaute and RNA-dependent RNA polymerase gene families in maize', *Plant Cell Reports*, (March). doi: 10.1007/s00299-011-1046-6.

Ray, A. *et al.* (1996) 'SHORT INTEGUMENT (SIN1), a gene required for ovule development in Arabidopsis, also controls flowering time.', *Development (Cambridge, England)*, 122(9), pp. 2631–8. Available at: http://www.ncbi.nlm.nih.gov/pubmed/8787738.

Reed, J. W. *et al.* (1993) 'Mutations in the gene for the red/far-red light receptor phytochrome B alter cell elongation and physiological responses throughout arabidopsis development', *Plant Cell*, 5(2), pp. 147–157.

Reinhart, B. *et al.* (2000) 'The 21-nucleotide let-7 RNA regulates developmental timing in Caenorhabditis elegans.', *Nature*, 403, pp. 901–906.

Reinhart, B. J. *et al.* (2002) 'MicroRNAs in plants', *Trends in Plant Science*, 7(11), pp. 1616–1626. doi: 10.1101/gad.1004402.of.

Reis, R. S. *et al.* (2015) 'Gene regulation by translational inhibition is determined by Dicer partnering proteins', *Nature Plants*. Nature Publishing Group, 1(February), pp. 1–6. doi: 10.1038/nplants.2014.27.

Ren, G. *et al.* (2012) 'Regulation of miRNA abundance by RNA binding protein TOUGH in Arabidopsis', *PNAS*, 109(31), pp. 12817–12821. doi: 10.1073/pnas.1204915109.

Robinson-Beers, K., Pruitt, R. E. and Gasser, C. S. (1992) 'Ovule development in wild-type Arabidopsis and two female-sterile mutants', *Plant Cell*, 4(10), pp. 1237–1249.

Robinson, O., Dylus, D. and Dessimoz, C. (2016) 'Phylo.io: Interactive Viewing and Comparison of Large Phylogenetic Trees on the Web', *Molecular Biology and Evolution*, 33, p. msw080. doi: 10.1093/molbev/msw080.

Rogers, K. and Chen, X. (2013) 'Biogenesis , Turnover , and Mode of Action of MicroRNAs', *The Plant Cell*, 25(July), pp. 2383–2399. doi: 10.1105/tpc.113.113159.

Rubio-somoza, I. and Weigel, D. (2011) 'MicroRNA networks and developmental plasticity in

plants', *Trends in Plant Science*. Elsevier Ltd, 16(5), pp. 258–264. doi: 10.1016/j.tplants.2011.03.001.

Salinas, M. *et al.* (2011) 'Genomic organization , phylogenetic comparison and differential expression of the SBP-box family of transcription factors in tomato', *Planta*, (November). doi: 10.1007/s00425-011-1565-y.

Samad, A. F. A. *et al.* (2017) 'MicroRNA and Transcription Factor : Key Players in Plant Regulatory Network', *Frontiers in Plant Science*, 8(April), pp. 1–18. doi: 10.3389/fpls.2017.00565.

Sang, Y. K., Yu, X. and Michaels, S. D. (2008) 'Regulation of Constans and Flowering Locus T expression in response to changing light quality', *Plant Physiology*, 148(1), pp. 269–279. doi: 10.1104/pp.108.122606.

Sawa, M. *et al.* (2007) 'FKF1 and GIGANTEA Complex Formation Is Required for Day-Length Measurement in Arabidopsis', *Science*, 318(October), pp. 261–266.

Schauer, S. E. *et al.* (2002) 'DICER-LIKE1: Blind men and elephants in Arabidopsis development', *Trends in Plant Science*, 7(11), pp. 487–491. doi: 10.1016/S1360-1385(02)02355-5.

Schauer, S. E. *et al.* (2013) 'DCL1 , a Protein that Produces Plant MicroRNA , Coordinates Meristem Activity', pp. 1–37.

Schwartz, B. W., Yeung, E. C. and Meinke, D. W. (1994) 'Disruption of morphogenesis and transformation of the suspensor in abnormal suspensor mutants of Arabidopsis', *Development*, 120(11), pp. 3235–3245.

Shimamura (2016) 'Marchantia polymorpha : Taxonomy , Phylogeny and Morphology of a Model System Special Focus Issue – Review', 0(December 2015), pp. 1–27. doi: 10.1093/pcp/pcv192.

Shimamura, M. (no date) 'Marchantia polymorpha: Taxonomy, Phylogeny and Morphology of a Model System'. doi: 10.1093/pcp/pcv192.

Simon, S. A., Meyers, B. C. and Sherrier, D. J. (2009) 'MicroRNAs in the Rhizobia Legume Symbiosis', *Plant Physiology*, 151(3), pp. 1002 LP – 1008. doi: 10.1104/pp.109.144345.

Speth, C. *et al.* (2013) 'RACK1 scaffold proteins influence miRNA abundance in Arabidopsis', *The Plant Journal*, 76, pp. 433–445. doi: 10.1111/tpj.12308.

Speth, C. and Laubinger, S. (2014) 'RACK1 and the microRNA pathway: is it déjà-vu all over again?', *Plant signaling & behavior*, 9(January), p. e27909. doi: 10.4161/psb.27909.

Stone, J. M., Nekl, E. R. and Stiers, J. J. (2005) 'Arabidopsis AtSPL14, a plant-specific SBP-domain transcription factor , participates in plant development and sensitivity to fumonisin B1'. doi: 10.1111/j.1365-313X.2005.02334.x.

Suarez, I. P. *et al.* (2015) 'Induced folding in RNA recognition by Arabidopsis thaliana DCL1', *Nucleic Acids Research*, 43(13), pp. 6607–6619. doi: 10.1093/nar/gkv627.

Sugano, S. S. *et al.* (2014) 'CRISPR/Cas9-mediated targeted mutagenesis in the liverwort Marchantia polymorpha L.', *Plant and Cell Physiology*, 55(3), pp. 475–481. doi: 10.1093/pcp/pcu014.

Sun, Z. *et al.* (2018) 'Coordinated regulation of Arabidopsis microRNA biogenesis and red light signaling through Dicer-like 1 and phytochrome-interacting factor 4', *PLoS Genetics*, 14(3), pp. 1–21. doi: 10.1371/journal.pgen.1007247.

Szweykowska-kulinska, Z., Jarmolowski, A. and Vazquez, F. (2016) 'The crosstalk between plant microRNA biogenesis factors and the spliceosome', *Plant Signaling & Behavior*, 2324(August). doi: 10.4161/psb.26955.

Telfer, A., Bollman, K. M. and Poethig, R. S. (1997) 'Phase change and the regulation of trichome distribution in Arabidopsis thaliana.', *Development (Cambridge, England)*, 124(3), pp. 645–54.

Available at: http://www.ncbi.nlm.nih.gov/pubmed/9043079.

Telfer, A. and Poethig, R. S. (1998) 'HASTY: a gene that regulates the timing of shoot maturation in Arabidopsis thaliana.', *Development (Cambridge, England)*, 125(10), pp. 1889–98. Available at: http://www.ncbi.nlm.nih.gov/pubmed/9550721.

Teotia, S. and Tang, G. (2015) 'To bloom or not to bloom: Role of micrornas in plant flowering', *Molecular Plant*. Elsevier Ltd, 8(3), pp. 359–377. doi: 10.1016/j.molp.2014.12.018.

Tétreault, N. and De Guire, V. (2013) 'MiRNAs: Their discovery, biogenesis and mechanism of action', *Clinical Biochemistry*. The Canadian Society of Clinical Chemists, 46(10–11), pp. 842–845. doi: 10.1016/j.clinbiochem.2013.02.009.

Thompson, B. E. *et al.* (2014) 'The dicer-like1 homolog fuzzy tassel is required for the regulation of meristem determinacy in the inflorescence and vegetative growth in maizew open', *Plant Cell*, 26(12), pp. 4702–4717. doi: 10.1105/tpc.114.132670.

Tripathi, R. K., Bregitzer, P. and Singh, J. (2018) 'Genome-wide analysis of the SPL / miR156 module and its interaction with the AP2 / miR172 unit in barley', (April), pp. 1–13. doi: 10.1038/s41598-018-25349-0.

Tsuzuki, M. *et al.* (2016) 'Profiling and characterization of small RNAs in the liverwort, Marchantia polymorpha, belonging to the first diverged land plants', *Plant and Cell Physiology*, 57(2), pp. 359–372. doi: 10.1093/pcp/pcv182.

Tsuzuki, M., Takeda, A. and Watanabe, Y. (2014) 'Recovery of dicer-like 1-late flowering phenotype by miR172 expressed by the noncanonical DCL4-dependent biogenesis pathway', *RNA*. doi: 10.1261/rna.044966.114.

Tu, B. *et al.* (2015) 'Distinct and Cooperative Activities of HESO1 and URT1 Nucleotidyl Transferases in MicroRNA Turnover in Arabidopsis', *PLoS Genetics*, 11(4). doi: 10.1371/journal.pgen.1005119.

Ueda, M., Koshino-Kimura, Y. and Okada, K. (2005) 'Stepwise understanding of root development', *Current Opinion in Plant Biology*, 8(1), pp. 71–76. doi: 10.1016/j.pbi.2004.11.014.

Unte, U. S. *et al.* (2003) 'SPL8 , an SBP-Box Gene That Affects Pollen Sac Development in Arabidopsis', *The Plant Cell*, 15(April), pp. 1009–1019. doi: 10.1105/tpc.010678.early.

Vazquez, F., Cre, P. and Bartel, D. P. (2004) 'The action of ARGONAUTE1 in the miRNA pathway and its regulation by the miRNA pathway are crucial for plant development', *Genes & Development*, 18, pp. 1187–1197. doi: 10.1101/gad.1201404.called.

Vazquez, F., Gasciolli, V. and Cre, P. (2004) 'The Nuclear dsRNA Binding Protein HYL1 Is Required for MicroRNA Accumulation and Plant Development , but Not Posttranscriptional Transgene Silencing', *Current Biology*, 14, pp. 346–351. doi: 10.1016/j.cub.2004.01.035.

Wang, B. *et al.* (2015) 'HOS1 regulates Argonaute1 by promoting transcription of the microRNA gene MIR168b in Arabidopsis', *Plant Journal*, 81(6), pp. 861–870. doi: 10.1111/tpj.12772.

Wang, H. *et al.* (2019) 'Genome-wide characterization of SPL family in Medicago truncatula reveals the novel roles of miR156 / SPL module in spiky pod development'. BMC Genomics, pp. 1–14.

Wang, Hai and Wang, Haiyang (2015) 'The miR156/SPL module, a regulatory hub and versatile toolbox, gears up crops for enhanced agronomic traits', *Molecular Plant*. Elsevier Ltd, 8(5), pp. 677–688. doi: 10.1016/j.molp.2015.01.008.

Wang, J.-W. *et al.* (2005) 'Control of Root Cap Formation by MicroRNA-Targeted Auxin Response Factors in Arabidopsis', *The Plant Cell*, 17(8), pp. 157–198. doi: 10.1105/tpc.105.033076.1.

Wang, J., Mei, J. and Ren, G. (2019) 'Plant microRNAs: Biogenesis, homeostasis, and degradation', *Frontiers in Plant Science*, 10(March), pp. 1–12. doi: 10.3389/fpls.2019.00360.

Wang, J. W., Czech, B. and Weigel, D. (2009) 'miR156-Regulated SPL Transcription Factors Define an Endogenous Flowering Pathway in Arabidopsis thaliana', *Cell*. Elsevier Ltd, 138(4), pp. 738–749. doi: 10.1016/j.cell.2009.06.014.

Wang, L. *et al.* (2013) 'NOT2 Proteins Promote Polymerase II – Dependent Transcription and Interact with Multiple MicroRNA Biogenesis Factors in Arabidopsis', *The Plant Cell*, 25(February), pp. 715–727. doi: 10.1105/tpc.112.105882.

Wang, W. *et al.* (2011) 'An importin β protein negatively regulates microRNA activity in Arabidopsis', *Plant Cell*, 23(10), pp. 3565–3576. doi: 10.1105/tpc.111.091058.

Willmann, M. R. and Poethig, R. S. (2007) 'Conservation and evolution of miRNA regulatory programs in plant development', *Elsevier*, (10), pp. 503–511. doi: 10.1016/j.pbi.2007.07.004.

Wu, Gang and Poethig, R. S. (2006) 'Temporal Regulation of Shoot Development in Arabidopsis Thaliana By Mir156 and its Target SPL3', *Development*, 133(18), pp. 3539–3547.

Wu, G. and Poethig, S. (2006) 'Temporal regulation of shoot development in Arabidopsis thaliana by miR156 and its target SPL3', *Development*, 133(18), pp. 3539–3547. doi: 10.1242/dev.02521.

Wu, X. *et al.* (2013) 'A role for the RNA-binding protein MOS2 in microRNA maturation in Arabidopsis', *Cell Research*, 23(5), pp. 645–657. doi: 10.1038/cr.2013.23.

Xie, K., Wu, C. and Xiong, L. (2006) 'Genomic Organization , Differential Expression , and Interaction of SQUAMOSA Promoter-Binding-Like Transcription Factors and microRNA156 in Rice 1 [ W ]', *Plant Physiology*, 142(September), pp. 280–293. doi: 10.1104/pp.106.084475.

Xu, M. *et al.* (2016) 'Developmental Functions of miR156-Regulated SQUAMOSA PROMOTER BINDING PROTEIN-LIKE (SPL) Genes in Arabidopsis thaliana', *PLoS Genetics*, 12(8), pp. 1–29. doi: 10.1371/journal.pgen.1006263.

Yamaoka, S. *et al.* (2018) 'Generative Cell Specification Requires Transcription Factors Evolutionarily Conserved in Land Plants', *Current Biology*. Elsevier Ltd., 28(3), pp. 479-486.e5. doi: 10.1016/j.cub.2017.12.053.

Yang, L. *et al.* (2006) 'SERRATE is a novel nuclear regulator in primary microRNA processing in Arabidopsis', *The Plant Journal*, 47, pp. 841–850. doi: 10.1111/j.1365-313X.2006.02835.x.

Yang, L., Conway, S. R. and Poethig, R. S. (2011) 'Vegetative phase change is mediated by a leaf-derived signal that represses the transcription of miR156', *Development*, 138(2), pp. 245–249. doi: 10.1242/dev.058578.

Yi, R. *et al.* (2003) 'Exportin-5 mediates the nuclear export of pre-microRNAs and short hairpin RNAs', *Genes and Development*, 17(24), pp. 3011–3016. doi: 10.1101/gad.1158803.

Yu, B. *et al.* (2005) 'Methylation as a Crucial Step in Plant microRNA Biogenesis', *Science*, 307(February), pp. 932–936.

Yu, B. *et al.* (2008) 'The FHA domain proteins DAWDLE in Arabidopsis and SNIP1 in humans act in small RNA biogenesis', *PNAS*, 105(29), pp. 10073–10078.

Zalewski, C. S. *et al.* (2013) 'Evolution of the Class IV HD-Zip Gene Family in Streptophytes', *Mol. Biol. Evol.*, 30(10), pp. 2347–2365. doi: 10.1093/molbev/mst132.

Zhang, S. *et al.* (2013) 'CDC5 , a DNA binding protein , positively regulates posttranscriptional processing and / or transcription of primary microRNA transcripts', *PNAS*, 110(43), pp. 17588–17593. doi: 10.1073/pnas.1310644110/-/DCSupplemental.www.pnas.org/cgi/doi/10.1073/pnas.1310644110.

Zhang, S. *et al.* (2015) 'Evolutionary Comparison of Two Combinatorial Regulators of SBP-Box Genes , MiR156 and MiR529 , in Plants', *Plos one*, 10(April), pp. 1–12. doi: 10.1371/journal.pone.0124621.

Zhang, S., Liu, Y. and Yu, B. (2014) 'PRL1 , an RNA-Binding Protein , Positively Regulates the

Accumulation of miRNAs and siRNAs in Arabidopsis', *PLOS Genetics*, 10(12). doi: 10.1371/journal.pgen.1004841.

Zhang, Y. *et al.* (2007) 'SPL8, a local regulator in a subset of gibberellin-mediated developmental processes in Arabidopsis', *Plant Molecular Biology*, 63(3), pp. 429–439. doi: 10.1007/s11103-006-9099-6.

Zhao, Y. *et al.* (2012) 'HESO1, a nucleotidyl transferase in Arabidopsis, uridylates unmethylated miRNAs and siRNAs to trigger their degradation', *Current Biology*, 22(8), pp. 689–694. doi: 10.1016/j.cub.2012.02.051.HESO1.